

Российский химико-технологический университет им. Д.И.Менделеева
D.Mendeleev University of Chemical
Technology of Russia

**Université D.Mendeleev de
Technologie Chimique de Russie
Fédération de Russie**



**Université Aix-Marseille II
Faculté des Sciences de Luminy
France**

THESE DE DOCTORAT EN CO-TUTELLE

En vue d'obtenir le grade
de Docteur de l'Université Aix-Marseille II et de l'Université Mendeleev

Spécialité : Chimie Organique

Pésentée par

Sergey PARAMONOV

**Benzo- et naphtopyranes annelés par des éthers couronnes :
synthèse, photochromisme et pouvoir complexant vis-à-vis des
cations métalliques et des acides aminés**

Crown ether annelated benzo- and naphthopyrans: synthesis,
photochromism, and coordination ability towards
metal cations and amino acids

Soutenue le 19 Novembre 2010 devant le jury composé de :

Jean-Luc POZZO	Professeur, Université Bordeaux 1 (France)	Rapporteur
Sergey KURBATOV	Professeur, Université Fédérale du Sud (Russie)	Rapporteur
Vladimir LOKCHINE	Chargé de Recherches, CINaM CNRS UPR 3118 (France)	Directeur de thèse
Vladimir KHODORKOVSKY	Directeur de Recherches, CINaM CNRS UPR 3118 (France)	Examineur
Olga FEDOROVA	Professeur, Université Mendeleev (Russie)	Codirecteur de thèse
Leonid KOVALENKO	Professeur, Université Mendeleev (Russie)	Examineur

Acknowledgments

This work was carried out in accordance with co-tutorship agreement between D.Mendeleev University of Chemical Technology of Russia (Moscow, Russia) and Université Aix-Marseille II (Marseilles, France). In France, the work was performed in Centre Interdisciplinaire de Nanoscience de Marseille (CINaM CNRS UPR 3118).

I would like to express my deepest gratitude to Prof. Olga Fedorova (Mendeleev University) and Dr. Vladimir Lokshin (Université Aix-Marseille II) for wise supervising of the work.

I would like to thank the members of the jury for kind accepting the invitation to judge the defense. I express my gratitude to Prof. Jean-Luc Pozzo (Université Bordeaux I, France) and Prof. Sergey Kurbatov (Federal Southern University, Rostov-on-Don, Russia) for being referees and thorough examination of the manuscript. Prof. Vladimir Khodorkovsky (Directeur de recherches, CINaM CNRS UPR 3118, Marseilles, France) and Prof. Leonid Kovalenko (Mendeleev University, Moscow, Russia) are kindly thanked for being examiners.

I am also grateful to Prof. André Samat (CINaM CNRS UPR 3118, Marseilles, France), Dr. Yurii Fedorov (A.N.Nesmeyanov Institute of Organoelement Compounds RAS, Moscow, Russia), Prof. Gaston Vermeersch, Dr. Stéphanie Delbaere (Université Lille II, France), Prof. Heiko Ihmels (Universität Siegen, Germany), Dr. Natalia Sanina (Institute of Problems of Chemical Physics RAS, Chernogolovka, Russia) as well as all other people who participated in the investigations or supported me during the whole period of the work.

Content

1. PREFACE	1
2. INTRODUCTION	2
2.1. Systems Based on Spiropyrans.....	3
2.1.1. Complex Formation of Spiropyrans with Metal Cations	3
2.1.1.1. Simple Substituted Spiropyrans	3
2.1.1.2. Molecular Systems Containing the Spiropyran Fragments.....	8
2.1.1.3. Spiropyran-Based Systems with Controlled Charge and Energy Transfer	13
2.1.1.4. Polymer Compositions Containing Spiropyrans	17
2.1.2. Coordinations of Spiropyrans with Biomolecules	18
2.2. Systems Based on Spirooxazines	21
2.3. Systems Based on Chromenes.....	26
3. RESULTS AND DISCUSSION	30
3.1. Synthesis of Benzo- and Naphthopyrans	31
3.1.1. Synthesis of Crown-Containing Benzo- and Naphthopyrans from Phenols and β -Naphthol Annelated by Crown Ether	31
3.1.2. Synthesis of Naphthopyrans Annelated to the Crown Ether Fragments of Various Size and Heteroatomic Composition.....	42
3.1.3. Synthesis of Benzopyrans Containing Positively Charged Fragments ..	48
3.2. Study of Photochromic Properties and Complex Formation of Several Compounds Synthesized.....	51
3.2.1. Study of Coordination ability of Several Crown-Annelated Chromenes.....	51
3.2.1.1. Complex Formation of Chromenes 1a and 3a with Metal Cations.....	51
3.2.1.2. Complex Formation of Chromenes 1b and 3b with Amino Acids.....	74
3.2.2. Study of Chromene 33 Intercalation into DNA.....	90
4. CONCLUSIONS	96

5. EXPERIMENTAL PART	97
5.1. Syntheses.....	98
5.1.1. Acylation Using Eaton's Reagent.....	98
5.1.2. Baeyer-Villiger Oxidation.....	99
5.1.3. Synthesis of Naphthols.....	101
5.1.4. Synthesis of Chromenes from Appropriate Phenols.....	102
5.1.5. Replacement of Terminal Groups in Chromenes 16a and 16b	106
5.1.6. Synthesis of Crown-Annulated Derivatives.....	107
5.1.7. Nitrosation of Naphthols 17a and 17b	110
5.1.8. Synthesis of Spironaphthoxazines.....	110
5.1.9. Synthesis of Photochromes Containing Positively Charged Fragments.....	112
5.2. Determination of Complex Stability Constants by Spectrophotometric Titration.....	114
5.3. Determination of Bleaching Rate Constants.....	115
5.4. Study of Chromene 33 Intercalation into DNA.....	116
6. BIBLIOGRAPHY	117
7. APPENDIXES	130
7.1. X-Ray Data.....	130
7.2. NMR Spectra.....	137
7.3. List of Publications.....	147

1. Preface

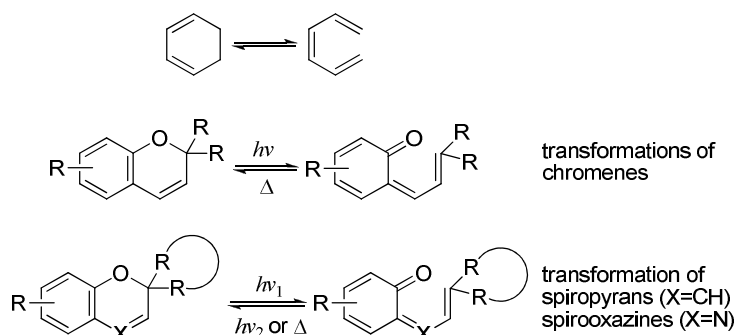
Photochromic fragments incorporation into a molecule enables photo-control of its characteristics. This approach expands the possibilities of practical use of already known materials. The most well-known and widely used photochromes are spiropyrans, spironaphthoxazines, and chromenes. The examples of photo-control of viscosity and size of polymer materials as well as characteristics and catalytic activity of biological molecules containing photochromic moieties are reported in literature [1-5]. Of interest is application of photochromes to the control both intramolecular (charge and energy transfer) and supramolecular (host-guest coordination and complex formation) processes. The development of the latter trend is of importance for creation of nano-scale molecular devices for information processing and storage; design of new drugs with photo-controlled pharmacological activity towards various diseases including cancer; and enhancement as well as elaboration of environmentally safe technologies used in many branches of modern industry.

Chromenes synthesized in this work have two important properties. When irradiated with light, they are able to undergo electrocyclization and *cis-trans* isomerization. The presence of crown ether or positively charged heterocyclic fragment in their structures defines the ability of such compounds to participate to the coordination with metal cations, amino acids, or DNA molecules, the process being accompanied by the change of their spectral characteristics. Thus, crown-containing chromenes may be used for creation of photo-controlled complexons, catalytic systems, etc. The possibility of adjusting photochromic properties of crown-containing naphthopyrans by complex formation makes these compounds suitable for developing new photochromic materials with tunable characteristics. Chromenes containing positively charged heterocyclic fragments may be used for creation of photochromic DNA tags for enhancement of cancer diagnostics and treatment methods.

The aim of this work was development of synthetic approaches towards benzo- and naphthopyrans, annelated to the crown ether fragments of various composition and size, and chromenes, containing positively charged heterocyclic fragments, as well as comprehensive study of the properties of the compounds and their complexes with metal cations, protonated amino acids, and DNA by NMR, optical spectroscopy, and X-ray structural analysis techniques.

2. Introduction

Photochromic compounds represent a large class of compounds able to participate in light-induced reversible electrocyclic transformations. Among photochromes undergoing a cyclohexadiene-1,3 – hexatriene-1,3,5 type phototransformation, of the greatest interest are spiropyrans, spirooxazines, and chromenes (Scheme 2.1) [1-3]. Photochromism of these compounds is due to photochemical conversion of the initial, the so-called “closed” or spiro- (SP), form to the isomeric merocyanine (MC), or “open”, form. In case of chromenes, the reverse process is thermal; whereas in case of spiropyrans and spirooxazines, it is both thermal and photochemical. Such transformations are accompanied by color change as closed and open forms usually absorb in the UV and visible region, respectively.



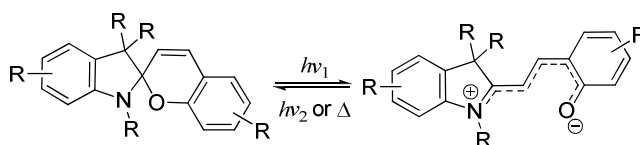
Scheme 2.1. Electrocyclic cyclohexadiene-1,3 – hexatriene-1,3,5 type transformations.

A number of publications and reviews are devoted to the development of synthetic approaches and investigation of this group of photochromes [1-5]. During the last years, the interest to such compounds was caused by a possibility of creation of molecular systems which properties may be reversibly changed by light irradiation. This principle is the basis of photoswitches and optical sensors.

The following literature review comprises publications devoted to spiropyran-, spirooxazine-, and chromene-based complexons, in which photochromic transformations and complex formation exhibit mutual influence on each other. Major part of reported works describes systems able to bind different metal ions. Yet, there are few articles which consider photochromic molecules as complexons for organic molecules. This review covers the papers published since 2003 until present time.

2.1. Systems Based on Spiropyrans

Spiropyrans are widely presented in modern scientific literature. Upon UV irradiation such molecules are able to transform into the MC forms, which reverse back into the SP forms both thermally and photochemically (by irradiation with visible light). The open forms of spiropyrans are characterized by a significant charge separation, which is usually depicted as zwitter-ionic structure (Scheme 2.2) [1-3]. Due to this, the phenolate oxygen atom, having higher electron density, may readily form complexes with metal cations. The latter process may be modulated by irradiating a sample with a light of different wavelength (UV or visible).



Scheme 2.2. Phototransformations of spiropyrans.

2.1.1. Complex Formation of Spiropyrans with Metal Cations

The major part of the reports describing complex formation by spiropyrans is devoted to complexing metal cations. They can be classified as follows:

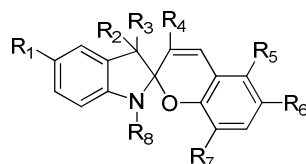
- simple substituted spiropyrans;
- molecular systems containing spiropyran fragments (e.g., crown ethers and calixarenes);
- spiropyran-based systems with controlled charge and energy transfer;
- polymer compositions containing spiropyrans.

2.1.1.1. Simple Substituted Spiropyrans

In the presence of metal ions, spiropyrans transform into the colored open forms spontaneously. As a rule, monovalent alkaline cations do not affect the MC-SP equilibrium, whereas addition of di- or trivalent cations results in considerable red shift of the absorption band as well as its intensity change. Additional UV irradiation of the solution containing both spiropyrans and metal ions usually leads to further increase of color intensity due to increasing concentration of the open forms. Thermal relaxation of such compounds in the metal ion presence is significantly lowered [6-11]. To attain the initial colorless state, samples are irradiated with visible light that induces MC to SP backward transformation [11, 12].

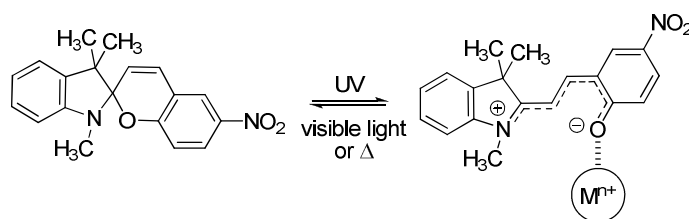
Table 2.1.

Spiropyrans with simple substituents.

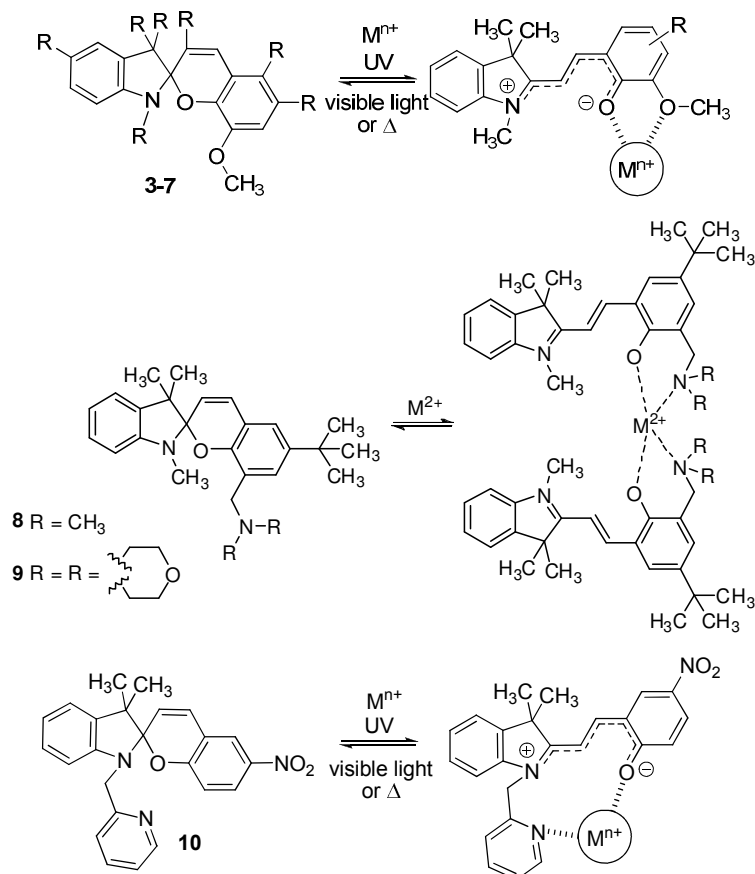


No.	R ₁	R ₂	R ₃	R ₄	R ₅	R ₆	R ₇	R ₈	Ref.
1	H	CH ₃	CH ₃	H	H	NO ₂	H	CH ₃	[6]
2	H	CH ₃	CH ₃	H	OH	CH=O	H	CH ₃	[7]
3	H	CH ₃	CH ₃	H	H	NO ₂	CH ₃ O	CH ₃	[8]
4	H	CH ₃	CH ₃	CH ₃	H	NO ₂	CH ₃ O	CH ₃	
5	H			H	H	NO ₂	CH ₃ O	CH ₃	
6	CF ₃			H	H	H	CH ₃ O	CH ₃	
7	CF ₃	CH ₃	CH ₃	H	H	H	CH ₃ O	CH ₃	
8	H	CH ₃	CH ₃	H	H	C(CH ₃) ₃		CH ₃	[9, 10]
9	H	CH ₃	CH ₃	H	H	C(CH ₃) ₃		CH ₃	
10	H	CH ₃	CH ₃	H	H	NO ₂	H		[11]
11	H	CH ₃	CH ₃	H	H	Cl		CH ₃	[12]
12	H	CH ₃	CH ₃	H	H	Cl		CH ₂ CH ₂ CH ₃	
13	H	CH ₃	CH ₃	H	H	Cl		CH ₂ CH(CH ₃) ₂	

Spiropyrans **1**, **2** (Table 2.1) form complexes with metal ions in MC state due to coordination with phenolate oxygen atom (Scheme 2.3) [6]. Introducing additional coordination centers (compounds **3-13**, Table 2.1) generally lead to greater stability of complexes formed upon irradiation (Scheme 2.4) [7, 8]. For several compounds, a specific and selective photo-response towards certain metal cations was observed. For instance, spiropyrans **8** and **9** were selective towards copper (II) ions [9, 10]; a high selectivity towards iron (III) ions was reported for compound **10** [11]. Therefore, spiropyrans may be successfully used as optical sensors for metal cations.

Scheme 2.3. Coordination of spiropyran **1** with metal ions.

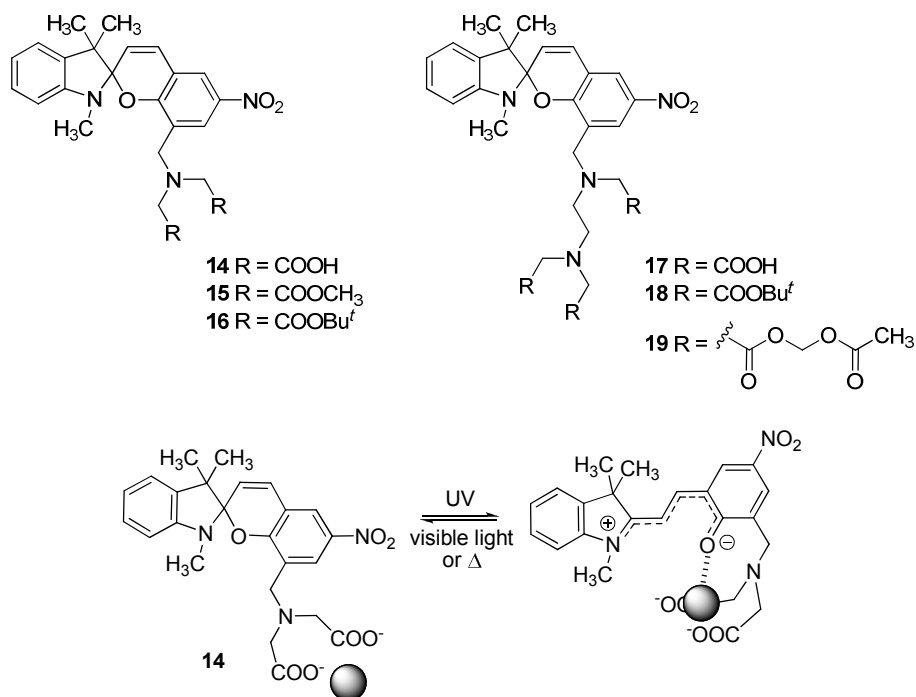
Spiropyran **14-19**, which contain carboxylic or ester groups, were shown to form complexes with cations in both the initial SP and photoinduced MC states (Scheme 2.5) [13],



Scheme 2.4. Additional coordination sites in spiropyrans **3-10**.

the stability of complexes with the open isomers being greater. The advantage of such systems is the possibility to study their properties in water solutions and in living cells. It is worth to mention that compound **17** exhibits relatively high affinity to calcium (II) cations.

An alternative interesting practical implementation of spiropyrans color changes upon metal ions addition is the use of compounds **20-23** in compositions with metals salts



Scheme 2.5. Complex formation of spiropyran **14**.

for color printing [14]. Thus, emulsions of spiropyrans and barium naphthenate, zinc naphthenate, and antimony chloride were made to reproduce pigments of CMYK color model: cyan, magenta, and yellow, respectively (Table 2.2).

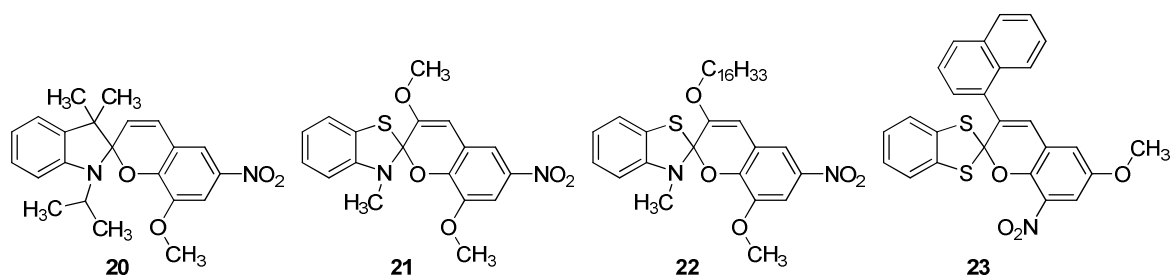


Table 2.2.

Using spiropyrans **20-23** for preparation of emulsions to reproduce CMYK pigments. (Absorption maxima, which are the closest to the required parameters, are in italics.)

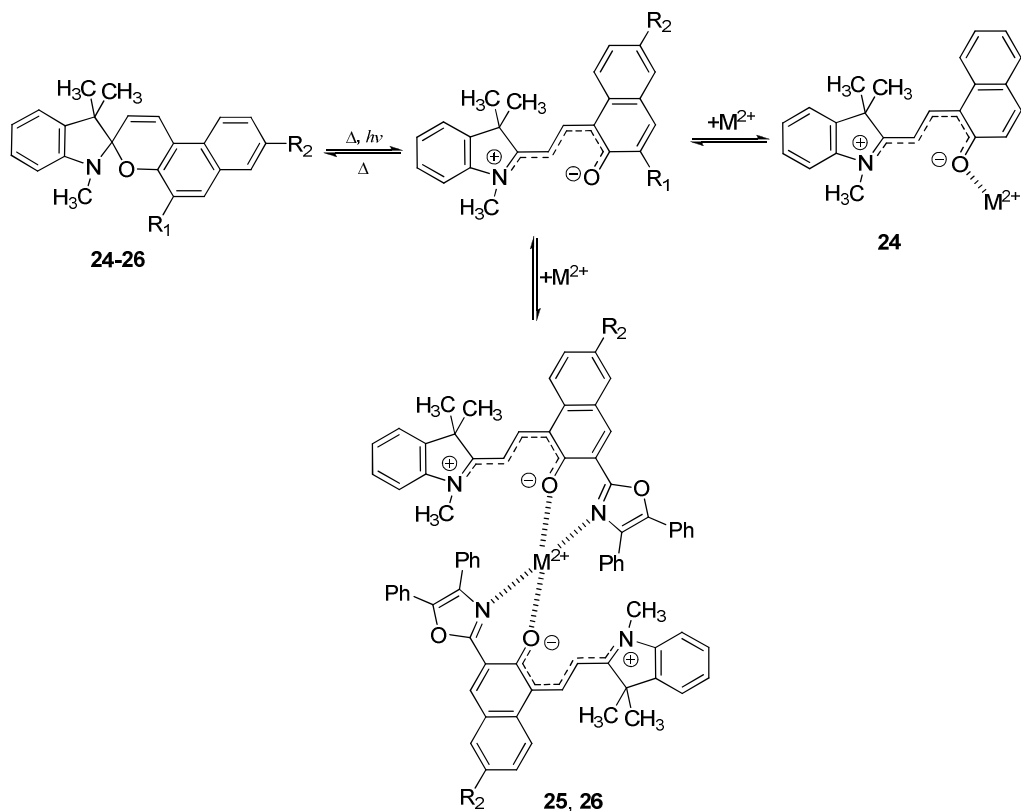
Pigment	Required λ_{\max} (nm)	20	21	22	23
Yellow (SbCl ₂)	456	<i>469</i>	<i>469</i>	<i>478</i>	<i>475</i>
Magenta (naphthenate Zn)	550	<i>521</i>	<i>539</i>	<i>548</i>	<i>540</i>
Cyan (naphthenate Ba)	660	<i>638</i>	<i>672</i>	<i>667</i>	<i>658</i>

Another type of spiropyrans modifications is annelation to the heterocyclic moieties (Table 2.3). It is reported that upon addition of solutions containing transition metal ions (Cd²⁺, Mn²⁺, Zn²⁺, Co²⁺, Ni²⁺, Cu²⁺) a spontaneous coloring of solutions of spiropyrans **24-26** was observed [15]. Comparing to the unsubstituted analogue **24**, compounds **25** and **26** were characterized by relatively high stability of complexes, which was due to the additional coordination with the oxazole fragment (Scheme 2.6). Cobalt (II), nickel (II), and copper (II)

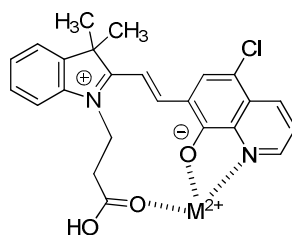
Table 2.3.

Spiropyrans with fused aromatic fragments.

	No.	R ₁	R ₂	R ₃	Ref.
	24	H	H	--	[15]
	25		H	--	
	26		OCH ₃	--	
	27	H	CH ₃	--	[16]
	28	H	C ₈ H ₁₆	--	
	29	H	CH(CH ₃) ₂	--	
	30	H	CH ₂ Ph	--	
	31	CH ₃	CH ₃	--	
	32	NO ₂	CH ₃	--	
	33	H	CH ₃	H	[17]
	34	NO ₂	CH ₃	H	
	35	H	CH ₃	Br	[18-20]
	36	H	CH ₃	Cl	
	37	H	CH ₂ Ph	Br	[19]
	38	Cl	CH ₃	Br	
	39	H	CH ₂ CH ₂ OH	Cl	[20]
	40	H	CH ₂ CH ₂ COOH	Cl	[19]



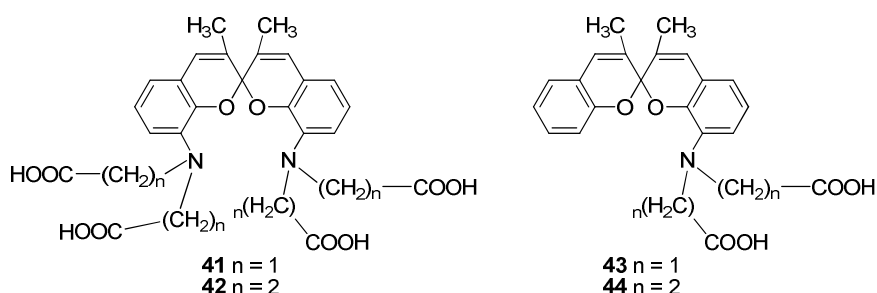
Scheme 2.6. Complex formation of spiropyrans **24-26** with metal cations.

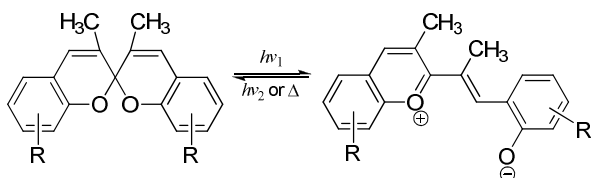


Scheme 2.7. Intramolecular stabilization of 1:1 complexes of spiropyran **40** [19].

cations were reported to form 2:1 (two ligand molecules per one metal ion) complexes with the open forms which remained colored even after irradiation with visible light. Similar behavior was detected for the compounds containing the chromenone (**27-32**, [16]) and quinoline (**33-40**, [17-20]) moieties. It should be noted however, that in case of spiropyrans **39** and **40**, 1:1 complex formation was favored due to the intramolecular stabilization of a cation by the HO⁻ or carboxylic group, respectively (Scheme 2.7).

Also, bis(spiropyran)s **41-44** were synthesized [21]. Similarly to compounds **14-19**, these compounds form complexes with metal ions in the initial SP state. However, the attempts to investigate the complex formation upon irradiation failed as the corresponding



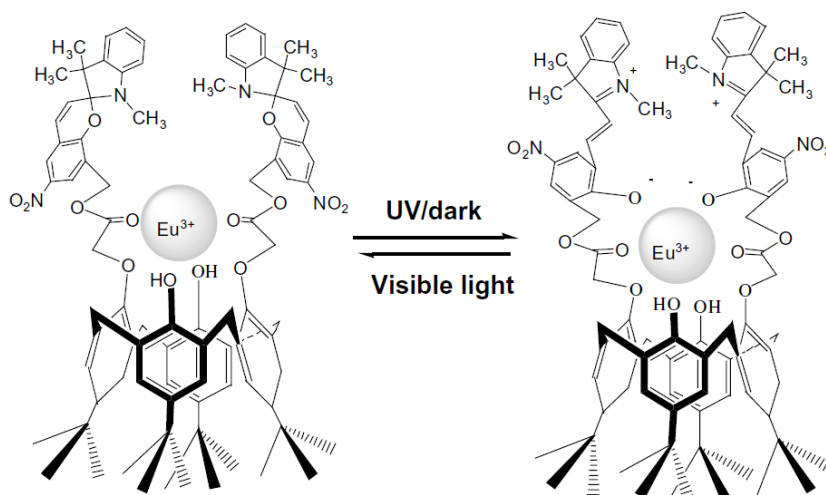


Scheme 2.8. Possible photochromic transformations of compounds **41-44**.

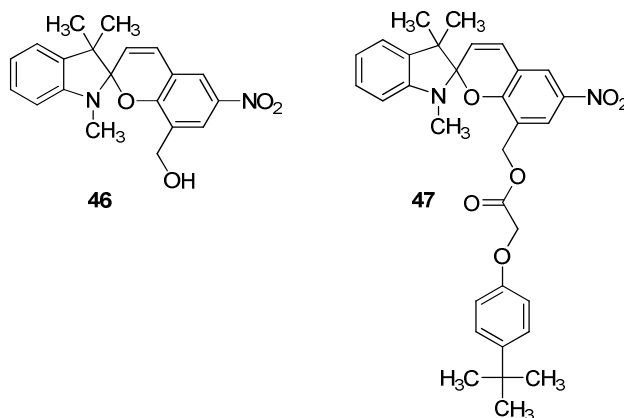
open forms were very unstable. It seems that the structure of the MC isomers disfavors the photochromic transformations (Scheme 2.8).

2.1.1.2. Molecular Systems Containing the Spiropyran Fragments

Macromolecules such as calixarenes and crown ethers are able to form very stable complexes due to their pre-organized structure. Attaching two nitrospiropyran moieties to calixarene **45** resulted in selectivity of the compound towards lanthanides ions (Scheme 2.9) [22-24]. In the presence of cations, a blue shift of MC form's absorption band was observed as well as noticeable decrease of bleaching rate. Similar effects, yet less pronounced, were detected in case of model compounds **46** and **47**.

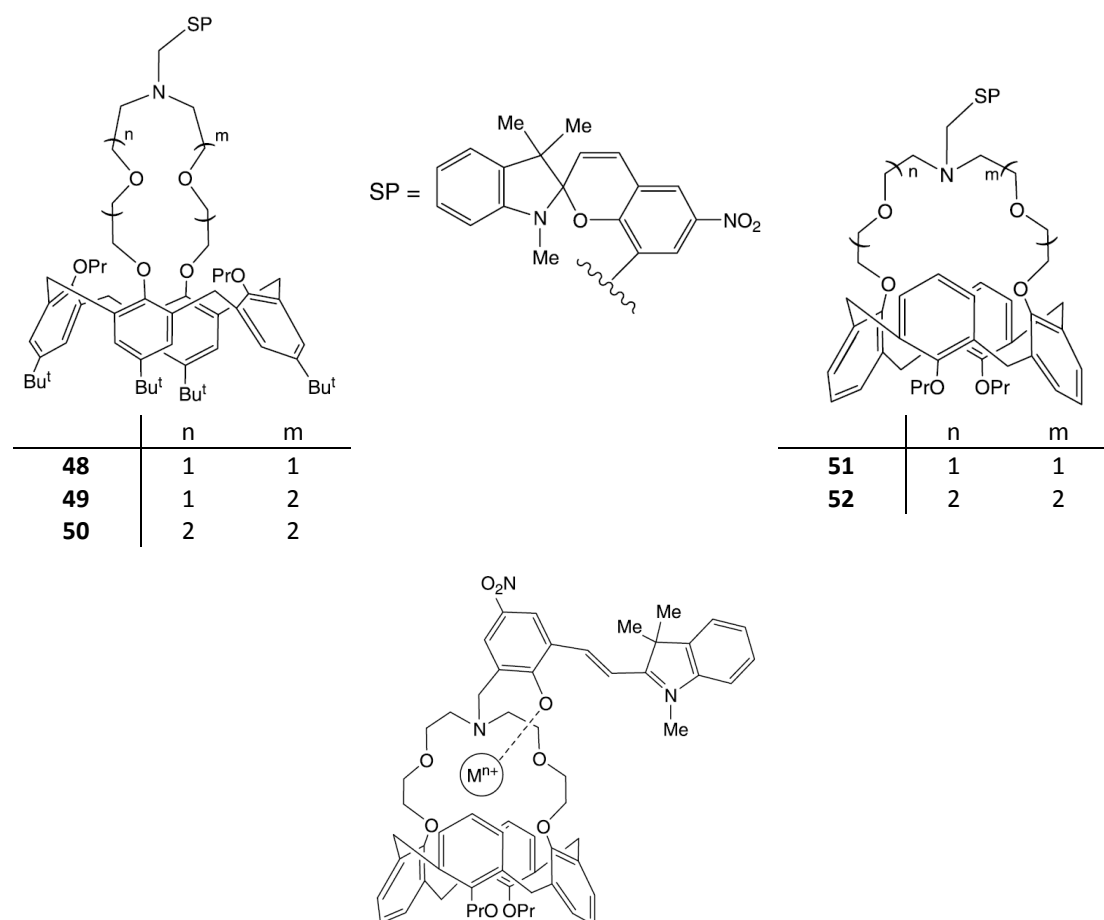


Scheme 2.9. Complex formation of calixarene **45** with cations.



Attaching a crown ether moiety to calixarenes **48-52** led to considerable enhancement of the complexes stability as the intramolecular cavity was formed [25]. It was found that charge density as well as size of cations is essential for stable coordination with

both the crown and spiropyran moieties. Thus, alkaline metal ions did not induce any considerable spectral changes of the calixarenes solution, whereas the divalent cations of alkaline-earth and transition metals caused coloration explained by cation-induced opening of the spiropyran fragments (Scheme 2.10).



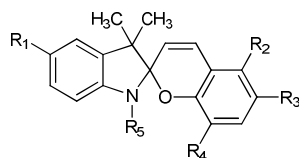
Scheme 2.10. Complex formation of calixarene **51**.

There are numerous publications describing spiropyran linked to a crown ether fragment. Such systems can be readily prepared providing the opportunity to design systems selective towards cations. The photochromic fragment affords compounds useful for photo-controlled complex formation or optical recognition of cations. The major part of the reported spiropyran contains a crown ether moiety tethered by an aliphatic spacer to 8th position of the benzopyran or 1st position of the indoline fragment (Table 2.4). Such substitution is mainly chosen because of proximity of the ionophoric fragment to the phenolate oxygen atom in the MC form.

Compounds **53-76** were found to form complexes by coordination of crown ether fragments or their analogues with metal cations. Upon irradiation, additional stabilization was provided by the phenolate oxygen atom of the open form (Scheme 2.11). Like those in the case of unsubstituted spiropyran, the greater spectral changes were observed with multicharged cations.

Table 2.4.

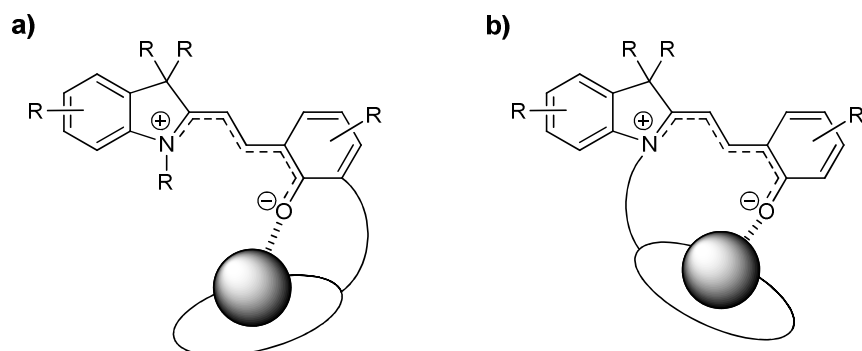
Spiroprans containing crown ether moiety.



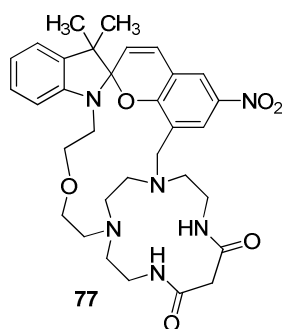
No.	R ₁	R ₂	R ₃	R ₄	R ₅	Ref.
53	H	H	NO ₂		CH ₃	[26, 27]
54	CF ₃	H	NO ₂		CH ₃	[26]
55	NO ₂	H	NO ₂		CH ₃	
56	H	H	NO ₂		C ₁₈ H ₃₇	[28, 29]
57	H	H	NO ₂		C ₁₈ H ₃₇	[28, 29]
58	H	H	NO ₂		C ₁₈ H ₃₇	
59	H	H	NO ₂		CH ₃	[17]
60	H	H	NO ₂		CH ₃	[30, 31]
61	NO ₂	H	NO ₂		CH ₃	[32]
62	H	H	NO ₂		CH ₃	[30]
63	H	H	NO ₂		CH ₃	[33]
64	H	H	NO ₂		CH ₃	
65	H	H	NO ₂		CH ₃	

Table 2.4 cont.

No.	R ₁	R ₂	R ₃	R ₄	R ₅	Ref.
66	H	H	H		CH ₃	[34]
67	H	H	H		CH ₃	
68	H	H	NO ₂		CH ₃	[35]
69	H	H	NO ₂			
70	H	H	NO ₂	H		[36]
71	H	H	H	H		[37, 38]
72	H	H	Br	H		
73	H	H	OCH ₃	H		
74	H	H	NO ₂	H		[30]
75	H	H		H	CH ₃	[40]
76	H	H		H	CH ₃	



Scheme 2.11. Coordination in complexes of spiroyrans (a) 53-65, 68, 69 and (b) 70-74 with metal cations.



In addition, spiropyran **77**, which contains an azacrown moiety linked to the both fragments of the photochromic molecule, is described [39]. The compound is reported to show high selectivity to copper (II) cations.

Another trend in crowned spiropyran is attaching several photochromic groups to a macrocycle. Generally, this leads to an increase in the complex stability upon irradiation as well as greater extent of the photo-control of complexation. There are crowned derivatives containing two (**78-84**), three (**85**), and even four (**86**) spiropyran moieties described in the literature (Table 2.5) [17, 28, 29, 34, 37-39, 41-44]. Attaching several chromophoric groups leads to the consequent intensity increase of the absorption band of the open forms upon irradiation. This, in turn, provides greater sensitivity of the ligands towards metal cations. Compounds **87-93**, which contain podand fragment that links two spiropyran, are reported (Table 2.6) [34]. In contrast to the crown-containing analogues, these compounds formed stable complexes with different metal ions and did not show pronounced selectivity towards any of them.

Table 2.5.

Crown ether derivatives containing two spiropyran fragments.

	No.	R	n	Ref.
	78	H	1	[41-43]
	79	H	2	[17, 28, 29, 34, 41-43]
	80	CF ₃	2	[17]
	81	NO ₂	2	
	82	H	--	[37-39]
	83	Br	--	
	84	OCH ₃	--	

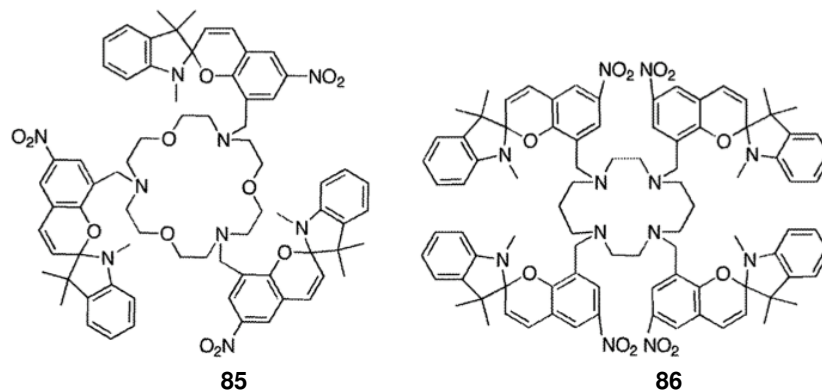


Table 2.6.

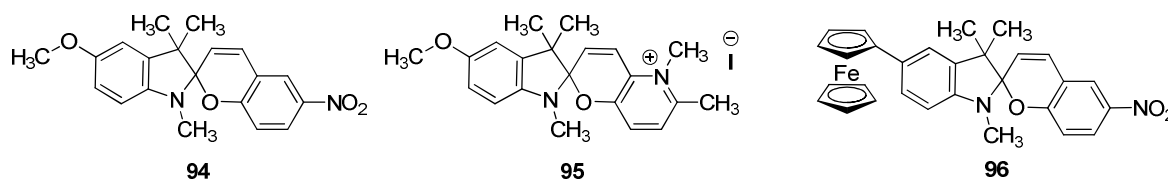
Spiroyrans linked by a podand fragment [34].

	No.	R	n
		87	H
	88	OCH ₃	1
	89	C(CH ₃) ₃	1
	90	CH(CH ₃) ₂	1
	91	Cl	1
	92	Br	1
	93	H	2

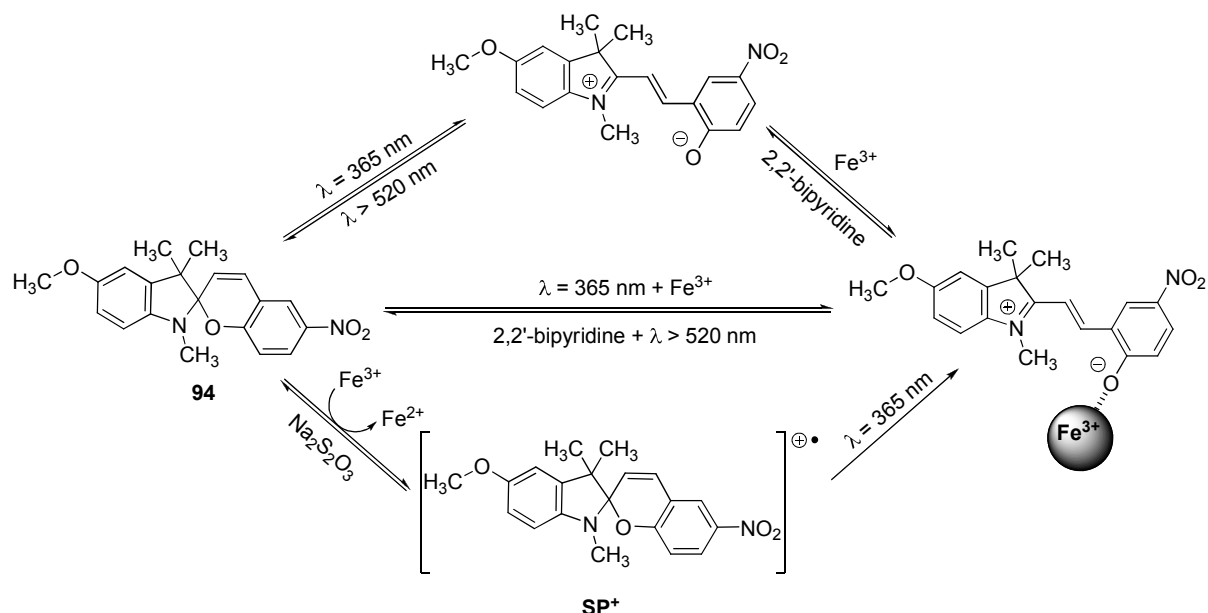
The compounds mentioned were proposed as potential candidates for implementing photo-control to such processes as extraction [26, 42-44] and transmembrane transport [28, 29, 36] of metal cations. However, the major part of publications is concentrated on the use of photochromic spiroyrans to optical recognition of metal ions [30, 33, 34, 37-40]. In addition, some derivatives were proved useful for other applications. For instance, complexes of compounds **60** and **61** with Gd³⁺ were successfully tested as promising contrast material for magnetic resonance imaging [31, 32].

2.1.1.3. Spiroiran-Based Systems with Controlled Charge and Energy Transfer

Since spiroiran state may be controlled by irradiation or addition of metal cations, systems, which contain a spiroiran moiety for controlling charge or energy transfer between different parts of a system, were described. This phenomenon implies the application of spiroyrans as Red-Ox switches and fluorescent sensors.

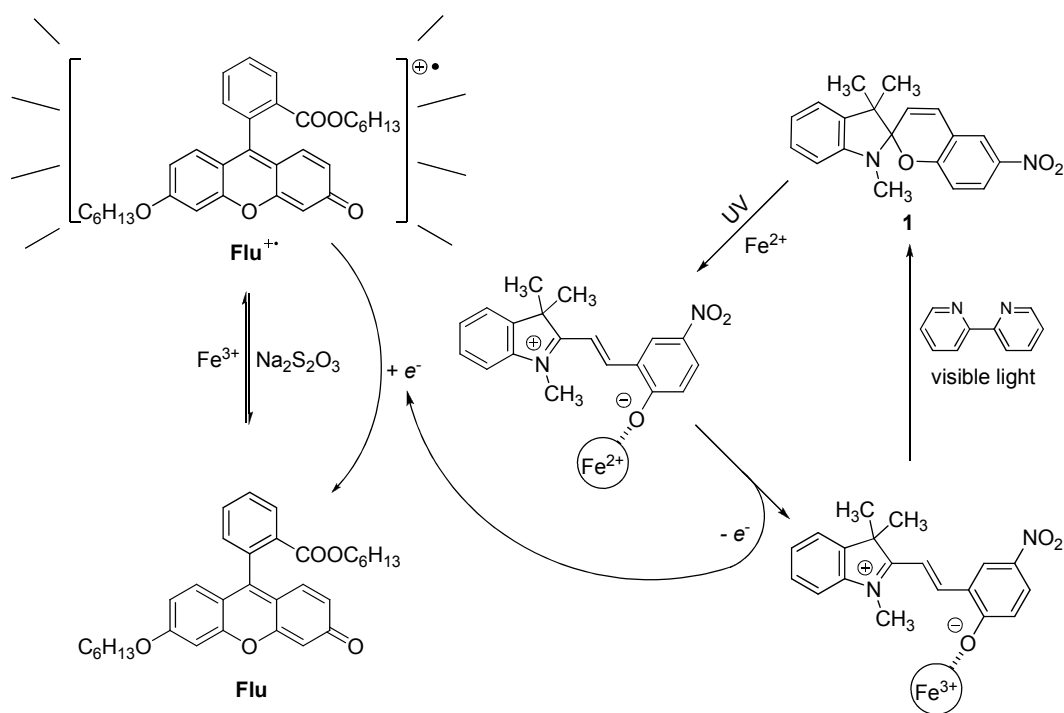


Compounds **94-96** were found to change their oxidation state in the presence of iron cations (or ferrocene moiety) and upon irradiation [45-47]. Thus, upon addition of the Fe (III) ions to spiroiran **94**, the SP form does not transform into the MC isomer but



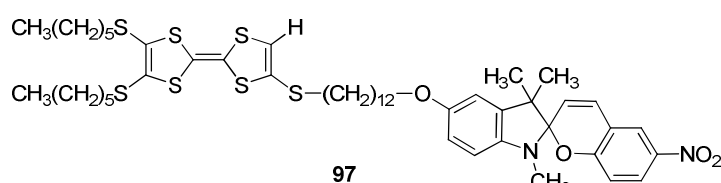
Scheme 2.12. Interconversions of spiropyran **94** upon UV and visible light irradiation and in the presence of iron cations [45].

converts into radical cation SP^+ whereas Fe^{3+} undergoes reduction to Fe^{2+} (Scheme 2.12). Upon UV irradiation and in the presence of the Fe (II) ions, SP^+ is reduced to form the open isomer which forms complexes with the generated Fe (III) ions. It is reported that such complexes are insensible to visible light while addition of 2,2'-bipyridine leads to usual photochromic reversibility. The same results were obtained when the Fe (III) ions were added to a solution of the open form. The similar behavior was observed in case of compound **95** and ferrocene derivative **96**.



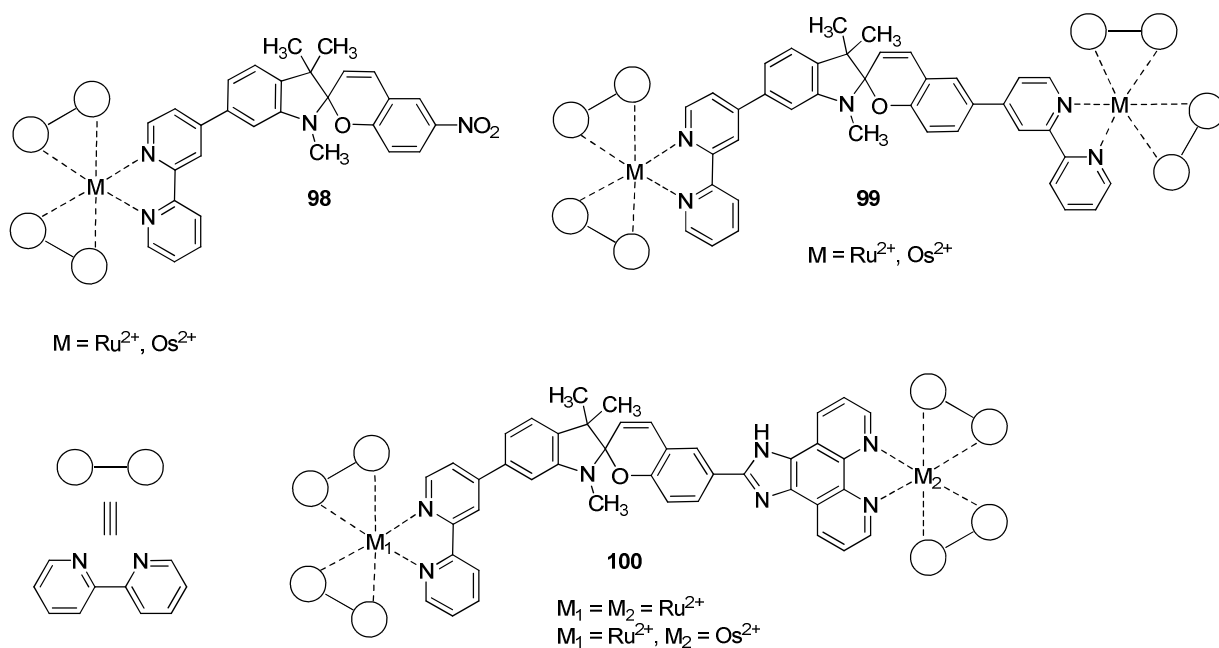
Scheme 2.13. Photochromic control of fluorescence in system fluorescein - spiropyran **1** in the presence of Fe^{3+} [49].

The red-ox pair $\text{Fe}^{3+}/\text{Fe}^{2+}$ was also used in a composition with photo-controlled fluorescence [48, 49]. Thus, addition of the Fe (III) ions to a solution of fluoreseine leads to considerable increase in the fluorescence intensity, the Fe (II) ions and fluoreseine radical cation Flu^+ being formed (Scheme 2.13). In the presence of spiroopyran **1**, UV irradiation of the latter solution results in the formation of the MC isomer which forms a complex with Fe^{2+} . Transfer of an electron from the complex to Flu^+ was found to be thermodynamically favorable and led to reduction of the latter to Flu and consequently to fluorescence quenching, the ions Fe^{2+} being oxidized to Fe^{3+} within the complex with the open form. Like that in the previous case, the photochromic reversibility was reached upon addition of a chelating agent (2,2'-bipyridine).



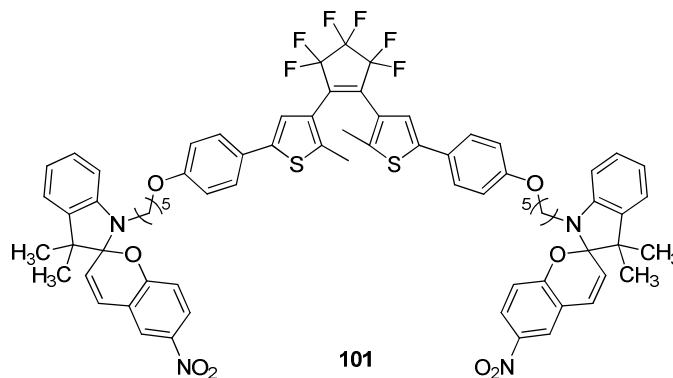
Similarly, electron transfer was controlled by photochromic transformation of spiroopyran **1** in the systems containing different tetrathiafulvalenes in the presence of Pb^{2+} and Sc^{3+} [50]. Also, tetrathiafulvalene **97** covalently bound to a spiroopyran moiety was reported [51].

An attempt to implement a spiroopyran fragment for electron and energy transfer control in bipyridine complexes of ruthenium (II) and osmium (II) was made [52-54]. For this purpose, compounds **98-100** and their complexes with metal ions were synthesized (Scheme



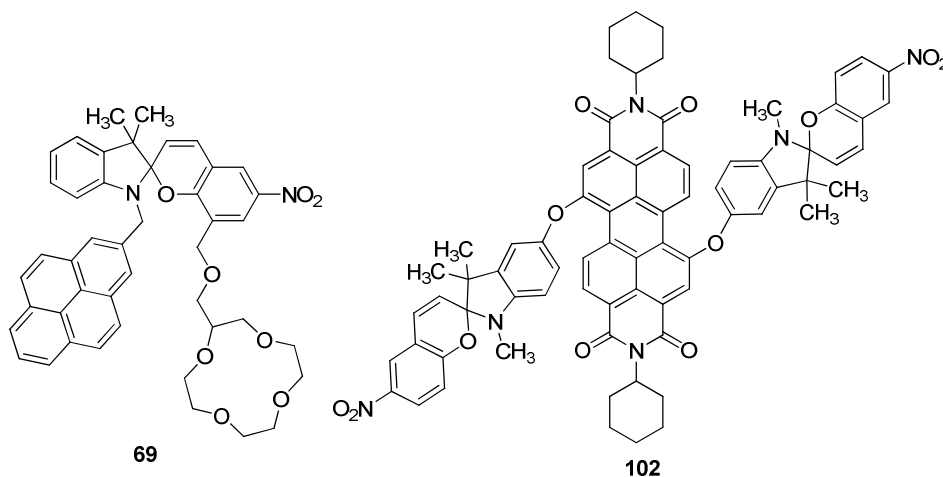
Scheme 2.14. Complexes of spiroopyrans **98-100** with ruthenium (II) and osmium (II) ions.

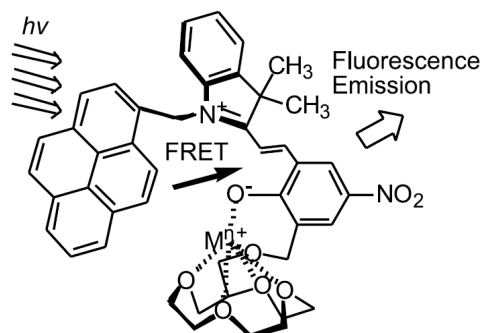
2.14). The authors assumed that in the initial state the charge and energy transfer is hindered due to a nonplanar structure of the spiropyran fragment; thus photoisomerization would resolve the problem as the MC state is planar. However, it was found that in such complexes the electron-withdrawing influence of the cations prevent the spiropyran fragment to isomerize upon irradiation.



There are reported studies on fluorescence of spiropyrans complexes with metal ions [9, 10, 12, 13, 18, 22-24, 28, 29, 55]. In general, the quantum yields of fluorescence in such systems are rather small. An alternative approach involving energy transfer (*via* FRET mechanism) between a spiropyran and a fluorophore, mixed in a solution or linked covalently, was explored. UV or visible light irradiation was used to control the fluorescence intensity in spiropyran **1** – bispyrene and compound **101** – anthracene mixtures in the presence of double- or triple-charged cations [56, 57]. Upon addition of cations or irradiation with UV light, the decrease in the fluorescence intensity was observed since the absorption band of the complexed MC form overlaps with the fluorescence band of the fluorophore. Irradiation with visible light led to the reverse effect. In the absence of cations irradiation does not affect the fluorescence intensity as the absorption band of the spiropyran open form is red shifted in comparison to that of the complex.

Covalently linked systems **69** and **102** were also reported [35, 58]. In the ground state, fluorescence quenching was observed due to photoinduced electron transfer (PET).



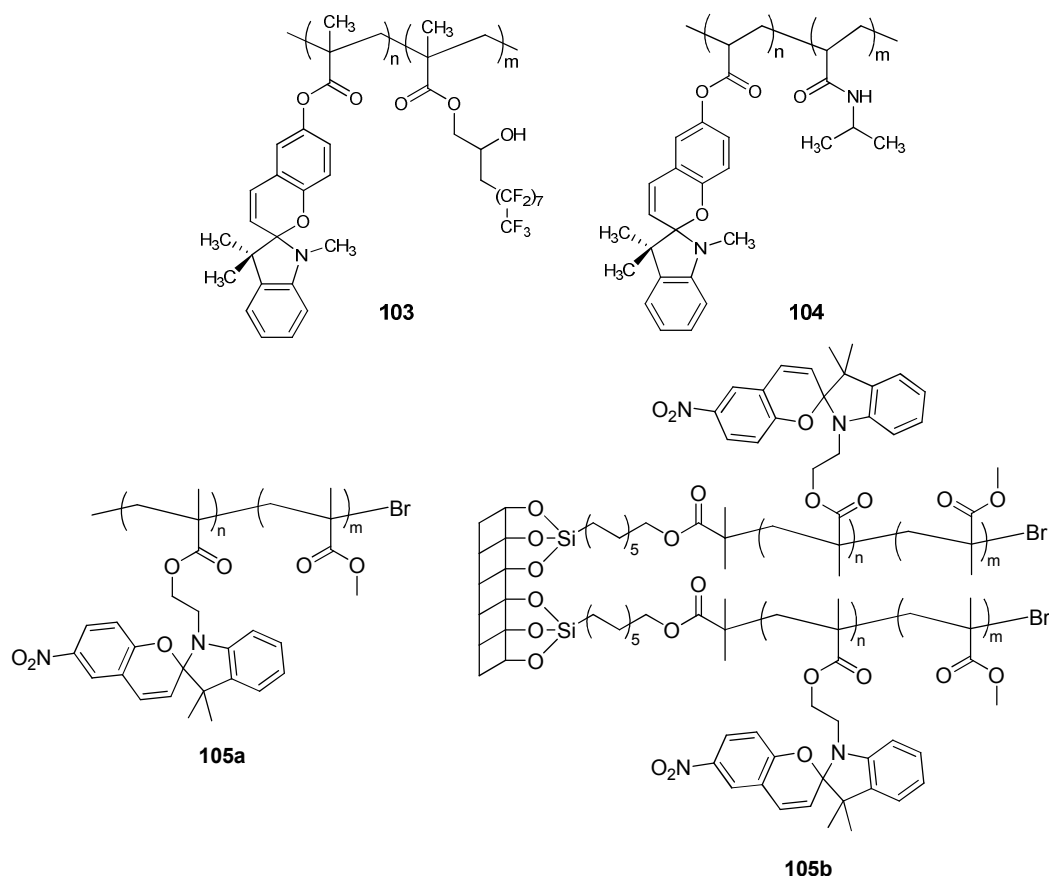


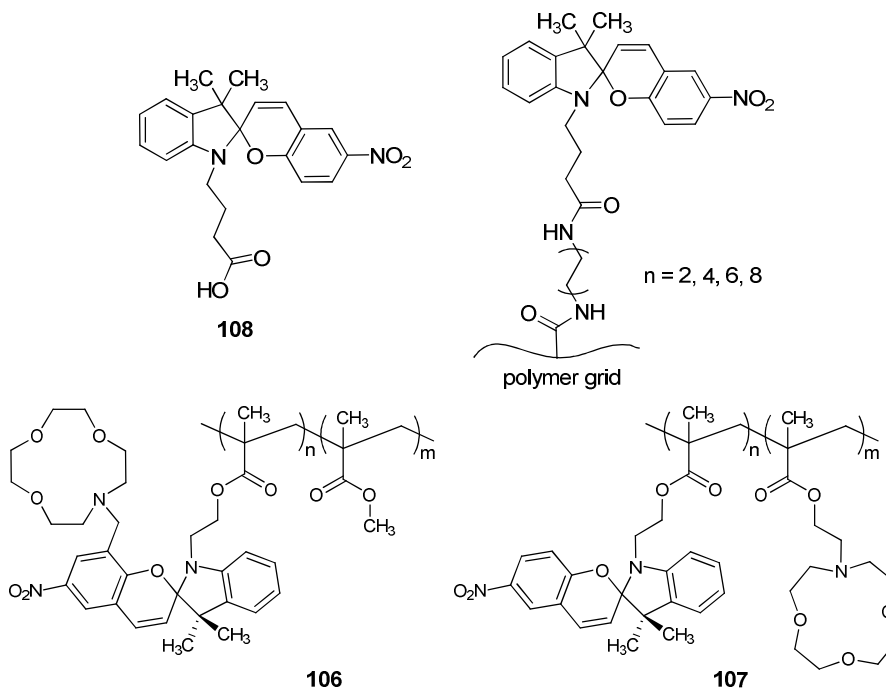
Scheme 2.15. Fluorescence quenching of compound **69** upon UV irradiation and in the presence of metal cations [35].

Upon irradiation and in the presence of metal ions, PET is blocked due to complex formation leading thus to fluorescence quenching. In case of compound **69** the authors reported that fluorescence of the MC form, originating from FRET between the fragments, was observed (Scheme 2.15). A mixture of the separated fragments, i.e. of spiropyran **68** and pyrene, demonstrated the same behavior [35].

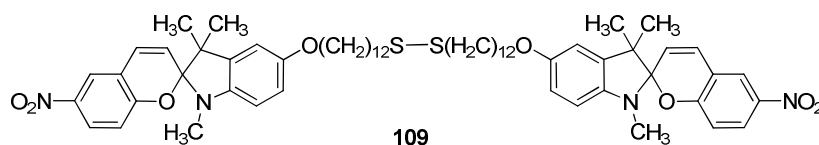
2.1.1.4. Polymer Compositions Containing Spiroyrans

Introducing photochromic fragments into polymer compositions affords materials suitable for practical use [59]. Employing the sensitivity of spiropyrans to the presence of metal cations, the polymers **103-105** were successfully tested for metal ion recognition or photo-reversible extraction [60-63]. To increase the stability of complexes, azacrown ether moieties were attached to polymers **106** and **107** [27].





A number of studies were devoted to spiropyran immobilized on a polymeric surface. Examples of spiropyran **108** fixed on polystyrene microbeads [64], polymethylmetacrylic films [65-67], or silicon surface [55] were described.



An alternative to polymers are self-assembling layers of spiropyran **109**, which are formed on the gold surface [68]. By means of UV or visible light irradiation, it was possible to control the electrode potential in solutions containing zinc (II) cations (Fig. 2.1).

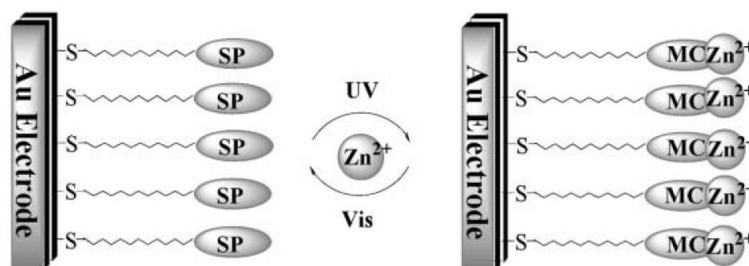


Figure 2.1. Using of spiropyran **109** to control the gold electrode potential by UV and visible light irradiation in the presence of zinc (II) cations [68].

2.1.2. Coordinations of Spiroyrans with Biomolecules

Several examples of photochromic systems sensible to a number of biological objects such as amino acids, proteins, and DNA were described. Spiroyrans **8**, **110-112** were proposed for amino acids recognition (Table 2.7) [69-71]. In all cases, the presence of the amino acid in solution led to the noticeable increase of the colored form stability as well as absorption maximum wavelength change. For better coordination and for selectivity reasons

as well, suitable substituents were attached to the molecules (Scheme 2.16). In case of compound **8**, the detection of cysteine and homocysteine was carried out in the presence of copper (II) or mercury (II) cations which gave rise to the amino acids dimerization followed by formation of the complexes comprising two spiropyran molecules and two cations for the sole dimeric (diCys) molecule (Scheme 2.16) [70]. Compounds **111**, **112** exhibited greater affinity to amino acids with relatively long carbon chain and also to tripeptide glutathione [71]. A significant disadvantage of the tested systems was their insolubility in water.

A selective binding with antibiotic vancomycin was demonstrated for spiropyran **113** [72]. The compound contains a specific D-Ala-D-Ala fragment responsible for the specific and selective interaction with the substrate. In control experiment isomeric spiropyran

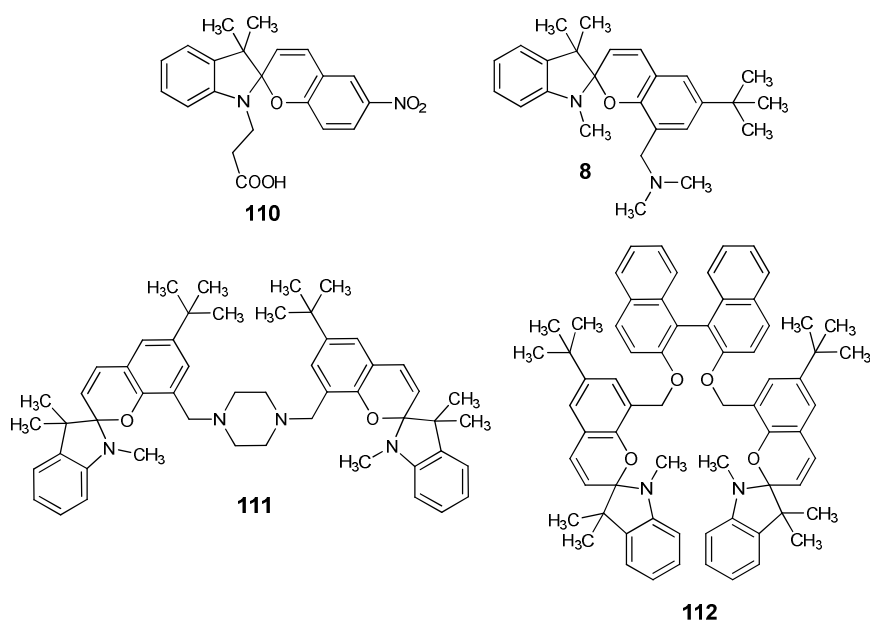
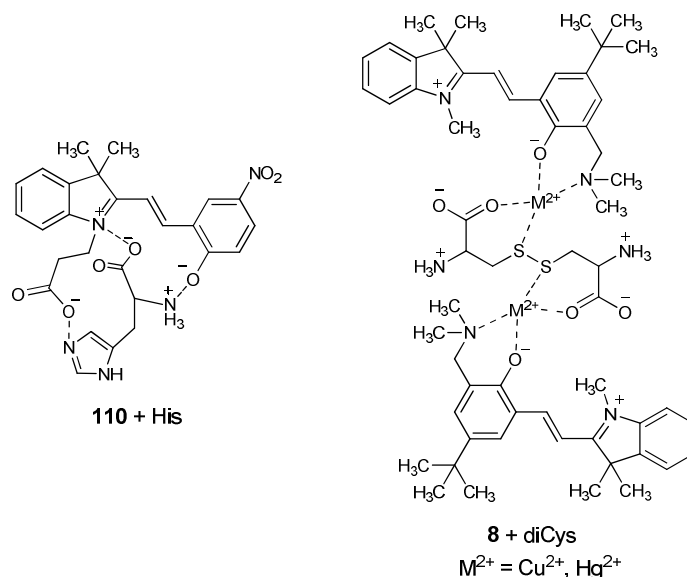


Table 2.7.

Tested spiropyrans and amino acids.

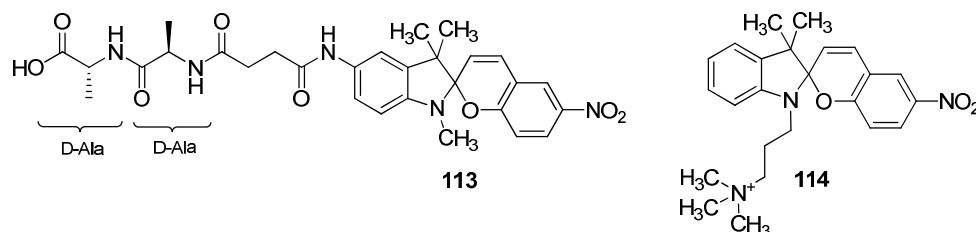
Spiropyran	Amino acid		Ref.
110	histidine (His)		[69]
	lysine (Lys)		
	arginine (Arg)		
8, 111, 112	cysteine (Cys)		[70, 71]
	homocysteine (Hcy)		
	glutamine (Glu)		



Scheme 2.16. Formation of complexes of spiropyran with amino acids.

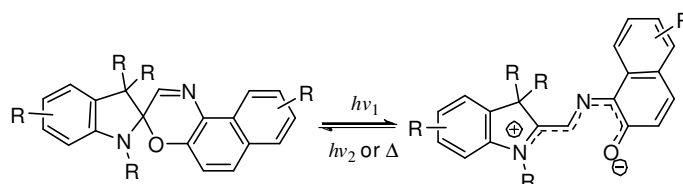
containing L-Ala-L-Ala fragment failed to bind to vancomycin. These results show the potential for developing specific photochromic tags for proteins.

Recently, spiropyran **114** was reported to participate in photo-induced DNA intercalation [73]. The initial bulk SP form prevent the molecule to bind strongly to DNA. Upon UV irradiation the planar MC isomer is formed which in turn is able to fit in between the base pairs of DNA. The reported stability constant ($\lg K \approx 4$) is within the average values for this type of interaction [74]. The photo-controlled intercalation provides development of new therapeutic agents for cancer treatment.



2.2. Systems Based on Spirooxazines

The number of publications devoted to complex formation involving spirooxazine molecules or fragments is approximately twice as less as that devoted to spiropyrans. Among them, the major part involves the naphthoxazine derivatives. Photo-induced forms of spironaphthoxazines are thermally unstable and transform back into the initial SP state over time (Scheme 2.17) [1-4]. Like the open forms of spiropyrans, those of spirooxazines may participate in the complex formation. Again, the greater number of reports describes complex formation with metal ions.

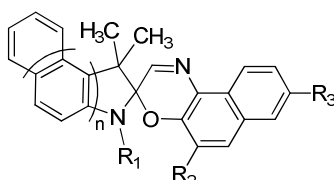


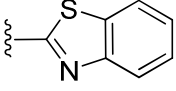
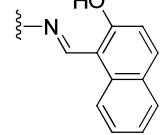
Scheme 2.17. Phototransformation of spirooxazines.

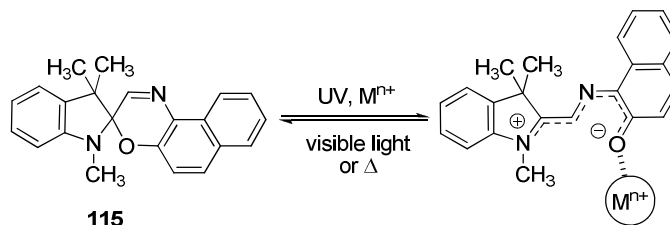
It was shown that unsubstituted spirooxazine **115** is sensitive to the presence of metal salts. Like in the case of spiropyrans, the decrease of the bleaching rate and the blue shift of the absorption maximum were observed (Scheme 2.18) [35, 75-78]. Introducing additional substituents able to coordinate with the cations led to a considerable increase of complex stability upon irradiation for compounds **116-125** (Table 2.8, Scheme 2.19).

Table 2.8.

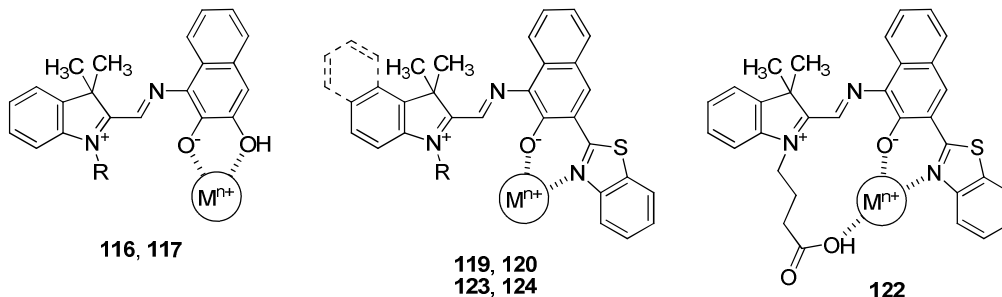
Spirooxazines with different substituents



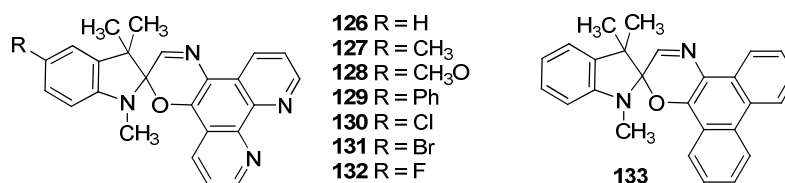
No.	n	R ₁	R ₂	R ₃	Ref.
116	0	CH ₃	OH	H	[78, 79]
117	0	C ₄ H ₉		H	
118	0	CH ₃		H	
119	0	CH ₃	COOH	H	[80, 81]
120	0	(CH ₂) ₃ CH ₃		H	
121	0	(CH ₂) ₃ COOCH ₃		H	
122	0	(CH ₂) ₃ COOH		H	
123	1	CH ₃		H	[80]
124	1	(CH ₂) ₃ CH ₃		H	
125	0	CH ₃		H	[82]



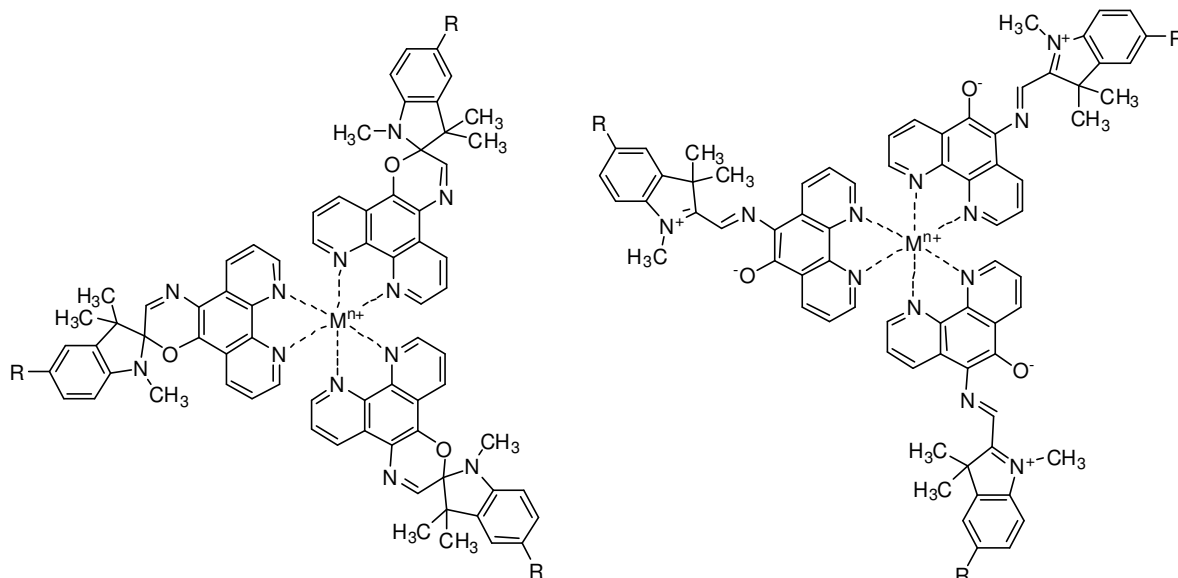
Scheme 2.18. Complex formation of the open form of compound **115** with metal cations.



Scheme 2.19. Additional coordination of substituents in some spirooxazines.

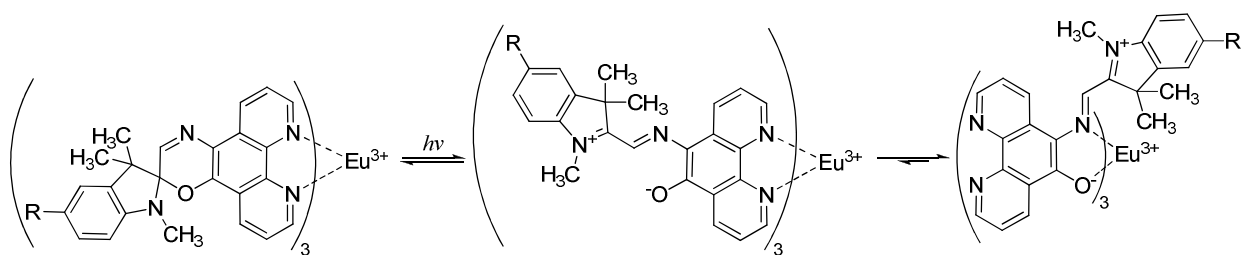


Spirooxazines **126-132** which contain fused phenanthroline fragment are also described [83-87]. These compounds are able to form complexes with the transition metal cations comprising three ligand molecules per one cation (Scheme 2.20). It is reported that the complexation noticeably affected the stability of the open forms upon UV irradiation, the bleaching being slowed down. At the same time, irradiating with visible light led to total decoloration of the solutions. The electron-donating groups were found to exhibit a stabilizing effect on the complexes, while the electron-withdrawing ones had the opposite influence.

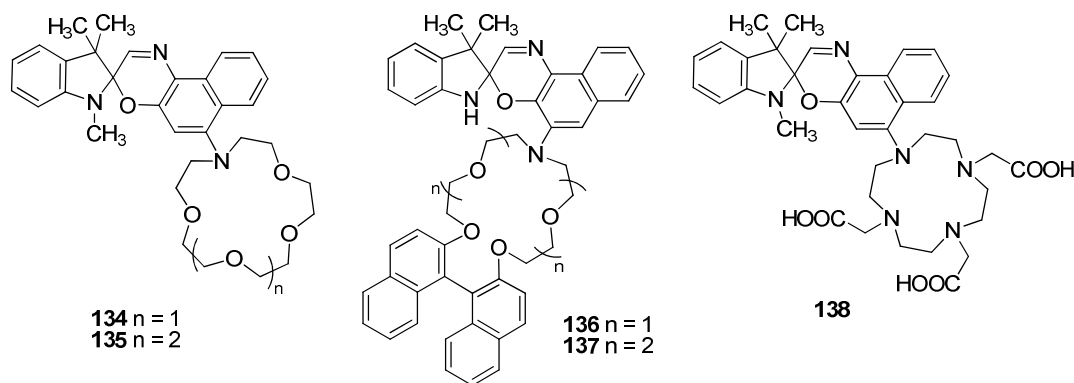


Scheme 2.20. Complexes of spirooxazines **126-132** with metal ions.

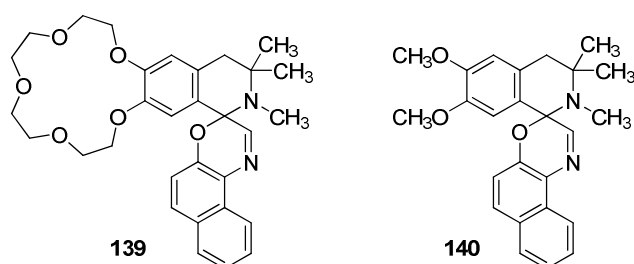
An interesting feature was detected in the mechanism of complex formation of compounds **126-128**, **132** and **133** with Eu^{3+} ions [86]. It was found that europium (III) ions form thermodynamically stable complexes with the open forms, in which the nitrogen atom of the former oxazine cycle coordinate with the metal ions.



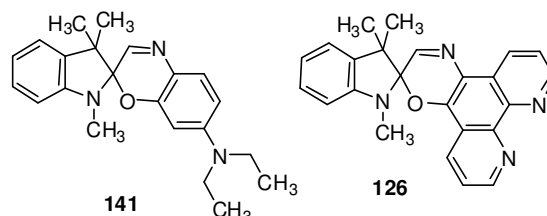
Scheme 2.21. Complex formation of the open forms of compounds **126-128** and **132** with europium (III) cations.



Spiro-naphthoxazines linked to a crown ether moiety are described. It is reported that, upon addition of the double-charged metal cations to compounds **134-137**, a spontaneous coloration was observed [33, 88]. The effect of different metals varied, yet coordination with both the crown ether and the oxygen atom of the open form was reported. Similarly to spiropyran **60**, spiro-naphthoxazine **138** was prepared and tested in the presence of Gd^{3+} as a contrast material in MRI [89]. The corresponding open form complex appeared to be thermally and photochemically stable. In addition, crown-containing spirooxazines **139**, **140** possessing dihydroisoquinoline fragment instead of indoline one were synthesized and investigated [90, 91].

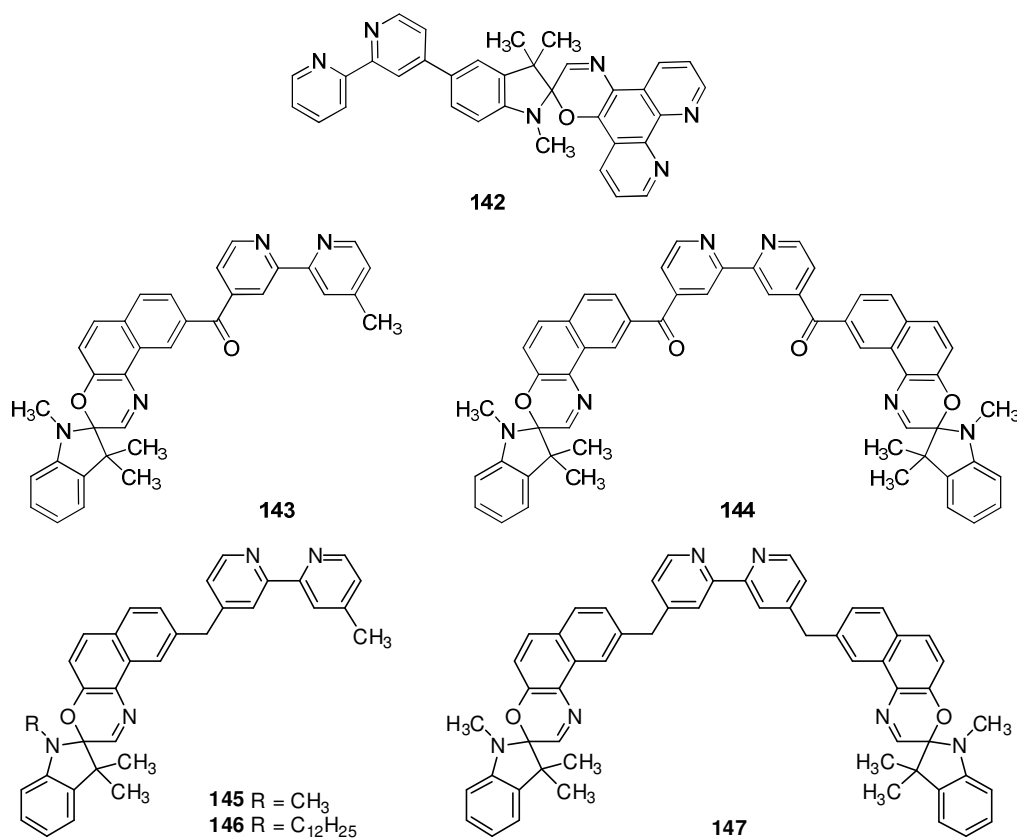


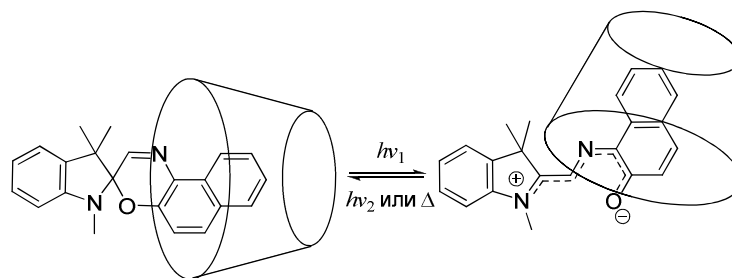
Several spirooxazines were explored for their ability to control the charge and energy transfers processes by photochromic transformations. Thus, compound **141** was found to transform into the MC state upon addition of Lewis acids (FeCl_3 , AlCl_3 , SnCl_4 ,



$\text{BF}_3\text{Et}_2\text{O}$, ZnCl_2) [92]. The colored isomers did not bleach even upon visible light irradiation, while the addition of a chelating agent (diethanolamine) led to the recovery of reversibility. The authors suggest that the strong interaction between a Lewis acid and electrons of the nitrogen atom of the amino group is responsible for the phenomenon. For compound **126**, a photo-control of the red-ox pair $\text{Co}^{2+}/\text{Co}^{3+}$ oxidation state was reported [87].

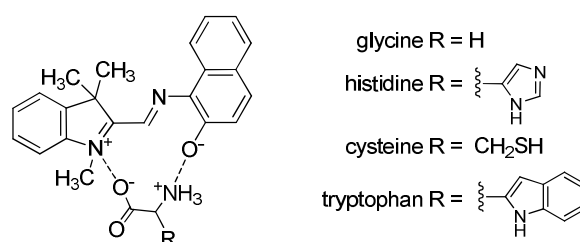
Similarly to spiropyrans **98-100**, compounds **142-147** were shown to control charge and energy transfer in the complexes with rhenium [93-95]. Still, the results were much similar to those of spiropyrans showing inhibition of the phototransformation.





Scheme 2.22. Noncovalent interaction of spirooxazine **115** and γ -cyclodextrine [97].

Less explored is the interaction of spirooxazines with uncharged molecules and biomolecules. Compound **148** is able to form assemblies with the $\text{Pd}(\text{PPh}_3)_2\text{Cl}_2$ catalyst [96]. These assemblies are stabilized due to π - π stacking between phenanthrene and triphenylphosphine fragments. Another example of noncovalent interaction with the uncharged particles is the spirooxazine **115** – γ -cyclodextrine system (Scheme 2.22) [97].

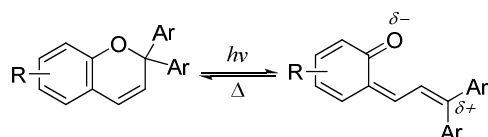


Scheme 2.23. Interaction of the open form of spirooxazine **115** with amino acids [98].

Also, compound **115** was tested for recognition of several amino acids (Scheme 2.23) [98]. Authors report that amino acids did not considerably change the spectral properties of the open forms, yet the stability of the MC isomers was increased.

2.3. Systems Based on Chromenes

In contrast with the spiropyrans and spirooxazines, chromenes (or benzopyrans) exhibit mostly thermal bleaching (Scheme 2.24) [1, 2, 5]. The studies of benzo- and naphthopyrans involved in the complex formation are poorly presented in literature. Most publications are devoted to the incorporation of a crown ether fragment into the naphthopyran molecules. Very few articles describe alternative coordinating functions.

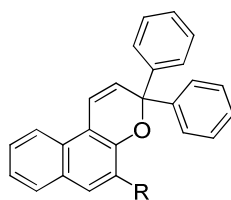


Scheme 2.24. Phototransformations of chromenes.

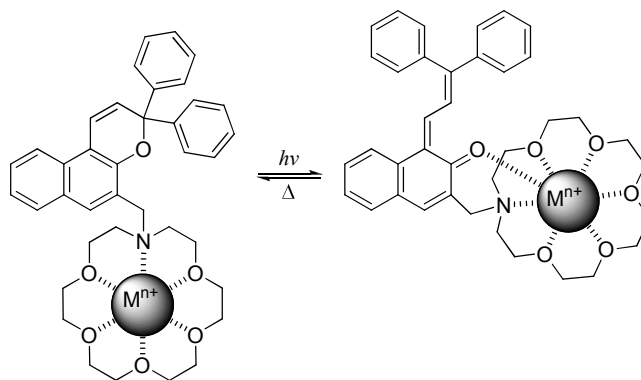
Naphthopyrans **149-156**, bearing different crown ether fragments, as well as model compounds **157-159**, containing podands or morpholine moieties, were studied (Table 2.9).

Table 2.9.

Crown-containing naphthopyrans.



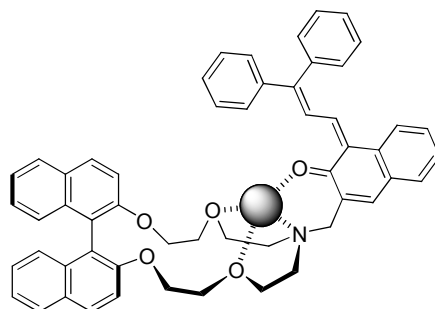
No.	R	n	Ref.
149		1	[99-102]
150		2	[99-102]
151		3	[99-102]
152		1	[103]
153		2	[103]
154		3	[103]
155		1	[33]
156		2	[33]
157		—	[103]
158		—	[103]
159		—	[99-101]



150

Scheme 2.25. Complex formation of chromenes containing a crown ether fragment with metal cations prior to and after irradiation (compound **150** is shown).

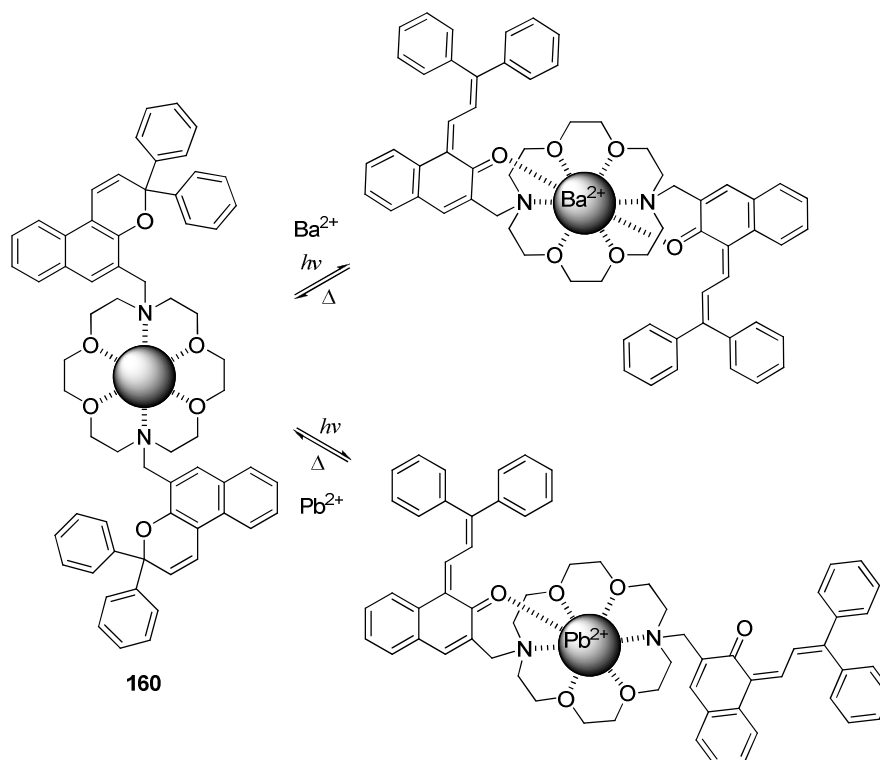
Addition of the cations led to spontaneous coloration of solutions in very rare cases. Upon irradiation and in the presence of metal ions, the absorption band of the open form was usually red shifted (up to 80 nm). In the model compounds **157-159**, these changes were frequently insignificant. Crowned chromenes are highly responsive to the presence of cations. In the complex, a cation binds to the crown ether fragment and, therefore, approaches to the carbonyl oxygen atom of the open form, thus stabilizing the latter due to coordination (Scheme 2.25) [99-102]. Chromenes **155**, **156** contain a bulky hydrophobic binaphthyl fragment that affects their ability to form complexes with the cations. Nevertheless, in the presence of the metal ions a red shift of the MC form absorption band was observed, confirming the carbonyl oxygen atom participation in coordination (Scheme 2.26) [33].



Scheme 2.26. Complex formation of the open form of naphthopyran **155**.

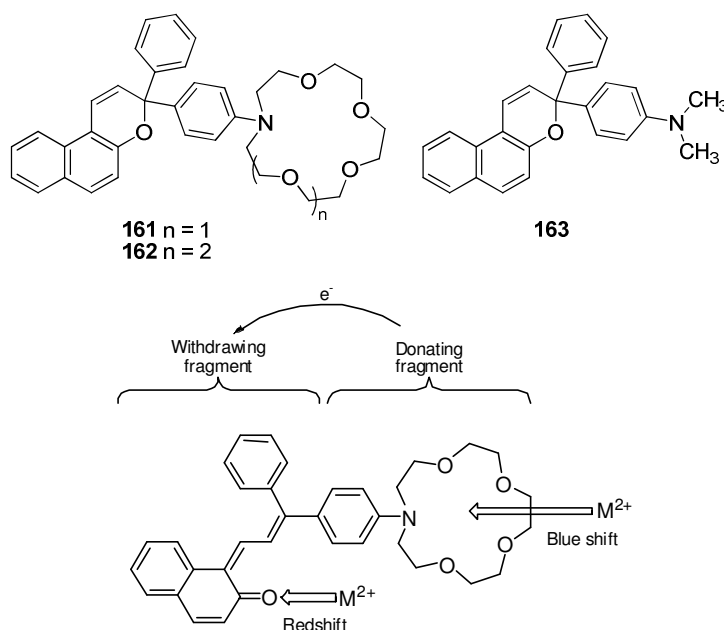
The formation of various structures of the open form complexes with divalent cations was suggested for bischromene **160** (Scheme 2.27) [99-101]. Obviously, the size and nature of the cations involved are of importance.

Chromenes **161**, **162** containing azacrown ethers in the phenyl ring, linked to the quaternary carbon atom of the pyran cycle, give another example of crown ether incorporation into the chromene molecule. The properties of these chromenes were compared with those of the model chromene **163**, containing the dimethylamino group [104-106]. Such structure suggests inclusion of a macrocycle into the chromophore system of the



Scheme 2.27. Complex formation of the open forms of chromene **160** with Ba^{2+} and Pb^{2+} .

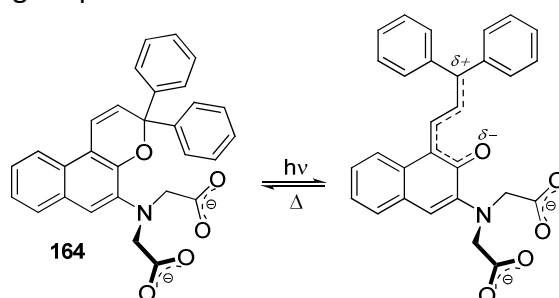
MC form and affords significant spectral changes upon complex formation. In this case, the open form of chromenes possesses two coordinating sites which coincide with electron-donating and electron-withdrawing fragments of the chromophore system. Thus, coordination with the carbonyl oxygen atom, which is the acceptor, increases its electron-withdrawing properties, leading to a red shift of the absorption band. When a complex is formed by the azacrown ether fragment, in which nitrogen atom is the donor, the metal cation reduces the electron-donating properties of the nitrogen atom and, as a result, a blue shift is observed (Scheme 2.28). This relationship was proven experimentally for compounds



Scheme 2.28. The effect of complex formation on spectral characteristics of the MC forms of chromene **161**.

161-163. Also, analysis of the bleaching rate changes upon addition of cations allowed determining the complex stability constants for the open forms which appeared to be lower than those for the closed ones.

The group of A. McCurdy et al. [107] suggested an alternative to a crown ether substituent able to form stable complexes with the metal cations (Scheme 2.29). Interaction of chromene **164** with alkaline-earth metal cations (Mg^{2+} , Ca^{2+} , and Sr^{2+}) was studied in the aqueous medium of various pH factor. Without irradiation, metal cations formed complexes of chromene to metal ratio equal to 1:1 and 2:1, the latter of which is more stable. Changes of the solution pH had a small effect on the complex stability. Remarkable is the ability of the compound to form stable complexes upon irradiation with the calcium cations, which are important for many biological processes.



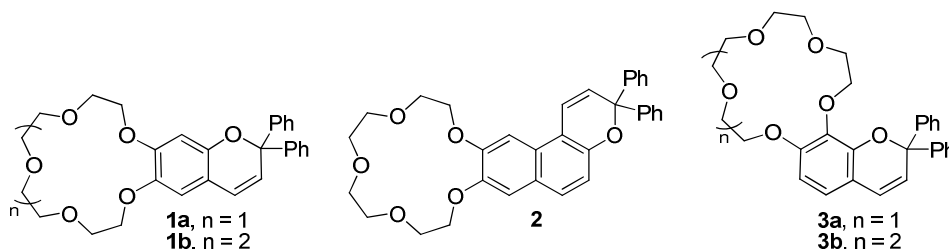
Scheme 2.29. Photochromic transformation of chromene **164** in the aqueous buffer. Deprotonated forms (pH 7.6 and 8.7) are shown.

Thus, by the present time, various complexons, containing spiropyran, spirooxazine, and chromene fragments, were synthesized and studied. Photochromic transformations significantly affect the complexing properties of such compounds. Comparing to the closed forms, the open isomers demonstrate higher stability constants of complexes with metal ions. In case of photochromes containing no coordinating sites, metal cations coordinate exclusively with the carbonyl oxygen atom of the open forms. The complex formation noticeably influences the photochromic properties of the ligands. Binding to various substrates causes considerable changes in the absorption spectra. For the thermoreversible systems, the transition of the MC form into the closed one in the complexes with metal ions is considerably slowed down.

Systems described in literature have various designs. However, the number of chromene derivatives is rather limited. Unfortunately, in the majority of works little attention is paid to the determination of quantitative characteristics of the complex formation. The studies of the coordination influence on the photochemical and photophysical properties of photochromes are frequently qualitative that significantly limits the evaluation of practical importance of the reported systems.

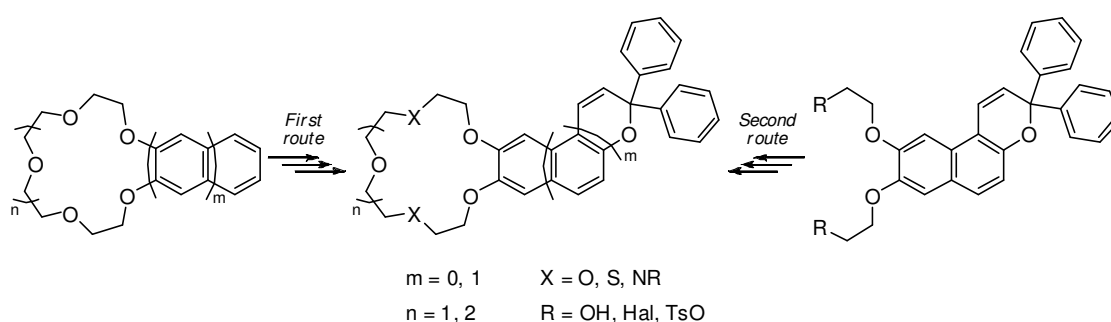
3. Results and Discussion

The use of the crown ether fragment as an additional functional group in the structure of photochromic compounds allows design of systems, in which photochromism and complex formation significantly affect each other. This is the basis for creation of systems with the photo-controlled complex formation or, *vice versa*, photochromic systems, which spectral and kinetic properties considerably depend on the presence of the metal cations (or other complexing agents). In the structure of the majority of crown-containing naphthopyrans, known in the literature, no macrocyclic fragment is included into the chromophore system of the photochrome, but bound to it *via* a bridge. However, the crown ether participation in the electron density redistribution upon photochromic transformations seems to be of the highest efficacy. Therefore, in this work, we chose chromenes containing annelated crown ether fragment as the target compounds. Since the investigation of mutual influence of photochromism and complex formation in the presence of metal cations and amino acids was of interest, primarily, the problem of synthesis of chromenes **1-3** fused with the 15-crown-5 and 18-crown-6 ether moieties was set as the target. There are no examples of such systems in the literature. Accordingly, the targets of the work included development of new synthetic approaches to benzo- and naphthopyrans, annelated to the crown ether fragments of different size and heteroatomic composition.



3.1. Synthesis of Benzo- and Naphthopyrans

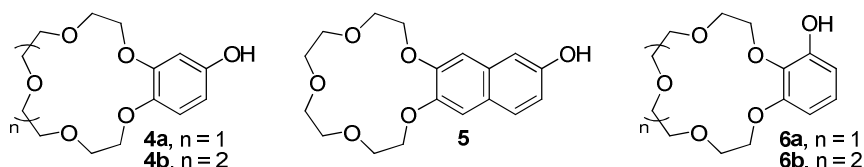
We developed two main approaches to the preparation of the target compounds with different synthetic direction (Scheme 3.1). The first, most obvious route consisted in the chromene fragment inclusion into the crown-containing aromatic substrate (benzo- or naphtho-15(18)-crown-5(6) ethers). In addition, we used an alternative synthetic route, which concluded, *vice versa*, in the crown ether fragment construction over the photochromic molecule. Though the second approach involved greater number of stages, it afforded naphthopyrans containing the crown ether fragments of different size and heteroatomic composition.



Scheme 3.1. Approaches to synthesis of the target benzo- and naphthopyrans.

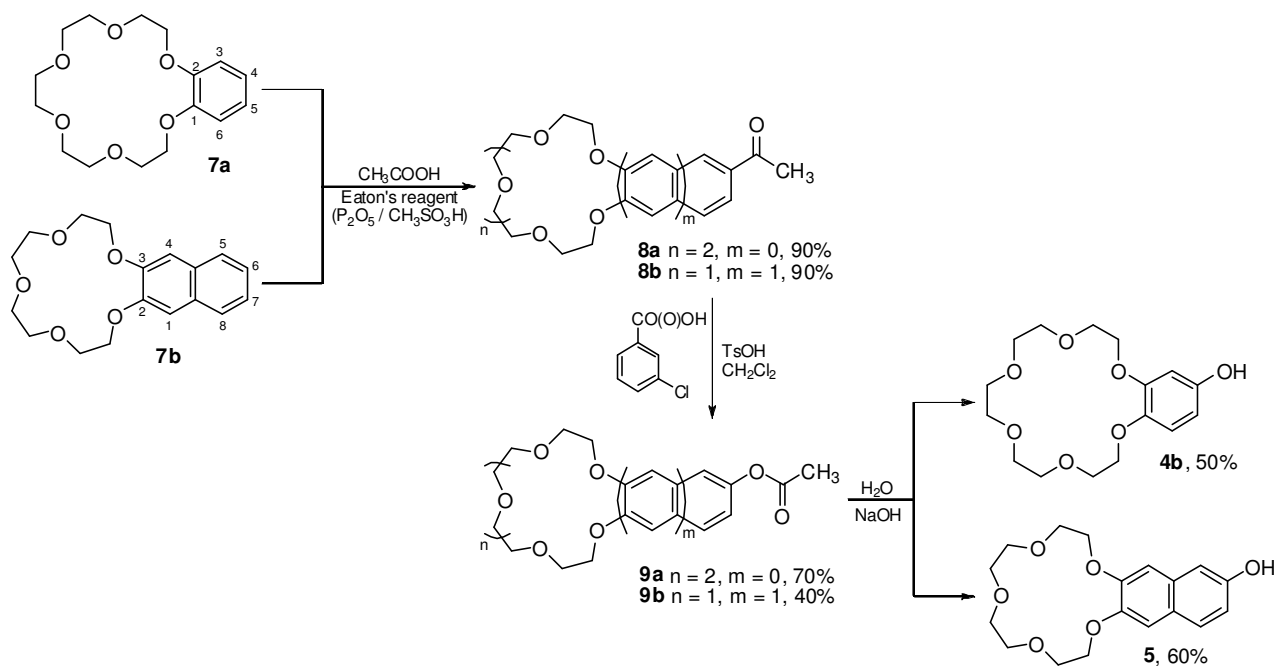
3.1.1. Synthesis of Crown-Containing Benzo- and Naphthopyrans from Phenols and β -Naphthol Annelated by Crown Ether

There are many known approaches to preparation of chromenes [1, 5]. However, the synthesis of chromenes from phenols or naphthols is the most widespread and accessible. At the first stage of the work, we concentrated on the developing of new or modernizing of existing methods for phenols **4-6**, containing the annelated crown ether fragment, preparation.



The approaches towards the synthesis of phenols **4**, **6** are known [108-113]; naphthol **5** is not described. With respect to the hydroxyl group position in relation to the crown ether fragment, two methods were employed.

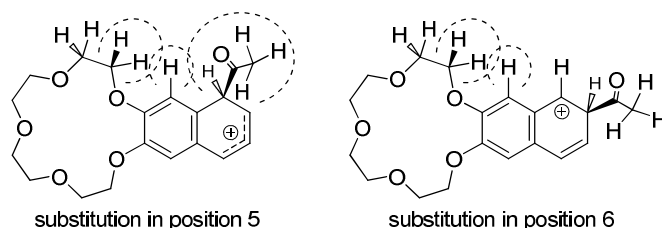
The first method consisted in hydroxyl group incorporation into the initial benzocrown ether (Scheme 3.2) [108-110]. It was applied by Dr. A.Chebunkova [114] in the



Scheme 3.2. Crowned phenol and naphthol synthesis from appropriate benzo- and naphthocrown ethers.

synthesis of phenol **4a**, but for the synthesis of **4b** and **5** some modifications were suggested, which increased the products yields. The synthesis included three stages: (i) acylation by the Eaton's reagent, (ii) Baeyer-Villiger oxidation, and (iii) hydrolysis. The yield-defining stage for the whole scheme was the oxidation, since it produced the greatest number of side products and was characterized by incomplete reaction proceeding.

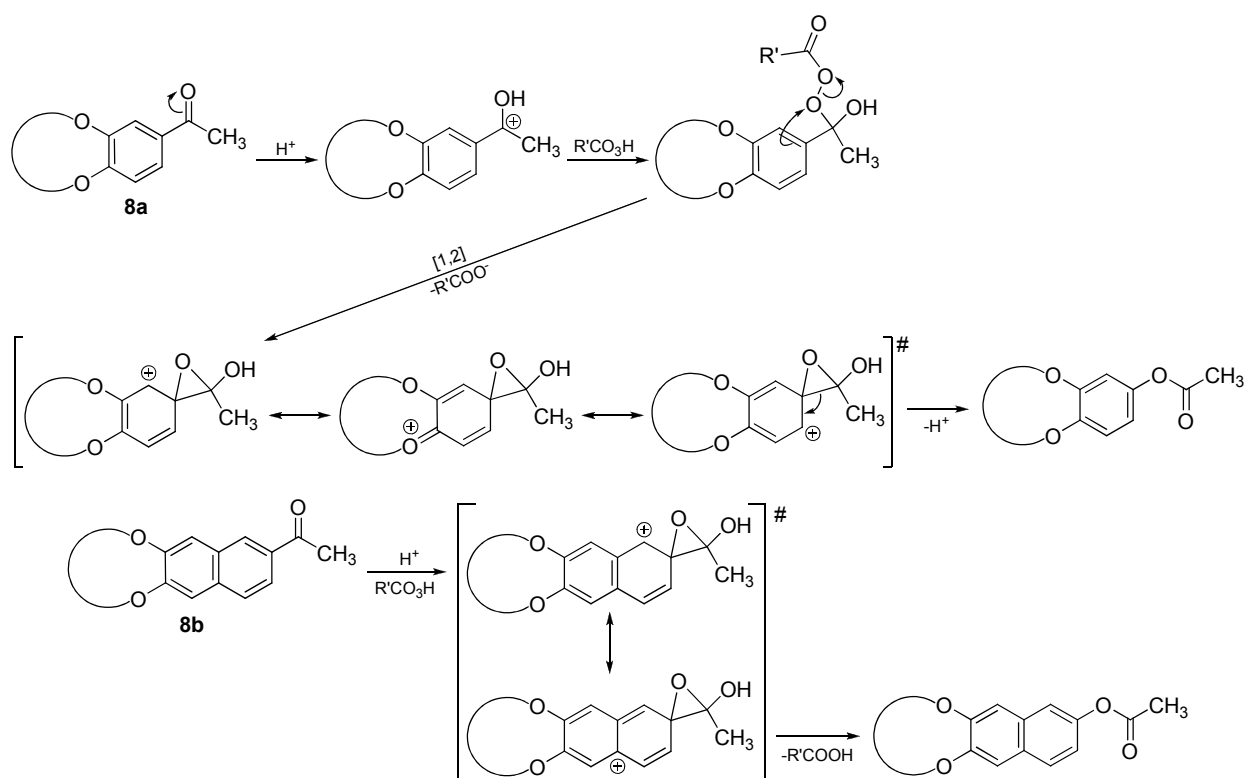
Benzo-18-crown-6 (**7a**) and naphtho-15-crown-5 (**7b**) ethers were acylated by acetic acid in the presence of the Eaton's reagent. The precursor **7a** is commercially available; crowned naphthalene **7b** was provided by A.V.Bogatsky Physicochemical Institute (Ukraine). The Eaton's reagent represents a solution of phosphorus oxide (V) in methanesulfonic acid. In the beginning of the work, a fresh solution containing phosphorus oxide (V) and methanesulfonic acid in the molar ratio of 1:10 (13% solution, approximately) was used. Later a commercial Eaton's reagent containing 7.5% of the oxide was used that resulted in a slight increase of the yield. In this reaction, the acylating agent is mixed acetic and methanesulfonic acids anhydride formed *in situ* [115]. The reaction proceeds during 6 hours at room temperature. As a result, 4- and 6-substituted derivatives of benzo-18-crown-6 and naphtho-15-crown-5 ethers, respectively, were prepared in good yields. On the one hand, the crown ether electron-donating character favored the reaction. On the other hand, the presence of the bulky macrocyclic fragment hindered acylating agent access to positions 3, 6 in benzocrown ether and positions 1, 4, 5, 8 in naphthocrown ether that provided high selectivity of the reactions. Substitution in position 6 in compound **7b** was probably promoted by the formation of the corresponding σ -complex, which was more stable than



Scheme 3.3. Spatial interaction of substituents in σ -complexes formed in course of naphthocrown ether **7b** acylation.

the one resulted from the acylating agent attack into position 5. The latter structure must be less stable as the acyl group is sterically affected by hydrogen atom in position 4, the influence being intensified due to close location of the methylene groups of the crown ether (Scheme 3.3).

The next stage of the synthesis was Baeyer-Villiger oxidation (rearrangement) consisting in the treatment of ketones with peroxyacids in the presence of acid catalysts. This reaction is widely applied to synthesis of esters and lactones by the mechanism of oxygen atom "insertion" [116]. Primarily, freshly prepared peroxyacetic acid, prepared by mixing glacial CH_3COOH with 35% H_2O_2 solution in the presence of H_2SO_4 , was used [108, 114]. However, since the control of the peracid concentration is difficult due to its instability, the use of commercially available *m*-chloroperoxybenzoic acid representing a solid with 25-30% water content was found preferable. For example, ester **9b** yields were 4 and 40% when using $\text{CH}_3\text{CO}(\text{O})\text{OH}$ and *m*- $\text{ClC}_6\text{H}_4\text{CO}(\text{O})\text{OH}$, respectively. Therefore, in further work peroxyacetic acid was not employed.



Scheme 3.4. Mechanism of the Baeyer-Villiger oxidation (rearrangement) of ketones **8**.

In the case of benzocrown ether derivative **9a**, the reaction yields were much higher. Such difference may result from a better stabilization of the positively charged transition state in the benzene derivative compared with the naphthalene one (Scheme 3.4). In this reaction, the intermediate structure resembles the σ -complex that forms in electrophilic substitution of benzene or naphthalene derivatives.

Nevertheless, the method using *m*-chloroperoxybenzoic acid has disadvantages, too. In all cases, product purification was complicated by the presence of the initial ketones. As products and initial compounds are structurally similar, separation of their mixtures was rather complicated. However, it was found experimentally that the initial ketones are better soluble in 96% ethanol, which was used for purification.

Incomplete reaction proceeding was apparently associated with relative instability of peroxybenzoic acid at room temperature. To optimize synthesis, the quantity of reagents and reaction time were varied. Nevertheless, a considerable improvement of yields failed. Moreover, increased amount of oxidant induced formation of larger quantity of yellow side products, specifically in the case of naphthalene derivative. For instance, NMR spectra of the reaction mixture indicated the presence of naphthoquinones **10** (Fig. 3.1). Conclusions about

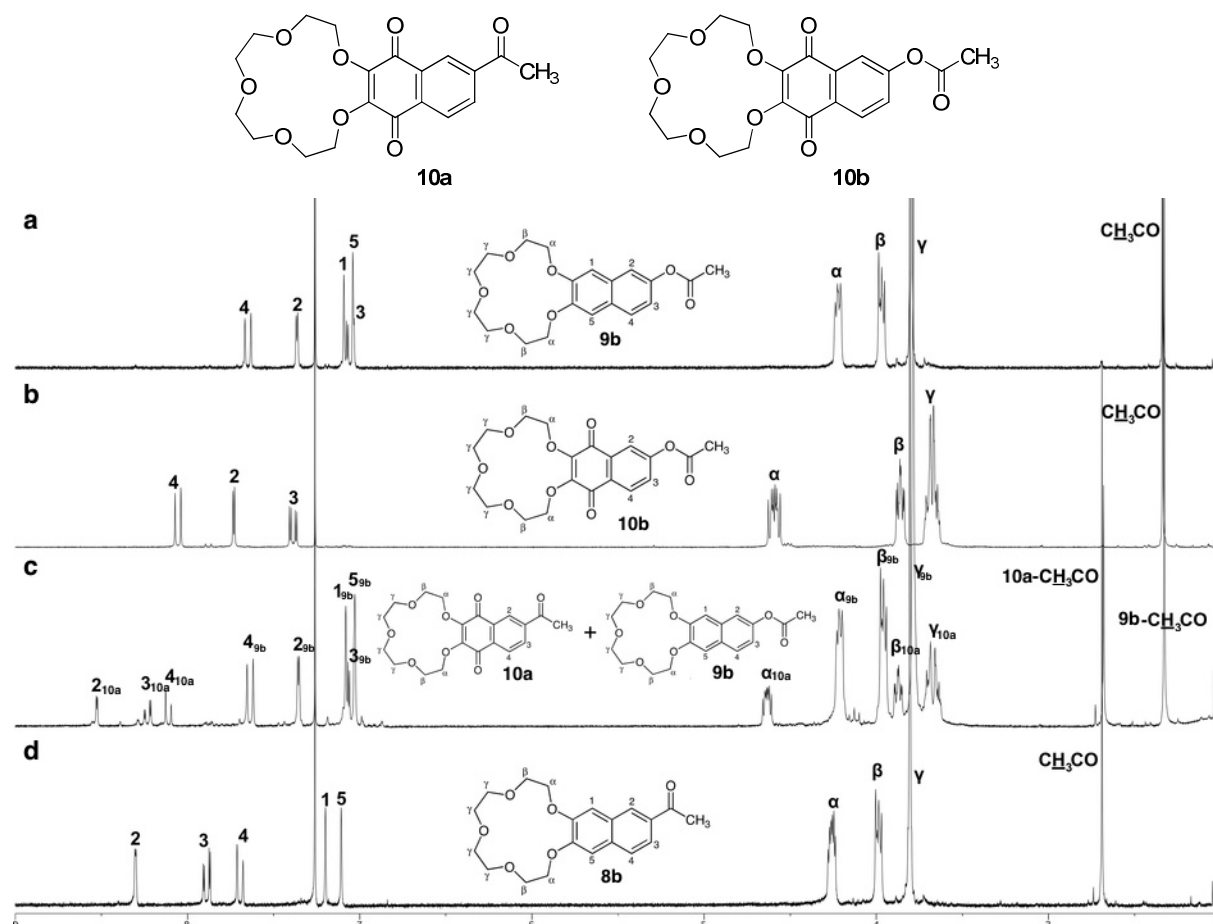


Figure 3.1. ^1H NMR spectra of oxidation reaction reagents and products: a) product **9b** of Baeyer-Villiger rearrangement; b) ester oxidation product **9b** (naphthoquinone **10b**); c) ester **9b** and ketone **8b** oxidation product (naphthoquinone **10a**) mixture; d) initial ketone **8b**.

the structure of the compounds were made on the basis of similarity in the NMR spectra for the initial ketone **8b** and ester **9b**, as well as specific location of methylene protons signals of the crown ether fragment and the number of aromatic hydrogen signals. Methyl group proton signals are typical for both cases. In the carbonylated structure they are characterized by the chemical shift of 2.69-2.70 ppm (Fig. 3.1c, d). In the ester group, the methyl proton signals are shifted upfield to 2.33-2.34 ppm (Fig. 3.1a-c). The quinone fragment proximity to the crown ether part promotes a noticeable downfield shift of the methylene proton signals due to the anisotropic effect of the two carbonyls (Fig. 3.1b, c). The resonances of the aromatic protons are also typical.

The final stage of the synthesis was the basic hydrolysis of the esters that produced phenol **4b** and naphthol **5** in moderate yields. Such yields are mostly caused by the ability of the crown ether derivatives to bind the metal cations in the aqueous medium with the formation of stable complexes. Free phenols were extracted by organic solvents. In the case of naphthol **5**, washing of the aqueous solution with dichloromethane was sufficient. However, 18-crown-6-phenol **4b** extraction by hot CH_2Cl_2 was carried out continuously during 24 h.

The structure of naphthol **5** was proved by X-ray structural analysis (Fig. 3.2). The crystal includes water molecules, which participate in hydrogen bonds formation. Each H_2O molecule is located in the crown ether cavity. In addition, water forms a hydrogen bond with hydroxyl hydrogen atom. Thus, the crystal consists of several infinite spirals formed due to head-to-tail naphthol and water molecules disposition.

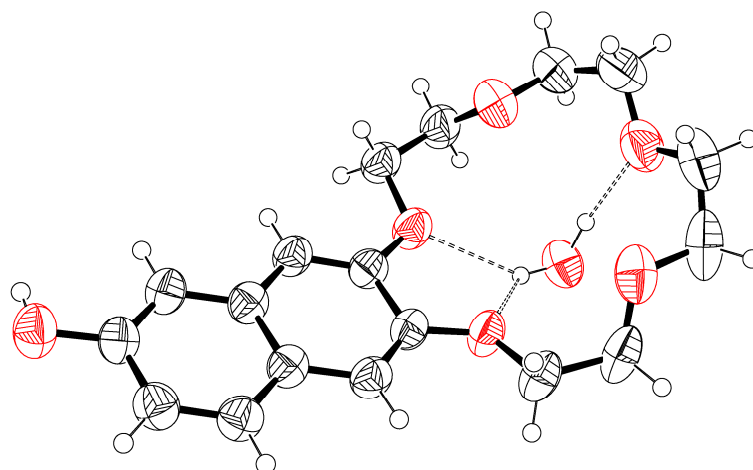
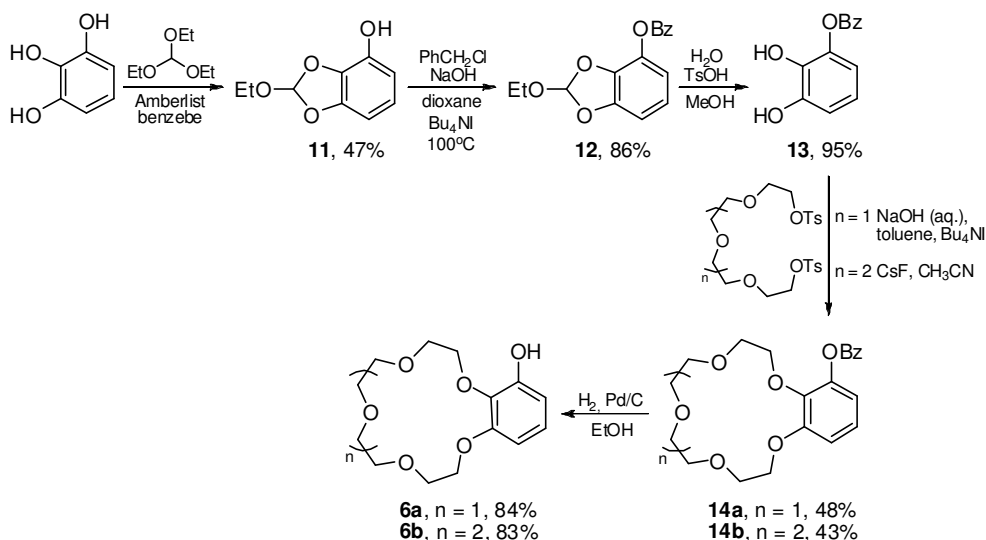


Figure 3.2. X-ray analysis data of naphthol **5**. A water molecule is located in the crown ether cavity.

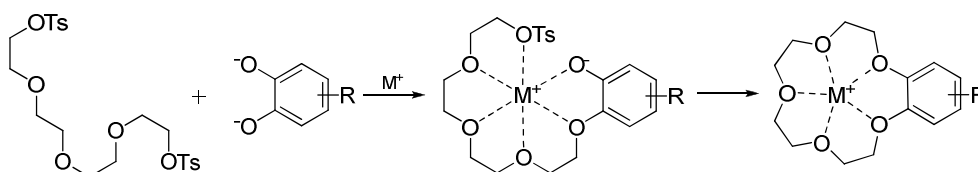
The phenols with vicinal disposition of the hydroxyl group and the crown ether fragment were prepared using another synthetic method, which included several alternating stages of protective groups incorporating into and removing from starting pyrogallol (Scheme 3.5) [111-113].



Scheme 3.5. Synthesis of crowned phenols by incorporating a macrocyclic fragment into pyrogallol molecule.

At the first stage, protection of two vicinal hydroxyl groups of pyrogallol, transforming it into an acetal derivative by the interaction with ortho-formiate in the presence of ion-exchange resin Amberlist 15, was used. Further on, phenol **11** was transformed in high yield to the corresponding benzyl derivative. The use of acetal (formyl) and benzyl groups allowed selective protection of hydroxyl groups in pyrogallol, because these protective groups have different stability. For example, under acidic conditions compound **12** was transformed to dihydroxy derivative **13** in nearly quantitative yield, the benzyl group being not involved. This enabled successful incorporation of the crown ether fragment by the two free hydroxyl groups, using appropriate oligoethyleneglycol ditosylate. 15-Crown-5 ether derivative **14a** was obtained employing NaOH as the base; the reaction was performed in toluene-water mixture with interphase catalysis [113]. In the case of 18-crown-6 ether (**14b**), the reaction was carried out in acetonitrile in the presence of CsF [112].

Beside high dilution, for crown ether synthesis the base selection is of importance, because metal cation is able to form a complex with the podand (oligoethyleneglycol), participating in the reaction, which promotes reagents pre-organization for the target product formation (the so-called template effect) (Scheme 3.6). Hence, the better correspondence of the podand (and crown ether formed) size to the cation diameter is, the higher the product yield is [117]. The only negative consequence of such effect is high stability of complexes, due to which, in some cases, difficulties of free ligand extraction may



Scheme 3.6. The template effect in crown ether synthesis.

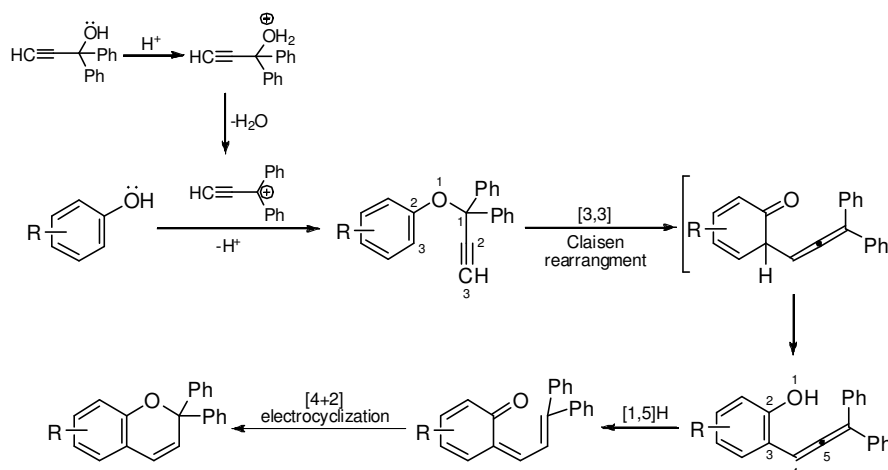
occur. Thus compromise conditions were chosen, which provided moderate yields and non-laborious product extraction.

The final stage was selective removal of the benzyl protection by hydrogen in ethanol in the presence of Pd/C. Mixture exposure at room temperature for several days gave high yields of target phenols **6**.

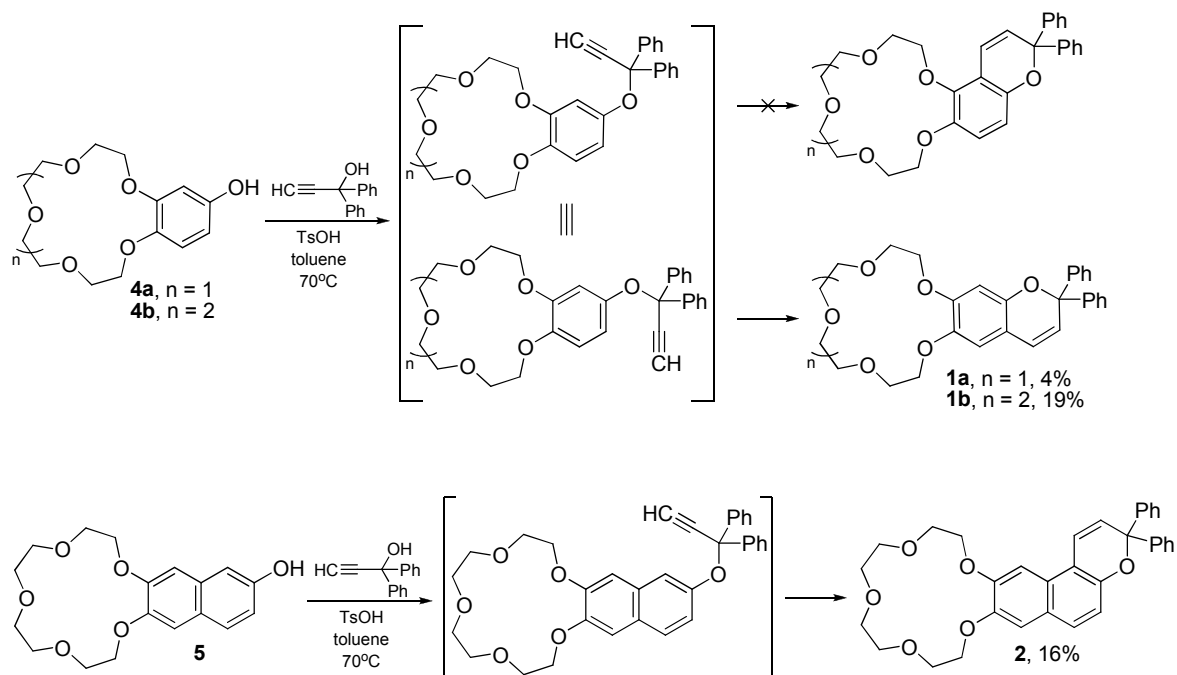
The target chromenes were prepared by two methods. The first method consisted in phenols interaction with diphenylpropargyl alcohol in the presence of an acid. This is one of the most frequently used approaches, which allows obtaining of chromenes in moderate to good yields [1, 5, 118-120]. According to the second method, photochromes were produced by phenols interaction with β -phenylcinnamaldehyde in the presence of titanium (IV) ethylate [119, 121-124]. Primarily, this approach was developed for the synthesis of chromenes containing heterocyclic (generally, nitrogen-containing) fragments and was rarely applied to the synthesis of carbocyclic chromenes.

The interaction of phenols with propargyl alcohol is catalyzed by acids and proceeds sequentially *via* *O*-alkylation, Claisen rearrangement ([3, 3] sigmatropic shift), [1, 5] sigmatropic hydrogen shift, and electrocyclization (Scheme 3.7) [119, 120]. *In situ* formation of arylpropargyl ether which enters the further Claisen rearrangement is the stage defining successful proceeding of the reaction.

Therefore, for phenols **4** the formation of two products is possible, namely: linear and angular chromenes (Scheme 3.8). In case of the angular isomer, however, the formation of the appropriate transition state is spatially hindered, which is associated with proximity of the crown ether fragment. As a result, linear isomers **1** in 4% ($n = 1$) (according to [114]) and 19% ($n = 2$) yield were obtained exclusively. Naphthol **5** afforded angular naphthopyran **2** in 16% yield.



Scheme 3.7. The mechanism of chromenes formation from phenols and diphenylpropargyl alcohol.

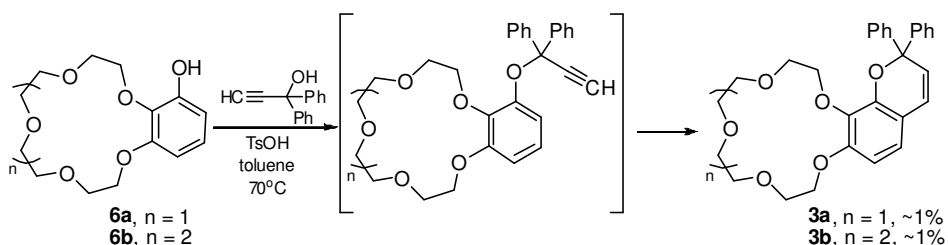


Scheme 3.8. Chromenes formation from phenols **1** and naphthol **2**.

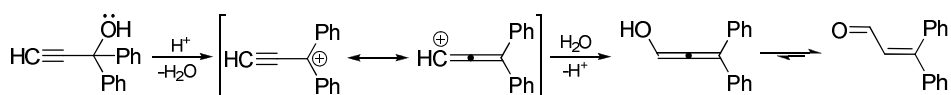
The vicinal position of hydroxyl group in phenols **6** unambiguously testifies about practical impossibility of obtaining appropriate chromenes with the help of this method (Scheme 3.9). Close location of the crown ether induces high spatial hindrances to propargyl ether formation. Preparation of chromenes **3** in satisfactory yields by this method failed.

This method has several essential disadvantages, primarily, due to side reactions. Acid presence in the reaction mixture makes possible transformation of propargyl alcohol to β -phenylcinnamaldehyde by the Meyer-Schuster rearrangement mechanism (Scheme 3.10) [125]. Thus, the alcohol amount is being reduced during the reaction that affects arylpropargyl ether formation.

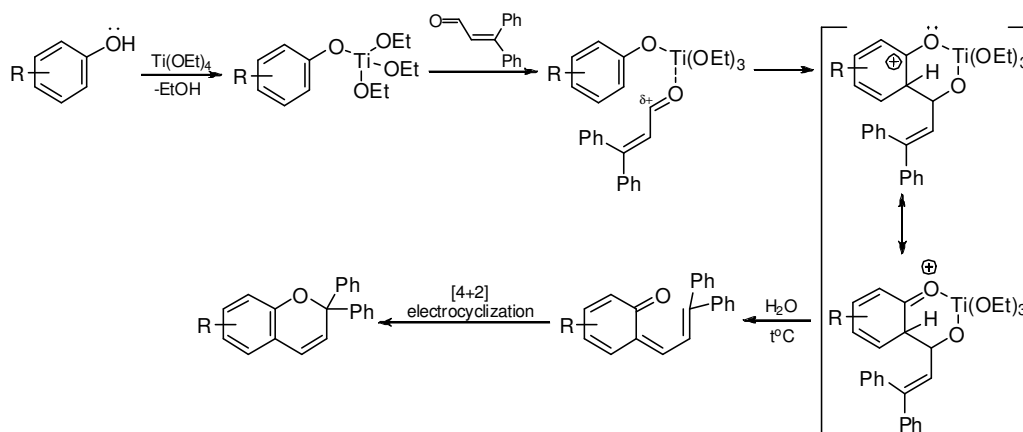
Another disadvantage of the method for the crown-containing systems was hydrolysis-induced partial degradation of the macrocyclic fragment. This caused formation of many products containing aliphatic residues of various lengths. It seemed rather difficult to



Scheme 3.9. The mechanism of angular chromenes **3** formation from phenols **6**.



Scheme 3.10. Mechanism of the Meyer-Schuster rearrangement.



Scheme 3.11. The mechanism of chromenes formation by phenols interaction with β -phenylcinnamaldehyde in the presence of $\text{Ti}(\text{OEt})_4$.

separate this mixture with the help of the column chromatography, because the R_f values were close, and NMR spectrum of the product was always characterized by the presence of alien proton peaks in the aliphatic part.

Therefore, the chromenes were synthesized by the method using β -phenylcinnamaldehyde in the presence of titanium tetraethoxide. In contrast with the first approach, the mechanism of this reaction includes no sequential pericyclic rearrangements and includes the stages of titanium (IV) ethylate attachment to hydroxyl oxygen atom, electrophilic substitution in the aromatic system, hydrolytic decomposition of a complex of the phenol with titanium, thermal dehydration, and electrocyclic leading to chromene formation (Scheme 3.11) [119, 121]. Application of the method allowed to prepare all the target chromenes in satisfactory yields that exceeded corresponding yields of the first method (Scheme 3.12). Moreover, extraction and purification of the products appeared less laborious.

In the case of phenols **4**, the linear chromenes were formed. No angular isomers were found in the reaction mixture that, apparently, is due to the spatial hindrance within the intermediate products (Scheme 3.12). In the reaction with naphthol **5**, the exclusive

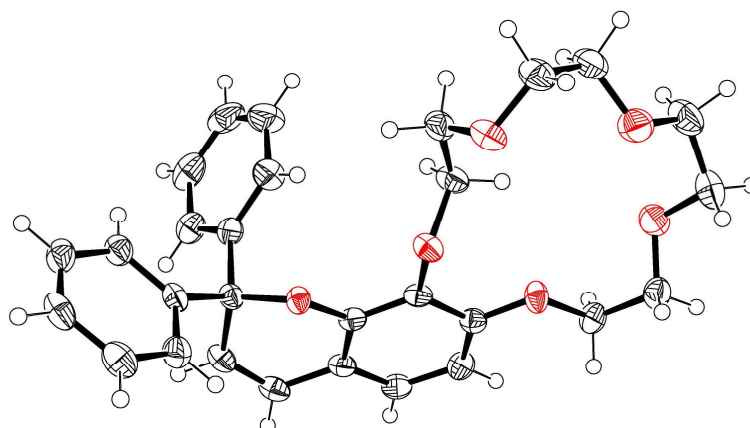
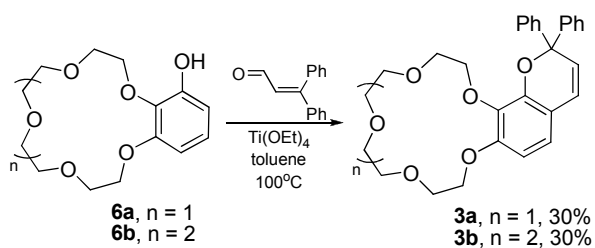
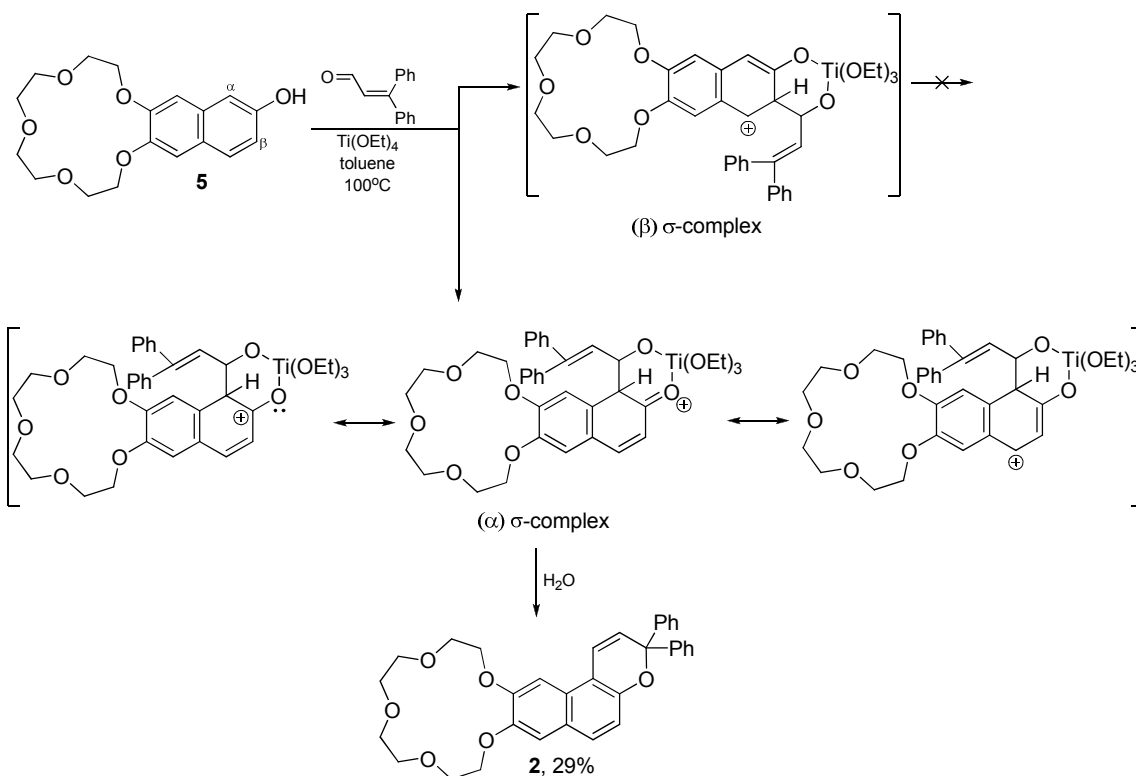
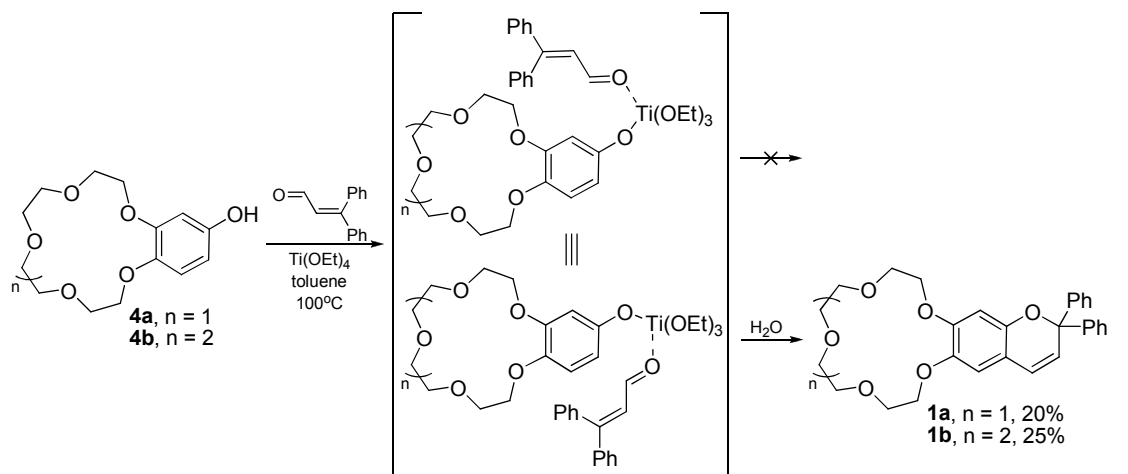
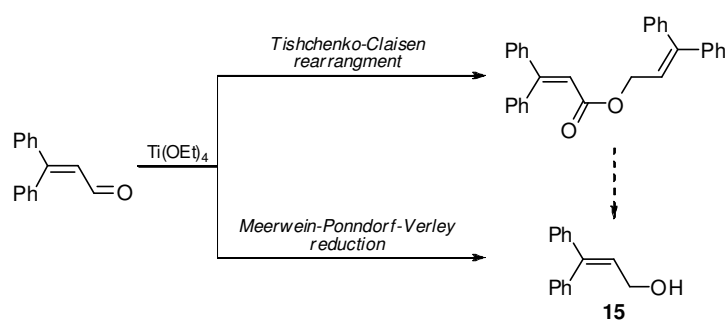


Figure 3.3. X-ray analysis data of chromene **3a**.



Scheme 3.12. Chromenes **1-3** formation by phenols **4-6** interaction with β -phenylcinnamaldehyde in the presence of $Ti(OEt)_4$.



Scheme 3.13. Side reactions with β -phenylcinnamaldehyde participation.

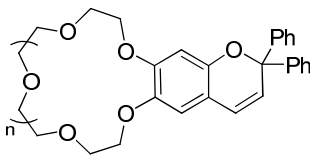
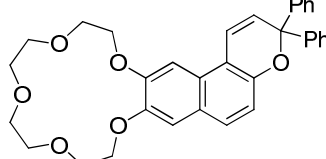
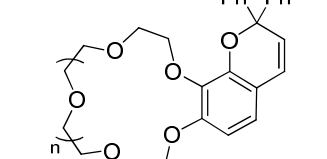
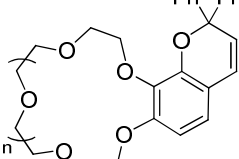
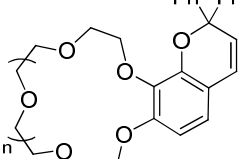
angular isomer **2** was formed that, apparently, was associated with the σ -complex stabilization in course of the electrophilic substitution stage (in α and β positions, Scheme 3.12). Chromenes **3** were prepared in moderate yields. Structure **3b** was also proved by X-ray analysis (Fig. 3.3).

We attempted to optimize the yields by varying the reaction conditions and the quantity of reagents. However, no noticeable improvement was achieved. The reaction has some disadvantages, which are, first of all, formation of multiple side products, most frequently of intense yellow color. In this case, however, admixtures may be successfully eliminated by chromatography. More substantial disadvantage is the possibility of aldehyde participation in the Tishchenko-Claisen rearrangement and the Meerwein-Ponndorf-Verley reduction with the participation of titanium tetraethoxide, which was proved by alcohol **15** separation from the reaction mixture (Scheme 3.13). This, in turn, limits variability of the conditions.

Thus, target chromenes **1-3** were synthesized by two alternative methods. Alongside with less laborious procedure of products extraction, the yields in the second method were found generally higher (Table 3.1). Both methods have disadvantages; however, in the case of chosen chromenes, annelated by crown ether fragments, the method applying β -phenylcinnamaldehyde is preferable and sometimes the only effective one (chromenes **3**). Therefore, in further work this approach was used for chromene syntheses.

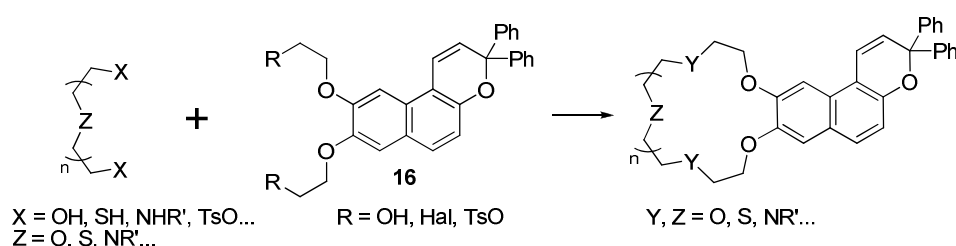
Table 3.1.

Chromene yields in two methods.

					
	1a n = 1	1b n = 2	2	3a n = 1	3b n = 2
<i>Method 1</i>	4% [114]	19%	16%	~1%	~1%
<i>Method 2</i>	20%	25%	29%	30%	30%

3.1.2. Synthesis of Naphthopyrans Annelated to the Crown Ether Fragments of Various Size and Heteroatomic Composition

For preparation of naphthopyrans, annelated to the crown ether fragments of different size and heteroatomic composition, we used an alternative synthetic approach based on introducing of a macrocyclic fragment into the naphthopyran molecule (Scheme 3.14). Chromenes **16**, containing various terminal groups in the aliphatic fragments, were suggested as the precursors. Derivatives with the hydroxy, chlorine, and iodine groups are necessary for the synthesis of oxa-, thia-, and azacrown ethers, respectively. Tosylate substituents are rather universal and may be used for preparation of macrocycles of any heteroatomic composition.

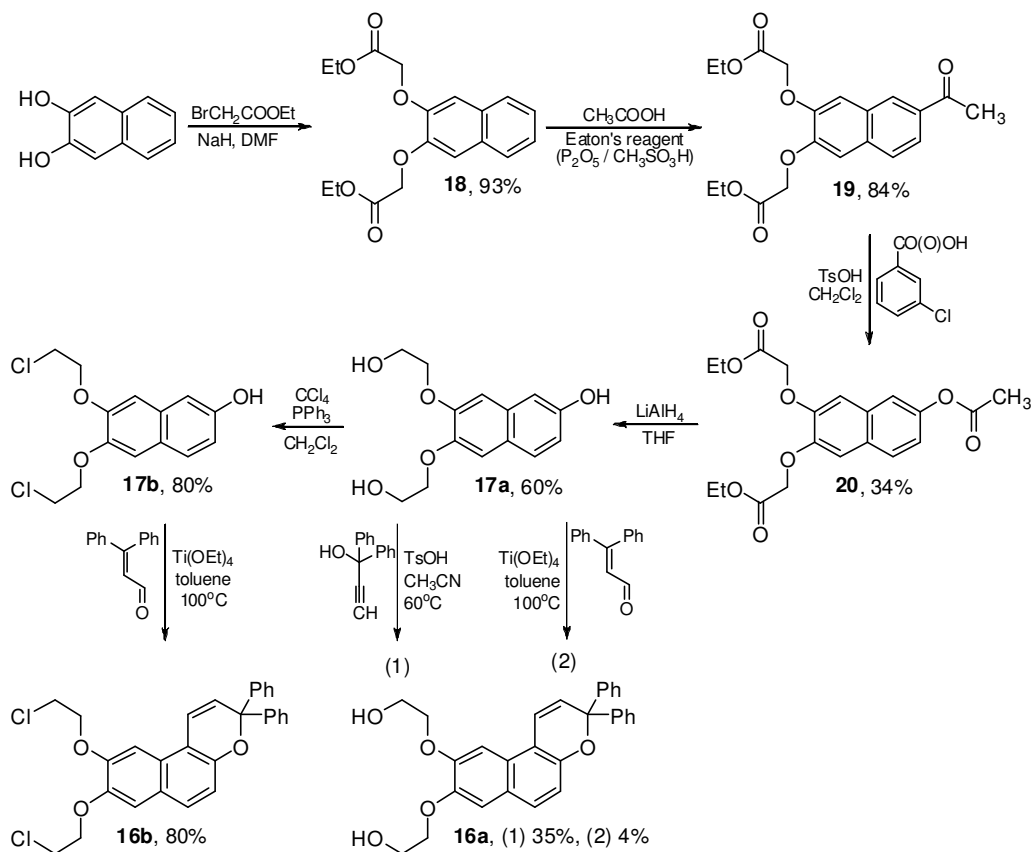


Scheme 3.14. The concept of crown ether fragment incorporation into chromene molecule.

The key compounds in the synthesis of chromenes **16** are the appropriate naphthols **17**. Such compounds have not been described. Therefore, synthetic techniques for the preparation of similar molecules and the methods used for obtaining crown-containing phenols were adapted from the literature [126-128]. As a result, we used a route for naphthols **17** synthesis from dihydroxynaphthalene by its successive *O*-alkylation, acylation, Baeyer-Villiger oxidation and LiAlH_4 reduction (Scheme 3.15). Similarly to the synthesis of 15-crown-5-naphthol **5**, in this case the most complicated stage was ketone **19** oxidation to ester **20**, which afforded 34% yield. Other stages gave high and moderate yields. Naphthol **17a** was also successfully converted to chloro substituted derivative **17b**.

The next stage was synthesis of chromenes from naphthols **17**. Due to high polarity, the compound **17a** was insoluble in toluene, which was usually used as a solvent in the reaction with β -phenylcinnamaldehyde. This led to extremely low reaction yield (4%). Accordingly, photochromic derivative **16a** was synthesized using the method with propargyl alcohol. Acetonitrile, in which compound **17a** solubility was much higher than in toluene, was used as a solvent. In this case, the yield was found satisfactory (35%). Chromene **16b** in high yield (80%), in turn, was obtained by the second method from naphthol **17b**.

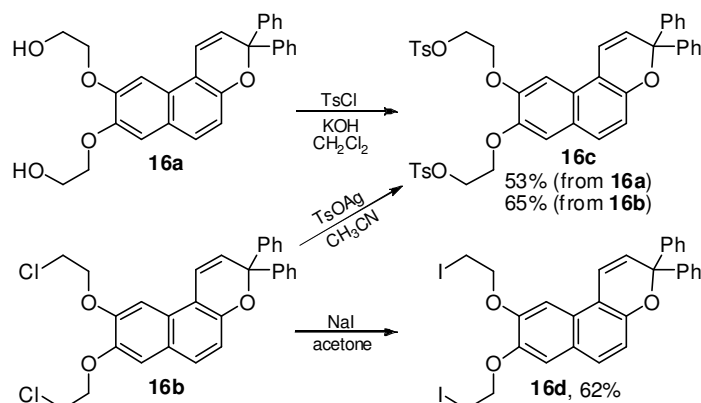
Terminal substituents in compounds **16a** and **16b** were replaced by tosylate groups and iodine (Scheme 3.16). Direct tosylation of compound **16a** with the use of TsCl in the



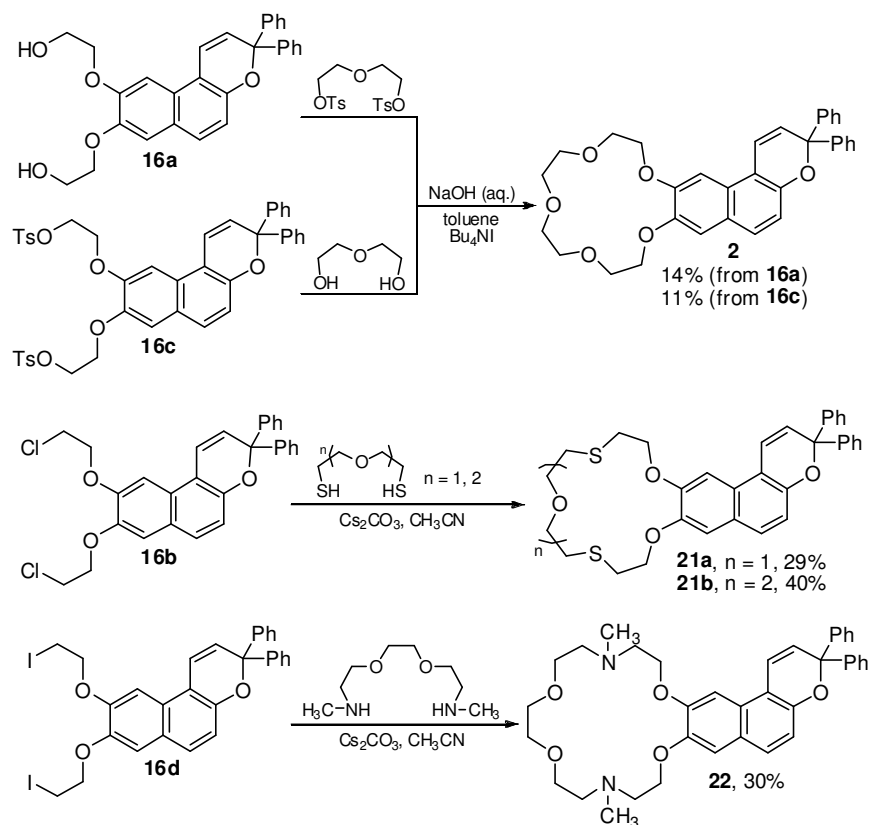
Scheme 3.15. Synthesis of chromenes-precursors **16a** and **16b**.

presence of a base gave chromene **16c** in 53% yield. Also, **16c** was obtained from compound **16b** by the interaction with TsOAg in acetonitrile. In this case, 4 days reflux of the reaction gave a mixture of the initial chromene and substitution products with predominant content of monosubstituted component (mixed terminal groups). The reaction mixture exposure to 140°C during 20 h increased conversion of compound **16b** and produced compound **16c** in 65% yield. Diiodo derivative **16d** was synthesized from **16b** according to the standard technique.

For obtaining the target crown-containing chromenes, the precursors reacted with oligoethyleneglycols containing various end groups. Compounds **16a** and **16c** were used for obtaining oxacrown derivative **2**; compounds **16b** and **16d** were employed for the synthesis



Scheme 3.16. Replacement of terminal groups in chromenes **16a** and **16b**.



Scheme 3.17. Synthesis of target chromenes from precursors **16**.

of dithia- (**21**) and diazacrown (**22**) derivatives, respectively (Scheme 3.17). It should be noted that obtained yields correspond to the average yields in crown ether syntheses. Nevertheless, naphthopyran **2** yield differs from analogous thia- and aza- derivatives by 2-4 times, which is probably associated with lower nucleophilic character of oxygen atoms of HO-groups in chromene **16a** or diethyleneglycol in the reaction with chromene **16c**. Structure of compound **21b** was proved by X-ray analysis (Fig. 3.4).

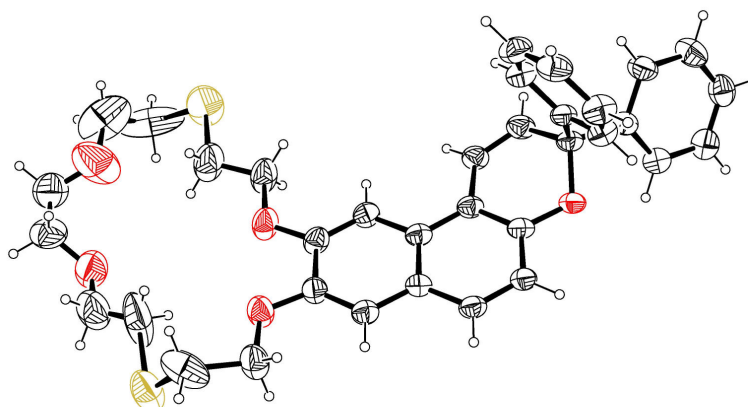


Figure 3.4. X-ray analysis data of naphthopyran **21b**.

In the synthesis of compound **21a**, a side non-photochromic product **23**, resulting from water molecule addition to the double bond of the pyran ring, was detected. The suggestion about its structure was made on the basis of 1D and 2D ¹H NMR spectra in CDCl₃, DMSO-*d*₆ (Figs. 3.5, 3.6).

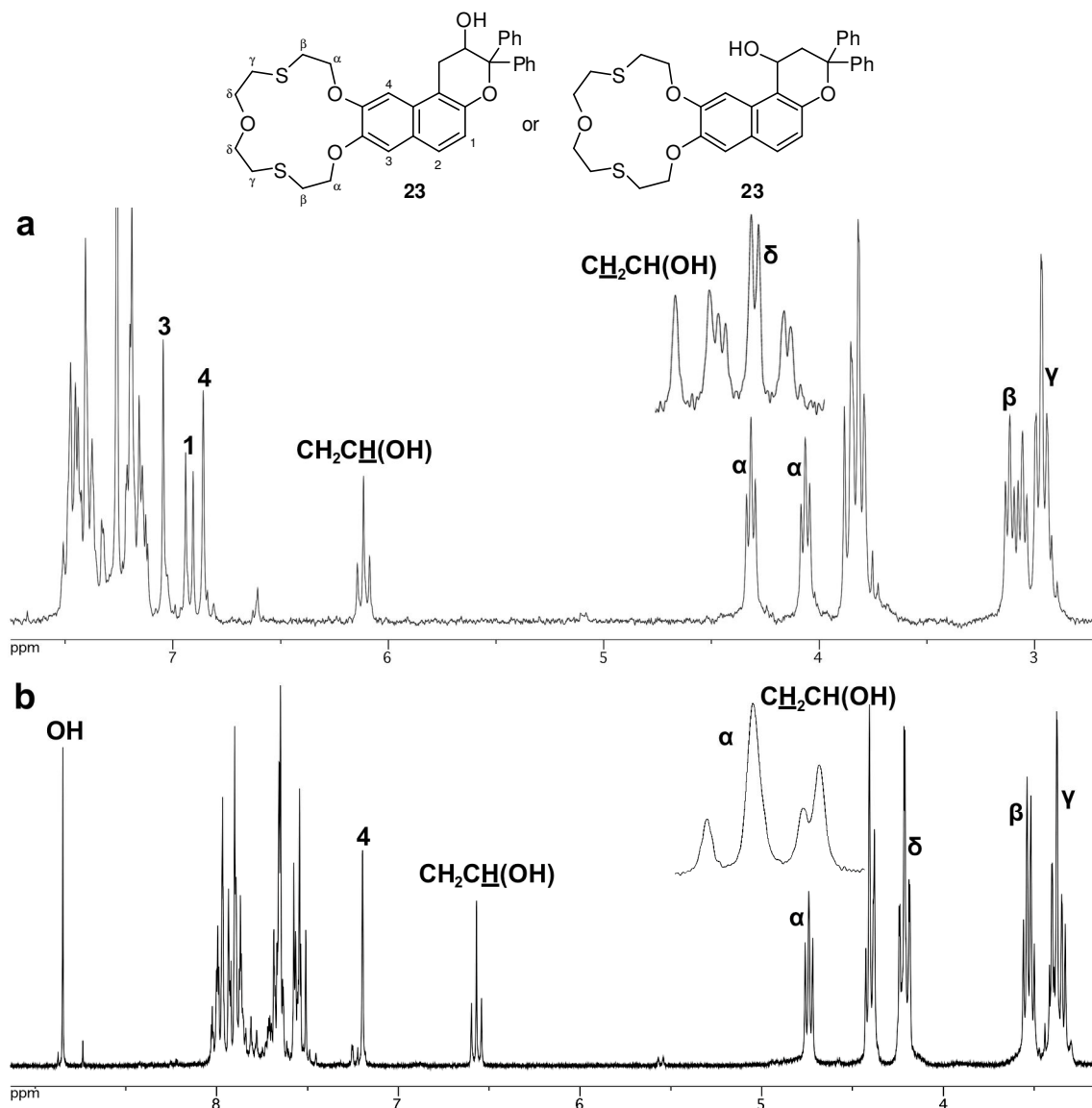


Figure 3.5. ^1H NMR spectra of compound **23** in (a) CDCl_3 and (b) $\text{DMSO}-d_6$. Insets correspond to zoomed (a) 3.76-3.90 and (b) 4.36-4.44 regions.

The NMR spectra possess a triplet signal of aliphatic proton (6.12 ppm and 6.57 ppm in CDCl_3 and $\text{DMSO}-d_6$ solutions, respectively) shifted downfield. This testifies about closely located electron-withdrawing group. In addition, the aliphatic part of the spectrum demonstrates a doublet proton signal (see zoomed spectrum fragments in Fig. 3.5). The coupling constants of the signals coincide and are equal to 7.2 Hz. COSY spectrum proves mutual coupling of the signals (Fig. 3.6). An indirect proof of HO-group presence is a singlet proton signal (8.85 ppm) in the NMR spectrum in $\text{DMSO}-d_6$ (Fig. 3.5b). The values of integral intensities also prove occurrence of three additional protons.

This approach to synthesis of target compounds is rather flexible and allows obtaining different photochromic systems. Hence, using phenols **17**, spironaphthoxazines **25** and **26** were synthesized (Scheme 3.18) [4, 129]. The key compounds in spironaphthoxazine synthesis are nitrosonaphthols obtained by nitrosation of corresponding naphthols. The low yield of compound **24a** compared with chloro substituted analogue is due to its good

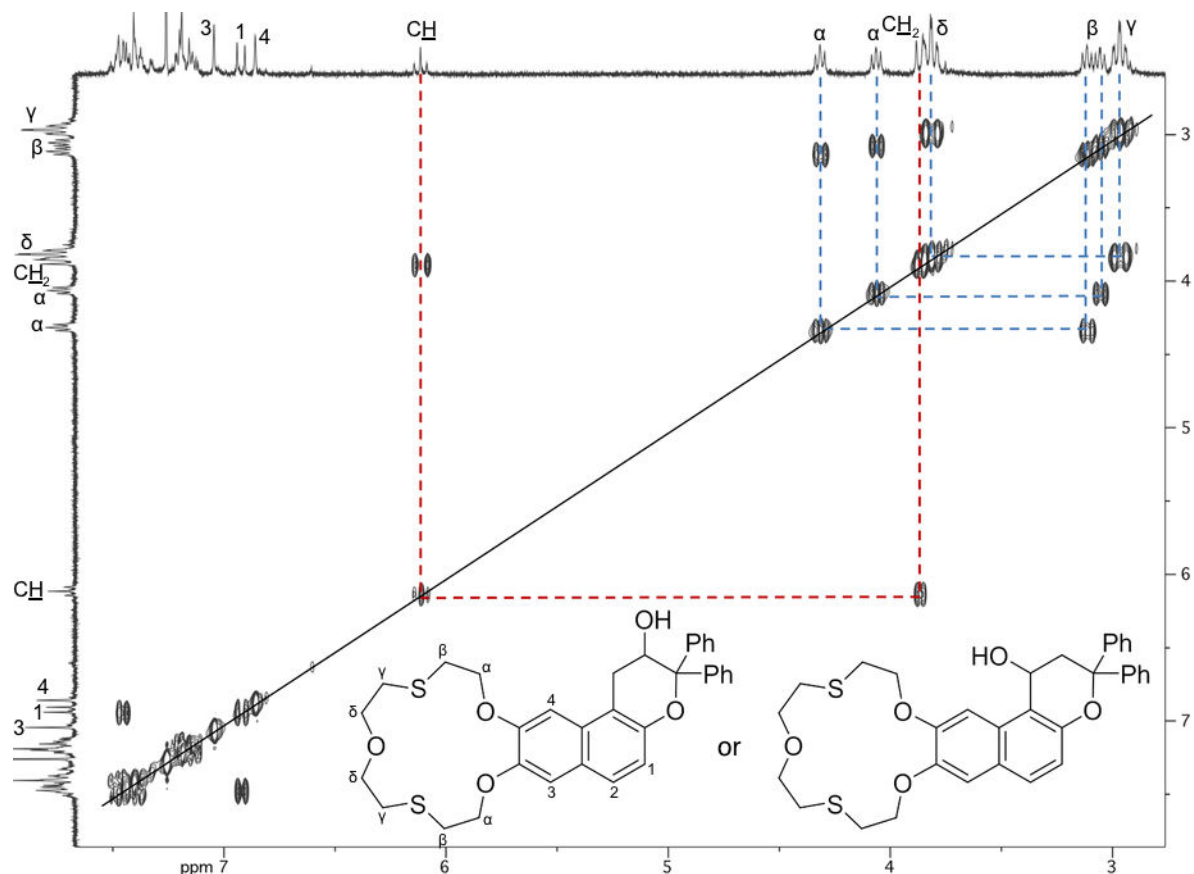
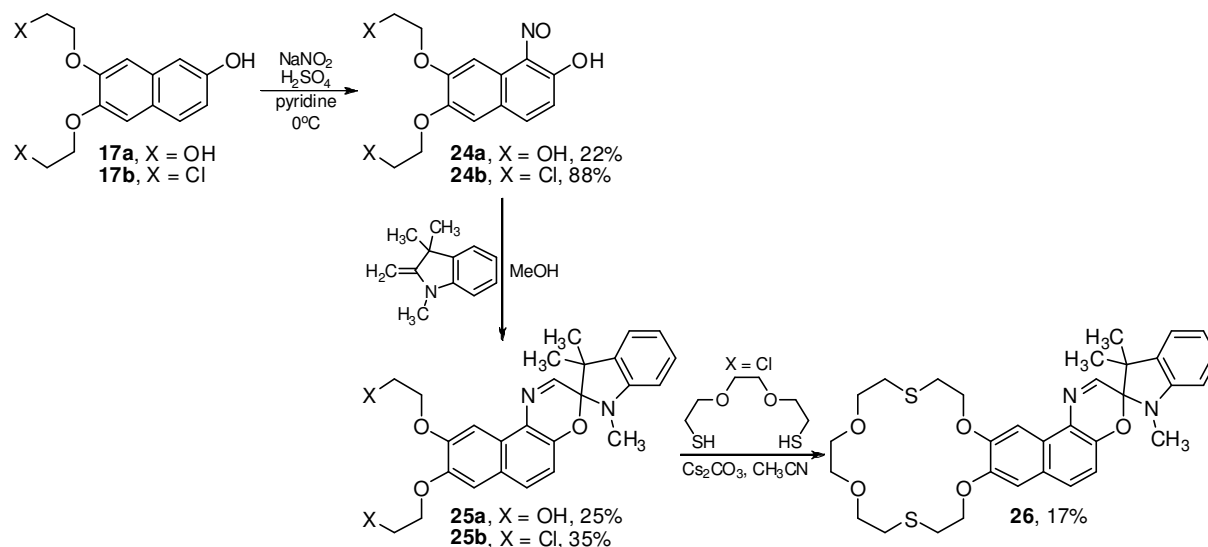


Figure 3.6. COSY NMR spectrum of compound **23** in CDCl_3 .



Scheme 3.18. Spironaphthoxazines synthesis.

solubility in water and poor solubility in organic solvents that significantly hindered its separation from the reaction mixture. On the contrary, derivative **24b** is insoluble in water that considerably favored the work up. Spironaphthoxazines **25** were synthesized from nitrosanaphthols by interaction with 2-methylenetetramine in methanol in traditionally low yields (25% and 35% for HO- and Cl-derivative, respectively). Similarly to the previously described procedures for chromene preparation, dithia-18-crown-6 ether derivative **26** was synthesized from precursor **25b**.

Thus, for the first time, an approach to synthesis of crown-annelated chromenes and spironaphthoxazines from available initial compounds was developed. By varying substituents of terminal alkyl fragments in precursors, several chromenes with oxa-, dithia- and diazacrown ethers were synthesized.

These two approaches were found effective in the synthesis of target chromenes. Primarily, they differ by the synthesis direction. The *first approach* suggests introduction of photochromic function into a substrate (benzene, naphthalene, etc.), already containing a crown ether fragment. In the *second approach*, a crown ether fragment is introduced into a photochromic molecule. Either approach possesses some advantages, however, disadvantages are also observed. Based on the work performed, comparison of the methods is provided below.

The accessibility of crown annelated substrates limits significantly the use of the first approach. Mostly, oxacrown ether containing derivatives of benzene or naphthalene are commercially available. Note also that the price of reagents may be rather high in this case. Moreover, similar to the case of phenols **6**, a certain type of substitution on the target chromene may require preliminary synthesis of the crown ether.

Another significant limitation for the first approach is the impossibility to use nonoxacrown ether derivatives, because acylation and oxidation conditions seem to be rather destructive for aza- or thiocrown ethers. This makes impossible preparation of the corresponding chromenes by the first approach.

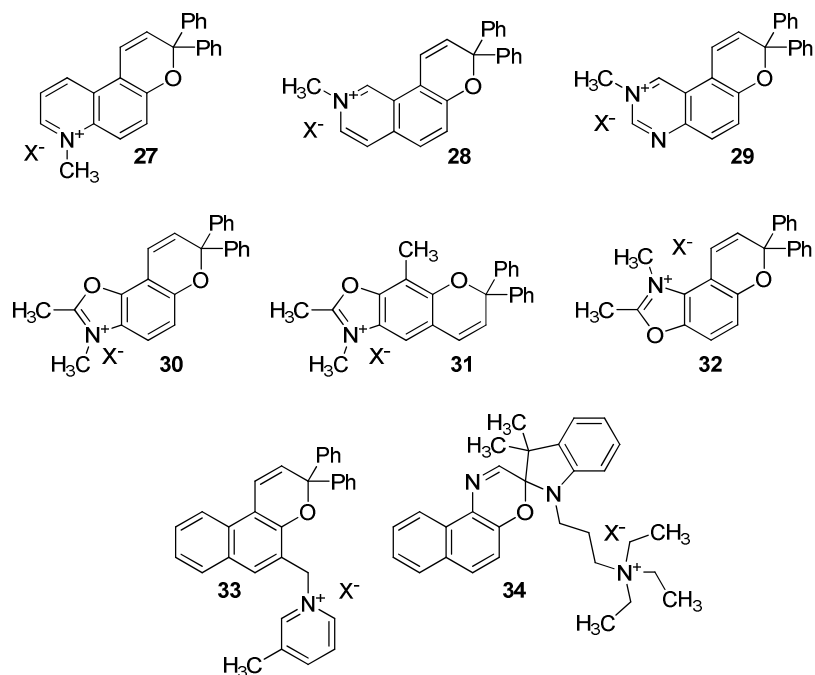
In most cases, the second approach has no such disadvantages, because the crown ether is formed at the final stage of the synthesis. Therefore, various macrocyclic derivatives with different heteroatomic composition and size may be synthesized. The advantage of the second approach is its flexibility and variability that also allows using the synthetic approach for other photochromic compounds, such as spironaphthoxazines which synthesis by the first method is rather difficult (first of all, at the nitrosation stage).

Note also that the general disadvantage of the suggested approaches is low yields in the Baeyer-Villiger oxidation. Hence, further development of the method requires optimization of this stage or elaboration of the alternative routes for hydroxyl group incorporation into the molecule.

The synthesis strategy is thus defined by the target compound. It could be concluded that for oxacrown ether derivatives, the first approach is more preferable. For the synthesis of chromenes, annelated by thia- and azacrown ether fragments, the best results can be obtained by the second approach.

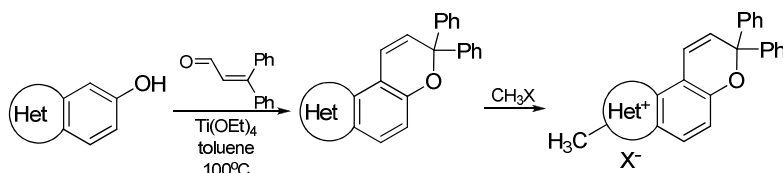
3.1.3. Synthesis of Benzopyrans Containing Positively Charged Fragments

Another target of the work was preparation of compounds able to participate in the photo-controlled DNA intercalation. In this case, the key requirement is the presence of positive charge in the structure. Therefore, we suggested several quaternary salts of heterocyclic chromenes **27-32** as well as chromene **33** and spironaphthoxazine **34**, possessing positively charged group in the side chain.



Heterocyclic chromenes **35-40** are described in literature [121, 123, 124]. They were prepared by interaction of the corresponding hydroxy-derivatives with β -phenylcinnamaldehyde in the presence of titanium tetraethoxide (Scheme 3.19, Table 3.2). In some cases, in the synthesis of compounds **35-40** linear isomers were detected and sometimes extracted (for **36** and **38**), however, their amount did not exceed 3-4%. Further alkylation of several chromenes led to corresponding quaternary salts (Scheme 3.19, Table 3.3).

Methyl iodide and methyl tosylate were used as alkylating agents. In the first case, the reaction was carried out without solvent with excessive amount of CH_3I in a closed ampoule heated up to 60°C . In the case of TsOCH_3 , the reactants were refluxed in acetonitrile. Although NMR spectra always indicated the alkylation products formation, not all products were isolated probably due to incomplete reactions and side products resulted from the redox processes with the iodide anion participation. In the case of chromene **39**, steric hindrance may also affect the reaction proceeding. Structures **27a** and **39** were proved by X-ray analysis (Fig. 3.7).



Scheme 3.19. Synthesis of chromenes possessing positive charge.

Table 3.2.

Synthesis of heterocyclic chromenes.

<i>Yield</i> 65%	45%	54%
<i>Yield</i> 27%	33%	28%

Table 3.3.

Synthesis of chromenes containing positively charged heterocyclic fragments.

27a , X = I ⁻	27b , X = TsO ⁻	28 , X = I ⁻	31 , X = I ⁻
<i>Yield</i> 96%	85%	87%	36%

In addition, we synthesized chromene **33**, containing positively charged picoline fragment in the side chain, and spironaphthoxazine **34** with triethylammonium cation, bound by a propylene bridge to the indoline fragment.

The starting compound for the synthesis of substance **33** was chromene **41** with the hydroxymethyl group in position 5 (Scheme 3.20). The hydroxyl group was converted to the

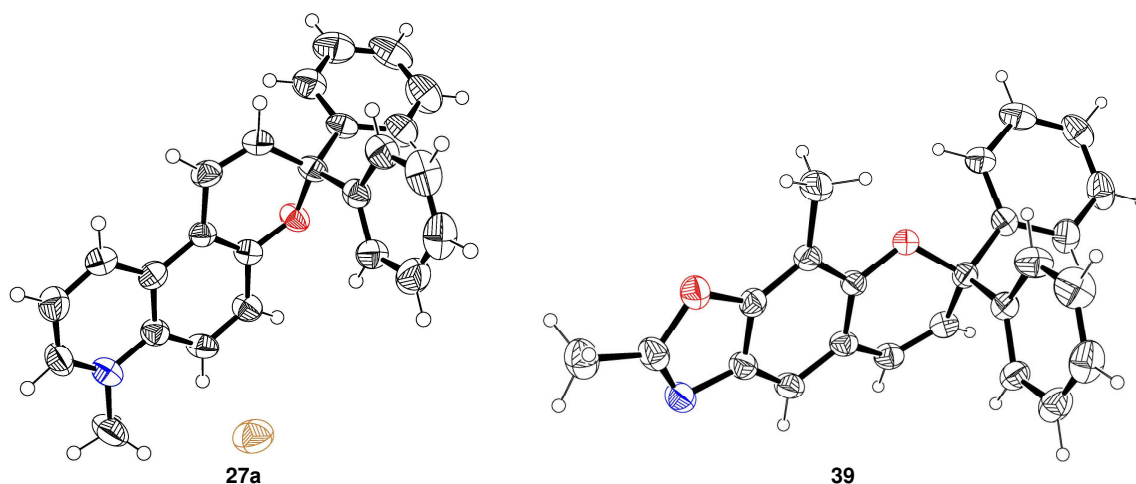
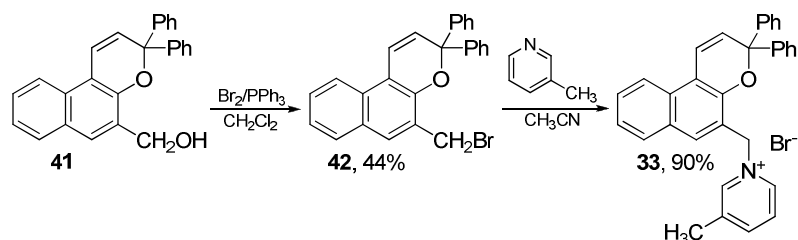


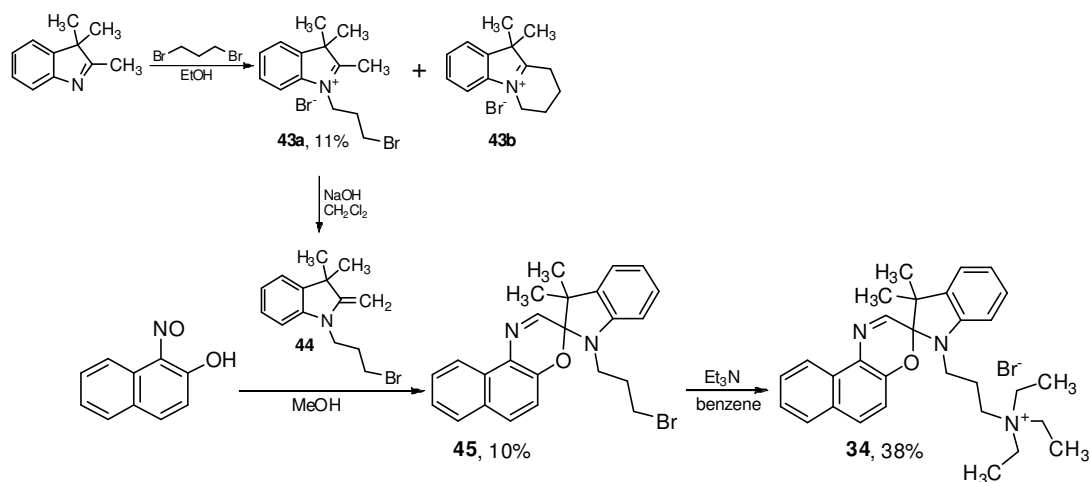
Figure 3.7. X-ray analysis data of iodide **27a** and chromene **39**.



Scheme 3.20. Chromene **33** synthesis.

corresponding bromo derivative **42** using Br_2/PPh_3 [129]. The reaction of β -picoline with chromene **42** gave quaternary salt **33** in high yield.

The synthesis of spironaphthoxazine **34** was more difficult (Scheme 3.21). In this case, the key compound was base **44** synthesized from 2,3,3-trimethylindoline and 1,3-dibromopropane [73]. At the first stage, quaternary salt **43a** was formed. Cyclic derivative **43b** was also identified in the reaction mixture. Isolation of compound **43a** was hindered by the presence of the starting indoline, which easily oxidized on air into a pink substance. Multiple rinsing of the reaction mixture by methanol/acetone (1/100) mixture gave almost pure product **43a**. At the next stage, indoline **44** was not purified and directly used in the reaction with 1-nitrosophthalen-2-ol. As a result, spironaphthoxazine **45** was obtained in only 10% yield that was probably the consequence of low purity of **44**. At the final stage, the reaction of compound **45** with triethylamine afforded the target spironaphthoxazine **34** in 38% yield.



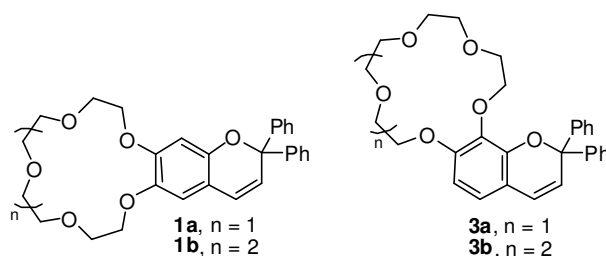
Scheme 3.21. Spironaphthoxazine **34** synthesis.

Thus, several chromenes and one spironaphthoxazine potentially able to interact with DNA were synthesized. Structures of compounds were proved by NMR spectroscopy and X-ray analysis. Investigation on the properties of the synthesized chromenes is discussed in Chapter 3.2.

3.2. Study of Photochromic Properties and Complex Formation of Several Compounds Synthesized

3.2.1. Study of Coordination Ability of Several Crown-Annulated Chromenes

The presence of oxa-15-crown-5 ether in **1a** and **3a** molecules determines their ability to form stable complexes with “hard” cations of alkaline and alkaline-earth metals. Thus, two metal cations of the group II, magnesium and barium, were chosen for the investigation. In addition, lead (II) cations were tested as they are able to form stable complexes with the crown ethers as well as to coordinate with the carbonyl oxygen atom occurring in the open form structure.



The fragment of 18-crown-6 ether in chromenes **1b** and **3b**, in turn, is characterized by the ability to bind strongly the ammonium cation due to the hydrogen bonds formation [130, 131]. As a result of photochromic transformation, one more strong coordination site, the carbonyl oxygen atom, appears in the structure. Using the protonated amino acids NH_3^+ -(CH_2) $_i$ -COOH as the guest molecules, one may expect the formation of ditopic complexes with the open form of chromenes **1b** and **3b**, in which the ammonium group is located in the crown ether cavity and the carboxyl group is coordinated with the carbonyl oxygen atom *via* hydrogen bond. In this case, amino acid coordination will depend on the amino acid alkyl chain length (i , the number of methylene groups).

The complex formation was studied using a combination of NMR and optical spectroscopy methods, enabling both the structure and stability of the complexes to be determined.

3.2.1.1. Complex Formation of Chromenes 1a and 3a with Metal Cations

The composition and stability of complexes of the SP forms were determined by spectrophotometric titration. Absorption spectra of the free ligands and those of complexes may differ due to the electronic density redistribution in the molecules. Indeed, addition of a metal solution aliquots to a ligand solution changes the absorption spectra (Figs. 3.8, 3.9, left

plots). The set of spectra obtained was used for determination of complex structures and calculation of their stability constants (see Experimental Part).

Plots on the left in Figs. 3.8 and 3.9 show titration experimental data; elucidated spectra of the complexes are shown on the right. With respect to metal cation in use, the analysis exclusively indicated formation of 1:1 complexes (for magnesium) or stepwise formation of two complexes, with ligand to metal ion ratio being 2:1 and 1:1 (for barium and lead). Dashed curves represent the free ligand spectrum, whereas solid lines correspond to 1:1 and 2:1 complexes spectra.

The presence of the metal cations induced blue shift of the longest wavelength absorption band of the ligand accompanied by a low hypochromic effect, which is more pronounced in case of compound **3a**. This evidences the occurrence of coordination between the cations and the crown ether fragment, since the oxygen atoms present in the chromophore system of the chromene substantially reduce their electron-donating ability, thus leading to the effects observed. The presence of two chromene molecules in a “sandwich” complex, in turn, provides twice higher extinction values for 2:1 complex spectra.

The obtained stability constants of complexes of chromenes **1a** and **3a** with metal cations are presented in Table 3.4. Among factors affecting the stability, cation nature, its charge and diameter, and correspondence of the latter to the crown ether cavity size should be noted.

Table 3.4.
Determined values of stability constants for 1:1 ($\lg \beta_{11}$) and 2:1 (ligand:metal) ($\lg \beta_{21}$) complexes of **1a** and **3a** with metal cations.

	Chromene 1a		Chromene 3a	
	$\lg \beta_{11}$	$\lg \beta_{21}$	$\lg \beta_{11}$	$\lg \beta_{21}$
Mg ²⁺	5.26 ± 0.04	–	4.14 ± 0.02	–
Ba ²⁺	5.39 ± 0.04	11.21 ± 0.06	5.53 ± 0.05	10.9 ± 0.1
Pb ²⁺	6.7 ± 0.3	13.7 ± 0.1	6.3 ± 0.2	12.9 ± 0.4

Estimated from X-ray crystallographic data, the cavity radius of 15-crown-5 ether is 0.86-0.92 Å. In turn, the ionic radii of the cations selected in this work vary from 0.72 Å for Mg²⁺ to 1.36 and 1.20 Å for Ba²⁺ and Pb²⁺, respectively [132]. Thus, formation of 1:1 complexes of the inclusive type, with the cation located in the crown ether cavity, is typical for magnesium cations. Having greater radius, barium and lead cations are inclined to form 1:1 complexes of the exclusive type, in which the ion is located outside the macrocyclic cavity, and more stable 2:1 complexes of the “sandwich” type stabilized considerably by stacking interaction between the ligand molecules.

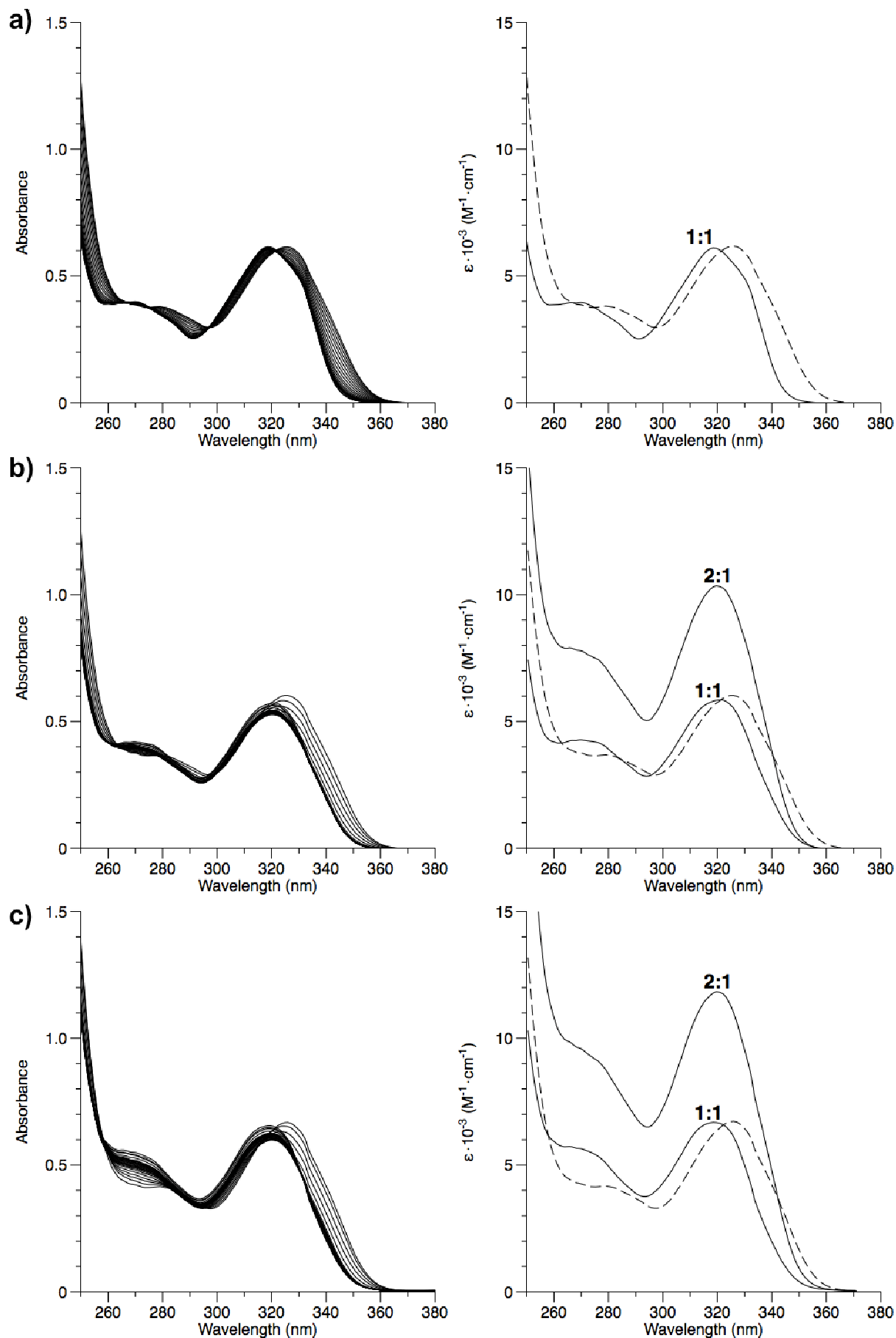


Figure 3.8. Spectrophotometric titration of chromene **1a** by (a) $\text{Mg}(\text{ClO}_4)_2$, (b) $\text{Ba}(\text{ClO}_4)_2$, and (c) $\text{Pb}(\text{ClO}_4)_2$ solutions in acetonitrile ($C_{1a} = 1 \cdot 10^{-4} \text{ M}$, $C_M/C_{1a} = 1 \div 64$). Elucidated from spectrophotometric titration data, absorption spectra of chromene **1a** (dashed line) and its complexes with metal cations of 1:1 and 2:1 composition (solid lines) are shown on the right. (ϵ is molar extinction coefficient, $\text{M}^{-1} \cdot \text{cm}^{-1}$)

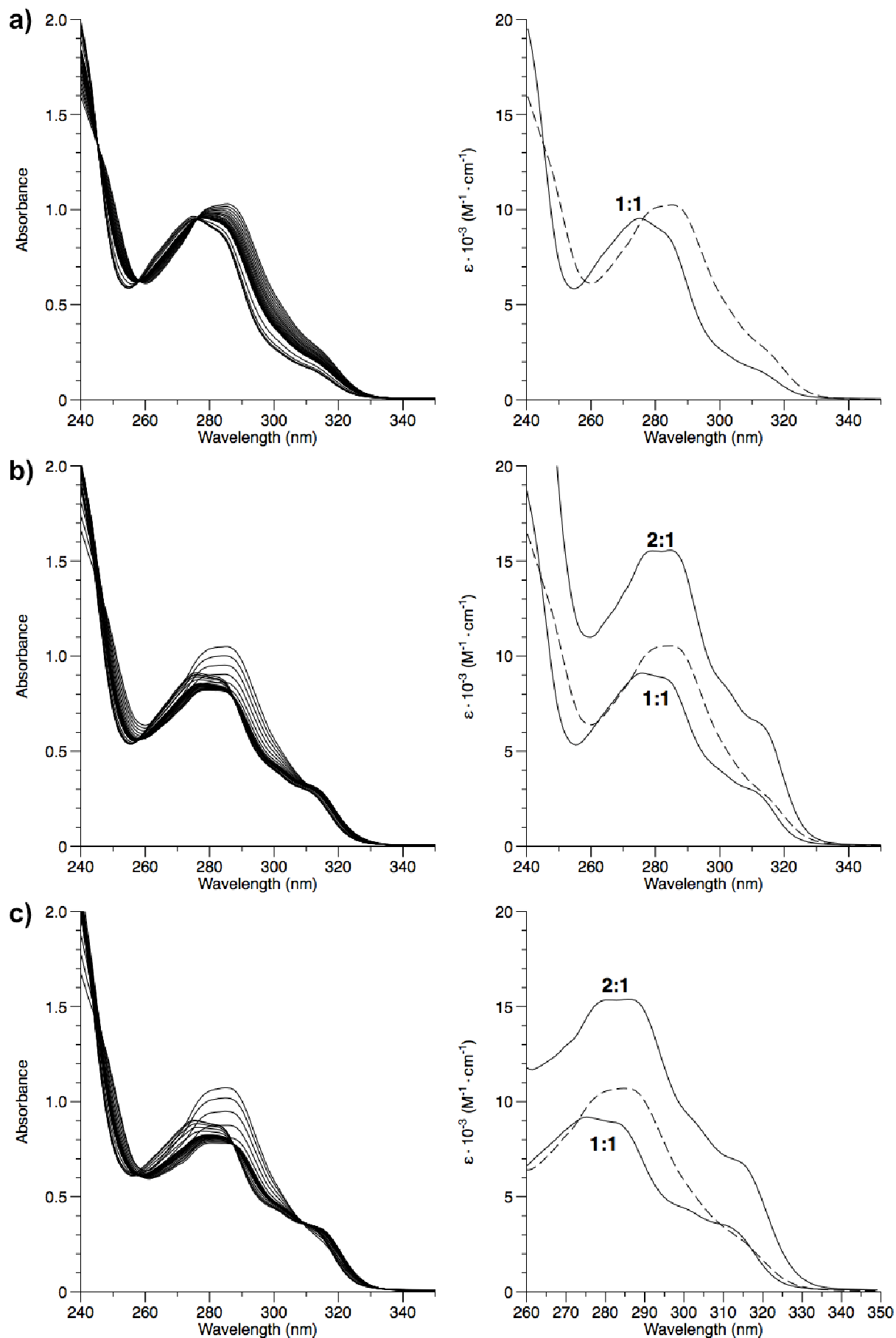
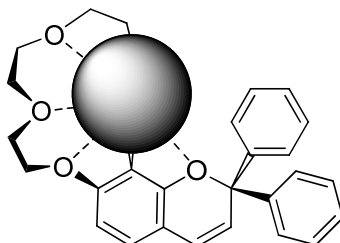


Figure 3.9. Spectrophotometric titration of chromene **3a** by (a) $\text{Mg}(\text{ClO}_4)_2$, (b) $\text{Ba}(\text{ClO}_4)_2$, and (c) $\text{Pb}(\text{ClO}_4)_2$ solutions in acetonitrile ($C_{1a} = 1 \cdot 10^{-4} \text{ M}$, $C_M/C_{1a} = 1 \div 64$). Elucidated from spectrophotometric titration data, absorption spectra of chromene **3a** (dashed line) and its complexes with metal cations of 1:1 and 2:1 composition (solid lines) are shown on the right. (ϵ is molar extinction coefficient, $\text{M}^{-1} \cdot \text{cm}^{-1}$)

For 1:1 complexes, stability constants were increasing in the sequence $Mg^{2+} < Ba^{2+} < Pb^{2+}$. For linear isomer **1a**, the difference in the complex stabilities with magnesium and barium cations is small. On the contrary, isomer **3a** constants differ by more than an order of magnitude. Large values of the stability constants for barium and lead in 1:1 complexes may be caused by possible participation of these cations in additional coordination with the oxygen atoms of the pyran cycle (Scheme 3.22).



Scheme 3.22. Formation of additional coordination between barium or lead cation and oxygen atoms of pyran cycle in chromene **3a**.

Despite the fact that lead cation radius is in the middle between magnesium's and barium's ones and the metal itself represents a "softer" acid, formation of the most stable complexes is typical for it. This is maybe associated with the high polarizability of the cations and the covalent character of the bonds they can establish [132].

The structure of the complexes was determined by NMR spectroscopy. Solutions in CD₃CN with ligand concentration of $1-2 \cdot 10^{-3}$ M in the presence of 0.5 and 1 molar equivalent of the cation were studied. Addition of metals significantly changes the NMR spectra of chromenes. However, under usual conditions (20°C) this resulted in peaks broadening (Fig. 3.10). When the temperature was decreased to -45°C, resolution was successfully improved (Fig. 3.11). The analysis of 1D spectra allowed determination of the number of components in the mixture. Additional 2D experiments made possible to determine structure of the complexes.

In the presence of the magnesium cations, a downfield shift of the aliphatic and aromatic protons was observed (Figs. 10b, 11b, Table 3.5), the phenyl group proton signals retaining their position. This indicated the formation of inclusive 1:1 complex with Mg^{2+} cation (Scheme 3.23, complex **A**). Of importance is the fact that the spectrum had a single group of signals that eliminated formation of several forms of complexes.

The absence of the free ligand signals also proved high stability of the complex. Atoms assignment was performed upon NOESY and HMBC spectra (see appendix). A peak at ~5.4 ppm, apparently, corresponds to water molecules, which are linked to magnesium ion (does not occur in HMBC and HSQC spectra).

With barium and lead cations, two solutions with different ligand to metal ratio (L/M) were studied. In both cases, occurrence of new signals, absent in the initial chromene **1a** spectrum, were observed (Fig. 3.11)

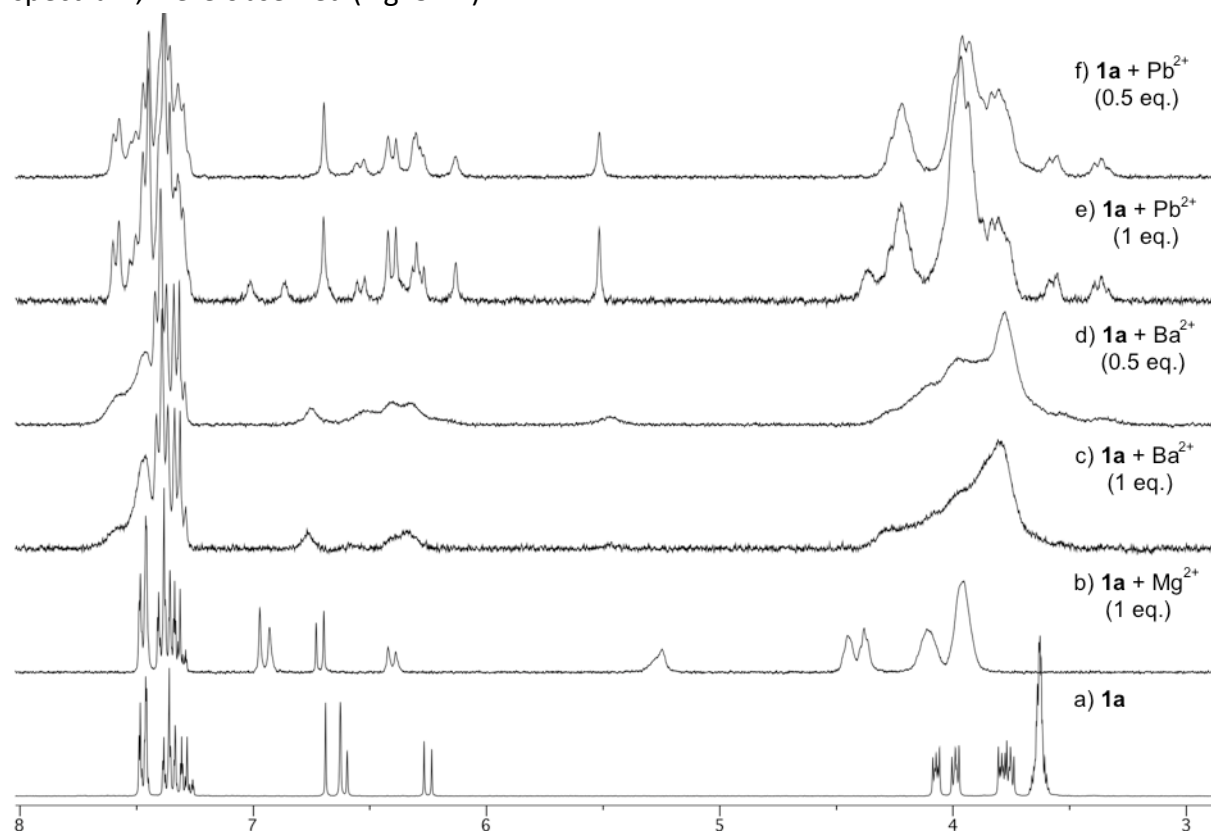


Figure 3.10. ^1H NMR spectra of chromene **1a** in the presence of metal cations at 20°C (a, b, e - $C_{1a} = 1 \cdot 10^{-3}$ M; d, f - $C_{1a} = 2 \cdot 10^{-3}$ M).

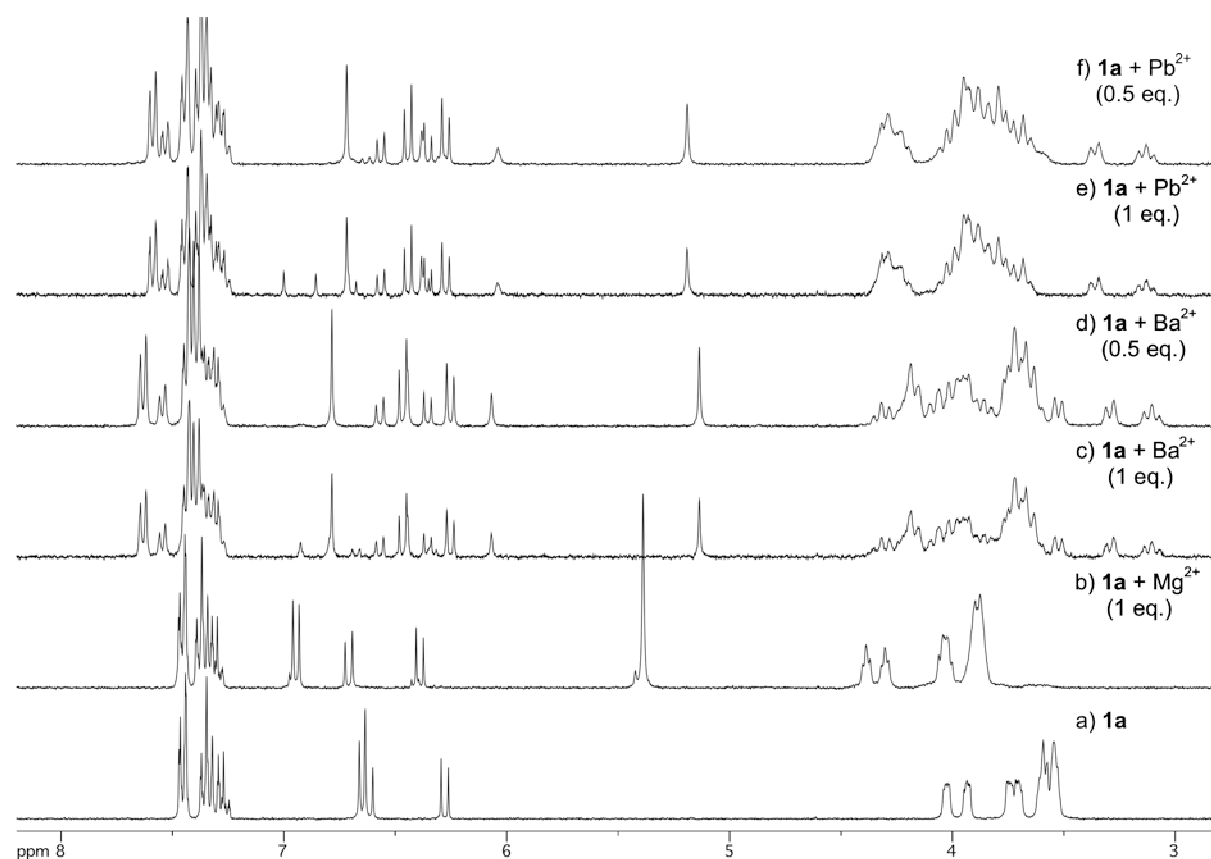
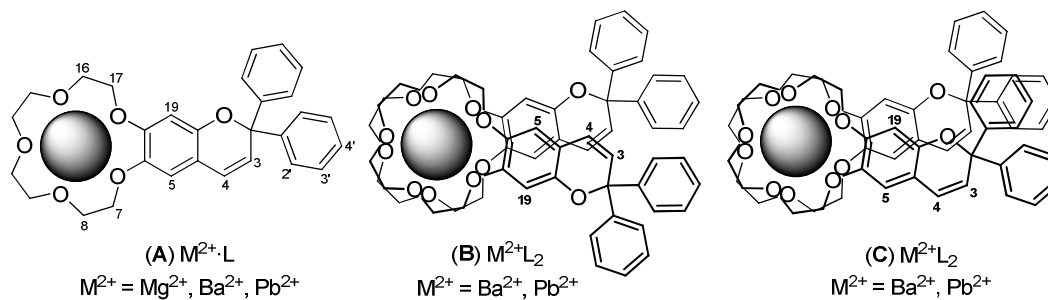


Figure 3.11. ^1H NMR spectra of chromene **1a** in the presence of metal cations at -45°C (a, b, e - $C_{1a} = 1 \cdot 10^{-3}$ M; d, f - $C_{1a} = 2 \cdot 10^{-3}$ M).



Scheme 3.23. Structures of chromene **1a** complexes with metal cations

Table 3.5.

Changes of aromatic proton signal shifts in complexes of **1a** with metal cations compared with the free ligand ($\Delta\delta = \delta_{\text{complex}} - \delta_{\text{1a}}$).

	Mg ²⁺	Ba ²⁺			Pb ²⁺			
	A (1:1)	A (1:1)	B (2:1)	C (2:1)	A (1:1)	B (2:1)	C (2:1)	D (2:1)
H-3	+0.11	+0.05	+0.19	+0.05	+0.08	+0.17	+0.08	+0.01
H-4	+0.09	+0.06	-0.36	+0.06	+0.09	-0.34	+0.06	+0.01
H-5	+0.29	+0.27	-1.52	-0.21	+0.34	-1.46	-0.27	+0.07
H-19	+0.29	+0.16	+0.15	-0.58	+0.16	+0.09	-0.59	+0.05

In the presence of Ba²⁺, analysis of NMR spectrum allowed elucidation of three groups of signals (**A**, **B** and **C**) (Fig. 3.12). For signal assignment, the 2D experiments (COSY, NOESY, HSQC, HMBC) were performed.

Intramolecular interactions of protons caused by nuclear Overhauser effect (NOE) allowed assignments of atoms in the complex (Fig. 3.13). For instance, among group **B** signals, interaction of protons at 5.14 ppm and protons at 3.10 and 3.29 ppm are indicative. This interaction may characterize H5 and H7 protons, the latter being magnetically nonequivalent (denoted as H_{7α} and H_{7β}), that causes occurrence of two signals (also proved by HSQC). Correlation of signals at 5.14 and 6.25 ppm confirms H5 assignment and detects H4. This is also proved by weak interaction of 6.25 (H4) and 6.47 (H3) ppm peaks (not shown in the fig.). The same way, cross-peaks at 6.78 ppm with several signals in the aliphatic region (3.72, 4.16 and 4.30 ppm) determine H19 position, which is also confirmed by peak at 6.78 ppm interaction with typical signals of the phenyl 2'-CH-groups at 7.42 and 7.63 ppm (these protons also became magnetically nonequivalent in the complex). Similar analysis of NOE signals for the group **C** makes possible assignment of hydrogen atoms in the complex. In addition, the assignment is proved by cross-peaks of protons participating in chemical exchange. Fig. 3.13 shows interactions of such signals related to groups **B** and **C**, namely: 5.14 and 6.43 ppm (H_{5B}-H_{5C}), 6.78 and 6.07 ppm (H_{19B}-H_{19C}), 6.25 and 6.57 ppm (H_{4B}-H_{4C}). Cross-peaks at 6.47 and 6.35 ppm, corresponding to H_{3B}-H_{3C} exchange (not shown), are also present.

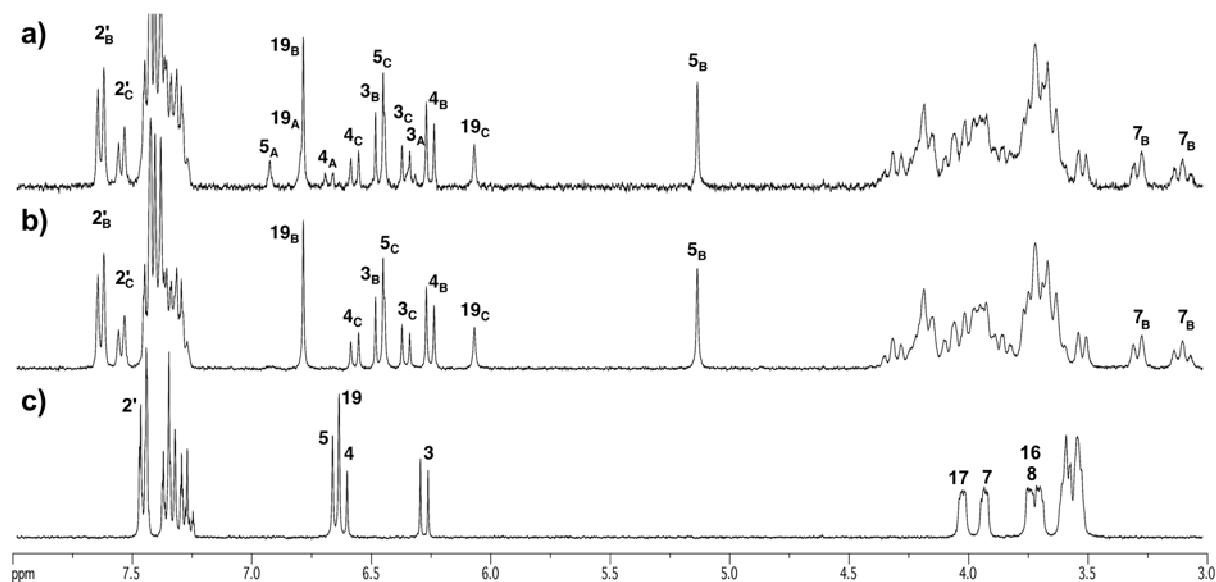


Figure 3.12. ^1H NMR spectra of chromene **1a** in the presence of barium cations at -45°C : a) $C_{1a} = 1 \cdot 10^{-3}$ M, $C_{Ba} = 1 \cdot 10^{-3}$ M; b) $C_{1a} = 2 \cdot 10^{-3}$ M, $C_{Ba} = 1 \cdot 10^{-3}$ M; c) $C_{1a} = 1 \cdot 10^{-3}$ M.

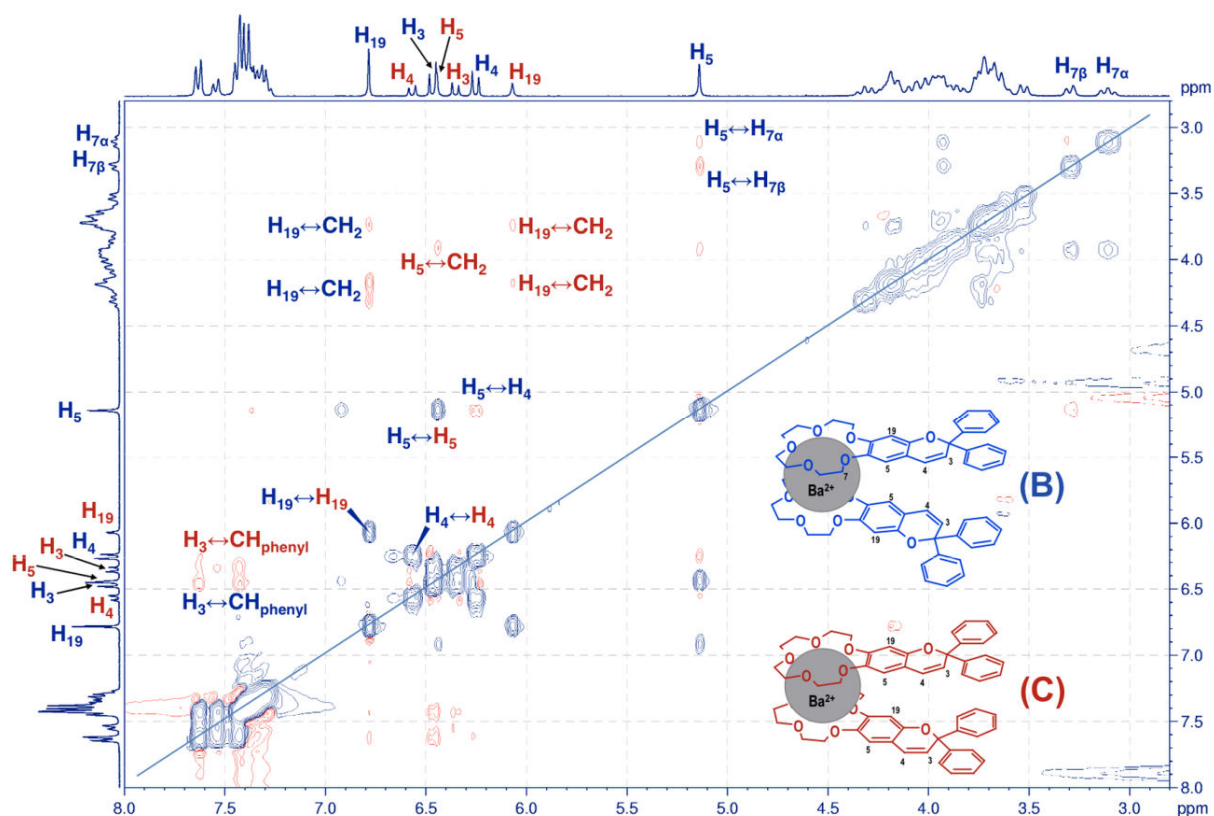


Figure 3.13. NOESY spectrum of chromene **1a** solution in the presence of barium cations at -45°C ($C_{1a} = 2 \cdot 10^{-3}$ M, $C_{Ba} = 1 \cdot 10^{-3}$ M).

Using complex stability constants determined from the UV investigations, concentrations of complexes in solutions for the NMR studies were calculated (Fig. 3.14). The solution containing $C_{1a} = C_{Ba} = 1 \cdot 10^{-3}$ M ($C_{Ba}/C_{1a} = 1$) (Fig. 3.12a) contains 77% of 2:1 complex and 23% of 1:1 complex; in the case of $C_{1a} = 2 \cdot 10^{-3}$ M and $C_{Ba} = 1 \cdot 10^{-3}$ M ($C_{Ba}/C_{1a} = 0.5$) (Figs. 3.12b, 3.13) ML_2 and ML concentrations are 96% and 2%, respectively. At low temperature, these values may vary, but the tendency will be preserved. Thus, NMR signals of groups **B** and **C** protons in the presence of barium cations correspond to 2:1 complexes of

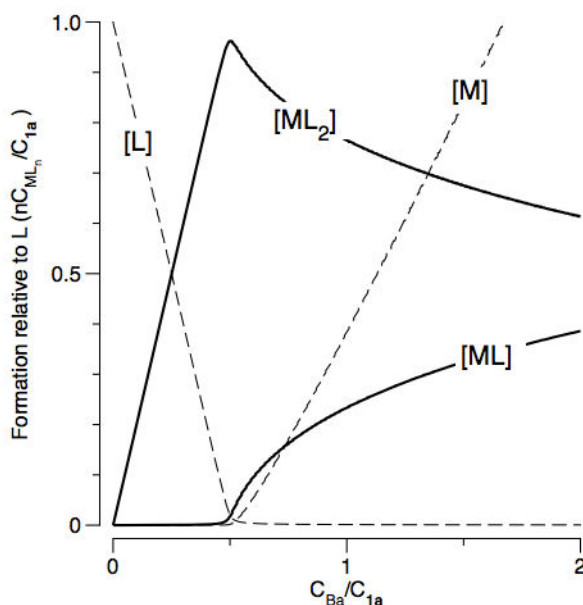


Figure 3.14. Calculated variations in the composition of **1a** solution with Ba^{2+} concentration increase ($\lg \beta_{11} = 5.39$, $\lg \beta_{21} = 11.21$, $C \sim 10^{-3}$ M) [133]. ([L], [M], [ML], [ML₂] correspond to equilibrium concentrations of ligand, metal, 1:1 and 2:1 complexes, respectively.)

various structure. Spectrophotometrically, these complexes are indistinguishable, probably, because of their absorption spectra being similar. In the NMR spectra, signals **B** and **C** are present in the approximate ratio of 2:1 in both cases. Signals **A**, appearing in the NMR spectra along with the increase of ligand/metal ratio, correspond to 1:1 complex. This assignment is also supported by the fact that, in the Ba^{2+} presence, the group **A** signals are shifted in the same way as those in the Mg^{2+} presence (Table 3.5, Scheme 3.23, complex **A**).

For the 2:1 complexes, we suggested two different structures with asymmetrical (**B**) and symmetrical (**C**) disposition of **1a** molecules in relation to cation, located in the crown ether fragment (Scheme 3.23). In case of such structure, the protons of the neighboring molecules will be affected by the anisotropic effects of the opposite aromatic systems, which is confirmed by NMR. Protons H5 and H4 upfield shifts by 1.52 and 0.36 ppm are observed for complex **B**. Due to the geometrical reasons, H5 is characterized by much greater shift than H4. At the same time, similarly to the 1:1 complex, protons H3 and H19 undergo the downfield shift (by 0.19 and 0.15 ppm, respectively). Such disposition of the chromene molecules implies that the crown ether hydrogen atoms, closest to the chromene moiety, are affected by the anisotropic effect of the aromatic system. Protons H7 are shifted upfield and exhibit magnetic nonequivalence. Similarly, atoms H2' of phenyl groups, located in the space between chromenes are downfield shifted, which is probably associated with deshielding effect of the benzene ring since fragments lie in the same plane. Similarly, the effects in the complex **C** are explained, only protons H5 and H19 being influenced on by anisotropic effect. Note also that, no other H5 and H19 signals of the same complex **C** were

observed, although one may assume that the magnetic nonequivalence between these very protons in different molecules may exist. The rotation of the molecules around the metal cation seem to level the differences.

The structure of the chromene **1a** complexes with the lead cations were determined by the same way (Fig. 3.15). Resonances of protons signals in the complexes are much alike on those of barium and magnesium cations (Table 3.5). The only difference is the presence of weak intensity signals of one more group of protons in the presence of the excess of the ligand (Fig. 3.15b, group **D**). These signals also emerge in the NOESY spectrum as the chemical exchange cross-peaks. Peaks shifts allow possible detection of one more conformation of the 2:1 complex of *anti*-configuration, in which the ligand molecules are located in the space with dihedral angle $90^\circ < \theta < 180^\circ$ (Scheme 3.24). In chromene rotation around the metal ion, such structure is an intermediate, which was frozen due to the low temperature. Determination of the precise structure of this conformer failed due to weak intensities of the signals. In addition, two possible configurations of the complex have no distinguishing features in the signal positions, since the molecules cause no anisotropic impact on one another. The *anti*-complex is distinguished from 1:1 complex by virtually unchanged H3 and H4 signals, lower downfield shifts of H5 and H19, and shifted signals of aliphatic protons; these effects being probably due to distribution of the cation electron-withdrawing influence on the two ligands.

For chromene **3a**, similar studies of the complex formation with magnesium, barium, and lead cations were performed (Fig. 3.16). Signal assignment was also carried out using 2D NMR spectroscopy. As a result, 1:1 complexes for all metals and 2:1 complexes for barium and lead were identified (Scheme 3.25, Table 3.6). In contrast with compound **1a**,

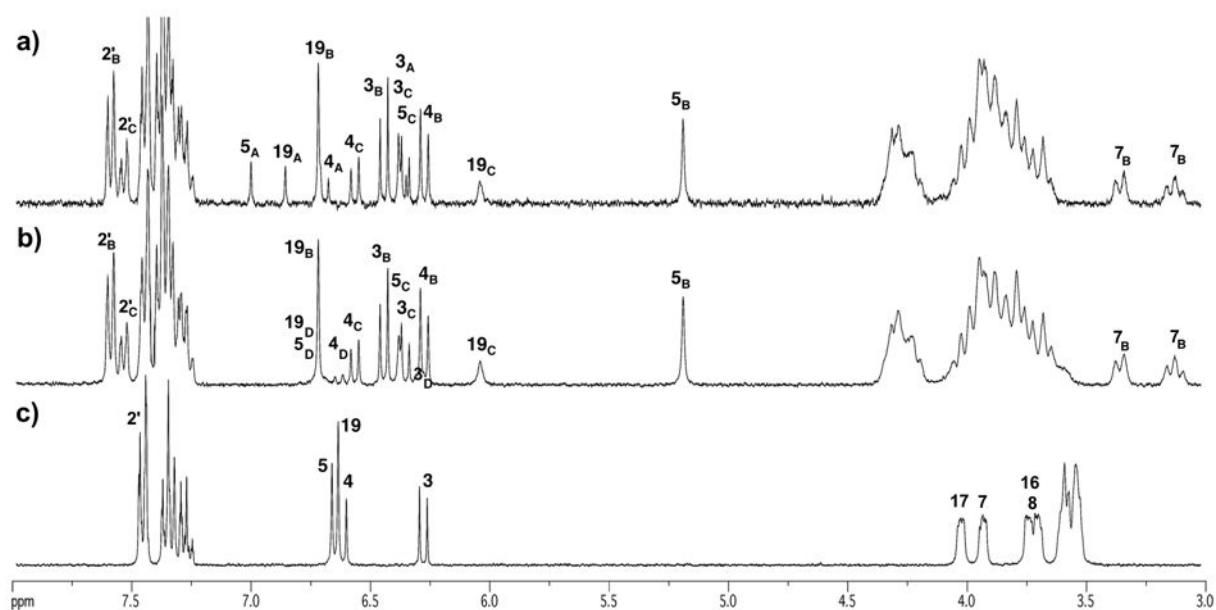
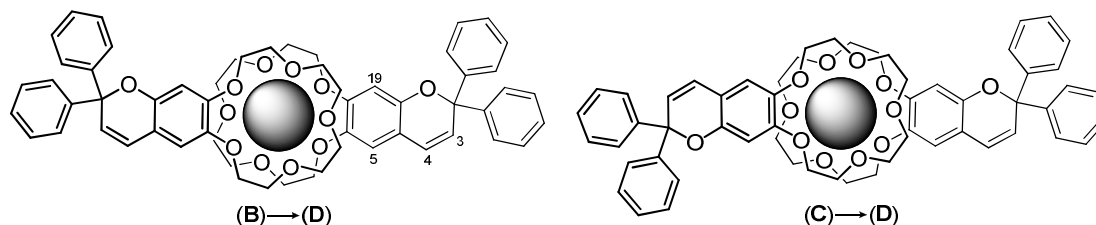


Figure 3.15. ^1H NMR spectra of chromene **1a** in the presence of lead cations at -45°C : a) $C_{1a} = 1 \cdot 10^{-3}$ M, $C_{Pb} = 1 \cdot 10^{-3}$ M; b) $C_{1a} = 2 \cdot 10^{-3}$ M, $C_{Pb} = 1 \cdot 10^{-3}$ M; c) $C_{1a} = 1 \cdot 10^{-3}$ M.



Scheme 3.24. Possible structures of *anti*-configuration (**D**) of the 2:1 complexes of chromene **1a** with lead cations.

temperature of the experiments caused different influence on the spectrum shape, not always giving the best results. Therefore, the temperature mode varied for different cases.

In the presence of magnesium cations, downfield shift of signals, like that in the case of **1a**, was observed (Fig. 3.16b). However, as the stability constant of 1:1 complex of the angular chromene is by an order of magnitude lower than that of 1:1 complex of the linear chromene, the spectrum also contained the free ligand signals. Temperature decrease shall also be taken into consideration, as stability of complexes depends on this parameter. The structure of **3a** complex with magnesium possesses some interesting features. For example, the signals of the methylene group protons 8 and 18 are significantly shifted downfield. Presumably, in the first case this is a consequence of the cation presence; in the second case, the reason is the deshielding effect of one of phenyl groups which approached the crown ether fragment. Thus, the second phenyl is located nearby atom H3 and, hence, shielding takes place resulting in the upfield shift of the signal. The rest of the aromatic protons affected by the electron-withdrawing effect of cation are farther shifted downfield (Table 3.6).

An interesting effect on the chromene is caused by the barium cations (Fig. 3.16c, d). Positions of group **B** signals are well described by the 2:1 complex structure (Scheme 3.25). Beside the electron-withdrawing effect of barium cation on H4 and H5 signals location, the deshielding effects of phenyl ring on H3 and chromene aromatic system on H6 are observed. The unexpected feature in this case is the formation of two conformations (**A1** and **A2**) of 1:1 complex. Signals **A1** are characterized by shifts similar to those in the presence of Mg^{2+} (Table 3.6). This allows to assume that the complexes have a similar structure. On the contrary, **A2** group is characterized by a downfield shift of all protons. Nevertheless, the observable spectral changes in the course of the experiments with varying temperature allowed a conclusion that **A2** signals correspond to another conformation of 1:1 complex (Fig. 3.17). As temperature increases, merging of **A1** and **A2** signals is observed that corresponds to rapid chemical exchange, typical for conformational interconversions. An additional proof of **A2** signals assignment to the 1:1 complex is similarity with the lead ions, where it is the only observed conformation. Apparently, the reason for such

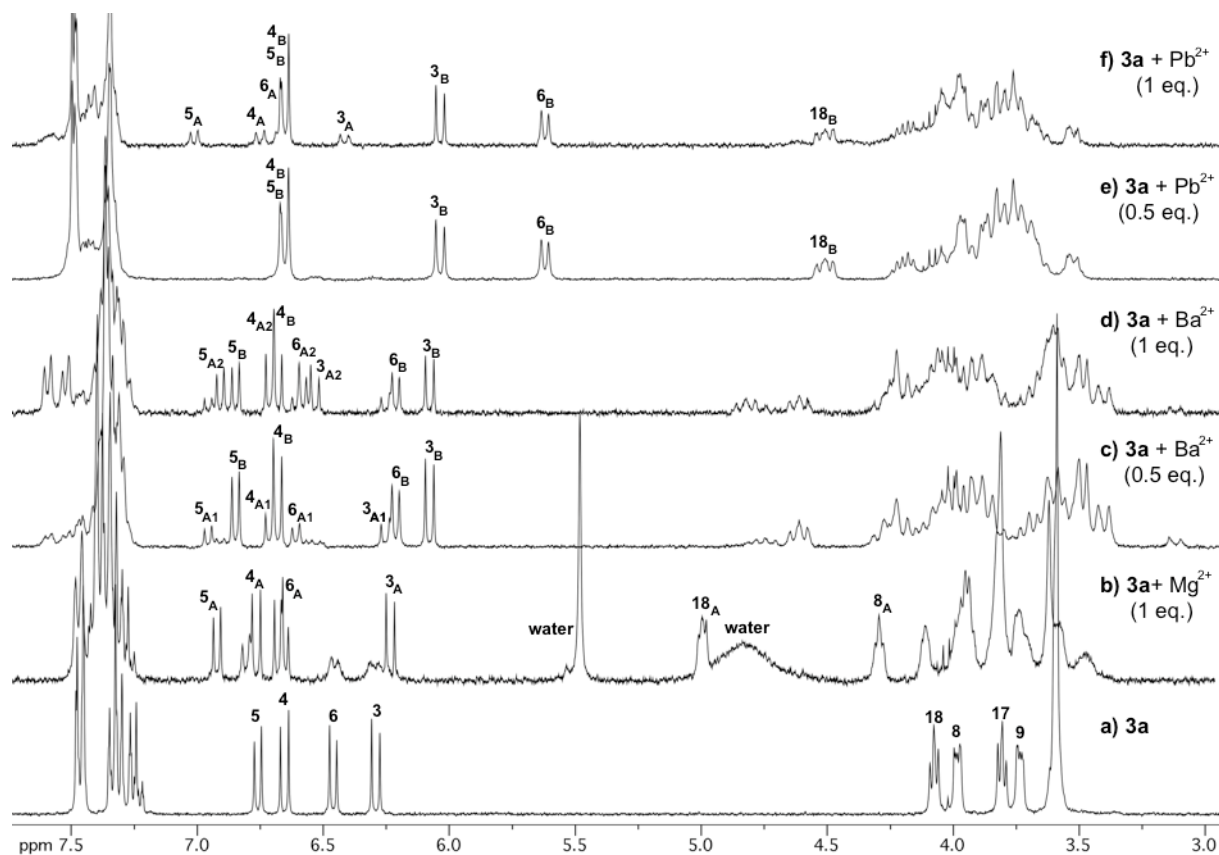
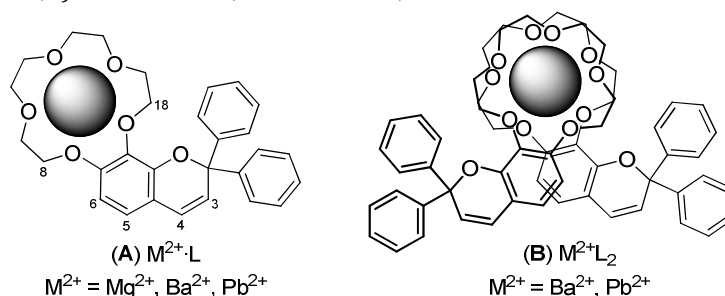


Figure 3.16. ^1H NMR spectra of chromene **3a** solutions in the presence of metal cations: a) $C_{3a} = 1 \cdot 10^{-3}$ M, -45°C ; b) $C_{3a} = 1 \cdot 10^{-3}$ M, $C_{\text{Mg}} = 1 \cdot 10^{-3}$ M, -45°C ; c) $C_{3a} = 2 \cdot 10^{-3}$ M, $C_{\text{Ba}} = 1 \cdot 10^{-3}$ M, -45°C ; d) $C_{3a} = 1 \cdot 10^{-3}$ M, $C_{\text{Ba}} = 1 \cdot 10^{-3}$ M, -45°C ; e) $C_{3a} = 2 \cdot 10^{-3}$ M, $C_{\text{Pb}} = 1 \cdot 10^{-3}$ M, 20°C ; f) $C_{3a} = 1 \cdot 10^{-3}$ M, $C_{\text{Pb}} = 1 \cdot 10^{-3}$ M, 20°C .



Scheme 3.25. Structures of **3a** complexes with metal cations.

Table 3.6.

Changes of aromatic proton signals shift in complexes of **3a** with metal cations compared with the free ligand ($\Delta\delta = \delta_{\text{complex}} - \delta_{3a}$).

	Mg^{2+}	Ba^{2+}		Pb^{2+}		
	A (1:1)	A1 (1:1)	A2 (1:1)	B (2:1)	A (1:1)	B (2:1)
H-3	-0.09	-0.05	+0.24	-0.21	+0.14	-0.23
H-4	+0.09	+0.04	+0.07	+0.03	+0.08	-0.03
H-5	+0.13	+0.19	+0.15	+0.09	+0.22	-0.15
H-6	+0.14	+0.13	+0.12	-0.25	+0.17	-0.90

intermediate position of barium in the sequence of cations is, on the one hand, its hardness, and on the other hand, its comparatively large size.

The “sandwich” complexes with lead cations, in contrast to barium, exhibited upfield shift of the aromatic protons what, which is possibly a consequence of the anisotropic influence of aromatic fragments of chromenes molecules (Fig. 3.16d, e). Such

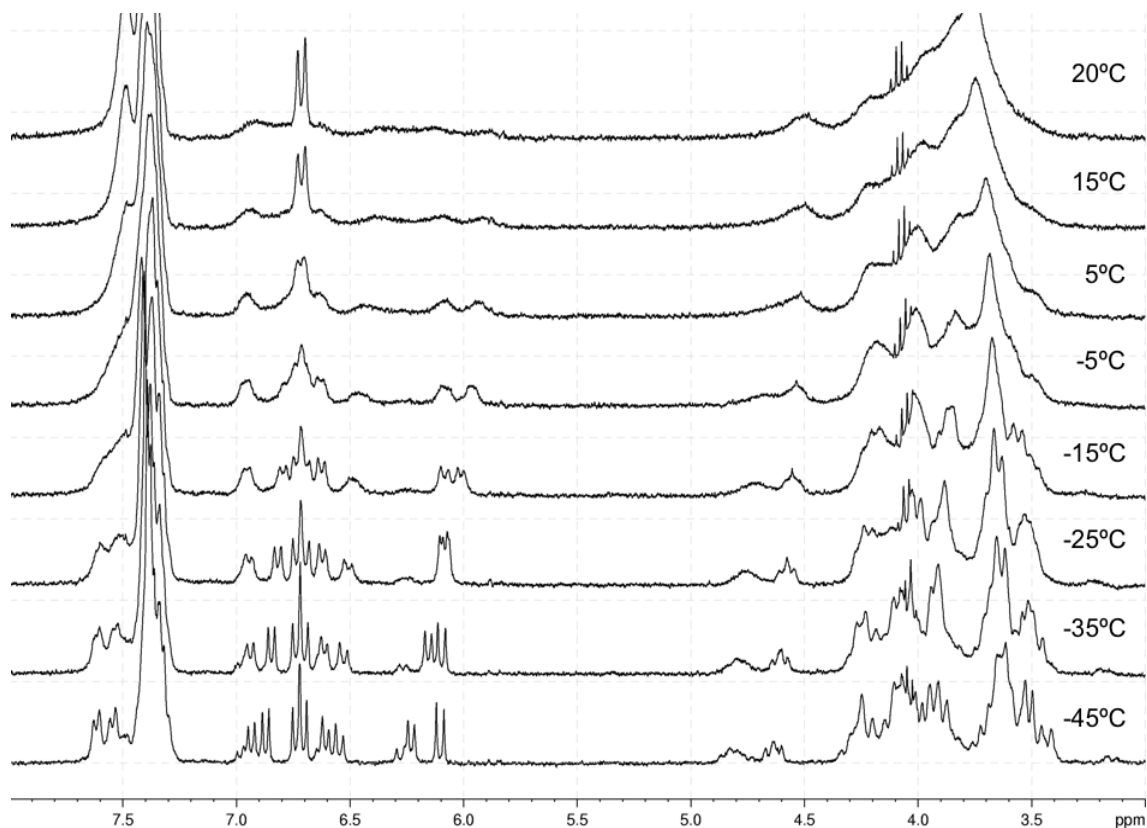
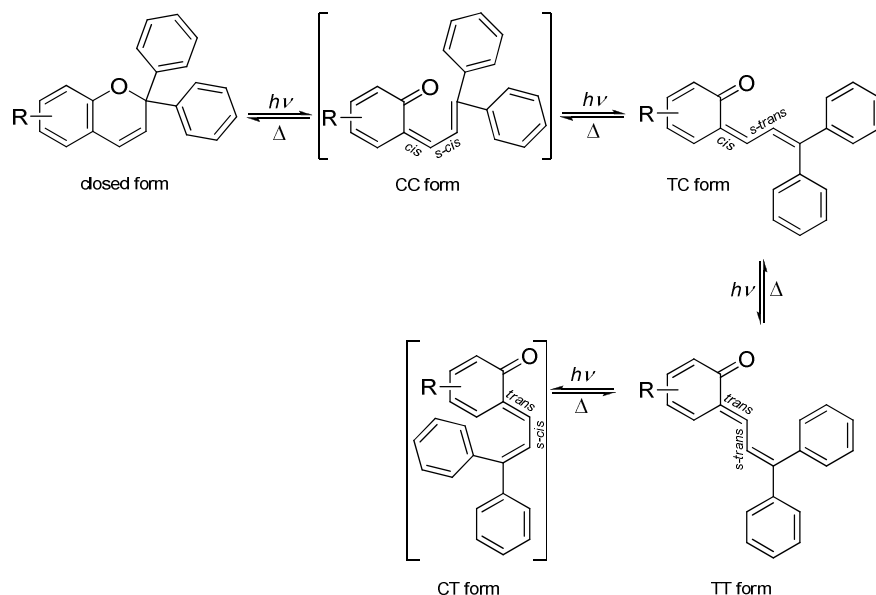


Figure 3.17. ^1H NMR spectra changes of **3a** solution in the presence of barium cations ($C_{1a} = 2 \cdot 10^{-3}$ M, $C_{Ba} = 1 \cdot 10^{-3}$ M) depending on the test temperature. The experiments at -45° , -35° , -25° , -15° , -5° , 5° , 15° , and 20°C are shown bottom-upwards.

effect may result from the proximity of the ligands and high conformational changes of phenyl group locations.

Upon UV-radiation, chromenes **1a** and **3a** undergo structural transformations, the two most stable isomers, the so-called TC and TT forms, being formed (Scheme 3.26). The pyran cycle is a $[4n+2]$ electron system that promotes the electrocyclic ring opening and reverse cyclization. Upon irradiation, at the first stage a spatially hindered CC (*s-cis-cis*) isomer is formed, which rapidly converts into a more stable TC (*s-trans-cis*) form. The consecutive *cis-trans* isomerization produces a TT (*s-trans-trans*) configuration. The latter isomer may also be transformed into a CT (*s-cis-trans*) form which, similarly to the CC, is the spatially hindered one. In the experiments, however, the CC and CT isomers are not detected by spectrophotometric methods.

The process of phototransformation may be tracked by UV-Vis spectroscopy. The open form is characterized by absorption in the visible region, which gradually disappears upon cessation of irradiation. Linear isomer **1a** exhibits two bands with $\lambda_{\text{max}} = 390$ and 470 nm. For the angular chromene **3a**, two bands with $\lambda_{\text{max}} = 410$ nm and $\sim 520\text{-}530$ nm (Fig. 3.18) are observed, low intensity of which is due to low stability of the open form in a polar solvent (acetonitrile) that is generally typical of chromenes.



Scheme 3.26. Chromenes phototransformation.

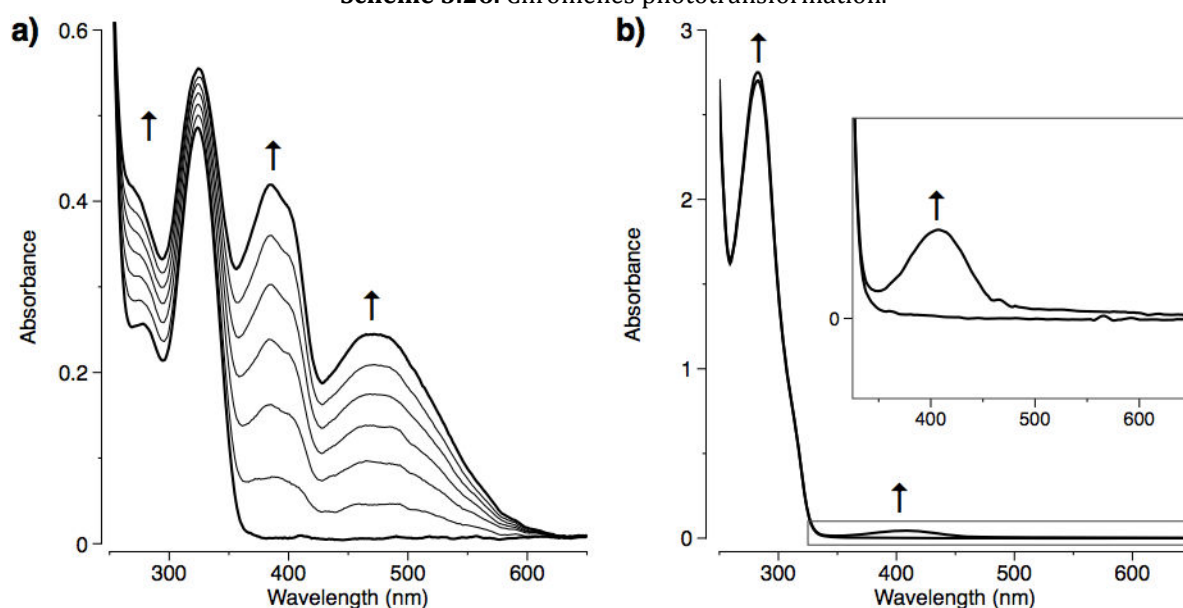


Figure 3.18. Changes in absorption spectra of chromenes **1a** and **3a** in acetonitrile upon irradiation: a) $C_{1a} = 7 \cdot 10^{-5} \text{M}$, 25°C , $\lambda_{\text{irrad.}} = 313 \text{ nm}$, 2 min; b) $C_{3a} = 2.7 \cdot 10^{-4} \text{M}$, 10°C , $\lambda_{\text{irrad.}} = 317 \text{ nm}$, 2 min.

The stability of the photoinduced forms is defined by kinetic characteristics of thermal bleaching (relaxation), namely: the reaction rate constant (k) and half-life time ($\tau_{1/2}$). For chromene **1a**, optical density change at $\lambda = 400 \text{ nm}$ during irradiation (first 180 s) and after its termination (bleaching of the solution) is shown in Fig. 3.19. The thermal bleaching curve is properly described by a mono-exponential dependence. Therefore, only a single photoinduced form can be detected at room temperature; however, using the UV-Vis spectroscopy data, it cannot be ascribed to the TT or TC form. The attempts to determine the kinetic parameters of the angular chromene **3a** failed because of extremely rapid bleaching under normal conditions.

Using the NMR spectroscopy for the studying the photochrome transformations can determine the photoinduced species formed and evaluate their stability. Irradiation of a

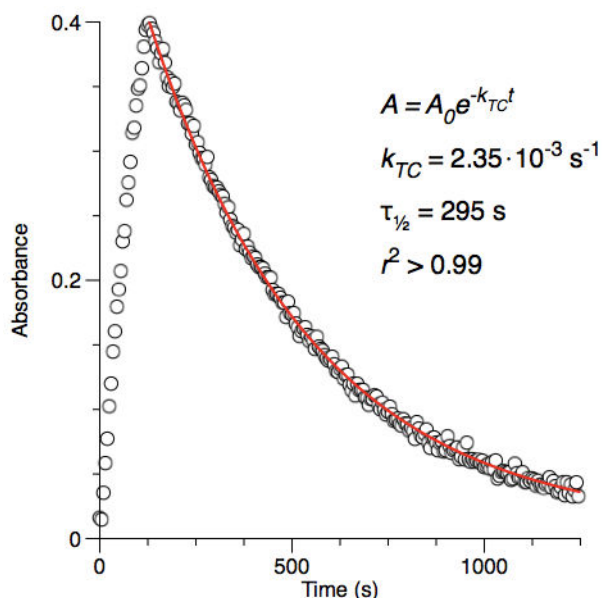


Figure 3.19. Kinetic parameters determination of chromene **1a** bleaching in acetonitrile at 25°C ($C_{1a} = 7 \cdot 10^{-5}$ M, $\lambda = 400$ nm). (A , A_0 are absorbances, r^2 is the correlation coefficient).

chromene solution causes occurrence of the open form signals in ^1H NMR spectrum; the intensity of the signals vary depending on the irradiation duration. Since at 25°C bleaching is relatively fast, the satisfactory NMR spectra were recorded at low temperature.

Chromene **1a** was studied at 0°C (Fig. 3.20). The open form signals, with the intensity increasing during irradiation, were observed in the spectrum. A signal that can be ascribed to the TC form is the signal of proton H3 at ~ 8.6 ppm, which resonance is caused by deshielding effect of carbonyl group nearby (Fig. 3.20a). Other signals were assigned on the basis of 2D spectroscopy (COSY, HSQC, HMBC). On cessation of irradiation, the reverse process was observed, the closed form signals being increased and those of the open form being decreased (Fig. 3.20b). Monitoring the signal ratio allowed to determine the kinetic parameters of the each form during bleaching (Fig. 3.21). At 0°C, bleaching is rather slow; the TC form has the bleaching constant of $8.25 \cdot 10^{-5} \text{ s}^{-1}$, whereas the TT form signal intensity is virtually unchanged. Taking into account that the bleaching rate increases with temperature, at 25°C thermal relaxation of the TC form is observed.

To observe the photoinduced products of angular chromene **3a** by the NMR technique, it was necessary to decrease the temperature down to -45°C (Fig. 3.22). In contrast to chromene **1a**, even after 20 minutes of irradiation, the spectrum of **3a** showed no TT species formation. A similar analysis of the bleaching kinetics gave the rate constant of $8.34 \cdot 10^{-5} \text{ s}^{-1}$. Therefore, compound **3a** is characterized by a low stability of open forms, which was insufficient for successful spectrophotometric detection.

With respect to this behavior of chromenes **1a** and **3a**, the experiments in the presence of metal cations were performed. Preliminary investigations have already shown

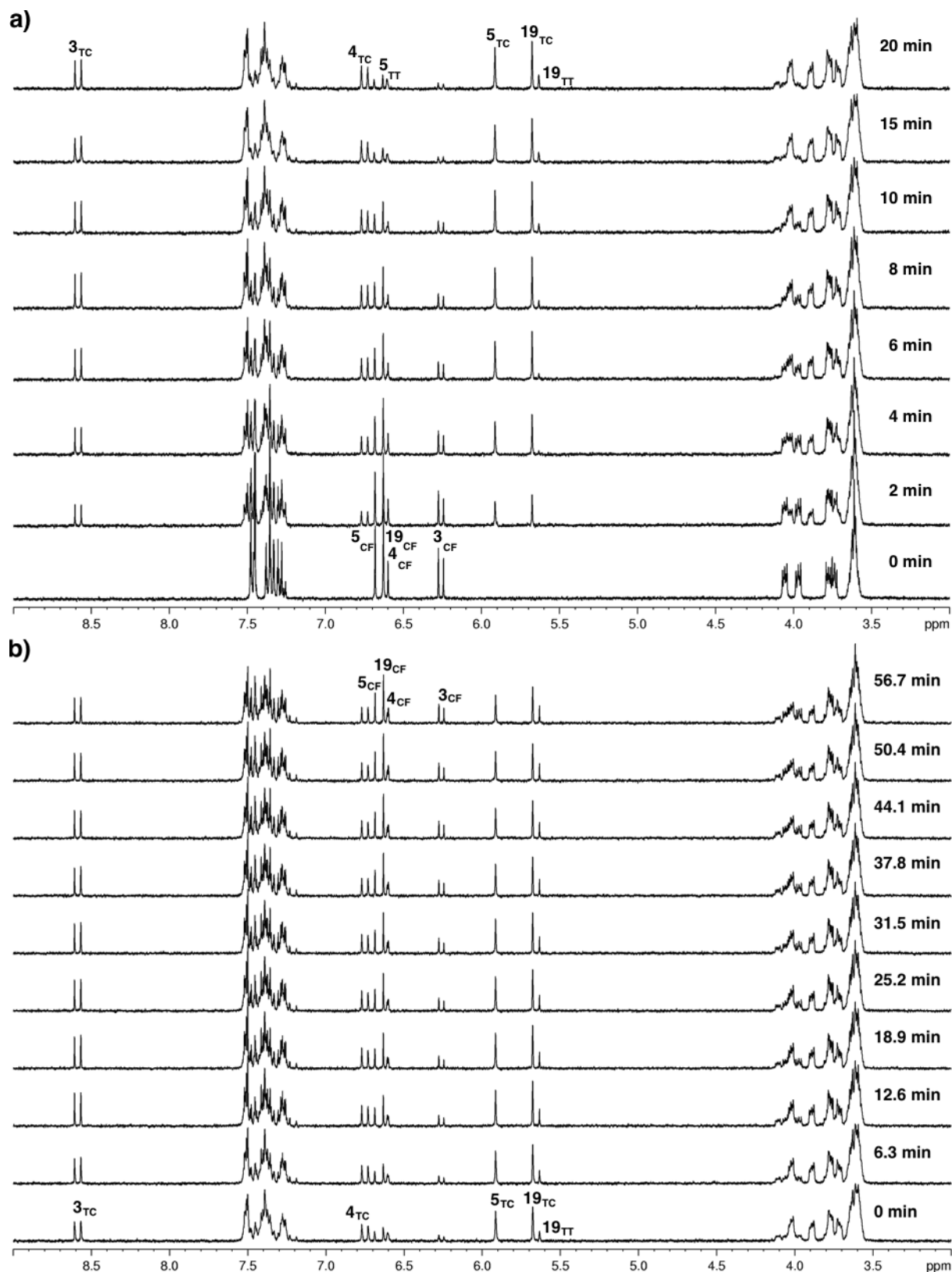


Figure 3.20. Chromene **1a** photochromism observation ($C_{1a} \sim 1 \cdot 10^{-3}\text{M}$, CD_3CN , 0°C) by ^1H NMR spectroscopy: a) irradiation at 313 nm (filtered light), total irradiation time shown on the right; b) thermal relaxation of the same solution after irradiation, spectra were recorded every 6.3 min (380 s).

that addition of cations significantly accelerates the bleaching process. Unfortunately, in the case of **3a**, even at -45°C this process was extremely fast that did not allow monitoring.

In the case of chromene **1a**, upon addition of the cations the bleaching rate increases to a maximum value that is insensitive to further growth of the ion concentration

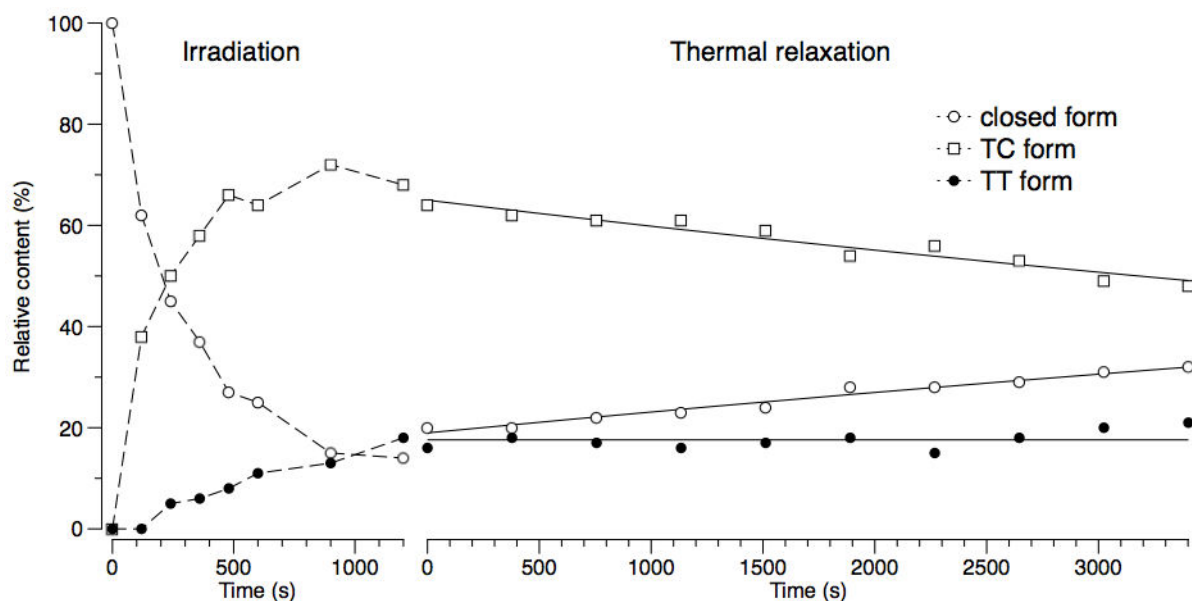


Figure 3.21. Variations of the intensities of the chromene **1a** closed and open forms signals in ^1H NMR spectrum during irradiation and bleaching at 0°C .

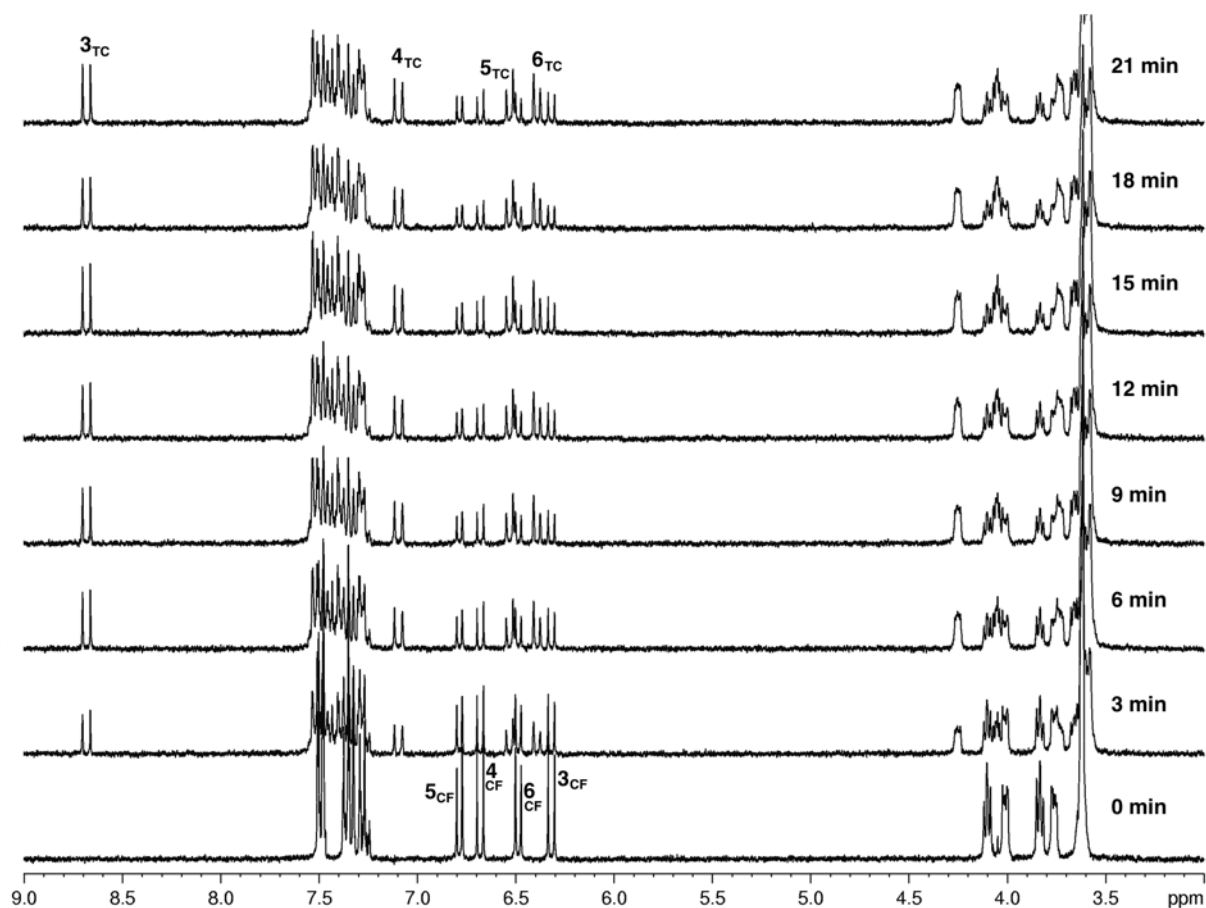


Figure 3.22. ^1H NMR spectrum change of chromene **3a** upon irradiation (313 nm) at -45°C .

(Fig. 3.23). In the presence of magnesium ions the changes terminated at $C_{\text{Mg}}/C_{1\text{a}} > 2$ with indicative inflection of the titration curve at $C_{\text{Mg}}/C_{1\text{a}} = 1$ (Fig. 3.23d). Prior to irradiation, the solution with ratio $C_{\text{Mg}}/C_{1\text{a}} < 1$ contains both the free ligand and the ligand as part of the complex. When irradiated, both these species produce the open forms, which ratio is to define the bleaching kinetics. As the quantity of metal increases ($C_{\text{Mg}}/C_{1\text{a}} > 1$), all the ligand

molecules appear to be complexed both prior to and after irradiation. Bleaching of the open form (TC) complex with magnesium becomes the main process that defines the kinetics as the quantity of the free colored form is extremely low and makes no significant contribution into the reaction rate. Thus, providing $C_{Mg}/C_{1a} > 2$, the relaxation of the open form complex (TC) with magnesium ion is observed, the rate constant of bleaching being 0.1 s^{-1} that is over 40-fold higher than the corresponding value of the free TC form. In other words, 7 and 295 s are required for a two-fold decrease of absorbance intensity of the complex and the free form, respectively.

In the case of barium and lead cations, two types of complexes are generated, 2:1 and 1:1 complexes being formed in deficient and excessive content of metal cations, respectively. Chromene solutions with Ba^{2+} or Mg^{2+} demonstrated mono-exponential bleaching kinetics (Fig. 3.23b). In the case of Pb^{2+} , the absorbance change after irradiation was clearly biexponential (Fig. 3.23c). The thermal relaxation rate constants of barium and lead complexes varied similarly to that of magnesium complexes, namely: the gradual increase was followed by a plateau. At $C_M/C_{1a} > 3$, the rate constant change stopped; the maximal value for barium and lead were ~ 0.06 and 0.075 s^{-1} , respectively (Fig. 3.23d), being 25- and 32-times higher than that for the free open form ($k = 2.35 \cdot 10^{-3} \text{ s}^{-1}$). Thus, destabilizing influence on photoinduced forms decreases in the sequence $\text{Mg}^{2+} > \text{Pb}^{2+} > \text{Ba}^{2+}$. This dependence coincides with the cation size increase and, consequently, the surface charge density decrease, which affects the electron density distribution in the complex.

All the above considerations are based on the assumption that short irradiation time leads to predominant formation of a single photoinduced isomer (most likely the TC). Such suggestion is proven experimentally. The bleaching curve is mono-exponential both without metals (Fig. 3.19) and with magnesium or barium cations added (Fig. 3.23a, b). Moreover, the solution is almost completely bleached, concentration of nonbleaching or extremely slowly bleaching ($k < 1 \cdot 10^{-4}$) component being very low and comparable with the measuring inaccuracy. Such a component may be the TT form, which due to a short-term irradiation is formed in negligible quantity or is not formed at all.

In contrast to the magnesium and barium cations, in the presence of the lead cations, the TT species were formed in measurable amount. When metal content was low ($C_M/C_{1a} < 1$), the quantity of the nonbleaching component was increasing along with the Pb^{2+} concentration. Starting from $C_M/C_{1a} = 1$ the kinetic curve became biexponential simultaneously with increase of the second component concentration (Fig. 3.23c). Thus, along with lead concentration increasing, the ratio of the TC and TT species formed was

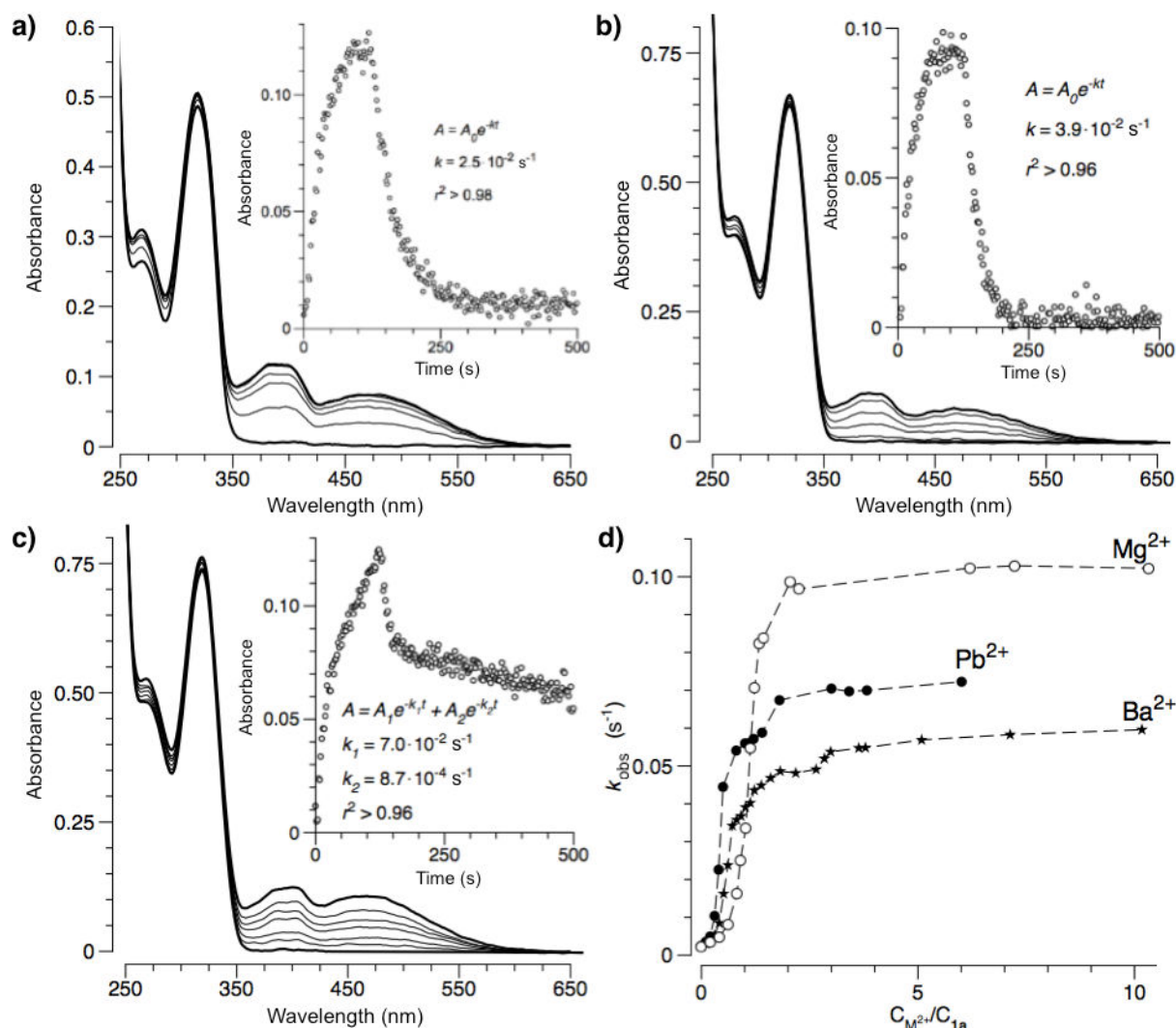
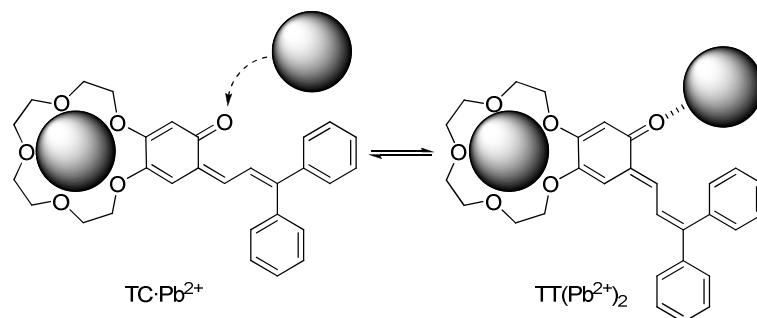


Figure 3.23. The study of chromene **1a** complex formation upon irradiation (25°C): a) in the presence of Mg^{2+} ($C_{1a} = 7.33 \cdot 10^{-5} \text{ M}$, $C_{Mg}/C_{1a} = 0.9$); b) in the presence of Ba^{2+} ($C_{1a} = 1.17 \cdot 10^{-4} \text{ M}$, $C_{Ba}/C_{1a} = 1$); c) in the presence of Pb^{2+} ($C_{1a} = 1.17 \cdot 10^{-4} \text{ M}$, $C_{Pb}/C_{1a} = 3$); d) bleaching rate constants dependence on the metal concentration ($\lambda = 400 \text{ nm}$). (A , A_0 , A_1 , A_2 are absorbances; k , k_1 , k_2 are bleaching rate constants for colored forms; r^2 is the correlation coefficient.)

changing so that at high Pb^{2+} excess ($C_M/C_{1a} = 7 - 50$) the TC isomer contribution to the observed bleaching kinetics was minimal, and the bleaching curve became mono-exponential again. Note that the absorption spectra of the open forms demonstrated a slight intensity increase of the long-wavelength absorption band (compare Figs. 18a, 23a-c). Such effect may be explained by lead cation coordination with the carbonyl oxygen atom of the open form. For the TC isomer, such interaction is hindered due to spatial configuration of the ligand. This, in turn, may provide an explanation of unusual thermal conversion of the TC form into the TT one. Metal coordination with the carbonyl oxygen atom should significantly affect the chromophore system resulting in the red shift and an intensity increase of the long-wavelength absorption band (in contrast to coordination with the crown ether fragment). In this case, excessive metal may induce mutual compensation of all these effects in the TT form complex with two Pb^{2+} cations (LM_2) that results just in a small variation of intensities



Scheme 3.27. Possible complex formation of the chromene **1a** TT form, in which lead cation coordinates with carbonyl oxygen atom.

ratio of the long-wavelength absorption bands (Scheme 3.27). The increase of the cation concentration also led to increase in the bleaching rate constant of the complex.

Irradiated solutions of chromene **1a** in the presence of cations were studied by NMR at low temperature (-45°C) that allowed slowing down the reverse transformation of the photoinduced forms. The use of more powerful radiation source (Xe-Hg lamp, 1000W) also caused high conversion of the initial chromene to the open isomers (up to *ca.* 90%, see Fig. 3.21). Nevertheless, interpretation of the spectra was complicated by the presence of numerous overlapped, frequently broadened, signals.

Irradiation of a solution of chromene **1a** in the presence of magnesium cations induced signals corresponding to the free TC form and to that in $\text{TC}\cdot\text{Mg}^{2+}$ complex (Fig. 3.24b). The free ligand signals were predominant and broadened. Few signals of the initial $\mathbf{1a}\cdot\text{Mg}^{2+}$ complex were also present. Further observation of the thermal relaxation (Fig. 3.24c -f) detected gradual elimination of $\text{TC}\cdot\text{Mg}^{2+}$ complex signals to be much faster than that of the free TC isomer. At the same time, gradual increase of the initial $\mathbf{1a}\cdot\text{Mg}^{2+}$ complex and the free TT form signals was observed.

To explain the observed effects, we suggested a scheme that shows processes in the solution after irradiation (Scheme 3.28). Prior to irradiation, the solution generally contains 1:1 complex of **1a** with magnesium. Its phototransformation produces $\text{TC}\cdot\text{Mg}^{2+}$ complex, which has low stability constant and decomposes, resulting in the free TC isomer signals emerging. Upon cessation of irradiation, the free TC species transform into the initial chromene **1a**, which immediately forms a complex with magnesium. At the same time, $\text{TC}\cdot\text{Mg}^{2+}$ complex, beside equilibrium with the free TC form, may participate in conversion into $\text{TT}\cdot\text{Mg}^{2+}$ complex, the latter being unstable, too. This explains the presence of the TT form signals, stable at experiment temperature, in the spectrum. Note also that, in the absence of metal ions, thermal transformation of the TC form into the TT one is not observed. Consequently, this process may be stimulated only by cations. The described effect, in turn, was not observed during spectrophotometric studies at higher temperature

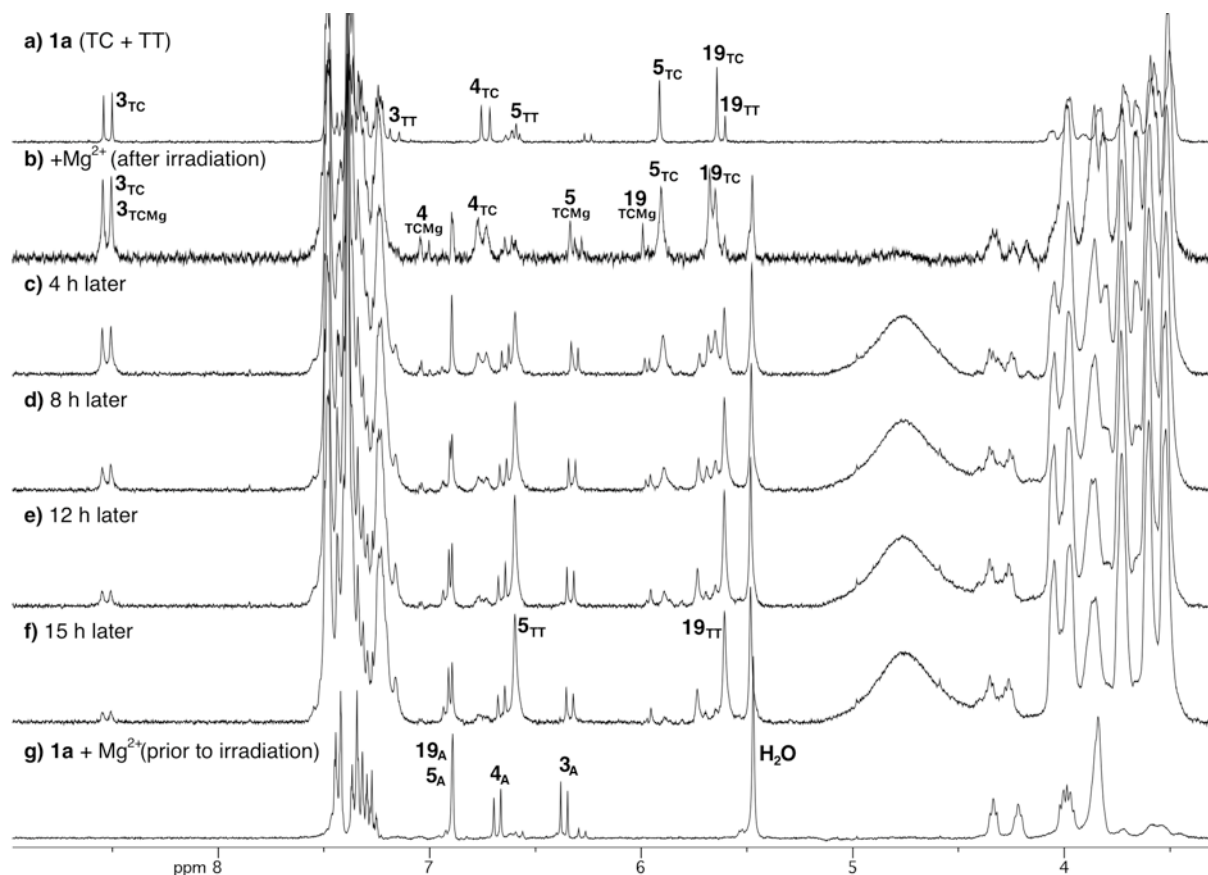
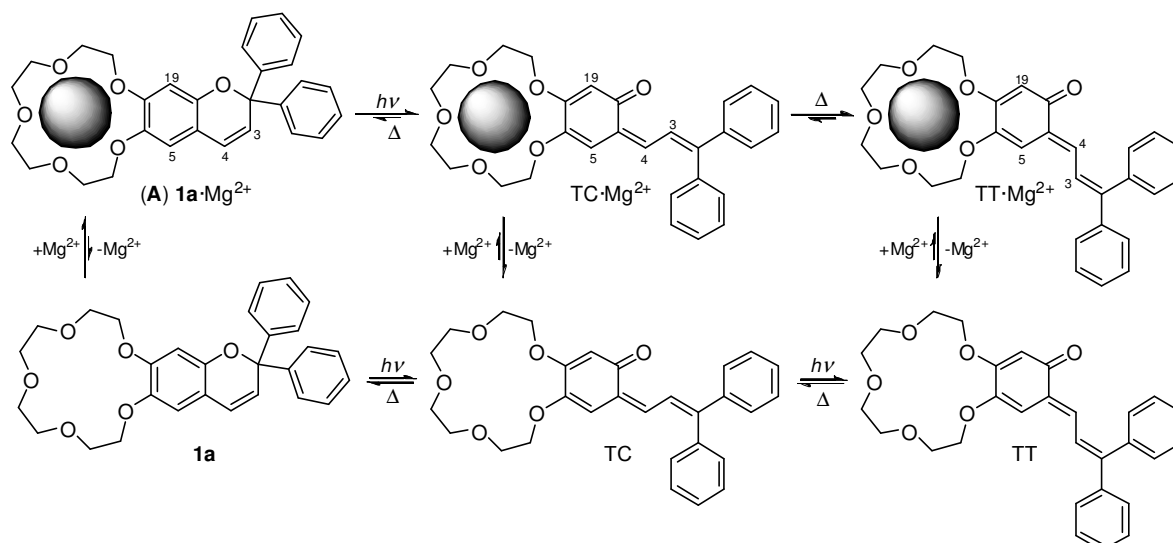


Figure 3.24. Changes in ^1H NMR spectra of chromene **1a** solution in the presence of magnesium cations during and after irradiation at -45°C ($C_{1a} = 1 \cdot 10^{-3} \text{ M}$, $C_{\text{Mg}}/C_{1a} = 1$): a) **1a** after irradiation in the absence of metal; b) **1a** after irradiation in the presence of cations; c)-f) spectra 4, 8, 12, and 15 hours after cessation of irradiation, respectively; g) **1a** in the presence of cations prior to irradiation.

(25°C). Hence, it could be concluded that at higher temperature (25°C), a thermally stable product ($\text{TC} \cdot \text{Mg}^{2+}$ in this case) predominates in the solution, whereas at low temperature (-45°C), formation of a kinetically stable product ($\text{TT} \cdot \text{Mg}^{2+}$) becomes possible.

In the presence of barium or lead cations, the interpretation of spectra after irradiation was very complicated due to numerous broadened (especially for barium) and



Scheme 3.28. Presumable behavior of chromene **1a** complex with magnesium cations during and after irradiation.

overlapped peaks (Fig. 3.25). This is due to the formation of multiple, compared with magnesium, possible complexes that formed during irradiation. The analysis of the signal intensities as well as 2D spectroscopy data indicated formation of the TC form in a complex with typical proton H3 resonance at 8.6 ppm. Nevertheless, our attempts to assign signals to 1:1 or 2:1 complexes failed.

For both cations, the formation of the mixed 2:1 complex, containing chromene molecule in the closed and open (TC) forms, was also observed (Fig. 3.25, Scheme 3.29). Apparently, this is a transient state of one of 2:1 complexes in course of step-wise transformation upon irradiation. Characteristic are the aromatic protons signals distinct from

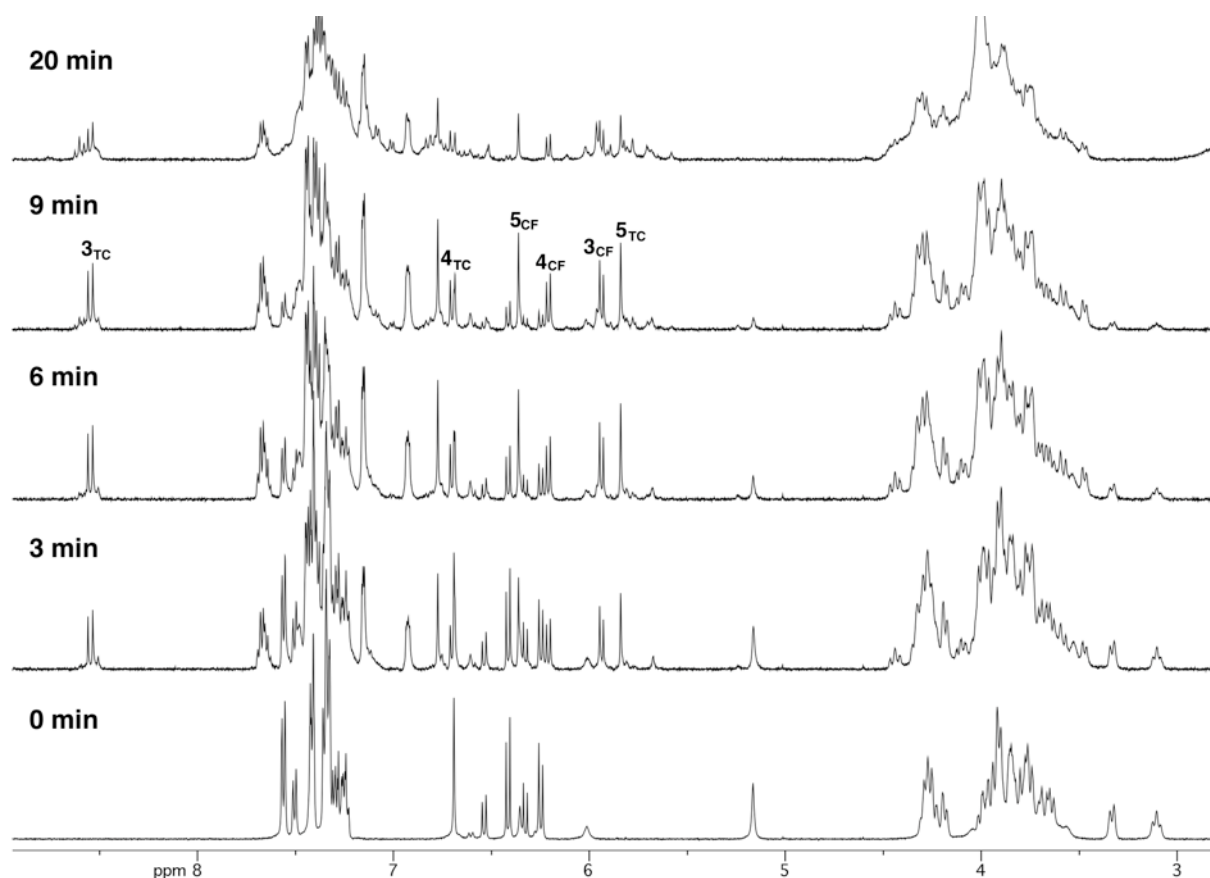
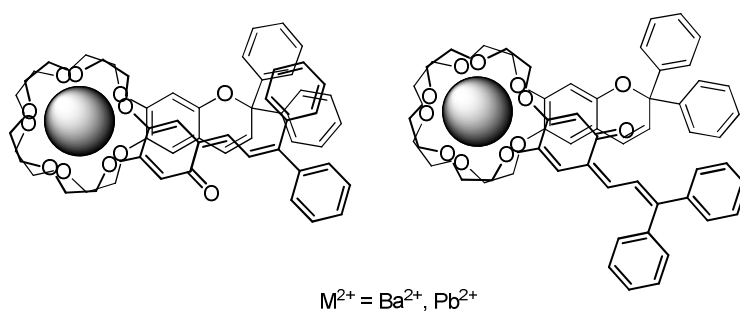


Figure 3.25. Changes in ^1H NMR spectrum of chromene **1a** solution in the presence of lead cations during and after irradiation exposure of 0, 3, 6, 9, and 20 min ($C_{1a} = 1 \cdot 10^{-3}$ M, $C_{\text{Pb}}/C_{1a} = 0.5$). The TC and CF signals correspond to the TC and closed form in the mixed 2:1 complex.



Scheme 3.29. Structures of chromene **1a** mixed 2:1 complexes with barium and lead cations.

Table 3.7.

Changes of aromatic proton signal shifts in complexes of **1a** with metal cations compared with the free ligand ($\Delta\delta = \delta_{\text{complex}} - \delta_{\text{1a}}$).

	Mg ²⁺	Ba ²⁺			Pb ²⁺	
	TC·Mg ²⁺	TC·Ba ²⁺ or TC ₂ Ba ²⁺	TC·Ba ²⁺ ·CF (2:1)		TC·Pb ²⁺ ·CF (2:1)	
			TC	CF	TC	CF
H-3	+0.01	+0.01	+0.01	-0.36	+0.03	-0.31
H-4	+0.30	+0.11	0.00	-0.40	-0.04	-0.38
H-5	+0.44	-0.14	-0.03	-0.24	-0.07	-0.26
H-19	+0.36	+0.40	+1.18	+0.19	--	--

those of the free forms and other complexes described above (Table 3.7). Similar to magnesium, thermal relaxation of irradiated solutions demonstrated the TC-TT conversion; however, the accurate measurements failed because of poor spectrum resolution.

Thus, the study of chromene **1a** complex formation with metal cations under irradiation was impeded, on the one hand, by low stability of the open forms in the presence of metals, which required lowering the temperature, and, on the other hand, by numerous complexes of various composition formed under irradiation. While magnesium ions may form only few complexes, barium and lead turned out to form various mixed complexes.

As a result, photochromism and complex formation with metal cations of chromenes **1a** and **3a**, containing the annelated 15-crown-5 ether fragment, were studied using UV-Vis absorption and NMR spectroscopies. The annelation position causes a strong impact on the photochromic properties of the compounds described. Upon irradiation, **1a** converts into the colored forms of various stability, namely: the TC isomer has relatively slow bleaching kinetics ($k^{25^\circ\text{C}} = 2.35 \cdot 10^{-3} \text{ s}^{-1}$, $k^{0^\circ\text{C}} = 8.25 \cdot 10^{-5} \text{ s}^{-1}$) and is stable at -45°C , whereas the TT isomer is stable in the entire temperature range used ($-45 \dots 25^\circ\text{C}$). Angular chromene **3a** has a poor colorability and low thermal stability of the photoinduced forms in acetonitrile even at -45°C ($k^{-45^\circ\text{C}} = 8.34 \cdot 10^{-5} \text{ s}^{-1}$); these properties impeded the study of the isomer.

Using UV-Vis absorption and the NMR spectroscopy methods, the quantity, composition and stability of **1a** and **3a** complexes with magnesium, barium, and lead cations were determined. For all metals, 1:1 complexes were detected; for barium and lead, 2:1 sandwich complexes were also observed. In addition, in the case of the linear isomer, the formation of two types of 2:1 complexes with different ligand symmetry in relation to metal cation was observed. Complexes stability constants are similar for the metals investigated, although stability of the complexes with lead cations is slightly higher.

Studies under irradiation indicated (on the example of compound **1a**) the mutual influence of photochromism and complex formation on each other. According to the NMR

spectroscopy data, complexes of the open forms with cations are less stable than those of the closed species. On the other hand, the destabilizing effect of the metal ions (and hence, the complex formation) onto thermal stability of the open forms, bleaching rate constant being increased by 1-2 orders of magnitude was demonstrated (Table 3.8).

In addition, an unusual isomerization of the TC form into the TT form in the presence of cations at low temperature was observed. At 25°C, this process was only detected with the lead cations and at high metal excess. This allows a suggestion that a complex of the TT form, with coordination between the Pb^{2+} cations and the carbonyl oxygen atom, was formed.

Table 3.8.

Comparison of bleaching rate constants (k) of the chromene **1a** free forms and in complexes with metal cations (maximal experimental value) at 25°C (acetonitrile).

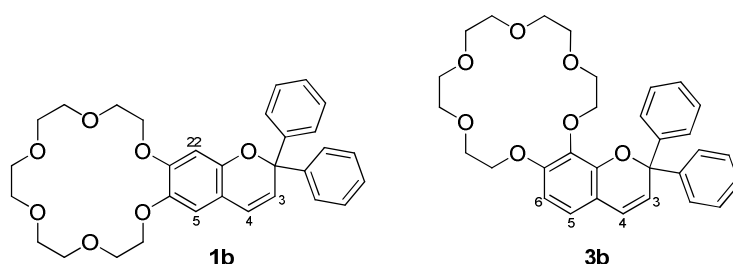
	1a	1a + Mg^{2+}	1a + Ba^{2+}	1a + Pb^{2+}
k_{TC} (s^{-1})	$2.35 \cdot 10^{-3}$	$1 \cdot 10^{-1}$	$6 \cdot 10^{-2}$	$7.5 \cdot 10^{-2}$
k_{TT} (s^{-1})	—*	—*	—*	$1 \cdot 10^{-2}$

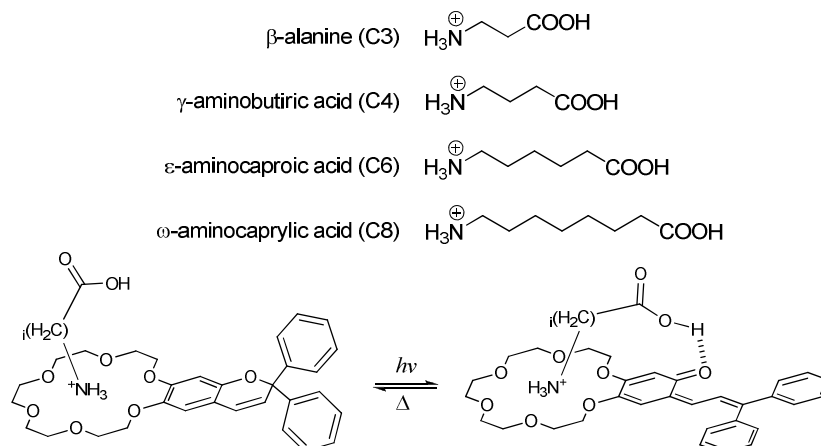
* formation was not detected at short-term irradiation by Hg lamp, 120 W.

3.2.1.2. Complex Formation of Chromenes **1b** and **3b** with Amino Acids

The complex formation of chromenes **1b** and **3b** with the protonated amino acids $NH_3^+-(CH_2)_i-COOH$ of different chain length was studied. Perchlorates of four amino acids were used, namely those of β -alanine ($C3$, $i = 2$), γ -aminobutyric ($C4$, $i = 3$), ϵ -aminocaproic ($C6$, $i = 5$), and ω -aminocaprylic ($C8$, $i = 7$) acid. As the model compound, ammonium perchlorate was used, which is able to coordinate with the crown ether fragment exclusively. For the amino acids of interest, a monotopic coordination with the closed forms and, depending on the carbon skeleton length, ditopic coordination with the open forms.

Preliminary molecular modeling using MOPAC/PM6 package [134] showed a potential possibility of such complexes to be formed (Fig. 3.26). For the linear isomer, the ditopic complex formation was possible for a number of methylene fragments $i > 4$ ($C5$ or higher); for the angular chromene, with a closer position of the two coordination sites, the modeling showed such possibility even for $i = 2$ ($C3$, β -alanine) and higher.





Scheme 3.30. Scheme of chromene **1b** complex formation with protonated amino acids prior to and after irradiation.

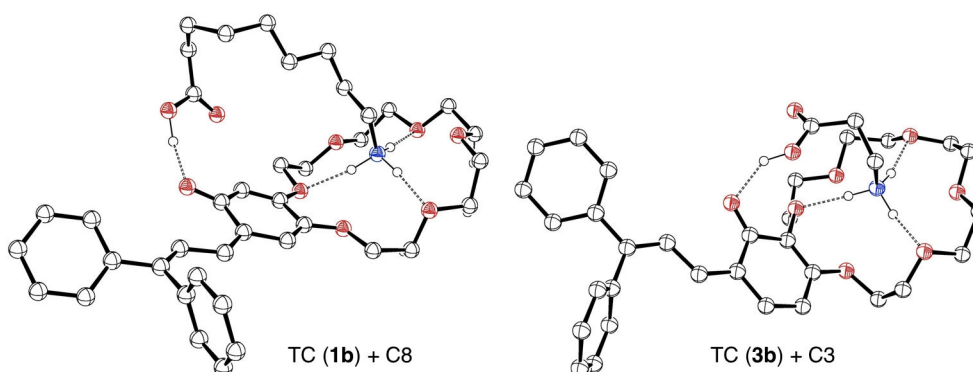


Figure 3.26. MOPAC/PM6 optimized structures of ditopic **1b** and **3b** TC form complexes with amino acids (for convenience, hydrogen atoms not participating in hydrogen bonds are omitted).

Similarly to the investigations of chromenes **1a** and **3a**, the complex formation with metal ions, compounds **1b** and **3b** were studied by UV-Vis absorption and NMR spectroscopy. Protonated amino acids were prepared by the reaction of their neutral forms with perchloric acid in acetonitrile.

Coordination with the crown ether fragment was proved by the NMR data (Fig. 3.27) showing that in the presence of the amino acids the major changes were aliphatic protons signals shape and position. Proton peaks of the crown ether fragment were shifted downfield that was caused by the electron-withdrawing group (ammonium cation) presence in the macrocycle cavity. Changes of the aromatic proton signals were less significant.

Spectrophotometric titration allowed determining of the quantity and stability of complexes. The analysis of data indicated the 1:1 complex presence in solution. In contrast to the metal ions, ammonium cations and amino acids caused no considerable effect on the long-wavelength absorption band, whereas in short-wavelength regions the effect of their presence was more noticeable (Fig. 3.28). The spectra of the complexes showed a slight blue shift. Such effects may provide evidence of the crown ether fragment coordination with the ammonium cation. Similar behavior was observed for angular isomer **3b**. Stabilities of

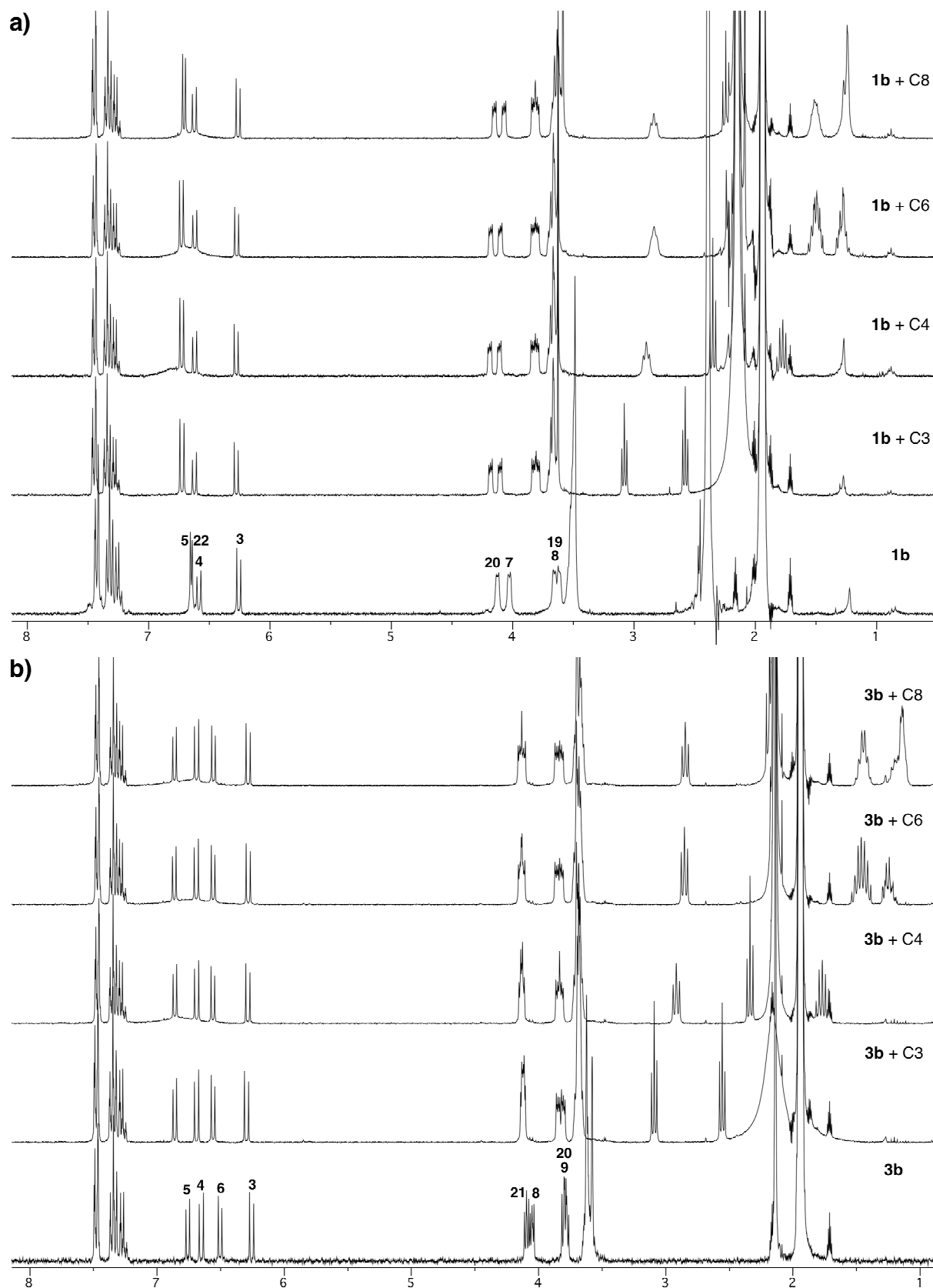


Figure 3.27. ^1H NMR spectra of chromenes **1b** and **3b** solutions in the presence of amino acids: a) **1b**, $C_{1b} = 1 \cdot 10^{-3}$ M, $C_{AA}/C_{1b} = 1$, -45°C ; b) **3b**, $C_{3b} = 1 \cdot 10^{-3}$ M, $C_{AA}/C_{3b} = 1$, 20°C .

complexes of the closed forms with amino acids and ammonium cations were comparable and ranged within 4.4-4.9 logarithmic units (Table 3.9).

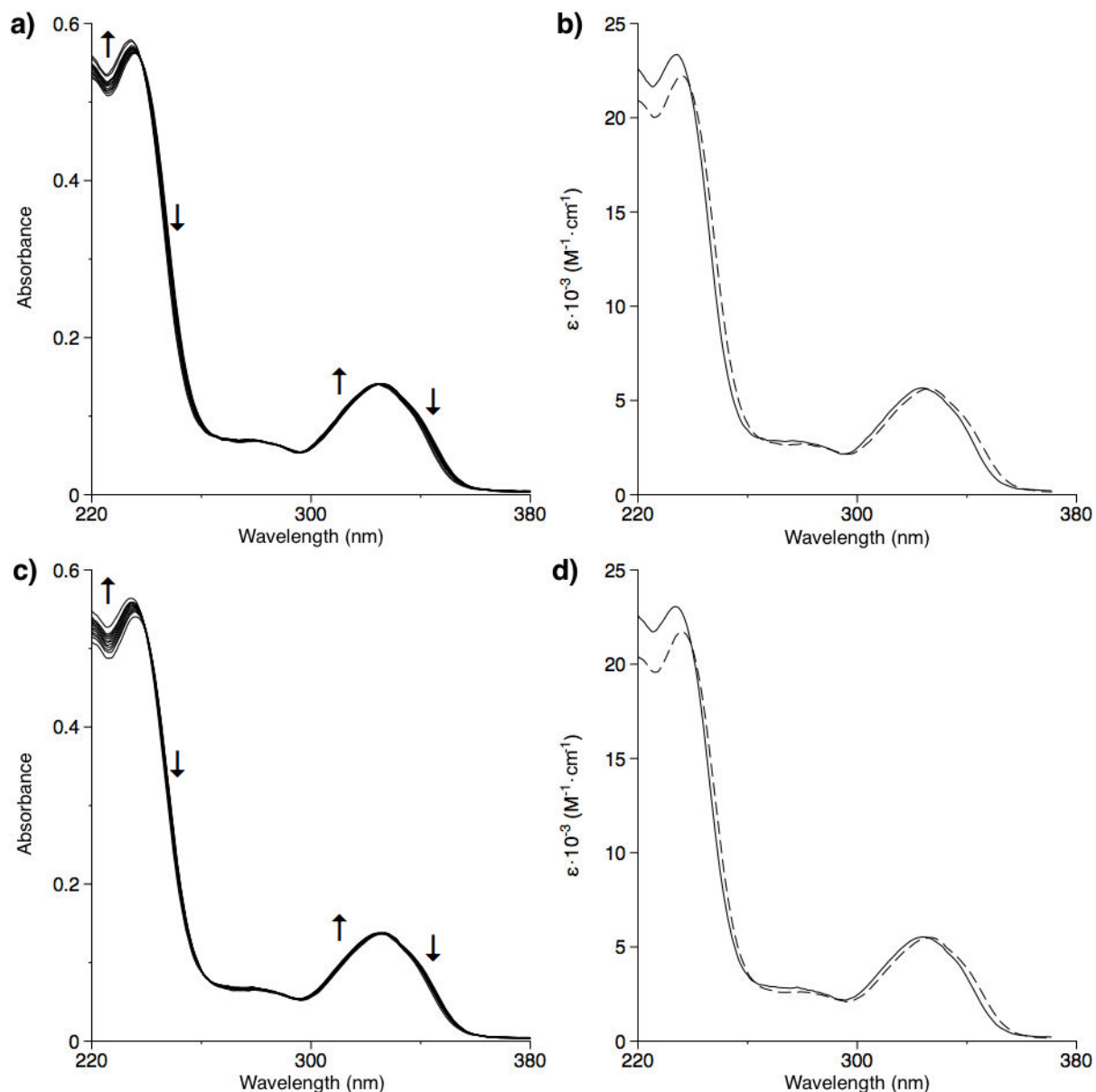


Figure 3.28. Spectrophotometric titration of chromene **1b** by ammonium perchlorate (a, b) and protonated ϵ -aminocaproic acid (c, d). $C_{1b} = 2 \cdot 10^{-5}$ M, $C_S/C_{1b} = 0 \rightarrow 8$ (C_S is NH_4ClO_4 or C6 concentration). (Dashed line shows the initial chromene spectrum, solid line shows the complex spectrum).

Upon irradiation, chromenes **1b** and **3b** are transformed into the colored forms. At 20°C, the linear isomer converts into the TC form predominantly, as evidenced by a mono-exponential dependence of the bleaching curve (Fig. 3.29a). The angular chromene is characterized by fast bleaching kinetics at 20°C. Irradiation of solution of **3b** in acetonitrile by unfiltered light (Hg-lamp, 120 W) also produced a small amount of the TT isomer. The

Table 3.9. Stability constant values ($\lg K_{11}$) for chromene **1b** and **3b** complexes with ammonium cations and amino acids (acetonitrile, 25°C).

	1b	3b
NH_4ClO_4	4.9 ± 0.1	4.66 ± 0.06
β -alanine (C3)	4.6 ± 0.1	4.85 ± 0.09
γ -aminobutyric acid (C4)	4.64 ± 0.05	4.45 ± 0.06
ϵ -aminocaproic acid (C6)	4.68 ± 0.08	4.75 ± 0.08
ω -aminocaprylic acid (C8)	4.42 ± 0.04	4.66 ± 0.06

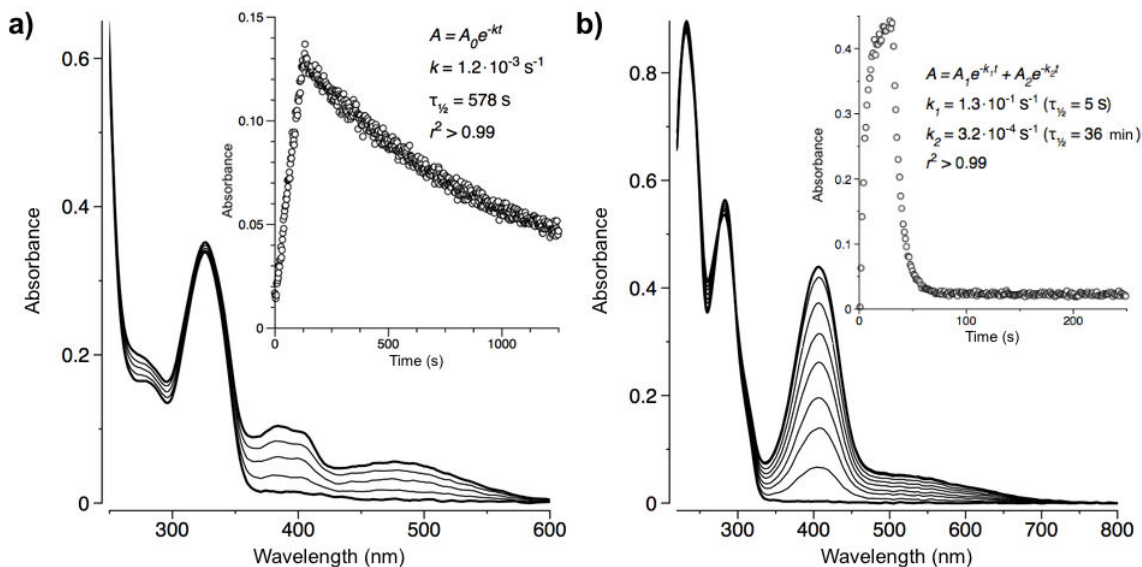


Figure 3.29. Changes in absorption spectra of chromenes **1b** and **3b** during irradiation and bleaching: a) **1b**, $C_{1b} = 5 \cdot 10^{-5}$ M, 20°C , 2-minute exposure to irradiation with filtered light (Hg lamp, 120 W, $\lambda = 315$ nm), kinetics at 385 nm is shown in the inset; b) **3b**, $C_{3b} = 7 \cdot 10^{-5}$ M, 20°C , 30-second exposure to irradiation with full light (Hg lamp, 120 W), kinetics at 410 nm is shown in the inset. (A , A_0 , A_1 , A_2 are absorbances; k , k_1 , k_2 are bleaching rate constants; r^2 is the correlation coefficient.)

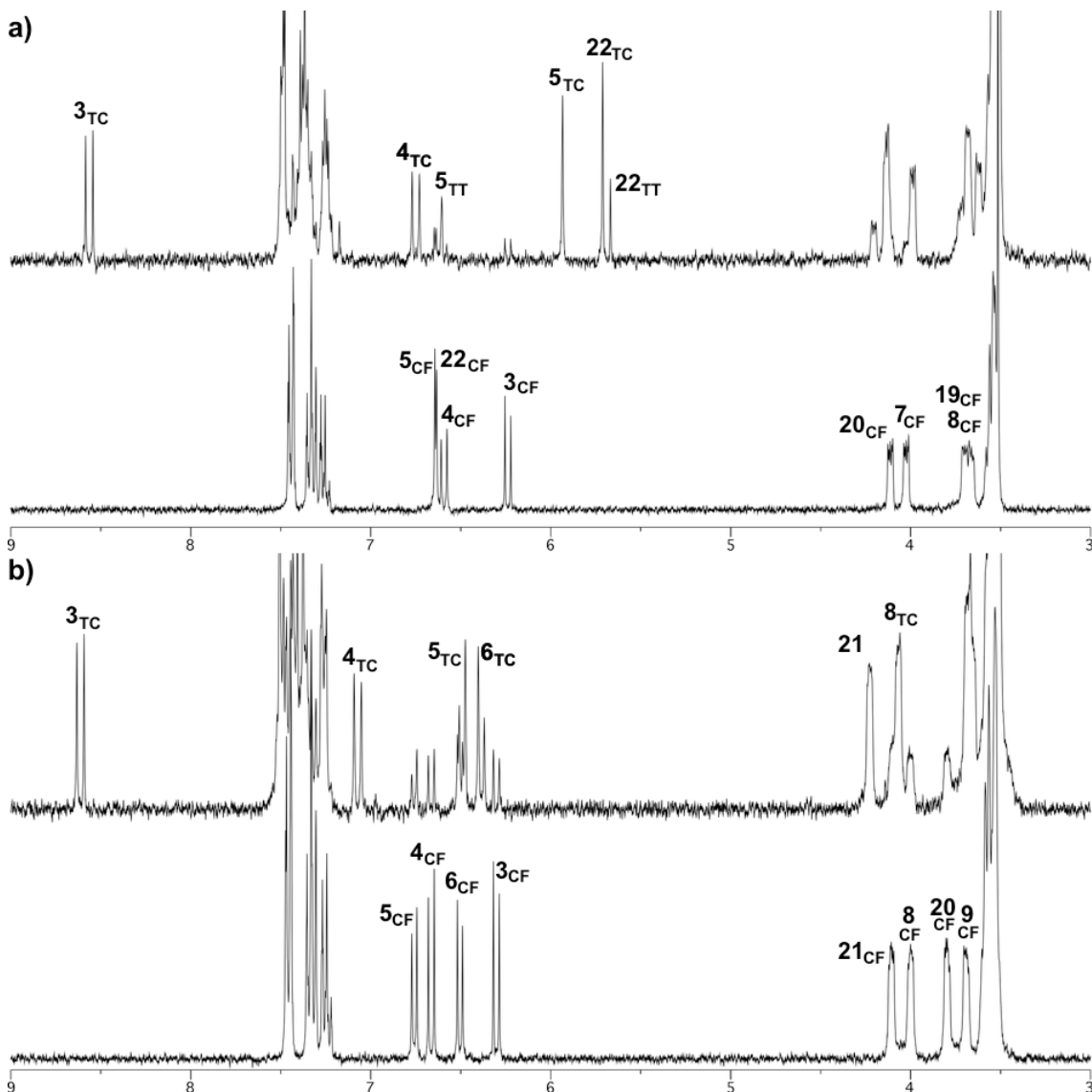


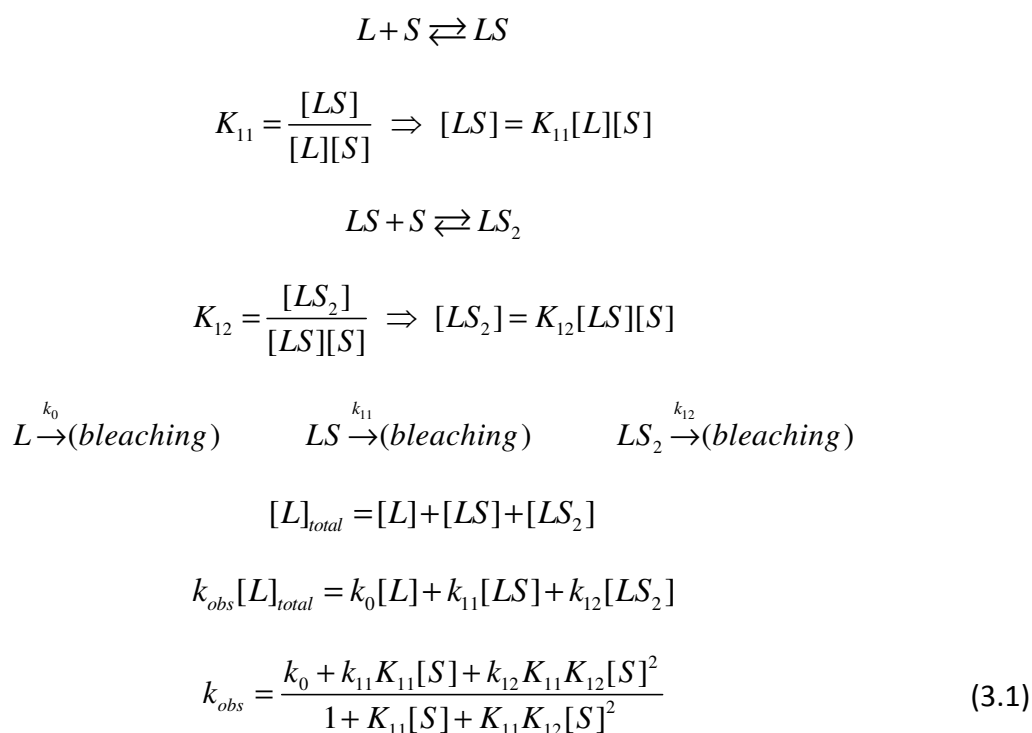
Figure 3.30. ^1H NMR spectrum changes for chromenes **1b** and **3b** upon irradiation with filtered light ($\lambda = 313$ nm) during 24 min (Hg-Xe lamp, 1000 W): a) **1b**, 0°C ; b) **3b**, -45°C .

corresponding relaxation rate constants of colored **3b** forms differed by 3 orders of magnitude ($k_1 = 1.3 \cdot 10^{-1} \text{ s}^{-1}$ for the TC and $k_2 = 3.2 \cdot 10^{-4} \text{ s}^{-1}$ for the TT).

The NMR studies of photochromic transformations at low temperature indicated that chromene **1b** produces two forms at 0°C, the TT isomer beginning to form after prolonged irradiation (Fig. 3.30a). The TT form was stable at 0°C while the TC form transformed into the initial closed form with $k = 1.1 \cdot 10^{-4} \text{ s}^{-1}$. Due to fast bleaching kinetics, photochromism of **3b** was studied at -45°C. In contrast with spectrophotometric investigations, after 24-minute irradiation with filtered light ($\lambda = 313 \text{ nm}$, Hg-Xe lamp, 1000 W), no signals of the TT form in NMR spectrum were observed (Fig. 3.30b). The TC isomer, in turn, converted into the initial closed form with the rate constant equal to $7.5 \cdot 10^{-5} \text{ s}^{-1}$ ($\tau_{1/2} = 2.57 \text{ hours}$).

The presence of the amino acids in the solution caused a substantial effect on the photochromic properties of the compounds. Similarly to the metal cations effect, destabilization of the colored forms was observed.

The processes were analyzed using the following general scheme:



where L denotes the open form; S denotes the amino acids or ammonium perchlorates; LS and LS_2 denote 1:1 and 1:2 complexes of the open forms with one and two amino acid or ammonium cations, respectively; k_0 , k_{11} , and k_{12} denote bleaching rate constants for the free chromene (L), 1:1 (LS), and 2:1 (LS_2) complexes, respectively.

Equation (3.1) describes the general case of the complex formation *via* consecutive addition of the cations to the ligand. When 1:1 complexes are formed exclusively, expression (3.1) is reduced to the form (3.2):

$$k_{obs} = \frac{k_0 + k_{11}K_{11}[S]}{1 + K_{11}[S]} \quad (3.2)$$

In the course of titration, a large excess of the amino acids or ammonium perchlorates was used. Therefore, it may be assumed that $[S] = C_S$:

$$k_{obs} = \frac{k_0 + k_{11}K_{11}C_S + k_{12}K_{11}K_{12}C_S^2}{1 + K_{11}C_S + K_{11}K_{12}C_S^2} \quad (3.1a)$$

$$k_{obs} = \frac{k_0 + k_{11}K_{11}C_S}{1 + K_{11}C_S} \quad (3.2a)$$

Thus, by analyzing dependencies of observed bleaching constant on the cation content in the solution, one may estimate the stability constants of the complexes formed and determine the thermal relaxation rate constants of the open forms in these complexes.

In the presence of the ammonium cations, irradiation of solution of **1b** with UV light ($\lambda = 313$ nm, Hg lamp, 120 W) for 2 minutes led to the formation of a single photoinduced form (TC), as evidenced by a mono-exponential pattern of the bleaching curve (Fig. 3.31). The curve of the relaxation rate constant dependence on cation concentration yielded to the plateau. Observed changes are well described by the model of 1:1 complex formation (formula 3.2a) (Fig. 3.31b).

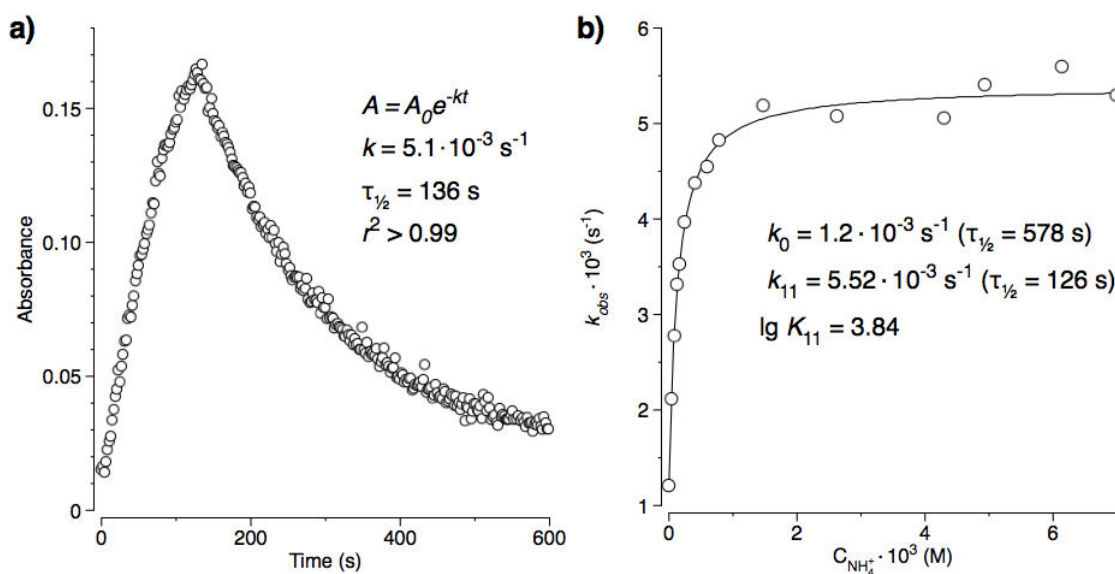


Figure 3.31. The effect of ammonium cation presence on the bleaching kinetics of chromene **1b** (acetonitrile, 20°C): a) bleaching kinetics at the ratio $C_{\text{ammon}}/C_{\text{1b}} = 160$, $C_{\text{1b}} = 4.2 \cdot 10^{-5}$ M; b) changes in the bleaching constant depending on ammonium perchlorate concentration in the solution. (A , A_0 are absorbances; k , k_0 , k_{11} are bleaching rate constants; r^2 is the correlation coefficient; $\lg K_{11}$ is the stability constant logarithm for 1:1 complex.)

In the experiments with the amino acids, the observed changes were dependent on their carbon skeleton length. In case of a slight excess of C3, C4, and C6 acids, a mono-exponential kinetics of thermal relaxation (the TC complex) was observed (Fig. 3.32a), accompanied by gradual accumulation of the slowly bleaching component (the TT complex) (Fig. 3.32b). Along with the increase of the TT form contribution, a further increase of the amino acid concentration induced a stepwise increase in its bleaching rate (Fig. 3.32c). Since in the absence of the amino acids no TT isomer was observed, it is possible to conclude that it existed in a form of a complex and was generated from the TC complex with amino acid. The rate constant of the TC isomer relaxation increased with the ligand concentration, too (Fig. 3.32d). This dependence is well described by the equation (3.1a) and corresponds to formation of two complexes.

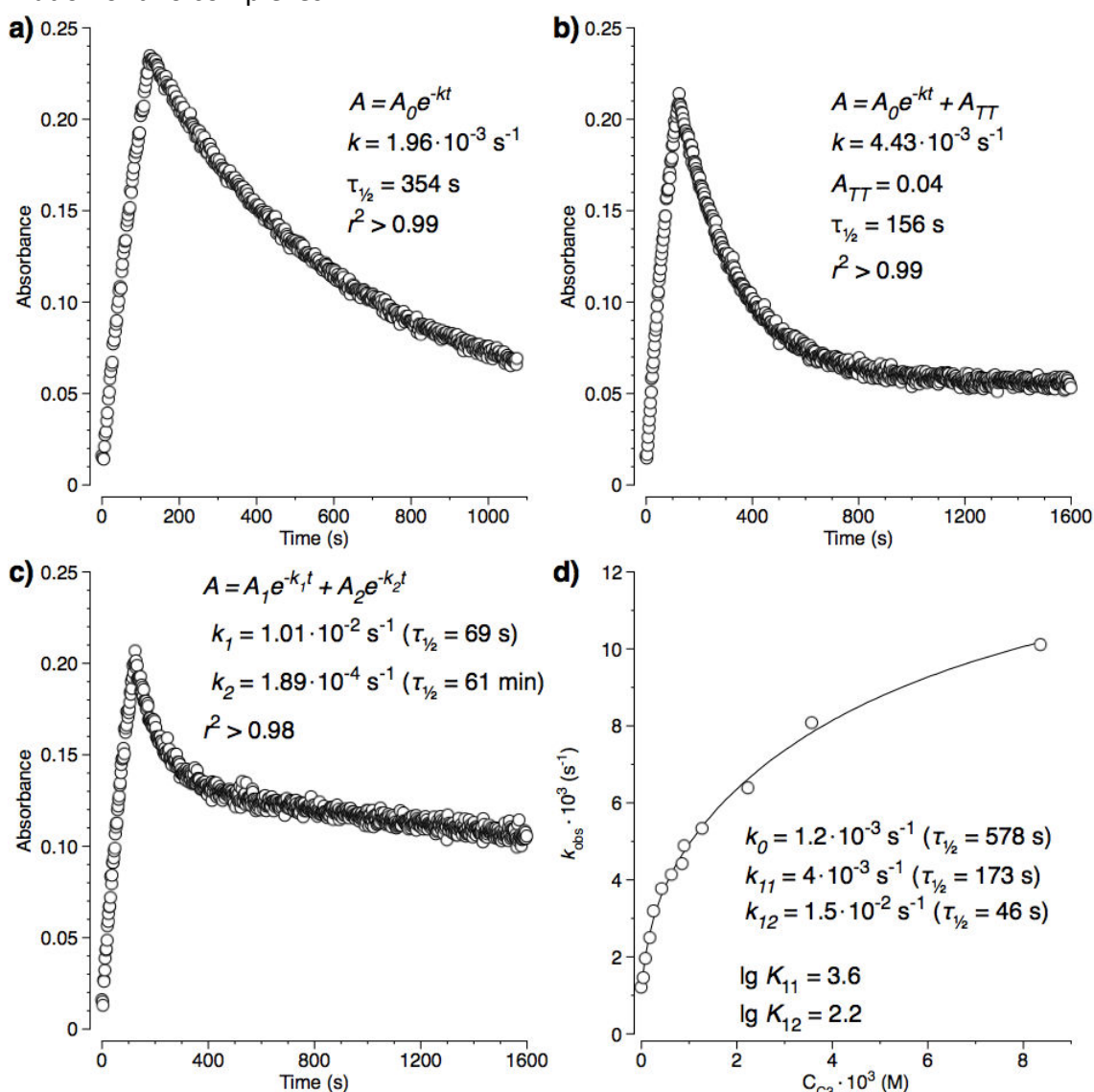
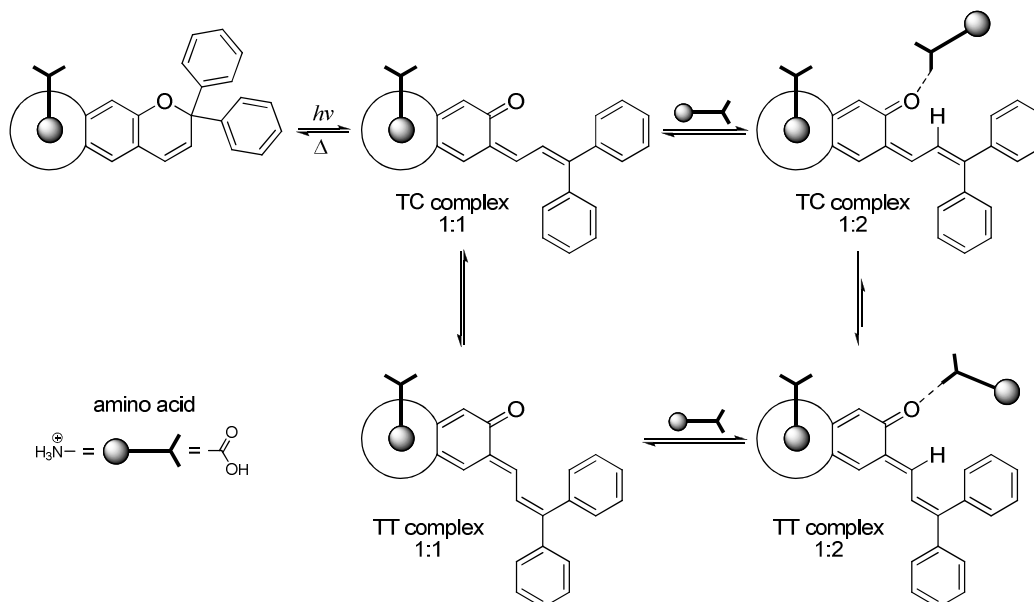


Figure 3.32. The influence of β -alanine (C3) presence on bleaching kinetics of **1b** solution after irradiation (acetonitrile, $C_{1b} = 4.2 \cdot 10^{-5} \text{ M}$, 20°C): a) $\lambda = 385 \text{ nm}$, $C_{AA}/C_{1b} = 2$; b) $\lambda = 385 \text{ nm}$, $C_{AA}/C_{1b} = 20$; c) $\lambda = 385 \text{ nm}$, $C_{AA}/C_{1b} = 195$; d) dependence of observed relaxation rate constant of TC form on amino acid concentration. (A , A_0 , A_1 , A_2 , A_{TT} are absorbances; k , k_0 , k_1 , k_2 , k_{11} , k_{12} are bleaching rate constants for the free colored forms and those in the complex; r^2 is the correlation coefficient; $\lg K_{11}$, $\lg K_{12}$ are logarithms of the complexes' stability constants.)



Scheme 3.31. Processes upon irradiation of chromene **1b** solution in the presence of amino acids C3, C4, or C6.

Thus, summarizing the results obtained, one may suggest that upon irradiation, the free chromene molecules as well as 1:1 complexes, present in the solution, the first transform into the corresponding TC forms (Scheme 3.31). Then, 1:1 complex of the TC form may join one more amino acid molecule to form 1:2 complex. The TC complexes are less stable (in particularly, 1:2 ones) and are readily transformed into the TT species.

In contrast with C3, C4, and C6 acids and similar to ammonium cations, ω -amino caprylic acid (C8) does not form 1:2 complexes with the open forms. But contrary to other ligands, even a small excess of C8 ($C_{AA}/C_{1b} = 2$) produces the both photoinduced forms (Fig. 3.33a, b). The amino acid quantity increase accelerates bleaching of the both colored forms; however, starting from a certain moment, further addition causes no substantial change in the bleaching rate (Fig. 3.33c, d). Such behavior allows a suggestion that a ditopic complex formation is realized in this case, preventing attachment of the second amino acid to the complex (Scheme 3.32). Like in the presence of C3, C4, or C6 acids, the abundance of the TT forms in the presence of C8 is due to a more favorable spatial arrangement of the fragments in the complex.

Analysis of the stability constants of the complexes and bleaching rate constants of the open forms also give an evidence in favor of the proposed schemes of complex formation (Table 3.10). The complex formation constant for C8 does not follow the general tendency to decrease along with the increasing number of carbon atoms, which is observed for the 1:1 complexes of the closed forms with amino acids C3, C4, C6 with open forms (Fig. 3.34a). These effects correlate well with the C8 ditopic coordination. Stability of such complexes, as compared with the monotopic ones, should be higher accounting for the two-site interaction.

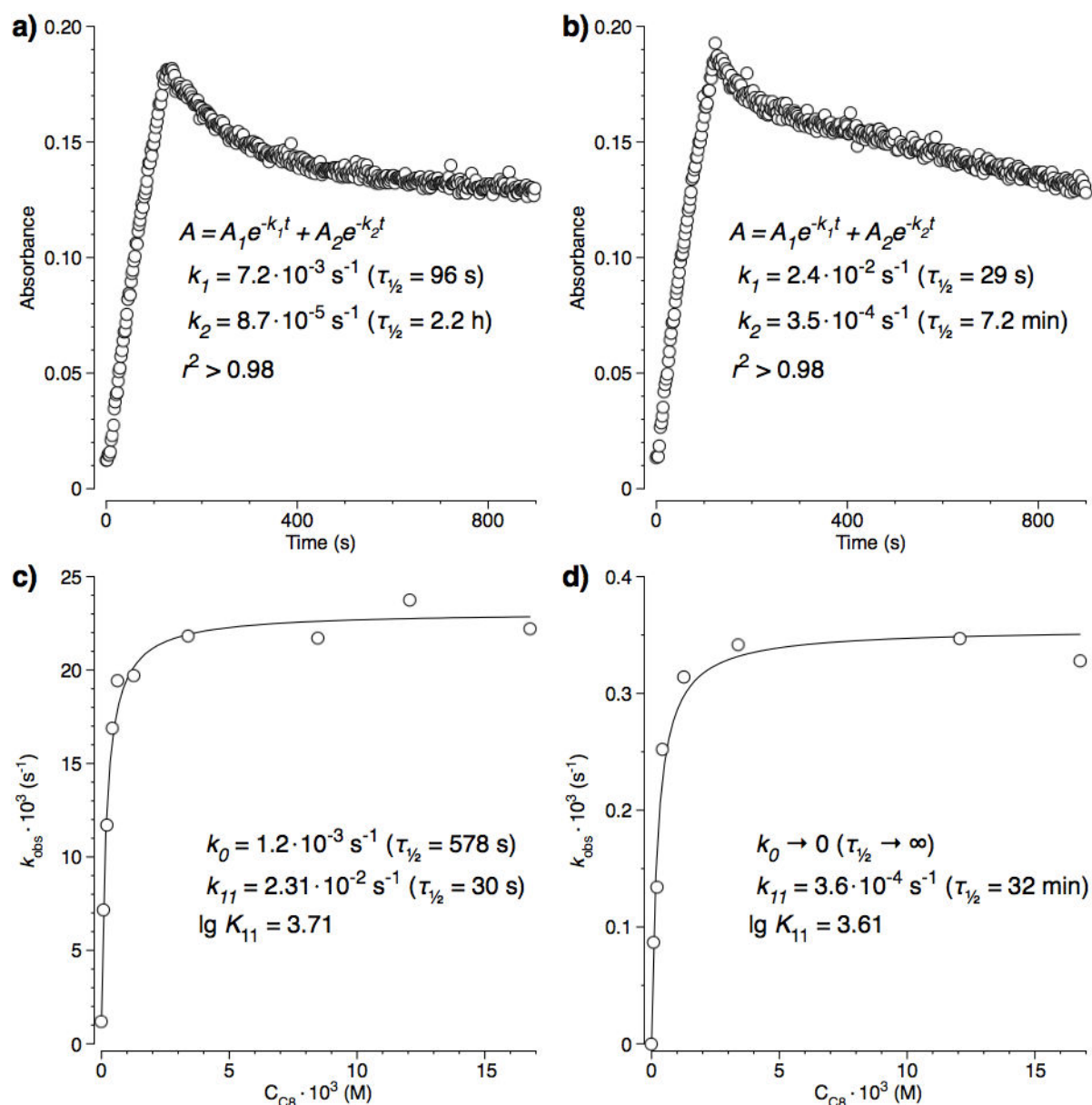
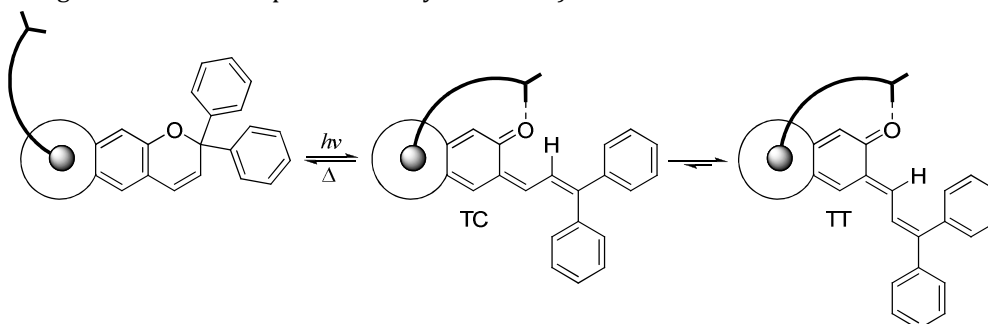


Figure 3.33. The influence of ω -aminocaproic acid (C8) on bleaching kinetics of chromene **1b** solution after irradiation (acetonitrile, $C_{1b} = 4.2 \cdot 10^{-5} \text{ M}$, 20°C): a) $\lambda = 385 \text{ nm}$, $C_{AA}/C_{1b} = 2$; b) $\lambda = 385 \text{ nm}$, $C_{AA}/C_{1b} \approx 300$; c) and d) dependencies of observed relaxation rate constant of the TC and TT forms, respectively, on the amino acid concentration. (A, A_1, A_2 are absorbances; k_0, k_1, k_2, k_{11} are bleaching rate constants for the free colored forms and those in the complex; r^2 is the correlation coefficient; $\lg K_{11}$ is logarithm of the complex's stability constants.)



Scheme 3.32. Formation of amino acid C8 ditopic complexes with the open forms of chromene **1a**.

As compared with the free ligand, in the presence of ammonium cations and the amino acids, the bleaching rate increases (Table 3.10). In the case of C8, rate constant value is much different from the corresponding values of other substrates (Fig. 3.34b). The

Table 3.10.

Characteristics of ammonium and amino acid cation complexes formed with chromene **1b** open forms (acetonitrile, 20°C). (k_{11} , k_{12} are bleaching rate constants of 1:1 and 1:2 TC complexes; $\tau_{1/2}$ is half-life time; $\lg K_{11}$, $\lg K_{12}$ are logarithms of the complexes stability constants.)

	Complex 1:1 (TC)			Complex 1:2 (TC)		
	$\lg K_{11}$	$k_{11} \cdot 10^3 \text{ (s}^{-1}\text{)}$	$\tau_{1/2} \text{ (s)}$	$\lg K_{12}$	$k_{12} \cdot 10^3 \text{ (s}^{-1}\text{)}$	$\tau_{1/2} \text{ (s)}$
1b *	–	$1.2 \pm 0.1^*$	578*	–	$1.2 \pm 0.1^*$	578*
1b + NH_4^+	3.84 ± 0.02	5.52 ± 0.05	126	–	–	–
1b + C3	3.6 ± 0.2	4 ± 1	173	2.2 ± 0.2	15 ± 2	46
1b + C4	3.41 ± 0.07	5.5 ± 0.4	126	1.6 ± 0.2	14 ± 2	50
1b + C6	3.4 ± 0.4	6.0 ± 0.7	117	1.7 ± 0.6	10 ± 2	69
1b + C8	3.71 ± 0.05	23.1 ± 0.5	30	–	–	–

* Data for the free colored forms is presented.

bleaching rate increase seems to be associated with high mobility of the long aliphatic fragment of the amino acids and related entropy of the system.

For the 1:2 TC complexes in the C3-C4-C6 sequence a tendency of stability constants and bleaching rate constants to decrease is observed. This is probably associated with the length of amino acids aliphatic chain, the latter also affecting the positive charge value of ammonium group. In the C3-C4-C6 sequence, the electron-withdrawing influence of carboxyl group is thus decreased, resulting to a slight decrease of stability constants of the complexes.

Unfortunately, it is impossible to make a conclusion about the TT complex stability for different amino acids. Nevertheless, it appears that the presence of amino acids in the solution promoted the TC→TT thermal transition, which was not observed for the free chromene.

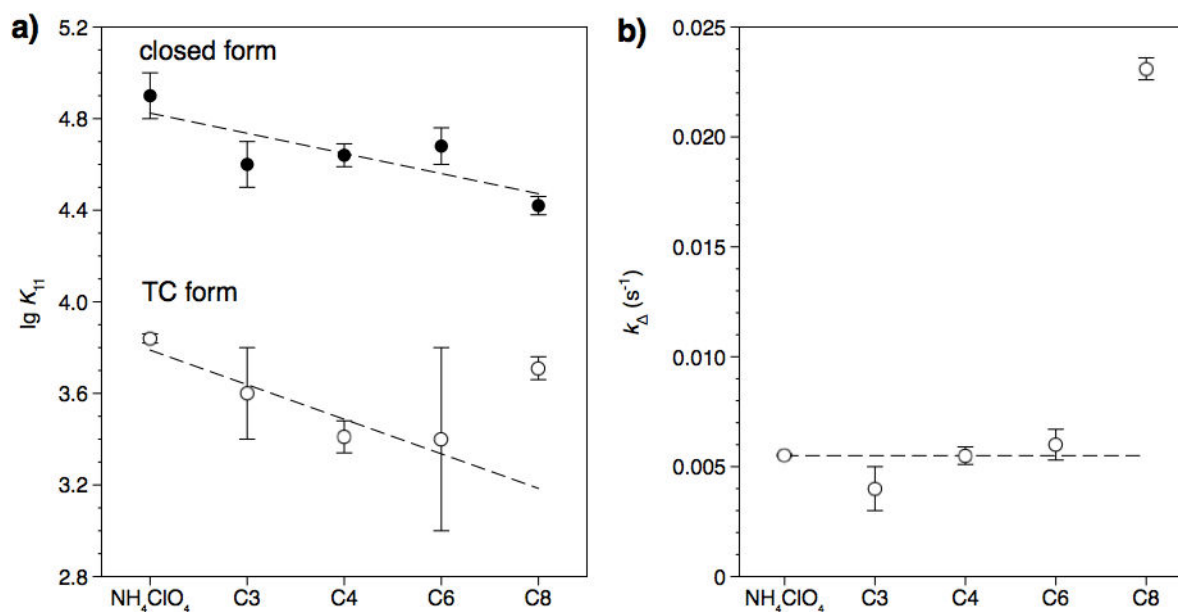


Figure 3.34. Parameters of chromene **1b** complex formation with amino acids: a) stability of the 1:1 TC complexes as compared with complexes of the closed form; b) the open form stability in 1:1 complexes (thermal relaxation rate constants). ($\lg K_{11}$ is logarithm of the complex stability constant; k is the bleaching rate constant of the 1:1 TC complexes.)

Using the NMR technique, solutions containing equimolar quantities of chromene **1b** and the amino acids were studied. Irradiation of the solutions with UV light ($\lambda = 313$ nm, Hg-Xe lamp, 1000 W) during 10 minutes at 20°C induced predominant formation of the TT form signals (Fig. 3.35a), the few TC form peaks being present. Temperature decrease to

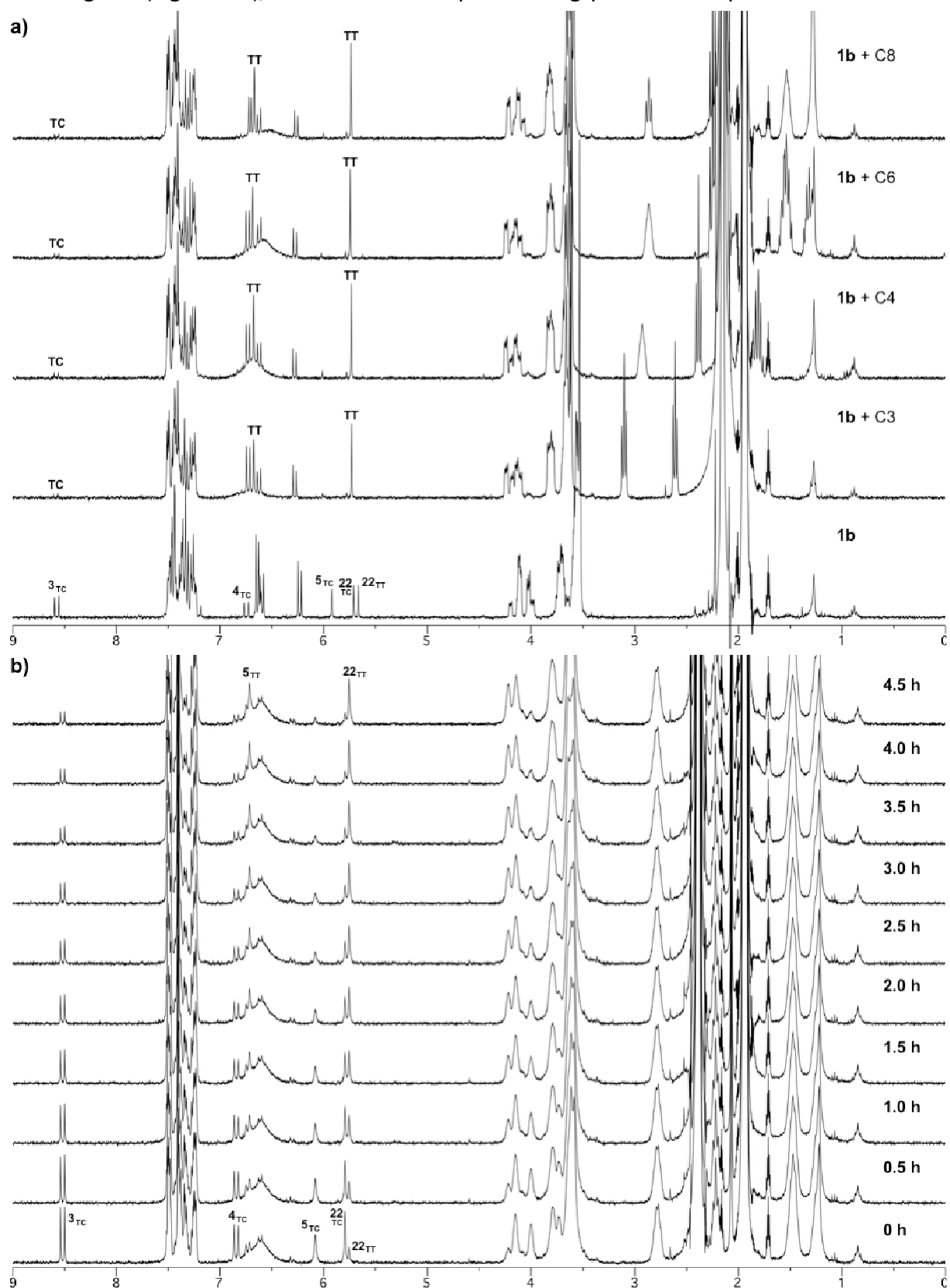


Figure 3.35. ^1H NMR spectra of chromene **1b** solutions in the presence of the amino acids after irradiation: a) after 10 minutes irradiation (20°C); b) thermal relaxation of **1b** + C6 solution after 10 minutes irradiation (-45°C).

-45°C allowed to detect the TC isomer formation. However, during relaxation, the TC→TT transition was observed (Fig. 3.35b). Thus, this data partly prove correctness of the previous conclusions made on the basis of spectrophotometric investigations.

The studies of the angular chromene **3b** were also performed at 20°C. However, high conversion of the initial molecules to the colored forms was reached by using a short-term (30 seconds) irradiation with unfiltered light of Hg lamp (120 W). This provided occurrence of the photoinduced forms absorption bands, which intensity being sufficient for observation of the bleaching kinetics. In all cases, the bleaching curve was of biexponential nature that gave evidence of material TT forms content (Fig. 3.36a). Moreover, upon high

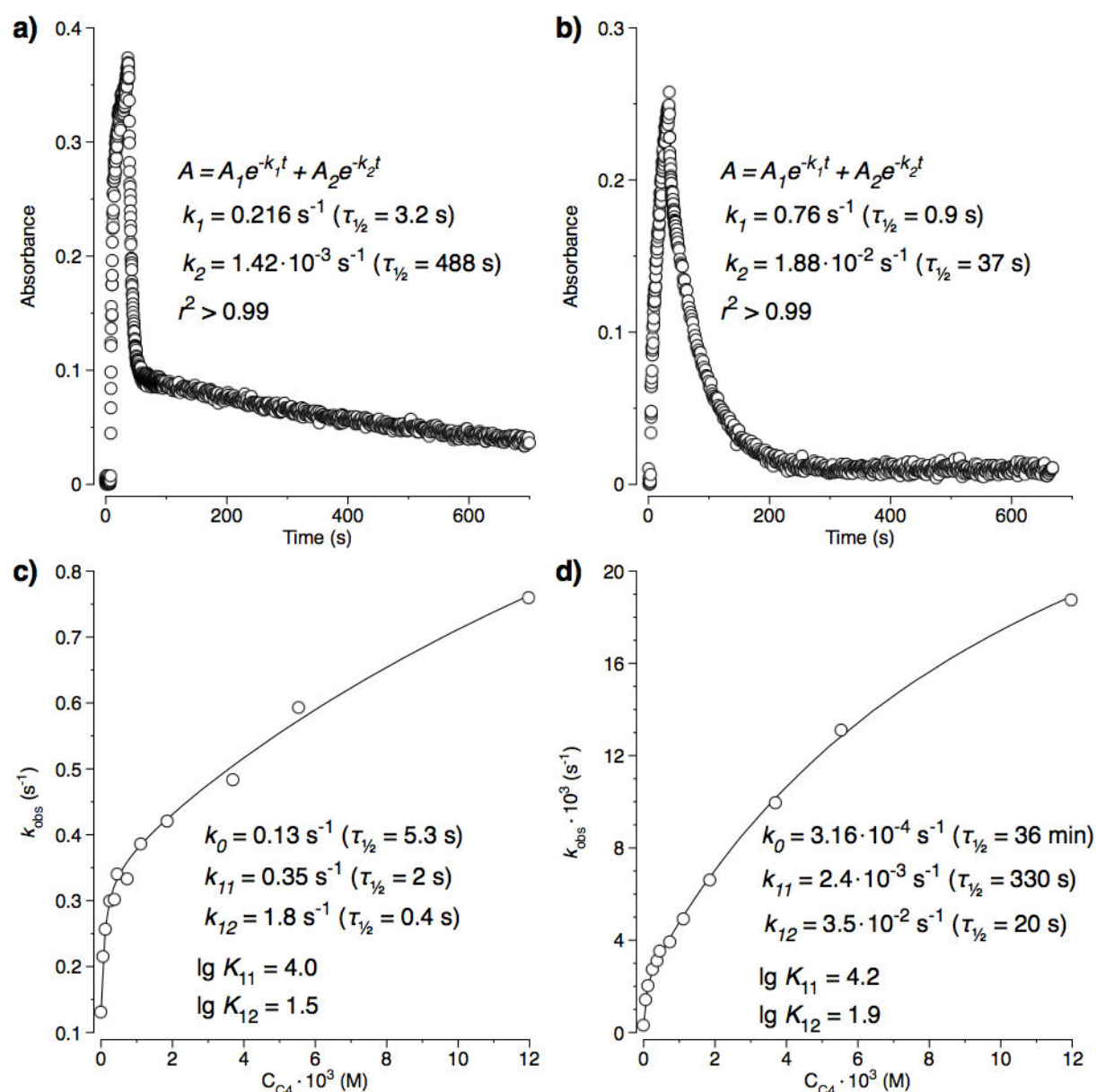


Figure 3.36. The influence of γ -aminobutyric acid (C4) on bleaching kinetics of chromene **3b** solution after irradiation (acetonitrile, $C_{3b} = 3.0 \cdot 10^{-5} \text{ M}$, 20°C): a) $\lambda = 410 \text{ nm}$, $C_{AA}/C_{3b} = 2$; b) $\lambda = 410 \text{ nm}$, $C_{AA}/C_{3b} = 400$; c) and d) dependencies of observed relaxation rate constant of the TC and the TT forms on amino acid concentration, respectively. (A , A_1 , A_2 are absorbances; k_0 , k_1 , k_2 , k_{11} , k_{12} are bleaching rate constants for the free colored forms and those in the complex; r^2 is the correlation coefficient; $\lg K_{11}$, $\lg K_{12}$ are logarithms of the stability constant for 1:1 and 1:2 complexes.)

ligand excess, the TC forms contribution into the observed relaxation kinetics was negligible (Fig. 3.36b). In the case of C3, C4, and C6, the overall character of the rate change agreed with the 1:1 and 1:2 complex formation for both photoinduced forms (Fig. 3.36c, d). Cations NH_4^+ did not form 1:2 complexes at all, whereas C6 formed 1:2 complexes with the TT isomer exclusively.

Table 3.11.

Logarithms of the stability constant for complexes of the chromene **3b** open forms with ammonium and amino acid cations (acetonitrile, 20°C). ($\lg K_{11}$, $\lg K_{12}$ are logarithms of the stability constant for 1:1 and 1:2 complexes.)

	TC complexes		TT complexes	
	$\lg K_{11}$	$\lg K_{12}$	$\lg K_{11}$	$\lg K_{12}$
3b + NH_4^+	3.29 ± 0.05	–	3.2 ± 0.4	1.4 ± 0.7
3b + C3	3.92 ± 0.02	2.15 ± 0.06	4.8 ± 1.5	2.40 ± 0.04
3b + C4	4.0 ± 0.1	1.5 ± 0.2	4.3 ± 0.2	1.94 ± 0.04
3b + C6	3.63 ± 0.04	–	2.5 ± 0.1	2.5 ± 0.3

Table 3.12.

Bleaching rate constants of the chromene **3b** open forms in the complexes with ammonium and amino acids cations (acetonitrile, 20°C). (k_{11} , k_{12} are rate constants of 1:1 and 1:2 complex bleaching.)

	TC complexes		TT complexes	
	k_{11} (s^{-1})	k_{12} (s^{-1})	$k_{11} \cdot 10^3$ (s^{-1})	$k_{12} \cdot 10^3$ (s^{-1})
3b	$0.13 \pm 0.02^*$	–	$0.32 \pm 0.02^*$	–
3b + NH_4^+	0.434 ± 0.006	–	3 ± 1	15 ± 13
3b + C3	0.394 ± 0.008	1.01 ± 0.05	3.6 ± 1.3	48 ± 1
3b + C4	0.35 ± 0.02	1.8 ± 0.5	2.4 ± 0.3	35 ± 2
3b + C6	0.69 ± 0.01	–	80 ± 30	59 ± 6

* Data for free colored forms are shown.

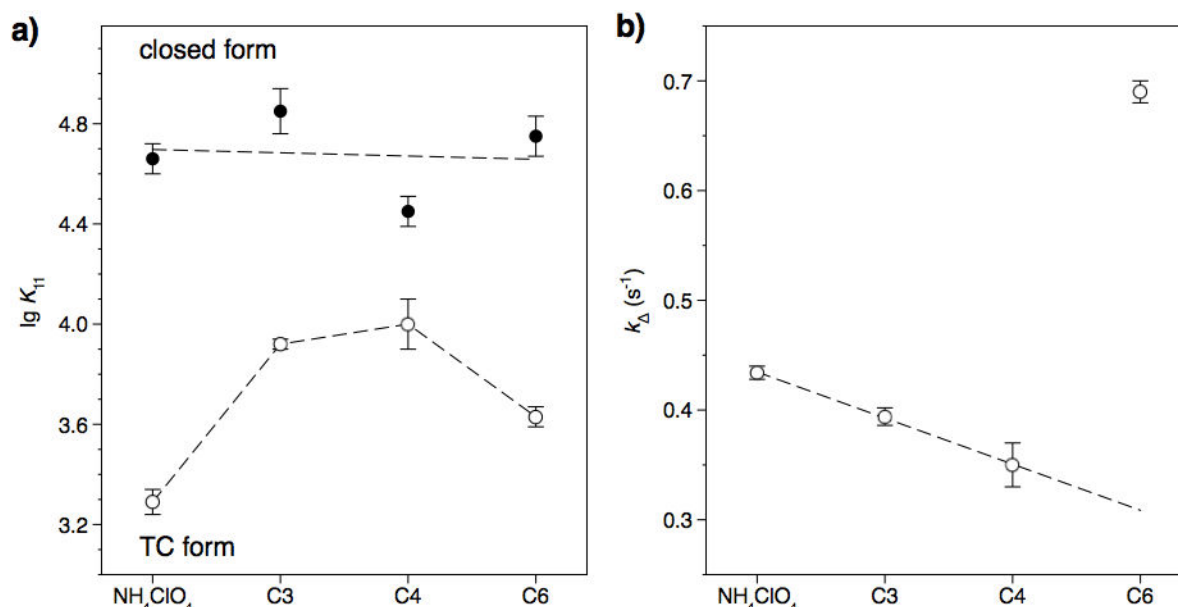


Figure 3.37. Parameters of chromene **3b** complex formation with amino acids: a) the 1:1 TC complex stability as compared with complexes of the closed form; b) the open form stability in the 1:1 TC complex (thermal relaxation rate constants). ($\lg K_{11}$ is stability constant logarithm for complexes; k is the bleaching rate constant of the 1:1 TC complexes.)

The stability constants of the complexes and rate constants of the TC and TT isomers bleaching varied for different ligands (Tables 3.11, 3.12). The stability of the 1:1 TC complexes with C3 and C4 is distinct from that of the complexes with the ammonium cations and C6 (Fig. 3.37a). This correlates well with the ditopic complex formation model. At the same time, the bleaching rate constant of the TC complex with C6 does not follow the general tendency to decrease. The latter, similar to the case of **1b**, is due to carbon chain length of the amino acid and its high mobility (Fig. 3.37b). Similar dependencies were observed for the TT complexes (Tables 3.11, 3.12). It should be noted, however, that in the case of C6, the contribution of the 1:1 TT complexes to general kinetics was much lower than of 1:2 ones.

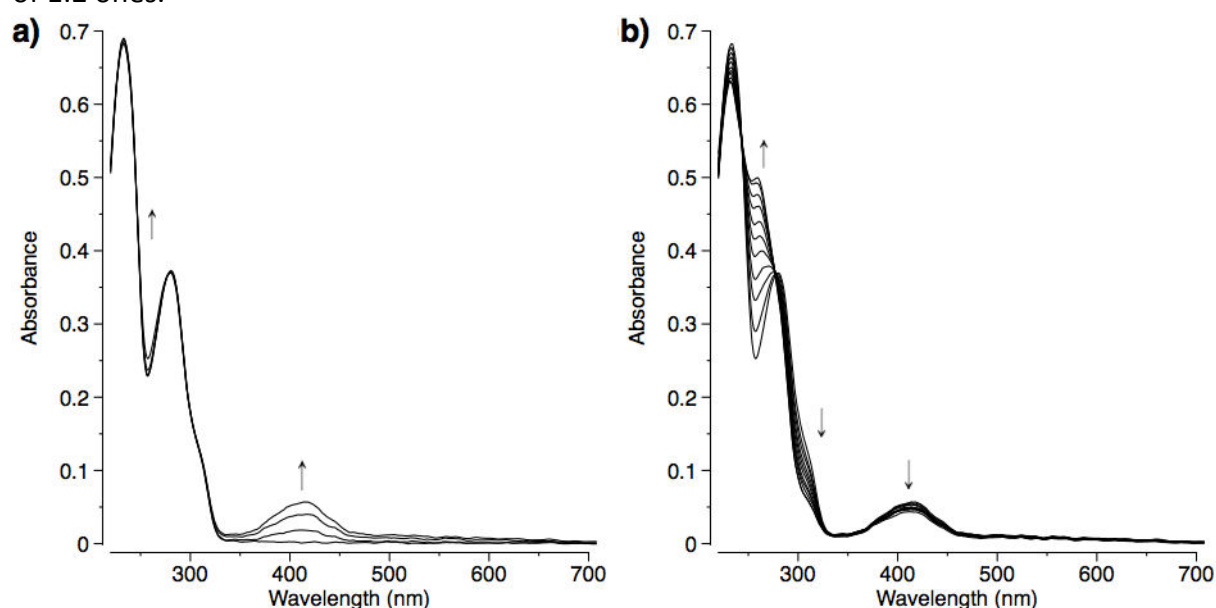
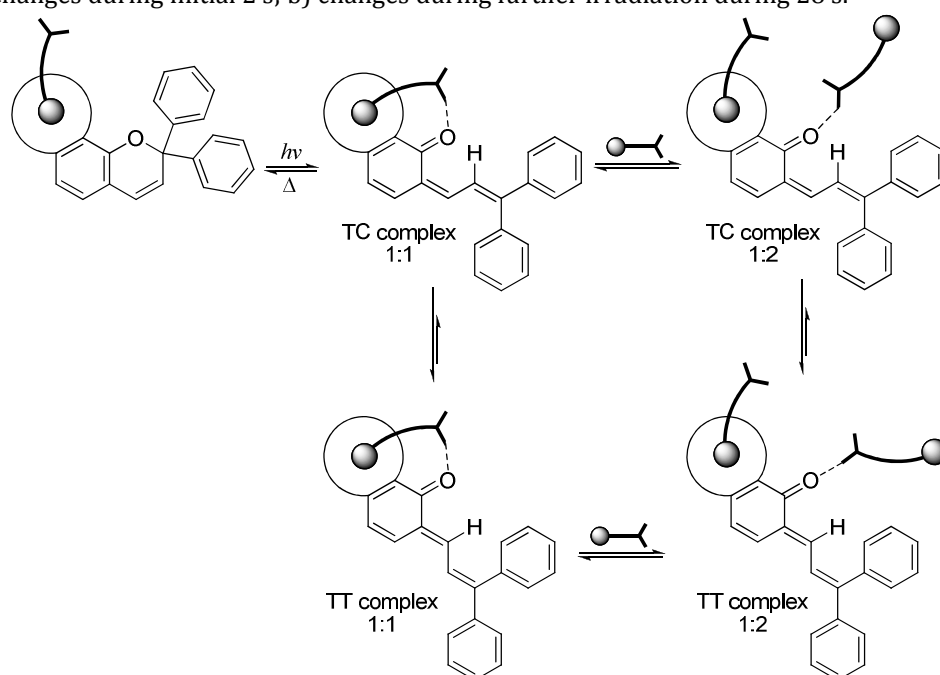


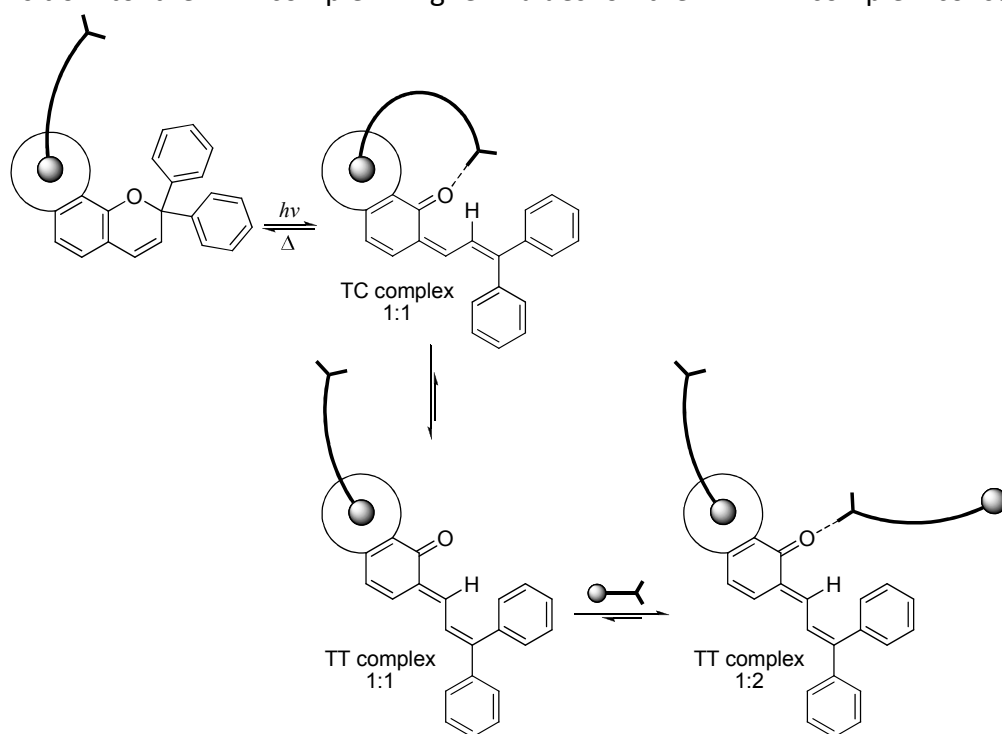
Figure 3.38. Changes in chromene **3b** absorption spectra upon irradiation (30 s, Hg lamp, 120 W, full light) in the presence of amino acid C8 (acetonitrile, 20°C): a) changes during initial 2 s; b) changes during further irradiation during 28 s.



Scheme 3.33. Formation of the chromene **3b** open form complexes with amino acids C3 and C4.

In the presence of amino acid C8, the behavior of the system was more complicated. When the solution was irradiated, the initial accumulation of the TC forms induced rapidly a noticeable the TC→TT transformation (Fig. 3.38), which was observed neither for other substrates, nor for the free chromene. Obviously, such behavior is exclusively caused by the size of the amino acid, which flexible aliphatic chain destabilized the open isomers formed. Unfortunately, precise determination of the complexes stability constant and the bleaching rate constants of components failed because of unusual behavior of the system and fast process proceeding.

Thus, the following rationalization of the observed experimental data may be suggested. Irradiation of solutions with amino acids C3, C4, and C6 induces the formation of the 1:1 TC complexes of higher stability than the complexes with ammonium cations (Scheme 3.33). This may be associated with the ditopic mode of the complex formation. Nevertheless, in the case of C3 and C4, at large amino acid excess, this complex may attach one more substrate molecule giving a 1:2 complex. In both cases, for the complex formation, the TT configuration is more spatially preferable. In the case of amino acid C6, the 1:2 TC complex formation was not observed that is, probably, associated with fast transition of the TC isomer into the TT one, the complexes with the latter being formed more favorable as evidenced by high contribution of this form to the observed bleaching kinetics (Scheme 3.34). As compared to complexes with the ammonium cations, a low stability constant of the 1:1 TT complex may mean that no ditopic interaction occurs. This may be associated with fast transition to the 1:2 complex. Higher values of the 1:2 TT complex constants, as



Scheme 3.34. Formation of the chromene **3b** open form complexes with amino acids C6.

compared with NH_4^+ , give evidence of coordination between carbonyl oxygen atom of the open form and carboxylic hydrogen of the amino acid. Processes, similar to those involving C6, may also proceed with amino acid C8, which preferably may form the TT complexes because of the long aliphatic chain.

The NMR studies of irradiated chromene **3b** could not be made owing to high transformation rate of the open forms to the closed ones. Moreover, even at -45°C , spectra possessed highly broadened signals that made their interpretation difficult.

Thus, depending on the carbon skeleton length, the formation of the ditopic complexes of the chromene **1b** and **3b** open forms with the amino acids was demonstrated. These complexes exhibited higher stability, as compared with other 1:1 complexes. For the linear isomer **1b**, such coordination was found possible in the case of amino acid C8. On the contrary, angular isomer **3b** forms the ditopic complexes with short amino acids (C3 and C4). The presence of the ammonium and amino acid cations accelerated bleaching independently of the complex type. However, a substantial rate increase was also associated with amino acid length, and C6, C8 were evaluated by a sharp increase of the bleaching rate that is, probably, due to nonspecific interaction of the open forms with the amino acids in space.

3.2.2. Study of Chromene **33** Intercalation into DNA

Relatively small organic molecules are capable of strong binding to DNA, and this property is of importance for designing of new chemotherapeutic agents and health safe DNA labels [74]. Three main interaction types are distinguished: (1) outside-stacking, (2) groove-binding, and (3) intercalation. The first type of interaction is the weakest and is generally due to electrostatic interactions of ligands with external phosphate skeleton of DNA. The other two types are based on the non-covalent binding, including π -stacking, hydrogen bond formation, van der Waals and hydrophobic interactions.

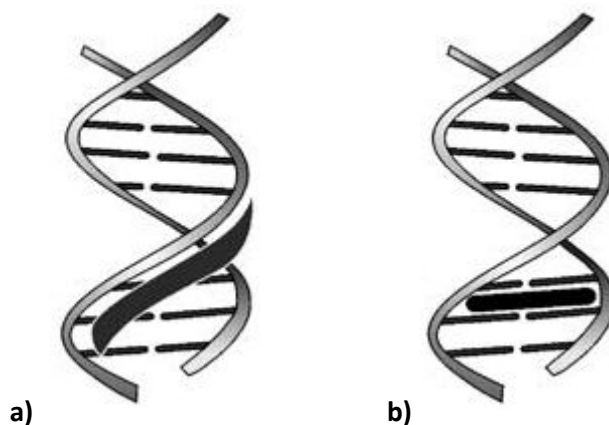


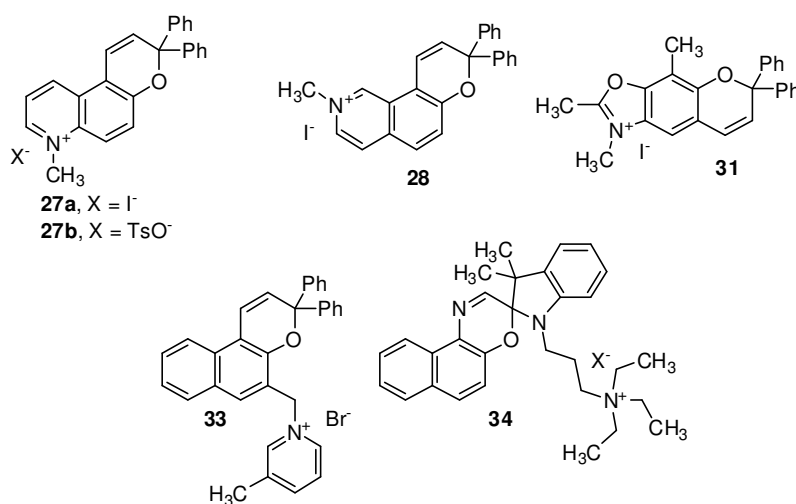
Figure 3.39. Types of interaction of small molecules with DNA: a) minor groove-binding; b) intercalation [74].

The DNA helix exhibits two grooves of different size, namely the minor and the major grooves, which may serve as binding sites for guest molecules. Whereas relatively large molecules such as proteins bind preferentially to the major groove, the minor groove is the preferred binding site for smaller ligands (Fig. 3.39a). Vital requirements to the structure of molecules for groove-binding are relative flexibility of the skeleton and the presence of functional groups capable of forming hydrogen bonds.

Intercalation is realized by molecule insertion between the neighboring pairs of DNA bases (Fig. 3.39b). Such binding is mostly stabilized by the hydrophobic and van der Waals interactions. Therefore, for effective intercalation the molecule should be planar, first of all. For small aromatic compounds (benzene, naphthalene), of importance is the presence of the positive charge in the molecule.

For interaction with DNA, various aromatic dyes are used most often. In the general case, intercalation provides weaker interaction of a substance with DNA ($\lg K = 4 - 6$), as compared with minor groove-binding ($\lg K = 5 - 9$), which is associated, in the first case, with greater conformational changes in DNA structure (distance between base pairs increases, small spiral unwinding).

Owing to their ability to transform upon irradiation into planar colored forms, photochromic benzo- and naphthopyrans may be used for reversible photo-control of DNA intercalation. In the initial state, these compounds are non-planar, as a result of the presence of two phenyl groups in the pyran ring. One may expect that before irradiation, due to spatial hindrances, no noticeable interaction with DNA will occur. Upon irradiation, the structure of the photochromes is substantially changed, it becomes planar, and, as a consequence, the probability that the open form gets inserted between the DNA base pairs increases. Thus, this property of the photochromes may be used to photo-control the intercalation process. For this purpose, several compounds containing a heterocyclic



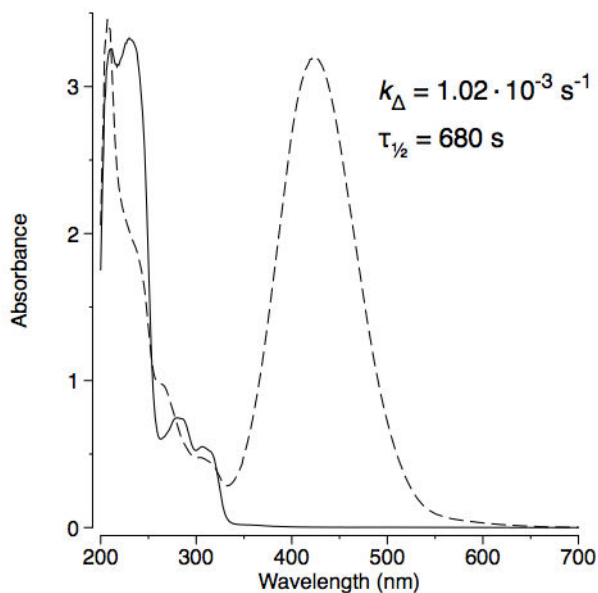


Figure 3.40. Absorption spectra of compound **31** in methanol ($C = 6.65 \cdot 10^{-5}$ M, 20°C) prior to (solid line) and after 1 min of irradiation by monochromatic light with $\lambda = 315$ nm (dashed line). (k is the bleaching rate constant; $\tau_{1/2}$ is the half bleaching time.)

fragment and a positive charge were synthesized. The photochromes possessed the charge located in the aromatic system (**27**, **28**, **31**) or in the side chain (**33**, **34**). However, at the preliminary stage, among five molecules, proposed for carrying out experiments with DNA, only naphthopyran **33** was selected.

Compounds **27** and **28** are well soluble in water. Unfortunately, they were fluorescent and did not exhibit photochromism sufficient for detection. In contrast, benzoxazole derivative **31** exhibit good photochromic properties (colorability and color stability upon cessation of radiation) in such polar solvents as acetonitrile and methanol (Fig. 3.40), which is unusual for

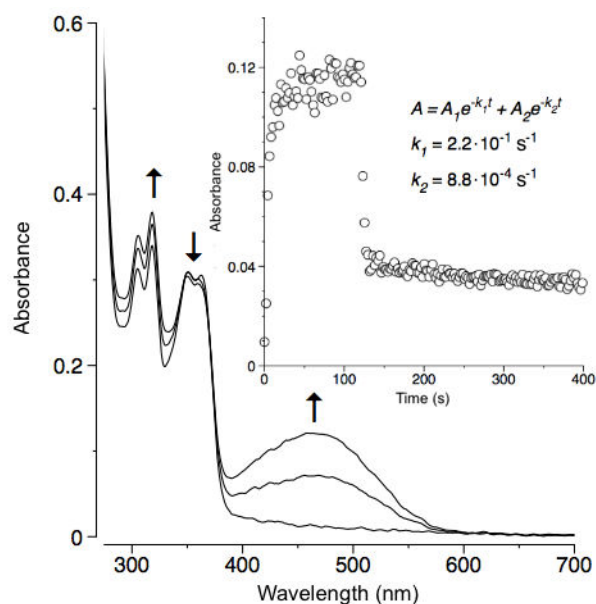


Figure 3.41. The change in absorption spectrum of compound **33** in BPE buffer solution at 10°C during irradiation (Hg lamp, 120 W, full light, 2 min). The insert corresponds to absorbance change at 480 nm during irradiation and after its termination. (A, A_1, A_2 are absorbances; k_1, k_2 are bleaching rate constants.)

chromenes (compare to **1** and **3**). Unfortunately, the chromene was insoluble in water and water/methanol, water/DMSO mixtures.

Finally, chromene **33** and spironaphthoxazine **34** are well soluble in water. These compounds exhibited the photochromic properties; however, the stability of the open forms in aqueous solutions at 20°C was extremely low, especially for compound **34**. Nevertheless, the temperature decrease down to 10°C helped in carrying out a number of experiments with compound **33**. At this temperature, chromene produces two open forms ($k_1 = 2.2 \cdot 10^{-2} \text{ s}^{-1}$, $k_2 = 8.8 \cdot 10^{-4} \text{ s}^{-1}$) (Fig. 3.41).

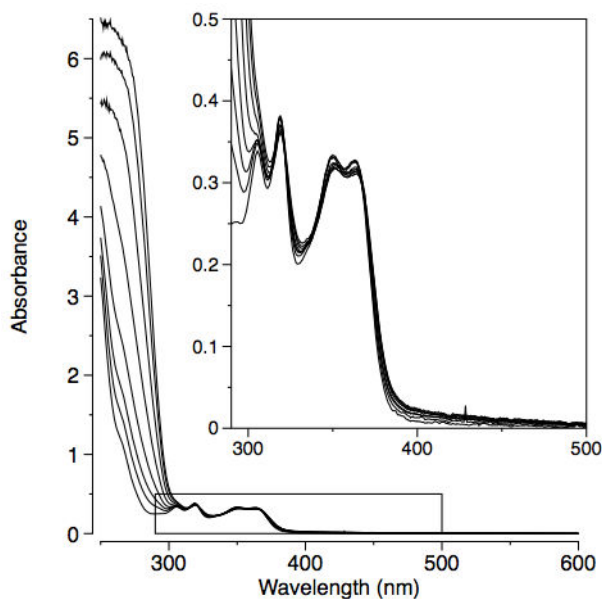


Figure 3.42. Spectrophotometric titration of chromene **33** by DNA solution in BPE buffer containing 5% vol. DMSO.

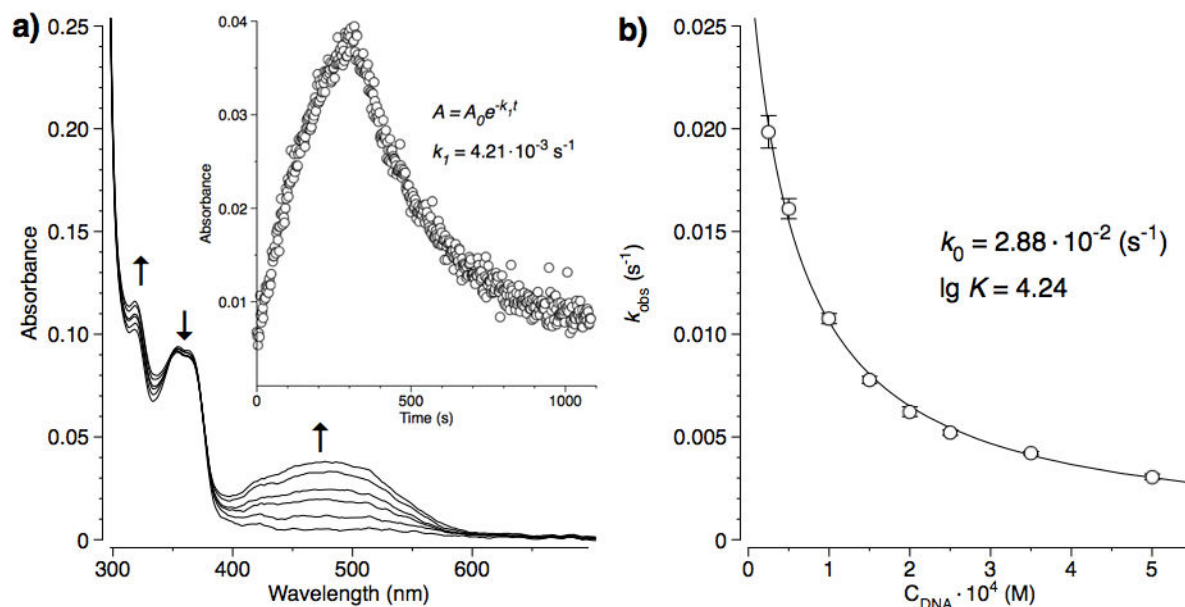
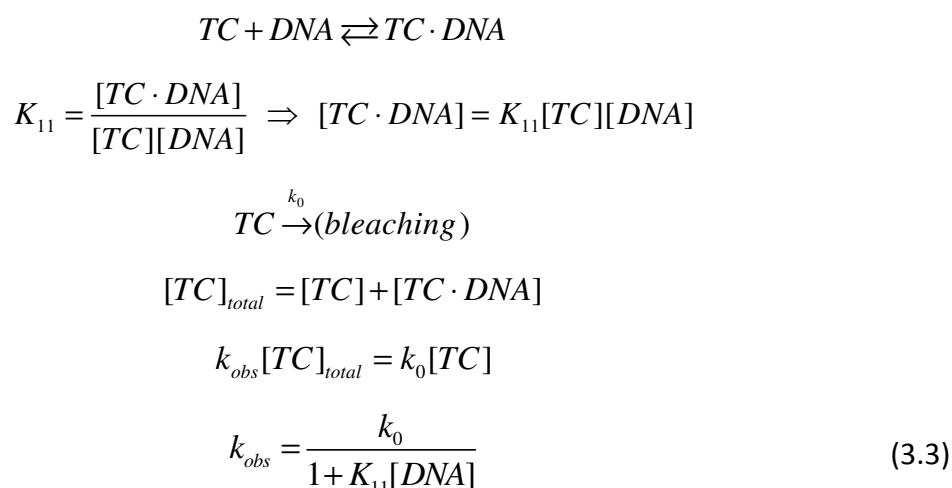


Figure 3.43. The effect of DNA on photochromic properties of chromene **33** (BPE buffer, 10°C, $C_{33} = 5.2 \cdot 10^{-5} \text{ M}$, irradiation by filtered light with $\lambda = 313 \text{ nm}$ during 5 min): a) spectrum change of solution with $C_{\text{DNA}}/C_{33} = 7$ upon irradiation, the insert corresponds to optical density change at 480 nm during and after irradiation; b) the change of observed rate constant of compound **33** solution bleaching depending on DNA concentration. (A , A_0 are absorbances; k , k_0 are bleaching rate constants; $\lg K$ is logarithm of stability constant for a complex with DNA. See explanation in the text.)

Stability constants of the DNA complexes with various ligands were determined by spectrophotometric titration in the buffer solution. In these experiments BPE buffer was used (2 mM NaH₂PO₄, 6 mM Na₂HPO₄, 1 mM Na₂EDTA, pH ~ 7.0). In the case of chromene **33**, addition of a large DNA excess led to precipitation. That is why, for titration a solution containing 5% vol. DMSO was used. As expected the closed form of chromene **33** (prior to irradiation) does not produce stable complexes. During titration no considerable changes in the absorption spectrum were observed, giving evidence of the absence of any specific interactions between the molecules (Fig. 3.42). Small changes, which were observed, were most likely associated with the chromene and DNA absorption bands overlap, the degree of the latter in the solution being increased in the course of titration.

Irradiation of solutions of compound **33**, containing different amount of DNA, produced absorption bands in the visible region. Thermal relaxation was characterized by a mono-exponential kinetic curve that gave evidence of only one photoinduced isomer formation under these conditions (Fig. 3.43a). Bleaching rate constants differed from corresponding initial values for the TC and TT forms. However, taking into account that increasing DNA amount led to stepwise decrease of the rate constant, changes in the spectrum were associated with the TC isomer formation (Fig. 3.43b).

To interpret the obtained dependencies, the following scheme of the process was assumed:



This scheme suggests that the TC isomer formed as a result of irradiation intercalates to DNA. Thus, the TC→TT transformation inside DNA will be rather difficult. Therefore, under these conditions, the TT isomer is not formed. However, due to the same reasons, the open form conversion to the closed form will also be impossible. Thus, only the free TC forms will contribute into the bleaching kinetics. However, taking into account that a part of them will occur inside DNA, the rate decrease upon increasing DNA concentration should be detected,

and it is indeed the case. Even if we assume that the open form conversion to the closed form may proceed inside DNA, bleaching will be caused by the free TC forms, because complex of the closed form with DNA is extremely unstable. Finally, accounting for the large DNA excess used in the experiments, it may be assumed that $[DNA] = C_{DNA}$. Then the expression (3.3) will give the following form:

$$k_{obs} = \frac{k_0}{1 + K_{11} C_{DNA}} \quad (3.3a)$$

The use of dependence (3.3a) helped in determining the stability constant of the TC complex with DNA (Fig. 3.43b). This value correlates well with the reported stability constant value for a photochromic spiropyran ($2 \cdot 10^4 \text{ M}^{-1}$) [73] and lies within the range of the average intercalation stability constants values ($10^4 - 10^6 \text{ M}^{-1}$) [74].

Nevertheless, the calculated bleaching constant value for the free TC form (0.0288 s^{-1}) is different from the one found in the experiment (0.22 s^{-1}). The reason for such deviation may be a simplified model of complex formation, which does not take into account all the details of complex formation with DNA. For instance, the most popular model in the literature is the so-called “neighbor exclusion model” [74, 135], based on the idea that an intercalator molecule, inserted between the base pairs, prevents another molecule from insertion between the neighbor base pairs, DNA molecule being considered as one infinitely long 1D lattice. The exclusion number, n , is introduced, representing the number of the free “cells” that separate two occupied intercalation sites. The expression describing this model was suggested by J. McGhee and P. von Hippel in 1974 [136]:

$$K = \frac{[DNA \cdot L]}{[L]} \cdot \frac{(C_{DNA} + [DNA \cdot L](n-1))^{n-1}}{(C_{DNA} - n[DNA \cdot L])^n}$$

It can be easily seen that with $n = 1$ this expression is reduced to a simpler one for the 1:1 complex formation constant, which, as applied to DNA, was called the Scatchard model. In the case of chromene **33**, this model adequately describes the experimental data and determines the intercalation constant, which is probably related to some general macroeffect, rather than the true value of the ligand interaction constant with a single site in DNA molecule (microinteraction). An indirect proof of the specific binding (intercalation) is also a considerable (by 1-2 orders of magnitude) reduction of the rate constant of the TC forms bleaching.

4. Conclusions

1. We developed two approaches to preparation of series of new benzo- and naphthopyrans, which involve annelated crown ether fragments of different size and heteroatomic composition, as well as chromenes, which contain positively charged heterocyclic fragment.
2. It was shown that the metal cations may effectively bind with crown ether moiety of the chromene molecule. Using NMR and UV-Vis spectroscopy, stability constants of such complexes were determined along with the bleaching rate constants of the open forms. The complex formation was proved to affect considerably the spectral and kinetical properties of the chromenes; and on the contrary, photochromic transformation leads to decrease of the chromene ability to form complexes. Such effects may be employed for photo-control of the complex formation.
3. It was demonstrated that the NMR spectroscopy may be used for investigation of the complex formation of crowned chromenes with the metal cations both in the initial and photoinduced states.
4. Depending on the carbon skeleton length, protonated amino acids were found to be able to form the ditopic complexes with the open forms of chromenes, in which the ammonium cation is located inside the crown ether cavity and the carboxylic hydrogen atom establishes a hydrogen bond with the carbonyl oxygen atom of the open form. At the same time, amino acids were demonstrated to form the monotopic complexes with the closed forms of chromenes. Thus, by means of irradiation it is possible to change the mode of complex formation as well as the stability of the complexes formed.
5. A new method for the analysis of the complex stability of chromenes, which contain positive charge, with DNA was proposed. It was demonstrated that such compounds may be used for photo-control of the intercalation process.

5. Experimental Part

NMR spectra were recorded on spectrometers «Bruker 250», «Bruker 400» using TMS as an internal standard. Chemical shifts were measured with 0.01 ppm accuracy; coupling constants were measured with 0.1 Hz accuracy. Deuterated solvents (CDCl₃, DMSO-*d*₆, CD₃CN) were purchased from «Aldrich».

Reactions were monitored by means of TLC plates DC-Alufolien Kieselgel 60 F₂₅₄ and Silica gel 60 F-254 purchased from Merck. Silica gel 60 with particles size 0.063-0.200 mm, Silica gel 60 0.043-0.060 mm, and Silica gel 60 RP-18 0.040-0.063 mm, all purchased from Merck, were used for column chromatography.

Elemental analysis was carried out in Universität Siegen (Siegen, Germany) and A.N.Nesmeyanov Institute of Organoelement Compounds RAS (Moscow, Russia).

Electronic absorption spectra were recorded on spectrophotometers «Specord M40», «Varian Cary 50», «Avantes AvaSpec-2048». Spectra of colored forms were obtained when samples in the spectrometer cell were simultaneously exposed to continuous irradiation, generated by Hg high pressure lamp 120W or Xe-Hg high pressure lamp 1000W.

Benzo[*b*]-15-crown-5 ether, benzo[*b*]-18-crown-6 ether, pyrogallol, triethylorthoformate, Eaton's reagent, phosphorous (V) oxide, ethyl bromoacetate, methalsulfonic acid, *p*-toluenesulfonic acid, *p*-toluenesulfonyl chloride, silver (I) *p*-toluenesulfonate, methyl *p*-toluenesulfonate, *m*-chloroperbenzoic acid, LiAlH₄, triphenylphosphine, iodomethane, 1,1-diphenylprop-2-in-1-ol, β-cinnamaldehyde, Ti(OEt)₄, tetraethylene glycol, pentaethylene glycol, diethylene glycol, 2,2'-oxydi(ethanethiol), 2,2'-(ethane-1,2-dioxy)di(ethanethiol), *N,N'*-dimethyl-2,2'-(ethane-1,2-dioxy)di(ethylamine), 2,3,3-trimethyl-3*H*-indole, 1,3,3-trimethyl-2-methyleneindoline, 1,3-dibromopropane, 1-nitroso-2-naphthol, acetic acid, organic solvents (acetonitrile, ethanol, methanol, tetrahydrofuran, toluene, pyridine) were purchased from either Aldrich, Merck, Fluka, or Alfa Aesar and used without additional purification. In appropriate cases, solvents were purified according standard procedures.

15-Hydroxybenzo[*b*]-15-crown-5 ether (**4a**) [108, 114], 18-hydroxybenzo[*b*]-18-crown-6 ether (**4b**) [108], 14-Hydroxybenzo[*b*]-15-crown-5 ether (**6a**), 17-Hydroxybenzo[*b*]-18-crown-6 ether (**6b**), 4-hydroxy-2-ethoxybenzo[*d*][1,3]dioxol (**11**), 4-(methylphenyl)oxy-2-ethoxybenzo[*d*][1,3]dioxol (**12**), 3-(methylphenyl)oxy-1,2-dihydroxybenzene (**13**), 14-(methylphenyl)oxybenzo[*b*]-15-crown-5 ether (**14a**), 17-(methylphenyl)oxybenzo[*b*]-18-crown-6 ether (**14b**) [111-113], 18-acetylbenzo[*b*]-18-crown-6 ether (**8a**) [139], diethyl 2,2'-

(naphthalene-2,3-diylbis(oxy))diacetate (**18**) [126], 3,3-diphenyl-3*H*-pyrano[3,2-*f*]quinolone (**35**), 3,3-diphenyl-3*H*-pyrano[2,3-*h*]isoquinoline (**36**), 3,3-diphenyl-3*H*-pyrano[3,2-*f*]quinazoline (**37**), 2-methyl-7,7-diphenyl-7*H*-chromeno[6,5-*d*]oxazole (**38**), 2,4-dimethyl-6,6-diphenyl-6*H*-chromeno[[6,7-*d*]oxazole (**39**), 2-methyl-7,7-diphenyl-7*H*-chromeno[5,6-*d*]oxazole (**40**) [121, 123, 124], (3,3-diphenyl-3*H*-benzo[*f*]chromene-5-yl)methanol (**41**), 5-bromomethyl-3,3-diphenyl-3*H*-benzo[*f*]chromene (**42**) [129], 1-(3-bromopropyl)-2,3,3-trimethyl-3*H*-indolinium bromide (**43a**), 1-(3-bromopropyl)-3,3-dimethyl-2-methyleneindoline (**44**) [73] were synthesized according to known procedures.

Barium (II), magnesium (II), lead (II) perchlorates were purchased from Aldrich and used without additional purification.

Protonated amino acids were prepared by dissolving neutral β -alanine, γ -aminobutyric, ϵ -aminocaproic, and ω -aminocaprylic acids (all purchased from Aldrich) in acetonitrile solution of perchloric acid at ambient temperature. After being stirred during 24 h, the solution was filtered and the solvent was evaporated. The residue was additionally kept in a lyophilizer during 20 h.

5.1. Syntheses

5.1.1. Acylation Using Eaton's Reagent

The procedure was adopted from lit. [139]. *Eaton's reagent* was prepared in argon atmosphere by mixing methanesulfonic acid (10 *eq.*) and phosphorous (V) oxide (1 *eq.*) until dissolved. The obtained solution contained *ca.* 13% by weight of P₂O₅. Also, the commercial reagent (7.5% P₂O₅, purchased from Alfa Aesar) was used.

At ambient temperature, glacial acetic acid (1.1 *eq.*) was mixed with *Eaton's reagent* (containing 2 *eq.* of P₂O₅) and the appropriate benzene or naphthalene derivative (1 *eq.*) was added. After 6 *h* of stirring in Ar atmosphere, the mixture was poured into cooled water followed by extraction with dichloromethane. The organic layer was washed several times with water, dried over MgSO₄ and the solvent was removed under diminished pressure.

1-(2,3,5,6,8,9,11,12-Octahydronaphtho[2,3-*b*][1,4,7,10,13]pentaoxacyclopentadecine-16-yl)ethanone (**8b**)

According to the general procedure, from 1.56 g (5.0 *mmol*) of naphtho-15-crown-5 ether, 0.33 g (5.5 *mmol*) of acetic acid, 19 g of *Eaton's reagent* (containing 10.0 *mmol* of P₂O₅)

and after the residue of evaporating was extracted by hot heptane, 1.62 g (90%) of **8b** was obtained as white crystals. M.p. 126-129°C. ¹H NMR (250MHz, CDCl₃, δ ppm, *J* Hz): 2.69 (s, 3H, CH₃), 3.78-3.76 (m, 8H, 4 × CH₂), 3.96-4.06 (m, 4H, 2 × CH₂), 4.22-4.32 (m, 4H, 2 × CH₂), 7.11 (s, 1H, H-20), 7.20 (s, 1H, H-14), 7.70 (d, *J* = 8.6, 1H, H-18), 7.89 (dd, *J* = 8.6 and 1.5, 1H, H-17), 8.31 (s, 1H, H-15). ¹³C NMR (63MHz, CDCl₃, δ ppm): 26.67, 68.50, 68.60, 69.32, 69.39, 70.37, 70.40, 71.41, 107.40, 109.15, 122.79, 126.72, 128.41, 128.60, 132.27, 133.14, 149.95, 151.48, 198.16. Calculated for C₂₀H₂₄O₆ (%): C, 66.65; H, 6.71. Found (%): C, 66.37; H, 6.68.

Diethyl 2,2'-(6-acetylnaphthalene-2,3-diylbis(oxy))diacetate (**19**)

According to the general procedure, from 8.15 g (24.5 mmol) of ester **18**, 1.62 g (27 mmol) of acetic acid, 93 g of Eaton's reagent (containing 49.0 g of P₂O₅) and after the residue of evaporating was treated with methanol, 7.70 g (84%) of **19** was obtained as beige solid. The sample amount for analysis was recrystallized from heptane. M.p. = 116-118°C. ¹H NMR (250MHz, CDCl₃, δ ppm, *J* Hz): 1.31 (t, *J* = 7.1, 6H, 2 × OCH₂CH₃), 2.69 (s, 3H, CH₃CO), 4.30 (q, *J* = 7.1, 4H, 2 × OCH₂CH₃), 4.84 (s, 2H, OCH₂CO), 4.85 (s, 2H, OCH₂CO), 7.10 (s, 1H, H-1), 7.22 (s, 1H, H-4), 7.70 (d, *J* = 8.6, 1H, H-8), 7.91 (dd, *J* = 8.6 and 1.7, 1H, H-7), 8.30 (s, 1H, H-5). ¹³C NMR (63MHz, CDCl₃, δ ppm): 14.11, 26.60, 61.53, 65.93, 66.11, 108.63, 110.59, 123.14, 126.79, 128.34, 128.56, 132.06, 133.41, 148.25, 149.70, 168.18, 168.34, 197.92. Calculated for C₂₀H₂₂O₇ (%): C, 64.16; H, 5.92. Found(%): C, 65.10; H, 6.08.

5.1.2. Baeyer-Villiger Oxidation

An appropriate ketone (1 eq.) and *p*-toluenesulfonic acid (0.7 eq.) was dissolved in dichloromethane (20 ml for 1 g of ketone) and *m*-chloroperbenzoic acid (2 eq.) was added to the solution. After being stirred at ambient temperature and in Ar atmosphere during 20 h, the mixture was filtered off the precipitate formed. The filtrate was consecutively washed by 10% NaHSO₃ solution (2×75 ml), saturated NaHCO₃ solution (3×75 ml), and brine (2×75 ml); then, dried over MgSO₄ and concentrated under diminished pressure.

2,3,5,6,8,9,11,12,14,15-Decahydrobenzo[*b*][1,4,7,10,13,16]hexaoxacyclooctadecine-18-yl acetate (**9a**)

According to the general procedure, from 2.22 g (6.3 mmol) of ketone **8a**, 0.84 g (4.41 mmol) of PTSA, and 3.10 g (12.6 mmol) of *m*CPBA (30% wet), after the residue of evaporating was treated with pentane, 1.62 g (70%) of **9a** was obtained as beige solid. The product was used in the next stage without additional purification. ¹H NMR (250MHz, CDCl₃, δ

ppm, *J* Hz): 2.27 (s, 3H, CH₃), 3.67-3.80 (m, 12H, 6 × CH₂), 3.88-3.95 (m, 4H, 2 × CH₂), 4.10-4.18 (m, 4H, 2 × CH₂), 6.62 (d, *J* = 9.2, 1H, H-19), 6.64 (s, 1H, H-17), 6.86 (d, *J* = 9.2, 1H, H-20). NMR data corresponds to lit. [139].

2,3,5,6,8,9,11,12-Octahydronaphtho[2,3-*b*][1,4,7,10,13]pentaoxacyclopentadecine-16-yl acetate (9b)

Procedure with the use of peracetic acid. A solution of *ca.* 9% peracetic acid was prepared by treating 10 g (0.167 mmol) of glacial acetic acid with 24.7 g of 35% H₂O₂ solution at 15-16°C and in the presence of 0.4 g of *conc.* H₂SO₄ and subsequent stirring the mixture at ambient temperature during 24 h. At 10-15°C, 6.3 g (*ca.* 7.42 mmol) of freshly-made peracetic acid was added dropwise to a solution of 1.53 g (4.25 mmol) of ketone **8b** in 10 ml of glacial acetic acid. The temperature was slowly increased up to 30°C and the reaction was stirred for 4 h. Then, the mixture was poured into a solution of sodium thiosulfate; the resulted solution was neutralized to pH 5-6. After extraction with dichloromethane, the organic layer was dried over MgSO₄ and then the solvent was evaporated. The residue was purified by column chromatography (ethyl acetate) to give 0.05 g (4%) of **9b** as white solid.

According to the general procedure, from 0.54 g (1.5 mmol) of ketone **8b**, 0.20 g (1.05 mmol) of PTSA, 0.74 g (3 mmol) of *m*CPBA, 0.23 g (40%) of ester **9b** was obtained as viscous oil. The product was used in the next stage without additional purification. A sample for analysis was crystallized from methanol to afford the product as colorless crystals. M.p. 133-134°C. ¹H NMR (250MHz, CDCl₃, δ ppm, *J* Hz): 2.33 (s, 3H, CH₃), 3.76-3.80 (m, 8H, 4 × CH₂), 3.94-4.00 (m, 4H, 2 × CH₂), 4.20-4.25 (m, 4 H, 2 × CH₂), 7.02-7.10 (m, 3H, H-14, H-18, H-19), 7.36 (s, 1H, H-15), 7.65 (d, *J* = 8.8, 1H, H-17). ¹³C NMR (63MHz, CDCl₃, δ ppm): 21.30, 68.40, 68.48, 69.33, 69.37, 70.33, 71.29, 107.59, 107.91, 117.33, 118.98, 127.34, 127.72, 129.73, 147.27, 149.15, 149.92, 169.93. Calculated for C₂₀H₂₄O₇·H₂O (%): C, 60.90; H, 6.64. Found (%): C, 60.96; H, 6.20.

6,7-Bis(ethoxycarbonylmethoxy)naphthalene-2-yl acetate (20)

According to the general procedure, from 1.00 g (2.67 mmol) of ketone **19**, 0.36 g (1.87 mmol) of PTSA, 0.92 g (5.34 mmol) of *m*CPBA, after the residue of evaporating was treated with pentane, 0.35 g (34%) of **20** as yellowish solid containing traces of the initial ketone. The product was used in the next stage without additional purification. ¹H NMR (250MHz, CDCl₃, δ ppm, *J* Hz): 1.26-1.34 (m, 6H, 2 × OCH₂CH₃), 2.34 (s, 1H, CH₃CO), 4.23-3.34

(m, 4H, 2 × OCH₂CH₃), 4.80 (s, 2H, OCH₂CO), 4.81 (s, 2H, OCH₂CO), 7.02-7.11 (m, 3H, H-14, H-18, H-19), 7.38 (d, *J* = 2.4, 1H, H-15), 7.67 (d, *J* = 8.9, 1H, H-17).

5.1.3. Synthesis of Naphthols

2,3,5,6,8,9,11,12-Octahydronaphtho[2,3-*b*][1,4,7,10,13]pentaoxacyclopentadecine-16-ol (**5**)

The procedure was adopted from lit. [108]. In 40 ml of water, 0.23 g (0.6 mmol) of ester **9b** was suspended and 20 ml of 30% NaOH solution was added. The mixture was stirred at 50°C for 3 h, then cooled to ambient temperature and washed once with dichloromethane. The aqueous phase was acidified with *conc.* HCl to pH 2 and extracted several times with dichloromethane. The combined fractions were washed with water; the organic layer was dried over MgSO₄ and the solvent was evaporated. The residue was treated with pentane to afford 0.12 g (60%) of **5** as brown solid. The sample amount for analysis was recrystallized from dichloromethane as colorless crystals. M.p. 157-158°C. ¹H NMR (250MHz, CDCl₃, δ ppm, *J* Hz): 3.70-4.20 (m, 16H, 8 × CH₂), 6.74 (s, 1H, H-15), 6.90 (dd, *J* = 8.7 и 2.3, 1H, H-17), 6.94-7.00 (m, 2H, H-14, H-19), 7.39 (d, *J* = 8.7, 1H, H-18). ¹³C NMR (63MHz, CDCl₃, δ ppm): 68.01, 68.41, 69.37, 69.50, 70.32, 70.36, 71.03, 106.61, 108.41, 108.88, 115.76, 123.99, 127.89, 130.60, 147.17, 149.66, 152.87. Calculated for C₁₈H₂₂O₆ (%): C, 64.66; H, 6.63. Found (%): C, 63.65; H, 6.55.

6,7-Bis(2-hydroxyethoxy)naphthalene-2-ol (**17a**)

The procedure was adopted from lit. [127]. A solution of 3.85 g (*ca.* 7 mmol) of ester **20** in 25 ml of *abs.* THF was added dropwise to a solution of 1.06 g (28 mmol) of LiAlH₄ in 250 ml of *abs.* THF. The suspension was stirred at ambient temperature for 3 h. Then, 4.48 g of 5% NaOH solution was added dropwise. After the resulted mixture was refluxed for 4 h, it was cooled, the precipitate was filtered off and the filtrate was washed several times with water. The aqueous phase was acidified with H₂SO₄ to pH 2 and then extracted with ethyl acetate (3 × 50 ml). The organic layer was dried over MgSO₄ and the solvent was evaporated. The residue was treated with ethanol to give 1.11 g (60%) of naphthol **17a** as beige solid. A sample for analysis was crystallized from methanol to afford the product as colorless crystals. M.p. 179-181°C. ¹H NMR (250MHz, DMSO-*d*₆, δ ppm, *J* Hz): 3.71-3.83 (m, 4H, OCH₂CH₂OH), 3.99-4.12 (m, 4H, OCH₂CH₂OH), 4.88 (m, 2H, OCH₂CH₂OH), 6.85 (dd, *J* = 8.7 and 2.4, 1H, H-3), 6.97 (d, *J* = 2.4, 1H, H-1), 7.10 (s, 1H, H-5), 7.19 (s, 1H, H-8), 7.54 (d, *J* = 8.7, 1H, H-4), 9.37 (s, 1H, Ar-

OH). ^{13}C NMR (75MHz, DMSO- d_6 , δ ppm): 59.47, 59.52, 69.98, 70.14, 106.51, 108.12, 108.40, 115.93, 122.96, 127.63, 130.44, 146.34, 149.18, 153.97. Calculated for $\text{C}_{14}\text{H}_{16}\text{O}_5$ (%): C, 63.63; H, 6.10. Found (%): C, 63.65; H, 6.35.

6,7-Bis(2-chloroethoxy)naphthalene-2-ol (17b)

The procedure was adopted from lit. [128]. To a solution of 2.35 g (8.9 mmol) of naphthol **17a** in 125 ml of dichloromethane 9.33 g (35.6 mmol) and 17.2 ml (0.178 mol) were added. The mixture was refluxed for 3 h. The solvent was evaporated and the residue was purified by column chromatography (ethyl acetate/c-hexane = 1/4) to give 2.15 g (80%) of naphthol **17b** as pinkish solid. M.p. 115-117°C. ^1H NMR (250MHz, DMSO- d_6 , δ ppm, J Hz): 3.94-4.05 (m, 4H, $\text{OCH}_2\text{CH}_2\text{Cl}$), 4.26-4.39 (m, 4H, $\text{OCH}_2\text{CH}_2\text{Cl}$), 6.90 (dd, $J = 8.7$ and 2.4 , 1H, H-3), 7.00 (d, $J = 2.4$, 1H, H-1), 7.18 (s, 1H, H-5), 7.28 (s, 1H, H-8), 7.57 (d, $J = 8.7$, 1H, H-4), 9.47 (s, 1H, Ar-OH). ^{13}C NMR (75MHz, DMSO- d_6 , δ ppm): 42.97, 43.01, 68.72, 69.11, 107.80, 108.17, 110.23, 116.48, 123.17, 127.87, 130.80, 145.51, 148.52, 154.34. Calculated for $\text{C}_{14}\text{H}_{14}\text{Cl}_2\text{O}_3$ (%): C, 55.83; H, 4.69. Found (%): C, 55.90; H, 4.70.

5.1.4. Synthesis of Chromenes from Appropriate Phenols

Method 1 (with the use of diphenylpropargyl alcohol). The procedure was adopted from lit. [118]. Substituted phenol or naphthol (0.6 mmol) and 1,1-diphenylprop-2-in-1-ol (0.6 mmol) were dissolved in 10 ml of toluene and PTSA (0.06 mmol) was added. The mixture was stirred at 50-60°C for 1 h and then at 70-80°C for additional 3 h. Afterwards the solvent was evaporated and the product was isolated by column chromatography.

Method 2 (with the use of β -phenylcinnamaldehyde). The procedure was adopted from lit. [122]. Substituted phenol or naphthol (1 mmol) and β -phenylcinnamaldehyde (1 mmol) were dissolved in 8 ml of toluene and a solution of titanium (IV) tetraethoxide (1.5 mmol) in 2 ml of toluene was added. The mixture was stirred at 100°C in Ar atmosphere for 6 h, then cooled to 30-40°C and 10 ml of toluene, 0.5 g of Silica gel, and 1 ml of water were added to it. The resulting suspension was stirred at 80°C for 30 min. After cooling to ambient temperature, the precipitate was filtered off, washed with dichloromethane several times and the organic solution was evaporated. The product was isolated by column chromatography.

2,2-Diphenyl-7,8,10,11,13,14,16,17-octahydro-2H-[1,4,7,10,13]pentaoxacyclopentadeca[2,3-*g*]chromene (1a)

For *Method 1* see lit. [114].

According to the general procedure for *Method 2*, from 0.57 g (2 mmol) of phenol **4a**, 0.42 g (2 mmol) of β -phenylcinnamaldehyde, 0.68 g (3 mmol) of titanium (IV) ethoxide, after the column chromatography (MeOH/CH₂Cl₂ = 1/9), 0.19 g (20%) of **1a** was obtained as orange solid. M.p. 110-113°C.

¹H NMR (300MHz, CD₃CN, δ ppm, *J* Hz): 3.58–3.70 (m, 8H, CH₂-5, CH₂-6, CH₂-8, CH₂-9), 3.72–3.83 (m, 4H, CH₂-3, CH₂-11), 3.96–4.02 (m, 2H, CH₂-2), 4.04–4.12 (m, 2H, CH₂-12), 6.25 (d, *J* = 9.8, 1H, H-17), 6.48–6.63 (m, 2H, H-18, H-14), 6.69 (s, 1H, H-19), 7.22–7.65 (m, 10H, H-Ar). ¹³C NMR (75MHz, CD₃CN, δ ppm): 68.5, 68.8, 69.2, 69.7, 69.8, 70.1, 70.4, 70.5, 82.0 (s, *quat*-C), 102.8, 112.9, 113.8, 123.3, 126.5, 126.8, 127.5, 128.2, 143.4, 145.3, 147.2, 150.4. Calculated for C₂₉H₃₀O₆ (%): C, 73.0; H, 6.4. Found (%): C, 73.2; H, 6.3.

2,2-Diphenyl-7,8,10,11,13,14,16,17,19,20-decahydro-2H-[1,4,7,10,13,16]hexaoxacyclooctadeca[2,3-*g*]chromene (1b)

According to the general procedure for *Method 1*, from 0.2 g (0.6 mmol) of phenol **4b**, 0.12 g (0.6 mmol) of 1,1-diphenylprop-2-in-1-ol, 0.01 g (0.06 mmol) of PTSA6 after the column chromatography (MeOH/CH₂Cl₂ = 1/9), 0.06 g (19%) of **1b** was obtained as viscous oil.

According to the general procedure for *Method 2*, from 0.33 g (1 mmol) of phenol **4b**, 0.21 g (1 mmol) β -phenylcinnamaldehyde, 0.34 g (1.5 mmol) of titanium (IV) ethoxide, after the column chromatography (MeOH/CH₂Cl₂ = 1/9), 0.19 g (20%) of **1a** was obtained as orange solid. M.p. 76-78°C.

¹H NMR (250MHz, CDCl₃, δ ppm, *J* Hz): 3.58-3.72 (m, 12H, CH₂-5, CH₂-6, CH₂-8, CH₂-9, CH₂-11, CH₂-12), 3.77-3.88 (m, 4H, CH₂-3, CH₂-14), 3.96-4.08 (m, 4H, CH₂-2, CH₂-15), 5.94 (d, *J* = 9.7, 1H, H-20), 6.39-6.52 (m, 3H, H-17, H-21, H-22), 7.11-7.29 (m, 6H, H-Ar), 7.30-7.38 (m, 4H, H-Ar). ¹³C NMR (63MHz, CDCl₃, δ ppm): 68.56, 69.34, 69.63, 69.91, 70.53, 70.59, 70.66, 70.68, 82.43 (s, *quat*-C), 102.61, 113.23, 113.38, 123.01, 126.35, 126.87, 127.34, 127.97, 142.80, 144.83, 147.33, 150.14. Calculated for C₃₁H₃₄O₇·2H₂O (%): C, 67.13; H, 6.91. Found (%): C, 67.68; H, 6.96.

3,3-Diphenyl-9,10,12,13,15,16,18,19-octahydro-3H-[1,4,7,10,13]pentaoxacyclopentadeca[2',3':4,5]benzo[*f*]chromene (2)

According to the general procedure for *Method 1*, from 0.096 g (0.29 mmol) of naphthol **5**, 0.06 g (0.29 mmol) of 1,1-diphenylprop-2-in-1-ol, 0.006 g (0.029 mmol) PTSA, after the column chromatography (MeOH/CH₂Cl₂ = 1/9), 0.024 g (16%) of **1b** was obtained as viscous oil.

According to the general procedure for *Method 2*, from 0.2 g (0.6 mmol) of phenol **4b**, 0.12 g (0.6 mmol) of β -phenylcinnamaldehyde, 0.21 g (0.9 mmol) of titanium (IV) ethoxide, after the column chromatography (MeOH/CH₂Cl₂ = 1/9), 0.09 g (29%) of **2** was obtained as beige solid. M.p. 147-148°C.

¹H NMR (250MHz, CDCl₃, δ ppm, *J* Hz): 3.74-3.78 (m, 8H, CH₂-12, CH₂-13, CH₂-15, CH₂-16), 3.87-3.95 (m, 4H, CH₂-10, CH₂-18), 4.10-4.22 (m, 4H, CH₂-9, CH₂-19), 6.24 (d, *J* = 9.9, 1H, H-2), 6.96 (s, 1H, H-21), 7.04 (d, *J* = 8.7, 1H, H-5), 7.14-7.34 (m, 8H, H-Ar, H-1, H-7), 7.41-7.51 (m, 5H, H-Ar, H-6). ¹³C NMR (75MHz, CD₃CN, δ ppm): 68.46, 68.48, 69.31, 70.24, 71.09, 82.17 (s, *quat*-C), 102.56, 109.17, 113.34, 116.15, 119.69, 124.88, 125.67, 126.97, 127.43, 127.54, 128.03, 128.11, 144.90, 147.36, 149.52, 149.96. Calculated for C₃₃H₃₂O₆ (%): C, 75.55; H, 6.15. Found (%): C, 75.23; H, 6.02.

2,2-Diphenyl-8,9,11,12,14,15,17,18-octahydro-2H-[1,4,7,10,13]pentaoxacyclopentadeca[2,3-*h*]chromene (3a)

According to the general procedure for *Method 1*, from 0.57 g (2 mmol) of phenol **6a**, 0.42 g (2 mmol) of 1,1-diphenylprop-2-in-1-ol, 0.04 g (0.2 mmol) of PTSA, after the column chromatography (ethyl acetate), < 0.01 g (< 1%) of chromene **3a** was obtained as viscous oil.

According to the general procedure for *Method 2*, from 1.14 g (4 mmol) of phenol **6a**, 0.84 g (4 mmol) of β -phenylcinnamaldehyde, 1.37 g (6 mmol) of titanium (IV) ethoxide, after the column chromatography (ethyl acetate), 0.56 g (30%) of chromene **3a** was obtained as yellowish solid. M.p. 72-74°C (pentane).

¹H NMR (250MHz, CDCl₃, δ ppm, *J* Hz): 3.70-3.79 (m, 8H, 4 \times CH₂), 3.83-3.94 (m, 4H, 2 \times CH₂), 4.04-4.20 (m, 4H, 2 \times CH₂), 6.08 (d, 1H, *J* = 9.8, H-17), 6.36 (d, 1H, *J* = 8.4, H-15), 6.55 (d, 1H, *J* = 9.8, H-16), 6.67 (d, 1H, *J* = 8.4, H-14), 7.17-7.35 (m, 6H, H-Ar), 7.41-7.50 (m, 4H, H-Ar). ¹³C NMR (63MHz, CDCl₃, δ ppm): 68.05, 69.31, 69.93, 70.15, 70.45, 70.50, 70.90, 73.12, 82.49 (s, *quat*-C), 105.06, 116.12, 120.93, 123.27, 126.72, 126.78, 127.29, 128.02, 136.82, 144.76, 146.16, 153.31. Calculated for C₂₉H₃₀O₆ (%): C, 73.40; H, 6.37. Found (%): C, 73.82; H, 6.59.

2,2-Diphenyl-8,9,11,12,14,15,17,18,20,21-decahydro-2H-[1,4,7,10,13,16]hexaoxacyclooctadeca[2,3-*h*]chromene (3b)

According to the general procedure for *Method 1*, from 0.33 g (1 mmol) of phenol **6b**, 0.21 g (1 mmol) of 1,1-diphenylprop-2-in-1-ol, 0.02 g (0.01 mmol) of PTSA, after the

column chromatography (ethyl acetate), < 0.01 g (< 1%) of chromene **3b** was obtained as viscous oil.

According to the general procedure for *Method 2*, from 0.30 g (0.91 mmol) of phenol **6b**, 0.31 g (1.37 mmol) of β -phenylcinnamaldehyde, 0.34 g (1.5 mmol) of titanium (IV) ethoxide, after the column chromatography (ethyl acetate), 0.14 g (30%) of chromene **3b** was obtained as white solid. M.p. 83-84°C (pentane).

^1H NMR (250MHz, CDCl_3 , δ ppm, J Hz): 3.65-3.86 (m, 14H, $7 \times \text{CH}_2$), 3.91-3.98 (m, 2H, CH_2), 4.06-4.16 (m, 4H, $2 \times \text{CH}_2$), 6.07 (d, 1H, $J = 9.8$, H-20), 6.39 (d, 1H, $J = 8.4$, H-18), 6.56 (d, 1H, $J = 9.8$, H-19), 6.68 (d, 1H, $J = 8.4$, H-17), 7.20-7.35 (m, 6H, H-Ar), 7.42-7.49 (m, 4H, H-Ar). ^{13}C NMR (63MHz, CDCl_3 , δ ppm): 68.53, 69.69, 70.34, 70.46, 70.64, 70.78, 71.04, 71.15, 72.53, 82.51 (s, *quat*-C), 105.66, 116.28, 121.06, 123.27, 126.82, 127.32, 128.04, 136.71, 144.79, 146.16, 153.24. Calculated for $\text{C}_{31}\text{H}_{34}\text{O}_7$ (%): C, 71.80; H, 6.61. Found (%): C, 71.96; H, 6.82.

8,9-Bis(2-hydroxyethoxy)-3,3-diphenyl-3H-benzo[f]chromene (16a)

According to the general procedure for *Method 1*, from 0.5 g (1.9 mmol) of naphthol **17a**, 0.39 g (1.9 mmol) of 1,1-diphenylprop-2-in-1-ol, 0.04 g (1.9 mmol) of PTSA, after the column chromatography ($\text{CH}_2\text{Cl}_2/\text{MeOH} = 20/1$), 0.31 g (35%) of chromene **16a** was obtained as grey solid.

According to the general procedure for *Method 2*, from 0.14 g (0.53 mmol) of naphthol **17a**, 0.11 g (0.53 mmol) of β -phenylcinnamaldehyde, 0.24 g (1.06 mmol) of titanium (IV) ethoxide, after the column chromatography ($\text{CH}_2\text{Cl}_2/\text{MeOH} = 10/1$), 0.01 g (4%) of chromene **16a** was obtained as grey-brown solid.

The product was used in the next stage without additional purification.

^1H NMR (250MHz, CDCl_3 , δ ppm, J Hz): 3.88-4.27 (m, 8H, $4 \times \text{CH}_2$), 6.27 (d, 1H, $J = 9.9$, H-2), 7.00 (s, 1H, H-10), 7.06 (d, 1H, $J = 8.8$, H-5), 7.15 (d, 1H, $J = 9.9$, H-1), 7.20-7.53 (m, 6H).

8,9-Bis(2-chloroethoxy)-3,3-diphenyl-3H-benzo[f]chromene (16b)

According to the general procedure for *Method 2*, from 0.30 g (1 mmol) of naphthol **17b**, 0.31 g (1.5 mmol) of β -phenylcinnamaldehyde, 0.34 g (1.5 mmol) of titanium (IV) ethoxide, after the column chromatography (ethyl acetate/*c*-hexane = 1/10), 0.39 g (80%) of chromene **16b** was obtained as colorless crystalline solid. M.p. 124-126°C (*n*-heptane). ^1H NMR (250MHz, CDCl_3 , δ ppm, J Hz): 3.80-3.95 (m, 4H, $2 \times \text{CH}_2\text{Cl}$), 4.25-4.42 (m, 4H, $2 \times \text{CH}_2\text{O}$), 6.27 (d, 1H, $J = 9.8$, H-2), 7.05-7.37 (m, 10H), 7.43-7.52 (m, 5H). ^{13}C NMR (63MHz, CDCl_3 , δ ppm): 41.97, 69.60, 82.45, 105.13, 111.76, 113.63, 117.08, 119.66, 125.37, 126.19, 127.11,

127.66, 128.04, 128.22, 128.42, 144.92, 146.71, 149.32, 150.06. Calculated for C₂₉H₂₄Cl₂O₃ (%): C, 70.88; H, 4.92. Found (%): C, 71.49; H, 4.98.

5.1.5. Replacement of Terminal Groups in Chromenes **16a** and **16b**

2,2'-(3,3-Diphenyl-3H-benzo[f]chromene-8,9-diylbis(oxy))diethyl di(*p*-toluenesulfonate) (16c**)**

From chromene 16a. The procedure was adopted from lit. [140]. At 0°C, to a solution, which contained 0.09 g (0.2 mmol) of chromene **16a**, 0.08 g (0.4 mmol) of *p*-toluenesulfonyl chloride, and 10 ml of dichloromethane, 0.11 g (2 mmol) of KOH was added portion-wise and the mixture was stirred for 3 h. Upon efflux of the allotted time, 10 ml of dichloromethane and 20 ml of water were added to the mixture; the aqueous layer was separated and washed with dichloromethane. The organic fractions were combined, washed consecutively with water and brine, dried over MgSO₄, and evaporated. The residue was purified by column chromatography (ethyl acetate/*c*-hexane = 1/4) to yield 0.08 g (53%) of chromene **16c** as beige solid.

From chromene 16b. In a thick-walled glass tube equipped with a threaded teflon stopper, 0.15 g (0.3 mmol) of chromene **16b** and 0.84 g (3 mmol) of silver (I) *p*-toluenesulfonate were mixed in 5 ml of dried acetonitrile. The mixture was heated at 140°C for 20 h, then cooled to ambient temperature and evaporated. The residue was washed with dichloromethane several times; the combined fractions were evaporated and the residue was purified by column chromatography (ethyl acetate/*c*-hexane = 1/4) to give 0.15 g (65%) of chromene **16c** as beige solid.

The product was used in the next stage without additional purification.

¹H NMR (250MHz, CDCl₃, δ ppm, *J* Hz): 2.35 (s, 3H, CH₃), 2.37 (s, 3H, CH₃), 4.15-4.49 (m, 8H, 4 × CH₂), 6.30 (d, 1H, *J* = 9.9, H-2''), 6.92 (s, 1H, H-7''), 7.05-7.57 (m, 18H), 7.72-7.90 (m, 4H, H-Ar_{tosylate}).

8,9-Bis(2-iodoethoxy)-3,3-diphenyl-3H-benzo[f]chromene (16d**)**

The procedure was adopted from lit. [117]. In 10 ml of dried acetone, 0.25 g (0.5 mmol) of chromene **16b** and 0.6 g (4 mmol) NaI were mixed and the reaction was refluxed for 120 h. The precipitate was filtered off. The product was recrystallized from the filtrate solution as colorless needles, yielding 0.21 g (62%) of chromene **16d**. M.p. 131-134°C (acetone). ¹H NMR (250MHz, CDCl₃, δ ppm, *J* Hz): 3.37-3.61 (m, 4H, 2 × CH₂l), 4.26-4.48 (m,

4H, 2 × CH₂O), 6.27 (d, 1H, *J* = 9.9, H-2), 7.04-7.37 (m, 10H), 7.43-7.52 (m, 5H). ¹³C NMR (63MHz, CDCl₃, δ ppm): 1.23, 1.32, 70.26, 82.48, 105.10, 111.75, 113.63, 117.10, 119.66, 125.36, 126.19, 127.13, 127.66, 128.07, 128.22, 128.40, 144.94, 146.41, 149.03, 150.10. Calculated for C₂₉H₂₄I₂O₃ (%): C, 51.65; H, 3.59. Found (%): C, 52.33; H, 3.69.

5.1.6. Synthesis of Crown-Annulated Derivatives

General procedure for preparation of oxacrown derivatives. The procedure was adopted from lit. [113]. A solution of an appropriate alcohol (0.2 mmol) and TBAI (0.1 mmol) in 5 ml of toluene was heated up to 50°C and 0.4 ml of 50% aq. NaOH solution was added. The mixture was stirred for 30 min, followed by addition of 5 ml toluene solution of ditosylate derivative (0.2 mmol). The reaction was refluxed for 16 h, then cooled and washed with water. The organic layer was separated and the solvent was removed. The residue was purified by column chromatography (CH₂Cl₂/MeOH = 100/1 going to 20/1).

General procedure for preparation of dithia- and diazacrown derivatives. The procedure was adopted from lit. [117]. Simultaneously, to a suspension of Cs₂CO₃ (2.5 mmol) in 100 ml of dried acetonitrile two 25 ml solutions in acetonitrile, each containing appropriate chromene (0.5 mmol) and thiol or amine (1.05 mmol), were added dropwise. The mixture was refluxed for 16 h. Upon cooling, the precipitate was filtered off and washed with acetonitrile. The combined organic fractions were evaporated and the residue was dissolved in dichloromethane. The resulted solution was washed with water and evaporated in the presence of slight amount of benzene. The residue was purified by column chromatography.

3,3-Diphenyl-9,10,12,13,15,16,18,19-octahydro-3H-[1,4,7,10,13]pentaoxacyclopentadeca[2',3':4,5]benzo[f]chromene (2)

According to the *general procedure for preparation of oxacrown derivatives*, from 0.09 g (0.2 mmol) of chromene **16a**, 0.08 g (0.2 mmol) of diethylene glycol di(tosylate), 0.04 g (0.1 mmol) TBAI, and 0.4 ml 50% aq. NaOH solution, 0.015 g (14%) of chromene **2** was obtained as viscous oil.

According to the *general procedure for preparation of oxacrown derivatives*, from 0.10 g (0.131 mmol) of chromene **16c**, 0.014 g (0.131 mmol) of diethylene glycol, 0.024 g (0.0655 mmol) TBAI, and 0.3 ml 50% aq. NaOH solution, 0.008 g (11%) of chromene **2** was obtained as viscous oil.

(See paragraph 5.1.4 for characteristics.)

3,3-Diphenyl-9,10,12,13,15,16,18,19-octahydro-3H-[1,4,10]trioxa[7,13]dithiacyclo-pentadeca[2',3':4,5]benzo[f]chromene (21a)

According to the *general procedure for preparation of dithia- and diazacrown derivatives*, from 0.25 g (0.5 mmol) of chromene **16b**, 0.15 g (1.05 mmol) of 2,2'-oxydi(ethanethiol), and 0.81 g (2.5 mmol) of Cs₂CO₃, after eluting with ethyl acetate/c-hexane = 1/5, 0.08 g (29%) of chromene **21a** was obtained as orange solid. M.p. 138-141°C (pentane). ¹H NMR (250MHz, CDCl₃, δ ppm, J Hz): 2.93-3.03 (m, 4H, 2 × SCH₂), 3.07-3.18 (m, 4H, 2 × SCH₂), 3.77-3.87 (m, 4H, CH₂OCH₂), 4.27-4.41 (m, 4H, 2 × OCH₂), 6.26 (d, 1H, J = 9.9, H-2), 7.00 (s, 1H, H-7), 7.06 (d, 1H, J = 8.7, H-5), 7.15-7.37 (m, 8H), 7.44-7.53 (m, 5H). ¹³C NMR (63MHz, CDCl₃, δ ppm): 31.34, 31.57, 70.98, 71.03, 71.80, 71.85, 82.36, 102.55, 109.11, 113.58, 116.50, 119.81, 124.97, 125.75, 127.14, 127.61, 127.87, 128.20, 128.27, 145.01, 147.20, 149.75, 149.79. Calculated for C₃₃H₃₂O₄S₂ (%): C, 71.19; H, 5.79. Found (%): C, 72.95; H, 5.92.

3,3-Diphenyl-9,10,12,13,15,16,18,19,21,22-decahydro-3H-[1,4,10,13]tetraoxa [7,16]dithiacyclooctadeca[2',3':4,5]benzo[f]chromene (21b)

According to the *general procedure for preparation of dithia- and diazacrown derivatives*, from 0.25 g (0.5 mmol) of chromene **16b**, 0.19 g (1.05 mmol) of 2,2'-(ethane-1,2-dioxy)di(ethanethiol), and 0.81 g (2.5 mmol) of Cs₂CO₃, after eluting with ethyl acetate/c-hexane = 1/5, 0.12 g (40%) of chromene **21b** was obtained as yellow solid. M.p. 189-192°C (*n*-heptane/benzene). ¹H NMR (250MHz, CDCl₃, δ ppm, J Hz): 2.92-3.04 (m, 4H, 2 × SCH₂), 3.08-3.25 (m, 4H, 2 × SCH₂), 3.54-3.83 (m, 8H, CH₂OCH₂CH₂OCH₂), 4.17-4.37 (m, 4H, 2 × OCH₂), 6.26 (d, 1H, J = 9.9, H-2), 6.97 (s, 1H, H-7), 7.05 (d, 1H, J = 8.7, H-5), 7.13-7.37 (m, 8H), 7.43-7.53 (m, 5H). ¹³C NMR (63MHz, CDCl₃, δ ppm): 30.99, 31.65, 70.39, 72.46, 72.61, 82.33, 101.06, 101.51, 108.03, 113.60, 116.30, 119.90, 124.82, 125.63, 127.14, 127.59, 127.81, 128.19, 128.22, 145.05, 146.87, 149.42, 149.69. Calculated for C₃₅H₃₆O₅S₂ (%): C, 69.97; H, 6.04. Found (%): C, 68.23; H, .97.

11,20-Dimethyl-3,3-duphenyl-9,10,12,13,15,16,18,19,21,22-decahydro-3H-[1,4,10,13]tetraoxa[7,16]diazacyclooctadeca[2',3':4,5]benzo[f]chromene (22)

According to the *general procedure for preparation of dithia- and diazacrown derivatives*, from 0.10 g (0.148 mmol) of chromene **16c**, 0.03 g (0.163 mmol) of *N,N'*-dimethyl-2,2'-(ethane-1,2-dioxy)di(ethylamine), and 0.22 g (0.668 mmol) of Cs₂CO₃, after eluting with ethyl acetate/methanol = 100/1 going to 0/1, 0.03 g (30%) of chromene **22** was obtained as yellow oil. ¹H NMR (250MHz, CDCl₃, δ ppm, J Hz): 2.39 (s, 3H, NCH₃), 2.41 (s, 3H, NCH₃), 2.75-

2.93 (m, 4H, 2 × NCH₂), 2.97-3.18 (m, 4H, 2 × NCH₂), 3.53-3.77 (m, 8H, CH₂OCH₂CH₂OCH₂), 4.07-4.32 (m, 4H, 2 × OCH₂), 6.25 (d, 1H, *J* = 9.9, H-2), 7.00 (s, 1H, H-7), 7.05 (d, 1H, *J* = 8.7, H-5), 7.13-7.37 (m, 8H), 7.43-7.53 (m, 5H). Calculated for C₃₇H₄₂N₂O₅ (%): C, 74.72; H, 7.12. Found (%): C, 72.08; H, 7.32.

9',10',12',13',15',16',18',19',21',22'-Decahydro-1,3,3-trimethylspiro[indoline-2,3'-[3H][1,4,10,13]tetraoxa[7,13]dithiaclooctadeca[2',3':6,7]naphtho[2,1-b][1,4]oxazine] (26)

According to the *general procedure for preparation of dithia- and diazacrown derivatives*, from 0.10 g (0.206 mmol) of spironaphthoxazine **25b**, 0.08 g (0.433 mmol) of 2,2'-(ethane-1,2-dioxy)di(ethanethiol), and 0.34 g (1.03 mmol) of Cs₂CO₃, after eluting with dichloromethane/*c*-hexane = 1/1 going to 1/0, 0.02 g (17%) of spironaphthoxazine **26** was obtained as beige solid. M.p. 184-186°C (acetonitrile). ¹H NMR (250MHz, CDCl₃, δ ppm, *J* Hz): 1.35 (s, 6H, 2 × CH₃), 2.76 (s, 3H, N-CH₃), 2.95-3.07 (m, 4H, 2 × SCH₂), 3.15-3.25 (m, 4H, 2 × SCH₂), 3.63 (s, 4H, OCH₂CH₂O), 3.71-3.81 (m, 4H, CH₂OCH₂CH₂OCH₂), 4.28 (t, 2H, *J* = 6.7, OCH₂), 4.43 (t, 2H, *J* = 6.7, OCH₂), 6.57 (d, 1H, *J* = 7.4, H-4), 6.85 (d, 1H, *J* = 8.8, H-6'), 6.89 (ddd, 1H, *J* = 7.4, 7.4, and 1.0, H-5), 7.01 (s, 1H, H-7'), 7.09 (dd, 1H, *J* = 7.6 and 1.2, H-7), 7.21 (ddd, 1H, *J* = 7.6, 7.6, and 1.2, H-6), 7.47 (d, 1H, *J* = 8.8, H-5'), 7.72 (s, 1H, H-24'), 7.84 (s, 1H, H-2'). ¹³C NMR (63MHz, CDCl₃, δ ppm): 20.86, 25.48, 29.71, 30.91, 30.93, 31.57, 51.82, 69.54, 70.29, 72.38, 72.53, 98.44, 100.83, 101.18, 107.12, 107.32, 114.40, 119.80, 121.49, 124.57, 125.21, 126.60, 128.01, 128.58, 135.91, 143.35, 147.25, 147.61, 149.81, 150.70. Calculated for C₃₂H₃₈N₂O₅S₂ (%): C, 64.62; H, 6.44. Found (%): C, 64.96; H, 6.51.

5.1.7. Nitrosation of Naphthols **17a** and **17b**

The procedure was adopted from lit. [4, 129]. A solution of an appropriate naphthol (1.9 mmol) in 5 ml of freshly distilled pyridine was cooled down to -10°C. Carefully, 2 g of 20% aq. NaNO₂ solution was added to the mixture. Then, watching the temperature, 12 ml of 30% aq. H₂SO₄ solution was added dropwise during 30 min. The reaction was stirred at 0°C for 1 h and then poured into 50 ml of water.

6,7-Bis(2-hydroxyethoxy)-1-nitrosonaphthalene-2-ol (**24a**)

According to the general procedure, from 0.5 g (1.9 mmol) of naphthol **17a**, after repeated extraction with ethyl acetate, evaporating of the organic solution, and subsequent treatment of the residue with diethyl ether, 0.12 g (22%) of **24a** was obtained as red-brown

solid. The product was used in the next stage without additional purification. ^1H NMR (250MHz, DMSO- d_6 , δ ppm, J Hz): 3.65-3.86 (m, 4H, $2 \times \text{CH}_2$), 3.96-4.19 (m, 4H, $2 \times \text{CH}_2$), 4.70-5.15 (m, 2H, $2 \times \text{OH}$), 6.29 (bd, 1H, $J = 9.5$), 7.29 (bs, 1H, H-5), 7.64 (bd, 1H, $J = 9.5$), 8.64 (bs, 1H, H-8).

6,7-Bis(2-chloroethoxy)-1-nitrosonaphthalene-2-ol (24b)

According to the general procedure, from 0.3 g (1 mmol) of naphthol **17b**, after the precipitate was treated with diethyl ether, 0.29 g (88%) of **24b** was obtained as red-brown solid. The product was used in the next stage without additional purification. ^1H NMR (250MHz, DMSO- d_6 , δ ppm, J Hz): 3.87-4.10 (m, 4H, $2 \times \text{CH}_2$), 4.19-4.51 (m, 4H, $2 \times \text{CH}_2$), 6.31 (bd, 1H, $J = 9.5$), 7.34 (bs, 1H, H-5), 7.63 (bd, 1H, $J = 9.5$), 8.61 (bs, 1H, H-8).

5.1.8. Synthesis of Spiro-naphthoxazines

The procedure was adopted from lit. [4, 129]. A solution of appropriate nitrosonaphthol (0.45 mmol) and 1,3,3-trimethyl-2-methyleneindoline in 10 ml of methanol was refluxed for 4 h. Upon efflux of the allotted time, the solvent was evaporated and the residue was purified by column chromatography.

6',7'-Bis(2-hydroxyethoxy)-1,3,3-trimethylspiro[indoline-2,3'-[3H]naphtho[2,1-b][1,4]oxazine] (25a)

According to the general procedure, from 0.12 g (0.45 mmol) of nitrosonaphthol **24a** and 0.08 g (0.45 mmol) of 1,3,3-trimethyl-2-methyleneindoline, after eluting with ethyl acetate, 0.05 g (25%) of spiro-naphthoxazines **25a** was obtained as white solid with a tint of pink. The sample amount for analysis was recrystallized from toluene as colorless needles. M.p. 172-174°C (toluene). ^1H NMR (250MHz, CDCl_3 , δ ppm, J Hz): 1.36 (s, 6H, $2 \times \text{CH}_3$), 2.75 (s, 3H, NCH_3), 3.93-4.43 (m, 8H, $4 \times \text{CH}_2$), 6.57 (d, 1H, $J = 7.6$, H-4), 6.84-6.95 (m, 2H), 7.06-7.25 (m, 3H), 7.51 (d, 1H, $J = 8.9$), 7.75 (s, 1H, H-10'), 8.00 (s, 1H, H-2'). Calculated for $\text{C}_{26}\text{H}_{26}\text{Cl}_2\text{N}_2\text{O}_3$ (%): C, 64.33; H, 5.40. Found (%): C, 65.53; H, 5.52.

1,3,3-Trimethyl-6',7'-bis(2-chloroethoxy)spiro[indoline-2,3'-[3H]baphtho[2,1-b][1,4]oxazine] (25b)

According to the general procedure, from 0.29 g (0.88 mmol) of nitrosonaphthol **24a** and 0.15 g (0.88 mmol) of 1,3,3-trimethyl-2-methyleneindoline, after eluting with ethyl acetate/c-hexane = 1/10, 0.15 g (35%) of spiro-naphthoxazines **25b** was obtained as white

solid with a tint of yellow. A sample for analysis was crystallized from methanol to afford the product as yellow needles. M.p. 126-128°C (methanol). ¹H NMR (250MHz, CDCl₃, δ ppm, *J* Hz): 1.36 (s, 6H, 2 × CH₃), 2.76 (s, 3H, NCH₃), 3.90 (t, 2H, *J* = 6.1, CH₂), 3.96 (t, 2H, *J* = 6.0, CH₂), 4.37 (t, 2H, *J* = 6.1, CH₂), 4.50 (t, 2H, *J* = 6.0, CH₂), 6.57 (d, 1H, *J* = 7.6, H-4), 6.89 (d, 1H, *J* = 8.7, H-6'), 6.90 (ddd, 1H, *J* = 7.4, 7.4, and 1.0), 7.09 (dd, 1H, *J* = 7.4 and 1.0), 7.17 (s, 1H), 7.23 (ddd, 1H, *J* = 7.6, 7.6, and 1.3), 7.50 (d, 1H, *J* = 8.8), 7.73 (s, 1H), 7.93 (s, 1H). ¹³C NMR (63MHz, CDCl₃, δ ppm): 20.93, 25.59, 29.82, 41.94, 52.00, 68.99, 69.93, 98.68, 103.31, 107.28, 111.68, 115.20, 120.02, 121.62, 122.23, 124.89, 127.36, 128.17, 128.96, 135.92, 143.88, 146.87, 147.64, 150.00, 150.98. Calculated for C₂₆H₂₈N₂O₅ (%): C, 69.63; H, 6.29. Found (%): C, 70.82; H, 6.46.

1-(3-Bromopropyl)-3,3-dimethylspiro[indoline-2,3'-[3*H*]naphtho[2,1-*b*][1,4]oxazine] (45)

According to the general procedure, from 0.22 g (1.28 mmol) of 1-nitrosonaphthalene-2-ol and *ca.* 0.30 g (1.06 mmol) of 1-(3-bromopropyl)-3,3-dimethyl-2-methyleneindoline **44**, after eluting with dichloromethane/hexane = 2/5, 0.046 g (10%) of spironaphthoxazine **45** was obtained as viscous oil. The product was used in the next stage without additional purification. ¹H NMR (400MHz, CDCl₃, δ ppm, *J* Hz): 1.25 (s, 6H, 2 × CH₃), 1.94-2.25 (m, 2H, CH₂), 3.17-3.42 (m, 4H, 2 × CH₂), 6.57 (d, 1H, *J* = 7.8), 6.80 (dd, 1H, *J* = 7.4 and 7.4), 6.89 (d, 1H, *J* = 8.9), 6.98 (d, 1H, *J* = 7.4), 7.11 (dd, 1H, *J* = 8.4 and 8.4), 7.30 (dd, 1H, *J* = 7.0 and 7.0), 7.48 (dd, 1H, *J* = 7.0 and 7.0), 7.57 (d, 1H, *J* = 8.9), 7.62-7.67 (m, 2H), 8.46 (d, 1H, *J* = 8.4).

5.1.9. Synthesis of Photochromes Containing Positively Charged Fragments

7-Methyl-3,3-diphenyl-3*H*-pyrano[3,2-*f*]quinolinium iodide (27a)

In a thick-walled glass tube equipped with a threaded teflon stopper, 0.34 g (1 mmol) of 3,3-diphenyl-3*H*-pyrano[3,2-*f*]quinoline **35** and 3 ml of iodomethane were mixed. The solution obtained was stirred at 60°C for 3 h. Then, the solvent was removed; and the residue was treated with diethyl ether to yield 0.46 g (96%) of salt **27a** as yellow solid. M.p. 210-213°C (ethanol). ¹H NMR (250MHz, CDCl₃, δ ppm, *J* Hz): 4.82 (s, 1H, NCH₃), 6.53 (d, 1H, *J* = 10.1, H-2), 7.25-7.46 (m, 11H), 7.82 (d, 1H, *J* = 9.6, H-5), 8.08 (dd, 1H, *J* = 8.8 and 5.8, H-9), 8.17 (d, 1H, *J* = 9.6, H-6), 9.17 (d, 1H, *J* = 8.8, H-10), 10.10 (d, 1H, *J* = 5.8, H-8). Calculated for C₂₅H₂₀I⁺NO⁻ (%): C, 62.90; H, 4.22; N, 2.93. Found (%): C, 63.88; H, 4.35; N, 3.01.

7-Methyl-3,3-diphenyl-3H-pyrano[3,2-f]quinolinium *p*-toluenesulfonate (27b)

A solution of 0.17 g (0.5 mmol) of 3,3-diphenyl-3H-pyrano[3,2-f]quinoline **35** and 0.19 g (1 mmol) of methyl *p*-toluenesulfonate in 10 ml of dried acetonitrile was refluxed in Ar atmosphere for 24 h. Upon cooling, a precipitate was formed, yielding 0.22 g (85%) of salt **27b** as yellow solid. M.p. 214-217°C. ¹H NMR (250MHz, CDCl₃, δ ppm, *J* Hz): 2.28 (s, 3H, H-Ts), 4.75 (s, 3H, NCH₃), 6.48 (d, 1H, *J* = 10.1, H-2), 7.07 (d, 2H, *J* = 8.0, H-Ts), 7.22-7.48 (m, 11H), 7.67-7.81 (m, 3H), 8.00-8.17 (m, 2H), 9.04 (d, 1H, *J* = 8.7, H-10), 9.95 (d, 1H, *J* = 5.1, H-8). Calculated for C₃₂H₂₇NO₄S (%): C, 73.68; H, 5.22. Found (%): C, 75.23; H, 5.35.

9-Methyl-3,3-diphenyl-3H-pyrano[2,3-h]isoquinolinium iodide (28)

In a thick-walled glass tube equipped with a threaded teflon stopper, 0.053 g (0.158 mmol) of 3,3-diphenyl-3H-pyrano[2,3-f]isoquinoline **36** and 2 ml of iodomethane were mixed. The solution obtained was stirred at 60°C for 3 h. Then, the solvent was removed; and the residue was treated with diethyl ether to yield 0.065 g (87%) of salt **28** as yellow solid. M.p. 218-222°C. ¹H NMR (250MHz, CDCl₃, δ ppm, *J* Hz): 4.80 (s, 3H, NCH₃), 6.56 (d, 1H, *J* = 10.1, H-2), 7.20-7.48 (m, 10H), 7.71 (d, 1H, *J* = 8.9), 7.83 (d, 1H, *J* = 8.9), 7.97-8.17 (m, 3H), 10.97 (s, 1H, H-10). Calculated for C₂₅H₂₀I₂NO (%): C, 62.90; H, 4.22. Found (%): C, 63.52; H, 4.28.

1,2,4-Trimethyl-6,6-diphenyl-6H-chromeno[6,7-d]oxazolium iodide (31)

In a thick-walled glass tube equipped with a threaded teflon stopper, 0.24 g (0.68 mmol) of 2,4-dimethyl-6,6-diphenyl-6H-chromeno[6,7-d]oxazole **39** and 3 ml of iodomethane were mixed. The solution obtained was stirred at 60°C for 3 h. Then, the solvent was removed; and the residue was treated with diethyl ether to yield 0.12 g (36%) of salt **31** as yellowish solid. M.p. 245-247°C. ¹H NMR (250MHz, CDCl₃, δ ppm, *J* Hz): 2.45 (s, 3H, 4-CH₃), 3.29 (s, 3H, 2-CH₃), 4.25 (s, 3H, 1-CH₃), 6.34 (d, 1H, *J* = 10.0, H-7), 6.82 (d, 1H, *J* = 10.0, H-8), 7.24-7.47 (m, 11H). ¹³C NMR (63MHz, CDCl₃, δ ppm): 8.88, 22.30, 36.46, 82.77, 114.02, 114.27, 122.14, 122.89, 123.41, 126.38, 126.76, 126.81, 127.41, 127.49, 128.16, 145.30, 151.19, 151.76, 173.22, 181.68. Calculated for C₂₅H₂₂I₂NO₂ (%): C, 60.62; H, 4.48. Found (%): C, 60.92; H, 4.53.

1-((3,3-Diphenyl-3H-benzo[*f*]chromene-5-yl)methyl)-3-methylpyridinium bromide (33)

In 15 ml of dried acetonitrile, 0.12 g (0.28 mmol) of 5-bromomethyl-3,3-diphenyl-3H-benzo[*f*]chromene **42** and 0.027 g (0.29 mmol) of freshly distilled *m*-picoline were dissolved. The solution was stirred in Ar atmosphere at ambient temperature for 20 h. Then, the solvent

was removed under diminished pressure and the residue was treated with diethyl ether to afford 0.18 g (90%) of salt **33** as orange solid. M.p. 166-168°C. ¹H NMR (250MHz, CDCl₃, δ ppm, *J* Hz): 2.35 (s, 3H, CH₃), 6.15 (d, 1H, *J* = 10.1, H-2'), 6.37 (s, 2H, CH₂), 7.11-7.61 (m, 14H), 7.81-8.06 (m, 3H), 8.52 (s, 1H), 8.93-9.15 (m, 2H). ¹³C NMR (75MHz, CDCl₃, δ ppm): 18.77, 60.64, 84.40 (*quat*), 114.18, 118.81, 120.71, 121.19, 124.95, 126.93, 127.11, 127.46, 128.33, 128.42, 128.65, 128.91, 129.70, 130.57, 133.69, 139.08, 142.23, 143.62, 144.65, 145.36, 147.78. Calculated for C₃₂H₂₆BrNO (%): C, 73.85; H, 5.04. Found (%): C, 72.92; H, 4.98.

3-(3,3-Dimethylspiro[indoline-2,3'-[3H]naphtho[2,1-b][1,4]oxazine]-1-yl)propyl-triethylammonium bromide (34)

In 5 ml of dried acetonitrile, 0.053 g (0.122 mmol) of spironaphthoxazines **45** and 0.123 g (1.22 mmol) of freshly distilled triethylamine were dissolved. The solution was stirred at 60°C for 24 h. Then, the solvent was removed under diminished pressure and the residue was treated with diethyl ether to afford 0.025 g (38%) of salt **34** as creamy-beige solid. M.p. 218-220°C. ¹H NMR (600MHz, DMSO-*d*₆, δ ppm, *J* Hz): 1.08 (t, 9H, *J* = 7.1, 3 CH₂CH₃), 1.26 (s, 3H, CH₃), 1.30 (s, 3H, CH₃), 1.75-1.88 (m, 1H, CH₂), 1.98-2.11 (m, 1H, CH₂), 3.10-3.27 (m, 10H), 6.81 (d, 1H, *J* = 7.8), 6.86 (dd, 1H, *J* = 7.4 and 7.4), 7.10-7.22 (m, 3H), 7.43 (dd, 1H, *J* = 7.6), 7.60 (dd, 1H, *J* = 7.6), 7.82 (d, 1H, *J* = 8.9), 7.86 (d, 1H, *J* = 8.2), 7.97 (s, 1H), 8.49 (d, 1H, *J* = 8.4). ¹³C NMR (150MHz, DMSO-*d*₆, δ ppm): 7.02, 20.55, 20.68, 25.12, 40.80, 51.73, 52.11, 53.72, 98.68, 106.90, 106.92, 116.63, 119.63, 120.97, 121.72, 122.00, 124.17, 127.15, 127.78, 127.82, 128.89, 130.12, 130.30, 135.21, 143.17, 146.14, 151.69. Calculated for C₃₀H₃₈BrN₃O (%): C, 67.16; H, 7.14. Found (%): C, 67.32; H, 7.20.

5.2. Determination of Complex Stability Constants by Spectrophotometric Titration

Spectrophotometric titration was employed for determining stability constants for complexes of chromenes **1** and **3** (their closed forms) with cations of metals and protonated amino acids [141, 142]. The procedure was as follows: To a solution of the ligand in acetonitrile ($\sim 10^{-4}$ M), aliquots of the substrate solution ($\text{Mg}(\text{ClO}_4)_2$, $\text{Ba}(\text{ClO}_4)_2$, $\text{Pb}(\text{ClO}_4)_2$, or β -alanine, γ -aminobutyric, ϵ -aminocaproic, or ω -aminocaprylic acids perchlorates in acetonitrile, $\sim 10^{-2}$ - 10^{-3} M) were added stepwise, recording an absorption spectrum on the each step. Analyzing spectral changes in course of titration, a conclusion about complexes' composition and stability may be drawn.

Absorbance of a solution is additive and depends on the concentration of components in the solution, the dependence being described by Beer–Lambert–Bouguer law:

$$A = \sum_{i=1}^n A_i = l \cdot \sum_{i=1}^n \epsilon_i C_i \quad (5.1)$$

where n is the number of components in the solution; A_i is the absorbance of component i , $i = 1, 2, \dots, n$; l is the optical path, cm; ϵ_i is the molar extinction coefficient of component i , $\text{M}^{-1} \cdot \text{cm}^{-1}$; C_i is the concentration of component i , M.

In the presence of a substrate (metal or amino acid ions), an equilibrium is establishes in the solution, the absorbance thus being determined by equilibrium concentrations of particles that participate in complex formation. The following are the equalities that describe the 1:1 complex formation:



2:1 Complex is formed in case of additional ligand molecule is bound to the complex LM:



Solving equations (5.1)-(5.3) simultaneously by means of numerical iterations methods gives the required parameters with desired accuracy. In this work, values of stability constants as well as individual absorption spectra (dependence of ε on λ) for each complex were determined using SPECFIT/32® software.

Stability constants for complexes of the open forms of chromenes **3** with protonated amino acids were determined upon analysis of changes in bleaching rate constants in the presence of different amount of the acids. For each determination, a fresh solution of chromene and amino acid was prepared. Using spectrometer «Avantes AvaSpec-2048», a spectrum was recorded (with 0.5 – 2 s interval between measurements) upon continuous irradiation of the sample solution. Each sample was irradiated during the same time (30 s – 5 min). Upon cessation of the irradiation, the spectrum was recorded until full bleaching or at least the intensity of a long-wavelength band was decreased twice.

5.3. Determination of Bleaching Rate Constants

Neglecting the formation of CC and CT forms upon irradiation (see scheme 3.26), the kinetic scheme for bleaching of the open forms may be described as follows



where TT and TC are different open forms; CF is closed (initial) form of chromene; k_{TT} and k_{TC} are bleaching rate constants for the two consecutive stages.

$$\frac{d[TT]}{dt} = -k_{TT}[TT]$$

$$\frac{d[TC]}{dt} = -k_{TC}[TC] + k_{TT}[TT]$$

Solving these differential equations, the following equations are obtained

$$[TT] = [TT]_0 e^{-k_{TT}t}$$

$$[TC] = [TC]_0 e^{-k_{TC}t} + [TT]_0 \frac{k_{TT}}{k_{TC} - k_{TT}} (e^{-k_{TT}t} - e^{-k_{TC}t})$$

Inserting the precedent expressions into the Beer-Lambert law formula, the following general expression is made

$$A = A_0^{TC} e^{-k_{TC}t} + A_0^{TT} e^{-k_{TT}t} + A_0^{TT} \frac{k_{TT}}{k_{TC} - k_{TT}} (e^{-k_{TT}t} - e^{-k_{TC}t})$$

Easy to notice that providing $k_{TC} \gg k_{TT}$, the equation may be considerably simplified

$$A = A_0^{TC} e^{-k_{TC}t} + A_0^{TT} e^{-k_{TT}t}$$

Thus, the bleaching kinetic curve exhibits biexponential pattern. However, in some cases a mono-exponential dependence may be observed. This may happen if the rate of $TC \rightarrow CF$ transformation is high; thus, the observed kinetics would virtually correspond to $TT \rightarrow CF$ process. Otherwise, mono-exponential dependence may occur in case of slow *cis-trans* isomerization $TC \rightarrow TT$ upon irradiation that leads to low TT concentration; thus, the observed kinetics would virtually correspond to $TC \rightarrow CF$ transition. To distinguish these processes by UV-Vis spectroscopy is practically impossible.

5.4. Study of Chromene **33** Intercalation into DNA

Calf-timus DNA (Sigma, St. Louis, MO, USA) (I type; polymerized sodium salt) was used as purchased without additional purification. A sample was dissolved in $1 \cdot 10^{-2}$ M BPE buffer ($6.0 \cdot 10^{-3}$ M Na_2HPO_4 , $2.0 \cdot 10^{-3}$ M NaH_2PO_4 , $1.0 \cdot 10^{-3}$ M Na_2EDTA ; total concentration of Na^+ is $16.0 \cdot 10^{-3}$ M; pH = 7.0) to prepare a solution containing $1\text{--}2 \text{ mg ml}^{-1}$ of DNA. The suspension was kept at 4°C during 20 h . After being kept for 10 min in an ultrasonic bath, the solution was filtered through PVDF membrane filter (porous size $0.45 \mu\text{m}$). The precise concentration of DNA was determined by measuring the absorbance of the solution 20 times diluted at 260 nm knowing that $e_{260} = 12824 \text{ cm}^{-1} \text{ M}^{-1}$ of base pairs (bp) [143]. The titration was performed with $0.5 - 2 \text{ eq.}$ step.

Experiments were carried out at 10°C . The aliquots of DNA solution were consecutively added to the solution of chromene **33** and each sample was irradiated for 5 min . The irradiation of Hg high pressure lamp 120W equipped with optical filter with $\lambda_{\text{max}} = 313 \text{ nm}$ was used. The bleaching was monitored until the total disappearance of the absorption band in visible region or at least until its intensity was reduced twice.

6. Bibliography

1. Organic photochromic and thermochromic compounds. Ed.: Crano, J.C.; Guglielmetti, R.J. New York: Plenum Press, **1999**, Vol. 1, 400 p., Vol. 2, 473 p.
2. Photochromism: molecules and systems. Ed.: Dürr, H.; Bouas-Laurent, H. Amsterdam: Elsevier BV, **2003**, 1044 p.
3. Minkin, V. Photo-, thermo-, solvato-, and electrochromic spiroheterocyclic compounds. *Chem. Rev.*, **2004**, *104*, pp. 2751-2776.
4. Lokshin, V.; Samat, A.; Metelitsa, A.V. Spirooxazines: synthesis, structure, spectral and photochromic properties. *Russ. Chem. Rev.*, **2002**, *71*, pp. 893-916.
5. Hepworth, J.D.; Heron, B.M. Photochromic naphthopyrans *in* Functional dyes. Ed.: Kim, S.-H. Amsterdam: Elsevier BV, **2006**, 271 p.
6. Lafuma, A., Chodorowski-Kimmes, S.; Quinn, F.X.; Sanchez, C. Photochromic properties of a spirooxazine and a spiropyran in alcoholic solutions of zirconium and aluminium alkoxides: Influence of the ethyl acetoacetate chelating agent on the optical properties. *Eur. J. Inorg. Chem.*, **2003**, *2*, pp. 331-338.
7. Attia, M.S.; Khalil, M.M.H.; Abdel-Mottaleb, M.S.A.; Lukyanova, M.B.; Alekseenko, Yu.A.; Lukyanov, B. Effect of complexation with lanthanide metal ions on the photochromism of (1,3,3-trimethyl-5'-hydroxy-6'-formyl-indoline-spiro-2,2'-[2H]chromene) in different media. *Int. J. Photoenergy*, **2006**, Article ID 42846.
8. Roxburgh, C.J.; Sammes, pp.G.; Abdullah, A. Photoreversible Zn²⁺ Ion Transportation Across an Interface Using Ion-Chelating Substituted Photochromic 3,3'-Indolospirobenzopyrans: Steric and Electronic Controlling Effects. *Eur. J. Inorg. Chem.*, **2008**, pp. 4951-4960.
9. Shao, N.; Zhang, Y.; Cheung, S.; Yang, R.; Chan, W.; Mo, T.; Li, K.; Liu, F. Copper ion-selective fluorescent sensor based on the inner filter effect using a spiropyran derivative. *Anal. Chem.*, **2005**, *77*, pp. 7294-7303.
10. Shao, N.; Jin, J.; Wang, H.; Zhang, Y.; Yang, R.; Chan, W. Tunable photochromism of spirobenzopyran via selective metal ion coordination: An efficient visula and ratioing fluorescent probe for divalent copper ion. *Anal. Chem.*, **2008**, *80*, pp. 3466-3475.
11. Ren J.; Tian H. Thermally stable merocyanine form of photochromic spiropyran with aluminum ion as a reversible photo-driven sensor in aqueous solution. *Sensors*, **2007**, *7*, pp. 3166-3178.

12. Zakharova, M.I.; Coudret, C.; Pimienta, V.; Micheau, J.C.; Delbaere, S.; Vermeersch, G.; Metelitsa, A.V.; Voloshin, N.; Minkin, V.I. Quantitative investigations of cation complexation of photochromic 8-benzothiazole-substituted benzopyran: towards metal-ion sensors. *Photochem. Photobiol. Sci.*, **2010**, *9*, pp. 199-207.
13. Sakata, T.; Jackson, D.K.; Mao, S.; Marriott, J. Optically switchable chelates: optical control and sensing of metal ions. *J. Org. Chem.*, **2008**, *73*, pp. 227-233.
14. Robillard, J.; Luna-Moreno, D.; Olmos, M. Study on the feasibility of a dry color printing process. *Opt. Mater.*, **2003**, *24*, pp. 491-495.
15. Chernyshev, A.V.; Voloshin, N.A.; Raskita, I.M.; Metelitsa, A.V.; Minkin, V.I. Photo- and ionochromism of 5'-(4,5-diphenyl-1,3-oxazol-2-yl) substituted spiro[indoline-naphthopyrans]. *J. Photochem. Photobiol., A*, **2006**, *184*, pp. 289-297.
16. Nikolaeva, O.G.; Tsukanov, A.V.; Shepelenko, E.N.; Lukyanov, B.S.; Metelitsa, A.V.; Kostyrina, O.Yu.; Dubonosov, A.D.; Bren, V.A.; Minkin, V.I. Synthesis of Novel Iono- and Photochromic Spiropyrans Derived from 6,7-Dihydroxy-8-Formyl-4-Methyl-2H-Chromene-2-One. *Int. J. Photoenergy*, **2009**, Article ID 238615.
17. Roxburgh, C.J.; Sammes, P.G. Synthesis of some new substituted photochromic N,N'-bis(spiro[1-benzopyran-2,2'-indolyl])diazacrown systems with substituent control over ion chelation. *Eur. J. Org. Chem.*, **2006**, pp. 1050-1056
18. Voloshin, N.A.; Chernyshev, A.V.; Metelitsa, A.V.; Besugliy, S.O.; Voloshina, E.N.; Sadimenko, L.P.; Minkin, V.I. Photochromic spiro[indoline-pyridobenzopyrans]: fluorescent metal-ion sensors. *Arkivoc*, **2004**, pp. 16-24.
19. Krikun, V.M.; Sadimenko, L.P.; Voloshina, E.N.; Voloshin, N.A. Polarographic and spectrophotometric studies of the spiro[indolin-pyridobenzopyrane] complexes with the heavy metal ions. *Russ. J. Gen. Chem.*, **2009**, *79*, pp. 1191-1196.
20. Chernyshev, A.V.; Metelitsa, A.V.; Gaeva, E.B.; Voloshin, N.A.; Borodkin, G.S.; Minkin, V.I. Photo- and thermochromic cation sensitive spiro[indoline-pyridobenzopyrans]. *J. Phys. Org. Chem.*, **2007**, *20*, pp. 908-916.
21. Kumar, S.; Chau, C.; Chau, G.; McCurdy, A. Synthesis and metal complexation properties of bisbenzospiropyran chelators in water. *Tetrahedron*, **2008**, *64*, pp. 7097-7105.
22. Liu, Z.L.; Jiang, L.; Liang, Z.; Gao, Y.H. Photochromism of a novel spiropyran derivative based on calix[4]arenes. *J. Mol. Struct.*, **2005**, *737*, pp. 267-270.
23. Liu, Z.L.; Jiang, L.; Liang, Z.; Gao, Y.H. Photo-switchable molecular devices based on metal-ionic recognition. *Tetrahedron Lett.*, **2005**, *46*, pp. 885-887.

24. Liu, Z.L.; Jiang, L.; Liang, Z.; Gao, Y.H. A selective colorimetric chemosensor for lanthanide ions. *Tetrahedron*, **2006**, *62*, pp. 3214-3220.
25. Grun, A.; Kerekes, P.; Bitter, I. Synthesis, characterization and cation-induced isomerization of photochromic calix[4](aza)crown-indolospiroopyran conjugates. *Supramol. Chem.*, **2008**, *20*, pp. 255-263.
26. Abdullah, A.; Roxburgh, C.J.; Sannes, P.G. Photochromic crowned spirobenzopyrans: Quantitative metal-ion chelation by UV, competitive selective ion-extraction and metal-ion transportation demonstration studies. *Dyes Pigm.*, **2008**, *76*, pp. 319-326.
27. Kimura, K.; Sakamoto, H.; Uda, R.M. Cation complexation, photochromism, and photoresponsive ion-conducting behavior of crowned spirobenzopyran vinyl polymers. *Macromolecules*, **2004**, *37*, pp. 1871-1876.
28. Sakamoto, H.; Takagaki, H.; Nakamura, M.; Kimura, K. Photoresponsive liquid membrane transport of alkali metal ions using crowned spirobenzopyrans. *Anal. Chem.*, **2005**, *77*, pp. 1999-2006.
29. Sakamoto, H.; Yamamura, T.; Takumi, K.; Kimura, K. Absorption- and fluorescence-spectral sensing of alkali metal ions in anionic micelle solutions containing crowned spirobenzopyrans. *J. Phys. Org. Chem.*, **2007**, *20*, pp. 900-907.
30. Machitani, K.; Sakamoto, H.; Nakahara, Y.; Kimura, K. Molecular design of tetraazamacrocyclic derivatives bearing a spirobenzopyran and three carboxymethyl moieties and their metal-ion complexing behavior. *Anal. Sci.*, **2008**, *24*, pp. 463-469.
31. Tu, C.; Louie, A.Y. Photochromically-controlled, reversibly-activated MRI and optical contrast agent. *Chem. Commun.*, **2007**, pp. 1331-1333.
32. Tu, C.; Osborne, E.A.; Louie, A.Y. Synthesis and characterization of a redox- and light-sensitive MRI contrast agent. *Tetrahedron*, **2009**, *65*, pp. 1241-1246.
33. Koszegi, E.; Grun, A.; Bitter, I. 1,1'-binaphtho(aza)crowns carrying photochromic signalling unit, I: Synthesis, characterization and cation recognition properties. *Supramol. Chem.*, **2006**, *18*, pp. 67-76.
34. Yagi, S.; Nakamura, S.; Watanabe, D.; Nakazumi, H. Colorimetric sensing of metal ions by bis(spiropyran) podands: Towards naked-eye detection of alkaline earth metal ions. *Dyes Pigm.*, **2009**, *80*, pp. 98-105.
35. Ahmed, S.A.; Tanaka, M.; Ando, H.; Tawa, K.; Kimura, K. Fluorescence emission control and switching of oxymethylcrowned spirobenzopyrans by metal ion. *Tetrahedron*, **2004**, *60*, pp. 6029-6036.

36. Khairutdinov, R.F.; Hurst, J.K. Light-driven transmembrane ion transport by spiropyran - Crown ether supramolecular assemblies. *Langmuir*, **2004**, *20*, pp. 1781-1785.
37. Liu, S.H. Synthesis of new spirobenzopyrans bearing a macrocyclic dioxopolyamine and their selective coloration for transition metal cations. *Mol. Cryst. Liq. Cryst.*, **2004**, *419*, pp. 97-101.
38. Liu, S.H. Synthesis of new spirobenzopyrans bearing macrocyclic dioxopolyamine and their selective coloration for transition metal cations. *Mol. Cryst. Liq. Cryst.*, **2004**, *420*, pp. 73-77.
39. Xiong, W.C.; Yuan, P.; Yin, J.; Liu, S.H. Synthesis of spirobenzopyrans bearing macrocyclic dioxopolyamine. *Mol. Cryst. Liq. Cryst.*, **2005**, *428*, pp. 127-130.
40. Khodonov, A.A.; Lukin, A.Y.; Laptev, A.V.; Shvets, V.I.; Demina, O.V.; Gromov, S.P.; Vedernikov, A.I.; Strokach, Y.P.; Venidiktova, O.V.; Valova, T.M.; Alfimov, M.V.; Barachevsky, V.A. Photochromic and cation-binding properties of new crowned spiropyran. *Mol. Cryst. Liq. Cryst.*, **2005**, *431*, pp. 515-521.
41. Machitani, K.; Nakamura, M.; Sakamoto, H.; Ohata, N.; Masuda, H.; Kimura, K. Structural characterization for metal-ion complexation and isomerization of crowned bis(spirobenzopyran)s. *J. Photochem. Photobiol., A*, **2008**, *200*, pp. 96-100.
42. Nakamura, M.; Fujioka, T.; Sakamoto, H.; Kimura, K. Application of photoionizable crowned spirobenzopyrans to flow-injection extraction-spectrophotometry for lithium ion. *Bunseki Kagaku*, **2003**, *52*, pp. 419-424.
43. Nakamura, M.; Takahashi, K.; Fujioka, T.; Kado, S.; Sakamoto, H.; Kimura, K. Evaluation of photoinduced changes in stability constants for metal-ion complexes of crowned spirobenzopyran derivatives by electrospray ionization mass spectrometry. *J. Am. Soc. Mass. Spectrom.*, **2003**, *14*, pp. 1110-1115.
44. Nakamura, M.; Kamoto, H.S.A.; Kimura, K. Photocontrollable cation extraction with crowned oligo(spirobenzopyran)s. *Anal. Sci.*, **2005**, *21*, pp. 403-408.
45. Guo, X.F.; Zhang, D.Q.; Zhang, G.X.; Zhu, D.B. Monomolecular logic: "Half-adder" based on multistate/multifunctional photochromic spiropyran. *J. Phys. Chem., B*, **2004**, *108*, pp. 11942-11945.
46. Kume, S.; Nishihara, H. Photochrome-coupled metal complexes: molecular processing of photon stimuli. *Dalton Trans.*, **2008**, pp. 3260-3271.
47. Nagashima, S.; Murata, M.; Nishihara, H. A ferrocenylspiropyran that functions as a molecular photomemory with controllable depth. *Angew. Chem. Int. Ed.*, **2006**, *45*, pp. 4298-4301.

48. Jiang, G.; Song, Y.; Guo, X.; Zhang, D.; Zhu, D. Organic functional molecules towards information processing and high-density information storage. *Adv. Mater.*, **2008**, *20*, pp. 2888-2898.
49. Guo, X.; Zhang, D.; Tao, H.; Zhu, D. Concatenation of two molecular switches via a Fe(II)/Fe(III) couple. *Org. Lett.*, **2004**, *6*, pp. 2491-2494.
50. Wu, H.; Zhang, D.; Su, L.; Ohkubo, K.; Zhang, C.; Yin, S.; Mao, L.; Shuai, Z.; Fukuzumi, S.; Zhu, D. Intramolecular electron transfer within the substituted tetrathiafulvalene-quinone dyads: facilitated by metal ion and photomodulation in the presence of spiropyran. *J. Am. Chem. Soc.*, **2007**, *129*, pp. 6839-6846.
51. Guo, X.F.; Zhang, D.Q.; Zhu, D.B. Photocontrolled electron transfer reaction between a new dyad, tetrathiafulvalene-photochromic spiropyran, and ferric ion. *J. Phys. Chem., B*, **2004**, *108*, pp. 212-217.
52. Belser, P.; De Cola, L.; Hartl, F.; Adamo, V.; Bozic, B.; Chriqui, Y.; Iyer, V.M.; Jukes, R.T.F.; Kuhni, J.; Querol, M.; Roma, S.; Salluce, N. Photochromic switches incorporated in bridging ligands: A new tool to modulate energy-transfer processes. *Adv. Funct. Mater.*, **2006**, *16*, pp. 195-208.
53. Jukes, R.T.F.; Bozic, B.; Hartl, F.; Belser, P.; De Cola, L. Synthesis, photophysical, photochemical, and redox properties of nitrospiropyrans substituted with Ru or Os tris (bipyridine) complexes. *Inorg. Chem.*, **2006**, *45*, pp. 8326-8341.
54. Jukes, R.; Bozic, B.; Belser, P.; De Cola, L.; Hartl, F. Photophysical and Redox Properties of Dinuclear Ru and Os Polypyridyl Complexes with Incorporated Photostable Spiropyran Bridge. *Inorg. Chem.*, **2009**, *48*, pp. 1711-1721.
55. Benito-Lopez, F.; Scarmagnani, S.; Walsh, Z.; Paull, B.; Macka, M.; Diamond, D. Spiropyran modified micro-fluidic chip channels as photonically controlled self-indicating system for metal ion accumulation and release. *Sens. Actuators, B*, **2009**, *140*, pp. 295-303.
56. Guo, X.F.; Zhang, D.Q.; Wang, T.X.; Zhu, D.B. Reversible regulation of pyrene excimer emission by light and metal ions in the presence of photochromic spiropyran: toward creation of a new molecular logic circuit. *Chem. Commun.*, **2003**, pp. 914-915.
57. Choi, H.; Ku, B.S.; Keum, S.R.; Kang, S.O.; Ko, J. Selective photoswitching of a dyad with diarylethene and spiropyran units. *Tetrahedron*, **2005**, *61*, pp. 3719-3723.
58. Guo, X.F.; Zhang, D.Q.; Zhu, D.B. Logic control of the fluorescence of a new dyad, spiropyran-perylene diimide-spiropyran, with light, ferric ion, and proton: Construction of a new three-input "AND" logic gate. *Adv. Mater.*, **2004**, *16*, pp. 125-130.

59. Koshkin, A.V. Synthesis, complex formation, and photochromic properties of crown-containing spironaphthoxazines. PhD thesis. Photochemistry Center of RAS, Moscow, **2005**, 128 p.
60. Suzuki, T.; Kawata, Y.; Kahata, S.; Kato, T. Photo-reversible Pb^{2+} -complexation of insoluble poly(spiropyran methacrylate-co-perfluorohydroxy methacrylate) in polar solvents. *Chem. Commun.*, **2003**, pp. 2004-2005.
61. Suzuki, T.; Kato, T.; Shinozaki, H. Photo-reversible Pb^{2+} -complexation of thermosensitive poly(*N*-isopropyl acrylamide-co-spiropyran acrylate) in water. *Chem. Commun.*, **2004**, pp. 2036-2037.
62. Fries, K.; Samanta, A.; Orski, S.; Locklin, J. Reversible colorimetric ion sensors based on surface initiated polymerization of photochromic polymers. *Chem. Commun.*, **2008**, pp. 6288-6290.
63. Fries, K.; Driskell, J.D.; Samanta, A.; Orski, S.; Locklin, J. Spectroscopic analysis of metal ion binding in spiropyran containing copolymer thin films. *Anal. Chem.*, **2010**, *82*, pp. 3306-3314.
64. Scarmagnani, S.; Walsh, Z.; Slater, C.; Alhashimy, N.; Paull, B.; Macka, M.; Diamond, D. Polystyrene bead-based system for optical sensing using spiropyran photoswitches. *J. Mater. Chem.*, **2008**, *18*, pp. 5063-5071.
65. Byrne, R.J.; Stitzel, S.E.; Diamond, D. Photo-regenerable surface with potential for optical sensing. *J. Mater. Chem.*, **2006**, *16*, pp. 1332-1337.
66. Radu, A.; Byrne, R.; Alhashimy, N.; Fusaro, M.; Scarmagnani, S.; Diamond, D. Spiropyran-based reversible, light-modulated sensing with reduced photofatigue. *J. Photochem. Photobiol., A*, **2009**, *206*, pp. 109-115.
67. Radu, A.; Scarmagnani, S.; Byrne, R.; Slater, C.; Lau, K.T.; Diamond, D. Photonic modulation of surface properties: a novel concept in chemical sensing. *J. Phys. D: Appl. Phys.*, **2007**, *40*, pp. 7238-7244.
68. Wen, G.; Yan, J.; Zhou, Y.; Zhang, D.; Mao, L.; Zhu, D. Photomodulation of the electrode potential of a photochromic spiropyran-modified Au electrode in the presence of Zn^{2+} : a new molecular switch based on the electronic transduction of the optical signals. *Chem. Commun.*, **2006**, pp. 3016-3018.
69. Liu, Y.; Fan, M.; Zhang, S.; Sheng, X.; Yao, J. Basic amino acid induced isomerization of a spiropyran: Towards visual recognition of basic amino acids in water. *New J. Chem.*, **2007**, *31*, pp. 1878-1881.

70. Shao, N.; Jin, J.Y.; Cheung, S.M.; Yang, R.H.; Chan, W.H.; Mo, T. A spiropyran-based ensemble for visual recognition and quantification of cysteine and homocysteine at physiological levels. *Angew. Chem. Int. Edit.*, **2006**, *45*, pp. 4944-4948.
71. Shao, N.; Jin, J.; Wang, H.; Zheng, J.; Yang, R.; Chan, W.; Abliz, Z. Design of bis-spiropyran ligands as dipolar molecule receptors and application to in vivo glutathione fluorescent probes. *J. Am. Chem. Soc.*, **2010**, *132*, pp. 725-736.
72. Qiu, Z.; Yu, H.; Li, J.; Wang, Y.; Zhang, Y. Spiropyran-linked dipeptide forms supramolecular hydrogel with dual responses to light and to ligand-receptor interaction. *Chem. Commun.*, **2009**, pp. 3342-3344.
73. Andersson, J.; Li, S.; Lincoln, P.; Andréasson, J. Photoswitched DNA-binding of a photochromic spiropyran. *J. Am. Chem. Soc.*, **2008**, *130*, pp. 11836-11837.
74. Ihmels, H.; Otto, D. Intercalation of Organic Dye Molecules into Double-Stranded DNA – General Principles and Recent Developments. *Top Curr. Chem.*, **2005**, *258*, pp. 161-204.
75. Nishikiori, H.; Tanaka, N.; Takagi, K.; Fujii, T. Chelation of spironaphthoxazine with zinc ions during the sol-gel-xerogel transitions in silicon alkoxide systems. *J. Photochem. Photobiol., A*, **2006**, *183*, pp. 53-58.
76. Nishikiori, H.; Sasai, R.; Takagi, K.; Fujii, T. Zinc chelation and photofluorochromic behavior of spironaphthoxazine intercalated into hydrophobically modified montmorillonite. *Langmuir*, **2006**, *22*, pp. 3376-3380.
77. Nishikiori, H.; Tanaka, N.; Takagi, K.; Fujii, T. Chelation of spironaphthoxazine with zinc ions and its photochromic behavior during the sol-gel-xerogel transitions of alkyl silicon alkoxide. *J. Photochem. Photobiol., A*, **2007**, *189*, pp. 46-54.
78. Kim, S.-H.; Wang, S.; Ahn, C.-H.; Cho, M.-S. High photostabilization of Zn²⁺ Chelating spironaphthoxazine. *Fibers Polym.*, **2007**, *8*, pp. 447-449.
79. Minkovska, S.; Fedieva, M.; Jeliaskova, B.; Deligeorgiev, T. Thermally activated and light-induced metal ion complexation of 5'-(hydroxy)spiroindolinonaphthoxazines in polar solvents. *Polyhedron*, **2004**, *23*, pp. 3147-3153.
80. Jeliaskova, B.G.; Minkovska, S.; Deligeorgiev, T. Effect of complexation on the photochromism of 5'-(benzothiazol-2-yl)spiroindolinonaphthoxazines in polar solvents. *J. Photochem. Photobiol., A*, **2005**, *171*, pp. 153-160.
81. Alhashimy, N.; Byrne, R.; Minkovska, S.; Diamond, D. Novel synthesis and characterisation of 3,3-dimethyl-5'-(2-benzothiazolyl)-spironaphth(indoline-2,3'-[3H] naphth[2,1-b][1,4]oxa-zine) derivatives. *Tetrahedron Lett.*, **2009**, *50*, pp. 2573-2576.

82. Strokach, Y.P.; Valova, T.M.; Barachevskii, V.A.; Shienok, A.I.; Marevtsev V.S. Photochromic properties of the bichromophore spirooxazine and its complexes with metal cations. *Russ. Chem. Bull.*, **2005**, *54*, pp. 1477-1480.
83. Kopelman, R.A.; Snyder, S.M.; Frank, N.L. Tunable photochromism of spirooxazines via metal coordination. *J. Am. Chem. Soc.*, **2003**, *125*, pp. 13684-13685.
84. Kopelman, R.A.; Paquette, M.M.; Frank, N.L. Photoprocesses and magnetic behavior of photochromic transition metal indoline[phenanthroline] spirooxazine complexes: Tunable photochromic materials. *Inorg. Chim. Acta*, **2008**, *361*, pp. 3570-3576.
85. Zhang, C.; Zhang, Z.; Fan, M.; Yan, W. Positive and negative photochromism of novel spiro[indoline-phenanthroline]oxazines. *Dyes Pigm.*, **2008**, *76*, pp. 832-835.
86. Zhang, Z.; Zhang, C.; Fan, M.; Yan, W. Synthesis and complexation mechanism of europium ion (Eu³⁺) with spiro[indoline-phenanthroline]oxazine. *Dyes Pigm.*, **2008**, *77*, pp. 469-473.
87. Paquette, M.M.; Kopelman, R.A.; Beitler, E.; Frank, N.L. Incorporating optical bistability into a magnetically bistable system: a photochromic redox isomeric complex. *Chem. Commun.*, **2009**, pp. 5424-5426.
88. Fedorova, O.A.; Koshkin, A.V.; Gromov, S.P.; Strokach, Y.P.; Valova, T.M.; Alfimov, M.V.; Feofanov, A.V.; Alaverdian, I.S.; Lokshin, V.A.; Samat, A. Transformation of 6'-aminosubstituted spironaphthoxazines induced by Pb(II) and Eu(III) cations. *J. Phys. Org. Chem.*, **2005**, *18*, pp. 504-512.
89. Tu, C.; Nagao, R.; Louie, A.Y. Multimodal magnetic-resonance/optical-imaging contrast agent sensitive to NADH. *Angew. Chem. Int. Ed.*, **2009**, *48*, pp. 6547-6551.
90. Korolev, V.V.; Vorobyev, D.Yu.; Glebov, E.M.; Grivin, V.P.; Plyusnin, V.F.; Koshkin, A.V.; Fedorova, O.A.; Gromov, S.P.; Alfimov, M.V.; Shklyaev, Yu.V.; Vshivkova, T.S.; Rozhkova, Yu.S.; Tolstikov, A.G.; Lokshin, V.A.; Samat, A. Synthesis and cation-dependent photochromism of spironaphthoxazines obtained from crown-containing dihydroisoquinolines. *Mendeleev Commun.*, **2006**, *16*, pp. 302-304.
91. Korolev, V.V.; Vorobyev, D.Yu.; Glebov, E.M.; Grivin, V.P.; Plyusnin, V.F.; Koshkin, A.V.; Fedorova, O.A.; Gromov, S.P.; Alfimov, M.V.; Shklyaev, Yu.V.; Vshivkova, T.S.; Rozhkova, Yu.S.; Tolstikov, A.G.; Lokshin, V.A.; Samat, A. Spironaphthoxazines produced from crown-containing dihydroisoquinolines: Synthesis and spectroscopic study of cation-dependent photochromism. *J. Photochem. Photobiol., A*, **2007**, *192*, pp. 75-83.
92. Guo, K.; Chen, Y. Lewis acid and base triggered molecular switch. *J. Mater. Chem.*, **2009**, *19*, pp. 5790-5793.

93. Querol, M.; Bozic, B.; Salluce, N.; Belser, P. Synthesis, metal complex formation, and switching properties of spiropyrans linked to chelating sites. *Polyhedron*, **2003**, *22*, pp. 655-664.
94. Ko, C.-C.; Wu, L.-X.; Wong, K.M.-C.; Zhu, N.; Yam, V.W.-W. Synthesis, characterization and photochromic studies of spirooxazine-containing 2;2'-bipyridine ligands and their rhenium(I) tricarbonyl complexes. *Chem. Eur. J.*, **2004**, *10*, pp. 766-776.
95. Bao, Z.; Ng, K.-Y.; Yam, V.W.-W.; Ko, C.-C.; Zhu, N.; Wu, L. Syntheses, characterization, and photochromic studies of spirooxazine-containing 2,2'-bipyridine ligands and their zinc(II) thiolate complexes. *Inorg. Chem.*, **2008**, *47*, pp. 8912-8920.
96. Kumar, S.; Watkins, D.L.; Fujiwara, T. A tailored spirooxazine dimer as a photoswitchable binding tool. *Chem. Commun.*, **2009**, pp. 4369-4371.
97. Zhang, S.-X.; Fan, M.-G.; Liu, Y.-Y.; Ma, Y.; Zhang, G.-J.; Yao, J.-N. Inclusion complex of spironaphthoxazine with gamma-cyclodextrin and its photochromism study. *Langmuir*, **2007**, *23*, pp. 9443-9446.
98. Gentili, P.L.; Ortica, F.; Favaro, G. Supramolecular interaction of a spirooxazine with amino acids. *Chem. Phys. Lett.*, **2007**, *444*, pp. 135-139.
99. Fedorova, O.A.; Maurel, F.; Chebun'kova, A.V.; Strokach, Yu.P.; Valova, T.M.; Kuzmina, L.G.; Howard, J.A.K.; Wenzel, M.; Gloe, K.; Lokshin, V.; Samat, A. Investigation of cation complexation behavior of azacrown ether substituted benzochromene. *J. Phys. Org. Chem.*, **2007**, *20*, pp. 469-483.
100. Chebun'kova, A.V.; Gromov, S.P.; Strokach, Y.P.; Valova, T.M.; Alfimov, M.V.; Fedorova, O.A.; Lokshin, V.; Samat, A. Investigation of the azacrown-ether substituted naphthopyranes. *Mol. Cryst. Liq. Cryst.*, **2005**, *430*, pp. 67-73.
101. Fedorova, O.A.; Strokach, Yu.P.; Chebun'kova, A.V.; Valova, T.M.; Gromov, S.P.; Alfimov, M.V.; Lokshin, V.; Samat, A. Synthesis and complexation properties of photochromic benzochromenes containing aza- and diaza-18-crown-6-ether fragments. *Russ. Chem. Bull.*, **2006**, *55*, pp. 287-294.
102. Ahmed, S.A.; Tanaka, M.; Ando, H.; Iwamoto, H.; Kimura, K. Synthesis and photochromism of novel chromene derivatives bearing a monoazacrown ether moiety. *Eur. J. Org. Chem.*, **2003**, pp. 2437-2442.
103. Ahmed, S.A.; Tanaka, M.; Ando, H.; Iwamoto, H.; Kimura, K. Oxymethylcrowned chromene: photoswitchable stoichiometry of metal ion complex and ion-responsive photochromism. *Tetrahedron*, **2004**, *60*, pp. 3211-3220.

104. Ushakov, E.N.; Nazarov, V.B.; Fedorova, O.A.; Gromov, S.P.; Chebun'kova, A.V.; Alfimov, M.V.; Barigelletti, F. Photocontrol of Ca^{2+} complexation with an azacrown-containing benzochromene. *J. Phys. Org. Chem.*, **2003**, *16*, pp. 306-309.
105. Fedorova, O.A.; Maurel, F.; Ushakov, E.N.; Nazarov, V.B.; Gromov, S.P.; Chebunkova, A.V.; Feofanov, A.V.; Alaverdian, I.S.; Alfimov, M.V.; Barigelletti, F. Synthesis, photochromic behaviour and light-controlled complexation of 3,3-diphenyl-3H-benzo[f]chromenes containing a dimethylamino group or an aza-15-crown-5 ether unit. *New J. Chem.*, **2003**, *27*, pp. 1720-1730.
106. Nazarov, V.B.; Fedorova, O.A.; Brichkin, S.B.; Nikolaeva, T.M.; Gromov, S.P.; Chebun'kova, A.V.; Alfimov, M.V. Complex formation of 2,2-diphenyl-2H-benzo[f]chromene containing the aza-18-crown-6-ether fragment in the polymeric layer. *Russ. Chem. Bull.*, **2003**, *52*, pp. 2661-2667.
107. Kumar, S.; Hernandez, D.; Hoa, B.; Lee, Y.; Yang, Y.S.; McCurdy, A. Synthesis, photochromic properties, and light-controlled metal complexation of a naphthopyran derivative. *Org. Lett.*, **2008**, *10*, pp. 3761-3764.
108. Wada, F.; Arata, R.; Goto, T.; Kikukawa, K.; Matsuda, T. New Application of Crown Ethers. III. Synthesis of 4'-Hydroxybenzocrown Ethers and Their Bis(benzocrown ether)s Linked by Poly(oxyethylene) Chain. *Bull. Chem. Soc. Jpn.*, **1980**, *53*, pp. 2061-2963.
109. Godfrey, I.M.; Sargent, M.V.; Elix, J.A. Preparation of methoxyphenols by baeyer-villiger oxidation of methoxybenzaldehydes. *J. Chem. Soc., Perkin Trans. 1*, **1974**, pp. 1353-1354.
110. Smyth, M.S.; Stefanova, I.; Horak, I.D.; Burke, T.R. Hydroxylated 2-(5'-salicyl)naphthalenes as protein-tyrosine kinase inhibitors. *J. Med. Chem.*, **1993**, *36*, pp. 3015-3020.
111. Dietl, F.; Gierer, G.; Merz, A. Chinone von Benzo- und Dibenzokronenethern. *Synthesis*, **1985**, pp. 626-631.
112. Hayakawa, K.; Kido, K.; Kanematsu, K. Synthesis and characterization of crowned 1,4-benzoquinones as ionophore-dienophile (redox) combined systems: double interaction with catecholamines and tryptamine. *J. Chem. Soc., Perkin Trans. 1*, **1988**, pp. 511-519.
113. Bogaschenko, T.; Basok, S.; Kulygina, C.; Lyapunov, A.; Lukyanenko, N. A Practical Synthesis of Benzocrown Ethers under Phase-Transfer Catalysis Conditions. *Synthesis*, **2002**, pp. 2266-2270.

114. Chebun'kova, A.V. Synthesis and cation-affected photochromic properties of crown-containing benzo- and naphthopyrans. PhD thesis. Photochemistry Center of RAS, Moscow, **2006**, 148 p.
115. Carey, F.A.; Sundberg, R.J. Advanced Organic Chemistry. Part A: Structure and Mechanisms. 5th ed. New York: Springer Science+Business Media, LLC, **2007**. 1199 p.
116. Renz, M.; Meunier, B. 100 Years of Baeyer–Villiger Oxidations. *Eur. J. Org. Chem.*, **1999**, pp. 737-750.
117. Fedorova, O.A.; Vedernikov, A.I.; Yescheulova, O.V.; Tsapenko, P.V.; Pershina, Y.V.; Gromov, S.P. Template effect in the synthesis of formyl derivatives of benzothiacrown compounds. *Russ. Chem. Bull.*, **2000**, *49*, pp. 1853-1858.
118. Iwai, I.; Ide, J. Studies on acetylenic compounds. 32. Ring closure of propargyl ethers. *Chem. Pharm. Bull.*, **1963**, *11*, pp. 1042-1049.
119. Harie, G.; Samat, A.; Guglielmetti, R. Comparative study of chromenes containing different spiro-carbocyclic moieties. *Mol. Cryst. Liq. Cryst.*, **1997**, *297*, pp. 263-268.
120. Carvalho, L.M.; Silva, A.M.S.; Martins, C.I.; Coelho, P.J.; Oliveira-Campos, A.M.F. Structural elucidation of the red dye obtained from reaction of 1,8-naphthalenediol with 1,1-diphenylprop-2-yn-1-ol. A correction. *Tetrahedron Lett.*, **2003**, *44*, pp. 1903–1905.
121. Pozzo, J.L.; Lokshin, V.A.; Guglielmetti, R.A. Convenient Synthesis of Azolo-fused 2H-[1] Benzopyrans. *J. Chem. Soc. Perkin Trans. 1*, **1994**, pp. 2591-2595.
122. Malatesta, V.; Hopley, J.; Giroladini, W.; Wis, M.L. Photochromic compounds in the solid state, process for their preparation and their use in polymeric materials. Eur. Pat. Appl., EP 1132449 A2. **2001**. 12 p.
123. Pozzo, J.L.; Lokshin, V.A. Guglielmetti, R. Newphotochromic 2,2-Diphenyl-[2H]-Chromenes Annellated With Nitrogenated Six-Membered Ring. *Mol. Cryst. Liq. Cryst.*, **1994**, *246*, pp. 75-78.
124. Pozzo, J.L.; Samat, A.; Guglielmetti, R.; Dubest, R.; Aubard, J. Synthesis and photochromic behaviour of naphthopyrans, pyranoquinolines, pyranoquinazolines and pyranoquinoxalines. *Helv. Chim. Acta*, **1997**, *80*, pp. 725-738.
125. Engel, D.A.; Dudley, G.B. The Meyer–Schuster rearrangement for the synthesis of α,β -unsaturated carbonyl compounds. *Org. Biomol. Chem.*, **2009**, *7*, pp. 4149–4158.
126. Desvergne, J.-P.; Lahrahar, N.; Gotta, M.; Zimmermann, Y.; Bouas-Laurent, H. 2,3-Anthraceno[2.2.2]cryptand. Mutual interactions between the receptor and the signal transducing subunit. *J. Mater. Chem.*, **2005**, *15*, pp. 2873-2880.

127. Brunet, E.; Alonso, M.T.; Juanes, O.; Velasco, O.; Rodríguez-Ubis, C. Novel polyaminocarboxylate chelates derived from 3-aryl coumarins. *Tetrahedron*, **2001**, *57*, pp. 3105-3116.
128. Delorme, D.; Ducharme, Y.; Brideau, C.; Chan, C.C.; Chauret, N.; Desmarais, S.; Dubé, D.; Falgueyret, J.P.; Fortin, R.; Guay, J.; Hamel, P.; Jones, T.R.; Lépine, C.; Li, C.; McAuliffe, M.; McFarlane, C.S.; Nicoll-Griffith, D.A.; Riendeau, D.; Yergey, J.A.; Girard, Y. Dioxabicyclooctanyl naphthalenenitriles as nonredox 5-lipoxygenase inhibitors: structure-activity relationship study directed toward the improvement of metabolic stability. *J. Med. Chem.*, **1996**, *39*, pp. 3951-3970.
129. Samat, A.; Lokshin, V.; Chamontin, K.; Levi, D.; Pepe, G.; Guglielmetti, R. Synthesis and unexpected photochemical behaviour of biphotochromic systems involving spirooxazines and naphthopyrans linked by an ethylenic bridge. *Tetrahedron*, **2001**, *57*, pp. 7349-7359.
130. Ehala, S.; Toman, P.; Makrlík, E.; Kašička, V. Application of affinity capillary electrophoresis and density functional theory to the investigation of benzo-18-crown-6-ether complex with ammonium cation. *J. Chromatogr. A*, **2009**, *1216*, pp. 7927-7931.
131. Spätha, A.; König, B. Ditopic crown ether-guanidinium ion receptors for the molecular recognition of amino acids and small peptides. *Tetrahedron*, **2010**, *66*, pp. 1859-1873.
132. Arnaud-Neu, F.; Delgado, R.; Chaves, S. Critical Evaluation of Stability Constants and Thermodynamic Functions of Metal Complexes of Crown Ethers. *Pure Appl. Chem.*, **2003**, *75*, pp. 71-102.
133. Alderighi, L.; Gans, P.; Ienco, A.; Peters, D.; Sabatini, A.; Vacca, A. Hyperquad simulation and speciation (HySS): a utility program for the investigation of equilibria involving soluble and partially soluble species. *Coord. Chem. Rev.*, **1999**, *184*, pp. 311-318.
134. MOPAC2009, Stewart, J.J.P. Stewart Computational Chemistry, Version 9.351M. [HTTP://OpenMOPAC.net](http://OpenMOPAC.net).
135. Rocha, M.S. Revisiting the Neighbor Exclusion Model and Its Applications. *Biopolymers*, **2010**, *93*, pp. 1-7.
136. McGhee, J.D.; von Hippel, P.H. Theoretical aspects of dna-protein interactions - cooperative and non-cooperative binding of large ligands to a one-dimensional homogeneous lattice. *J. Mol. Biol.*, **1974**, *86*, pp. 469-489.
137. Tkachev, V.V.; Aldoshin, S.M.; Sanina, N.A.; Lukyanov, B.S.; Minkin, V.I.; Utenyshev, A.N.; Khalanskiy, K.N.; Alekseenko, Yu.S. Photo- and thermochromic spirans. 29. Novel

- photo-chromic indolinospiropyrans containing a quinoline moiety. *Chem. Heterocycl. Compd.*, **2007**, *479*, pp. 690-702.
138. Carrington, A.; McLachlan, A.D. Introduction to magnetic resonance with application to chemistry and chemical physics. New York: Harper and Row, **1967**. 447 p.
 139. Parish, W.W.; Stott, P.E.; McCausland, C.W.; Bradshaw J.S. Modified crown ether catalysts. 1. Synthesis of alkanoyl-, aroyl-, and α -hydroxyalkylbenzo crown ethers. *J. Org. Chem.*, **1978**, *43*, pp. 4577-4581.
 140. Bongers, K.M.; van der Berg, R.J.B.H.N.; Heitman, L.H.; IJzerman, A.P.; Oosterom, J.; Timmers, C.M.; Overkleeft, H.S.; van der Marel, G.A. Synthesis and evaluation of homo-bivalent GnRHR ligands. *Bioorg. Med. Chem.*, **2007**, *15*, pp. 4841-4856.
 141. Connors, K.A. Binding constants: the measurement of molecular complex stability. New York: John Wiley and Sons, **1987**. 411 p.
 142. Beck, M.T.; Nagypál, I. Chemistry of complex equilibria. New York: John Wiley and Sons, **1990**. 402 p.
 143. Mamedov, Sh.; Khydyrov, D. Investigations of glycol ethers and their derivatives. *Zh. Obshch. Khim.*, **1958**, *28*, pp. 2812-2816.
 144. Aldoshin, S.M.; Sanina, N.A.; Minkin, V.I.; Voloshin, N.A.; Ikorskii, V.N.; Ovcharenko, V.I.; Smirnov, V.A.; Nagaev, N.K. Molecular photochromic ferromagnetic based on the layered polymeric tris-oxalate of Cr(III), Mn(II) and 1-[(1',3',3'-trimethyl-6-nitrospiro[2H-1-benzopyran-2,2'-indoline]-8-yl)methyl]pyridinium. *J. Mol. Struct.*, **2007**, *826*, pp. 69-74.

7. Appendixes

7.1. X-Ray Data

Table 7.1.

X-Ray data for compounds **3b**, **5**, **21b**.

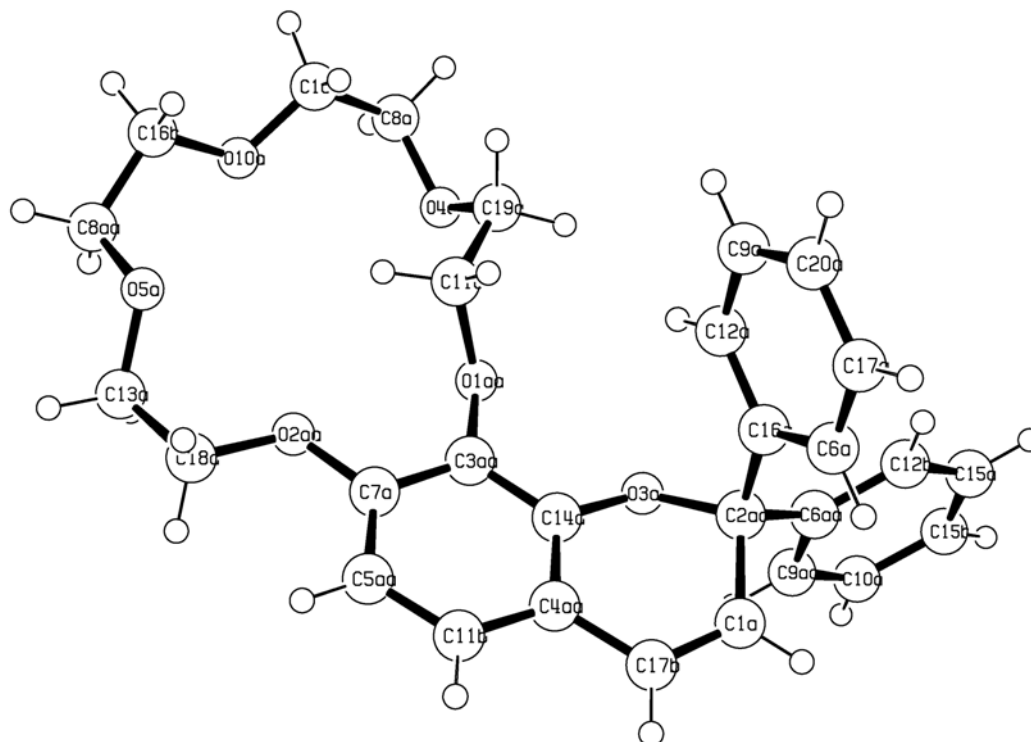
Parameter	3b	5*	21b
Empirical formula	C ₂₀ H ₂₀ N ₂ O ₂	C ₁₉ H ₂₆ Cl ₂ O ₇	C ₃₅ H ₃₆ O ₅ S ₂
Molecular weight	320.38	437.3	600.76
Crystal system	orthorhombic	monoclinic	monoclinic
Space group	<i>P</i> bca	<i>P</i> 2 ₁ /n	<i>P</i> 1 2 ₁ /c 1
Crystal size, mm ³	0.23 × 0.2 × 0.15	0.3 × 0.3 × 0.15	0.25 × 0.2 × 0.08
<i>a</i> , Å	9.6763(19)	9.1000(2)	9.1781(2)
<i>b</i> , Å	17.770(4)	8.2070(2)	36.0682(8)
<i>c</i> , Å	27.452(6)	28.9379(9)	9.4895(2)
α , °	90.00	90	90
β , °	90.00	90.0360(10)	96.027(2)
γ , °	90.00	90	90
<i>V</i> , Å ³	4720.2(16)	2161.19(10)	3124.02(12)
<i>Z</i>	12	4	4
<i>d</i> _{calc} , g cm ⁻³	1.352	1.344	1.277
μ , mm ⁻¹	0.088	0.337	0.211
<i>F</i> (000)	2040	920	1272
θ range, °	1.48 – 29.27	1.41 - 28.24	2.44 - 28.16
Observed reflections	25581	4994	20678
Independent reflections	6426	4994	7179
<i>R</i> _{int}	0.0741	0.071	0.084
Reflections [<i>I</i> > 2 σ (<i>I</i>)]	4246	2468	3087
Parameters	316	293	379
GOF	0.892	1.16	1.054
<i>R</i> [<i>I</i> > 2 σ (<i>I</i>)]			
<i>R</i>	0.0489	0.0786	0.1369
<i>wR</i> ₂	0.1271	0.2572	0.345
Final <i>R</i>			
<i>R</i>	0.0877	0.1629	0.232
<i>wR</i> ₂	0.1522	0.3226	0.4111

* In a crystal, there are presents CH₂Cl₂ molecules disordered in space with occupancies 0.75, 0.15, and 0.15 along the axes.

Table 7.2.X-Ray data for compounds **27a**, **39**.

Parameter	27a	39
Empirical formula	C ₂₅ H ₂₀ INO	C ₂₄ H ₁₉ NO ₂
Molecular weight	477.32	353.4
Crystal system	triclinic	monoclinic
Space group	<i>P</i> -1	<i>P</i> 2 ₁ / <i>n</i>
Crystal size, mm ³	0.2 × 0.1 × 0.1	0.2 × 0.15 × 0.15
<i>a</i> , Å	7.845(2)	8.5061(2)
<i>b</i> , Å	9.504(2)	16.8993(4)
<i>c</i> , Å	14.433(3)	13.7042(3)
α , °	95.45(2)	90
β , °	102.38(2)	107.827(1)
γ , °	100.07(2)	90
<i>V</i> , Å ³	1025.0(4)	1875.35(7)
<i>Z</i>	2	4
<i>d</i> _{calc} , g cm ⁻³	1.547	1.252
μ , mm ⁻¹	1.577	0.079
<i>F</i> (000)	476	744
θ range, °	2.20 - 25.01	2.79 - 28.72
Observed reflections	4208	17678
Independent reflections	3476	4679
<i>R</i> _{int}	0.0257	0.11
Reflections [<i>I</i> > 2 σ (<i>I</i>)]	2570	2424
Parameters	255	244
GOF	1.010	1.077
<i>R</i> [<i>I</i> > 2 σ (<i>I</i>)]		
<i>R</i>	0.0395	0.0713
<i>wR</i> ₂	0.0825	0.1598
Final <i>R</i>		
<i>R</i>	0.0646	0.1488
<i>wR</i> ₂	0.0919	0.2168

Table 7.3 .

Interatomic distances (d) and angles (ω) in structure of chromene **3b**.

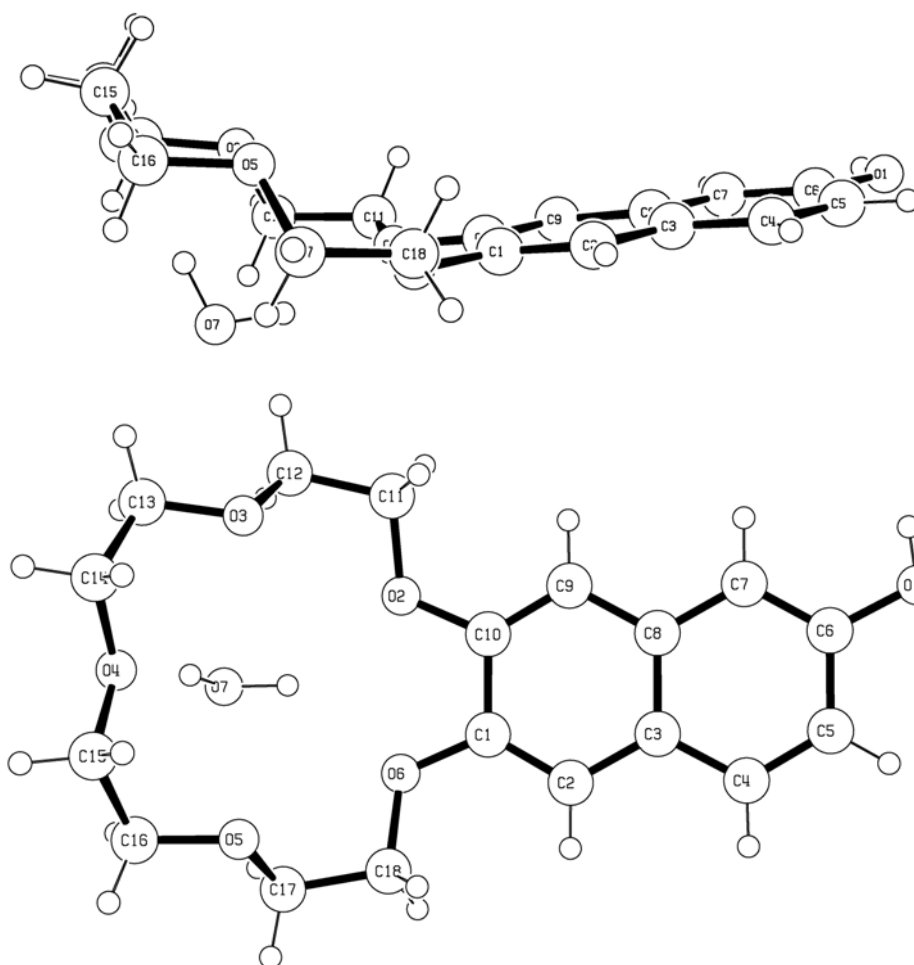
Bond		d (Å)
O2aa	C7a	1.358(2)
O2aa	C18a	1.4278(19)
O1aa	C3aa	1.3761(19)
O1aa	C11a	1.444(2)
O3a	C14a	1.3690(19)
O3a	C2aa	1.454(2)
C7a	C5aa	1.383(2)
C7a	C3aa	1.404(2)
O10a	C16b	1.415(2)
O10a	C1aa	1.417(2)

Bond		d (Å)
C1a	C17b	1.326(2)
C1a	C2aa	1.518(2)
C14a	C3aa	1.379(2)
C14a	C4aa	1.401(2)
C16a	C2aa	1.520(2)
C2aa	C6aa	1.522(2)
C4aa	C11b	1.383(2)
C4aa	C17b	1.447(2)
C5aa	C11b	1.385(2)
C8aa	C16b	1.496(3)

Angle			ω (°)
C7a	O2aa	C18a	118.64(13)
C3aa	O1aa	C11a	114.90(12)
C14a	O3a	C2aa	116.06(12)
O2aa	C7a	C5aa	124.75(15)
O2aa	C7a	C3aa	114.99(14)
C16b	O10a	C1aa	112.77(14)
O3a	C14a	C3aa	118.04(14)
O3a	C14a	C4aa	120.63(14)
O3a	C2aa	C16a	108.06(13)

Angle			ω (°)
O3a	C2aa	C6aa	105.30(13)
C16a	C2aa	C6aa	112.80(14)
O3a	C2aa	C1a	109.78(13)
O1aa	C3aa	C14a	119.17(14)
O1aa	C3aa	C7a	121.53(15)
C11b	C4aa	C17b	124.09(15)
C14a	C4aa	C17b	117.33(15)
O10a	C16b	C8aa	107.99(15)

Table 7.4.

Interatomic distances (d) and angles (ω) in structure of naphthol 5.

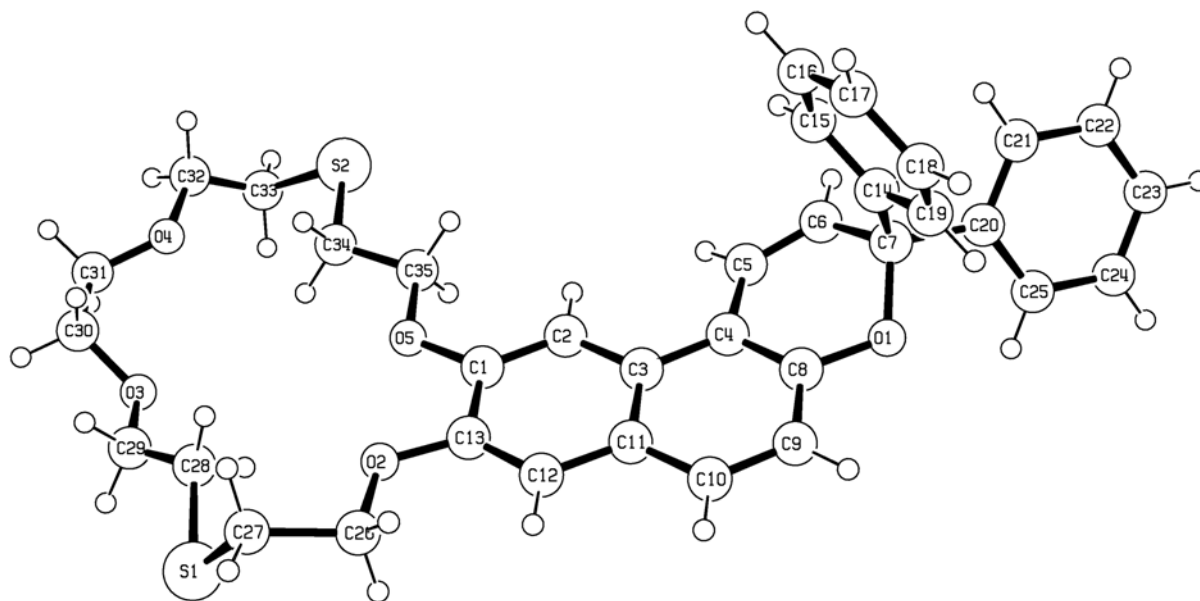
Bond		d (Å)
C1	C2	1.363(6)
C1	O6	1.373(5)
C1	C10	1.431(5)
C2	C3	1.416(5)
C3	C4	1.410(6)
C3	C8	1.423(5)
C4	C5	1.367(6)
C5	C6	1.406(6)
C6	O1	1.362(5)

Bond		d (Å)
C6	C7	1.364(6)
C7	C8	1.402(6)
C8	C9	1.419(5)
C9	C10	1.351(5)
C10	O2	1.370(5)
C11	O2	1.435(5)
C13	C14	1.487(8)
C14	O4	1.425(7)
C18	O6	1.433(5)

Angle			ω (°)
C2	C1	O6	126.2(3)
C2	C1	C10	119.8(4)
O6	C1	C10	114.0(3)
C4	C3	C2	122.9(4)
O1	C6	C7	123.4(4)
O1	C6	C5	117.3(4)
C7	C6	C5	119.3(4)
C7	C8	C9	122.1(4)

Angle			ω (°)
C9	C10	O2	125.6(3)
C9	C10	C1	120.6(4)
O2	C10	C1	113.8(3)
O4	C14	C13	107.5(4)
C10	O2	C11	117.4(3)
C15	O4	C14	115.2(4)
C1	O6	C18	117.9(3)

Table 7.5.

Interatomic distances (d) and angles (ω) in structure of chromene **21b**.

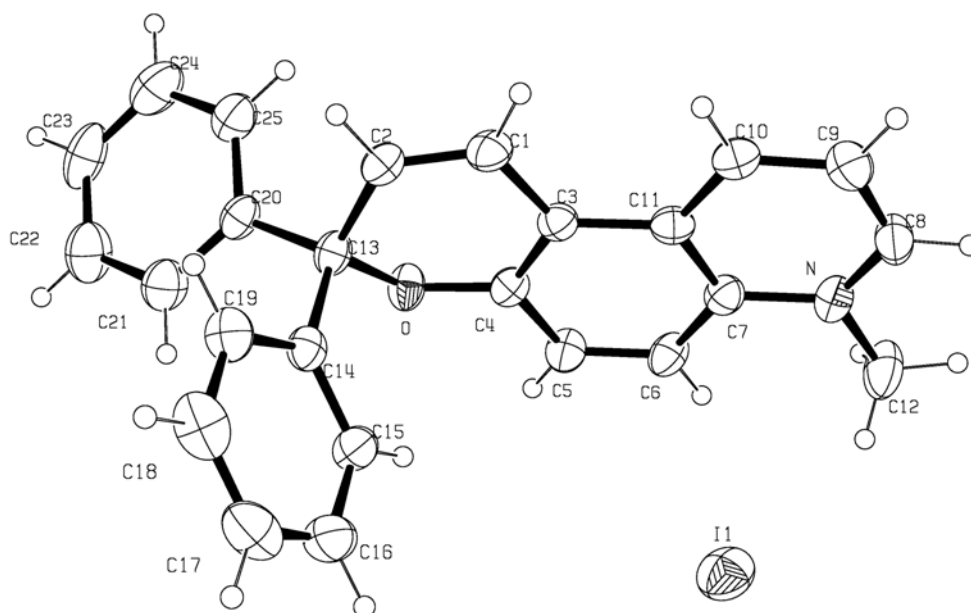
Bond		d (Å)
C30	C31	1.452(13)
C34	C35	1.395(11)
C34	S2	1.799(9)
C35	O5	1.466(8)
O4	C31	1.299(12)
O4	C32	1.393(15)
C1	O5	1.351(7)
C1	C2	1.364(8)
C1	C13	1.429(8)
C2	C3	1.415(8)
C3	C11	1.413(7)
C3	C4	1.414(7)
C4	C8	1.386(7)
C4	C5	1.454(7)

Bond		d (Å)
C5	C6	1.315(8)
C6	C7	1.508(8)
C7	O1	1.455(6)
C7	C20	1.519(8)
C7	C14	1.532(7)
C8	O1	1.380(6)
C11	C12	1.415(7)
C12	C13	1.350(8)
C13	O2	1.360(7)
C32	C33	1.26(2)
C33	S2	1.77(2)
C8	C9	1.394(7)
C9	C10	1.362(7)
C10	C11	1.417(7)

Angle			ω (°)
C35	C34	S2	110.7(7)
C34	C35	O5	108.2(7)
C31	O4	C32	120.8(13)
O5	C1	C2	125.6(5)
O5	C1	C13	114.2(5)
C2	C3	C4	122.3(5)
C8	C4	C5	116.2(5)
C3	C4	C5	125.2(5)
C6	C5	C4	120.1(5)
C5	C6	C7	120.3(5)
O1	C7	C6	108.5(4)
O1	C7	C20	106.4(4)
C6	C7	C20	110.5(4)

Angle			ω (°)
O1	C7	C14	107.3(4)
C6	C7	C14	112.5(5)
C20	C7	C14	111.4(4)
O1	C8	C9	116.4(5)
C10	C9	C8	118.7(5)
C12	C11	C10	121.9(5)
C12	C13	O2	126.5(5)
O2	C13	C1	114.3(5)
C33	C32	O4	109.6(15)
C32	C33	S2	114.7(12)
C8	O1	C7	114.2(4)
C1	O5	C35	117.7(5)
C33	S2	C34	103.6(6)

Table 7.6.

Interatomic distances (d) and angles (ω) in structure of chromene **27a**.

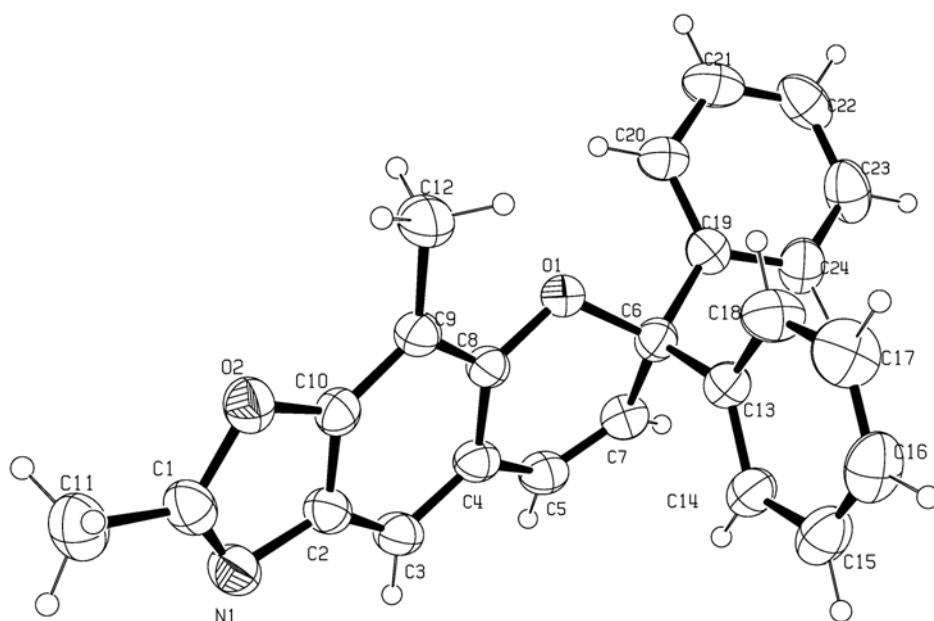
Bond		d (Å)
O	C4	1.363(4)
O	C13	1.464(4)
N	C8	1.323(5)
N	C7	1.392(5)
N	C12	1.472(5)
C13	C2	1.510(5)
C13	C20	1.518(5)
C13	C14	1.526(6)
C3	C4	1.375(5)
C3	C11	1.438(5)

Bond		d (Å)
C3	C1	1.451(5)
C4	C5	1.404(5)
C6	C5	1.358(5)
C6	C7	1.385(5)
C11	C10	1.404(5)
C11	C7	1.420(5)
C1	C2	1.322(5)
C10	C9	1.369(6)
C8	C9	1.364(6)

Angle			ω (°)
C4	O	C13	118.8(3)
C8	N	C7	121.6(4)
C8	N	C12	119.9(3)
C7	N	C12	118.5(3)
O	C13	C2	110.1(3)
O	C13	C20	104.1(3)
C2	C13	C20	113.2(3)
O	C13	C14	109.0(3)
C2	C13	C14	107.4(3)
C20	C13	C14	113.0(3)
C4	C3	C1	117.7(3)
C11	C3	C1	124.2(3)
O	C4	C3	122.5(3)

Angle			ω (°)
O	C4	C5	115.6(3)
C3	C4	C5	121.8(3)
C5	C6	C7	120.2(4)
C10	C11	C3	122.5(3)
C7	C11	C3	118.7(3)
C2	C1	C3	119.7(3)
C9	C10	C11	120.0(4)
C6	C7	N	121.4(3)
C6	C7	C11	120.8(3)
N	C7	C11	117.8(3)
C1	C2	C13	122.9(3)
N	C8	C9	121.9(4)
C6	C5	C4	120.5(4)

Table 7.7.

Interatomic distances (d) and angles (ω) in structure of chromene **39**.

Bond		d (Å)
C1	N1	1.282(4)
C1	O2	1.381(3)
C1	C11	1.476(4)
C2	C3	1.378(4)
C2	C10	1.382(4)
C2	N1	1.408(4)
C3	C4	1.395(4)
C4	C8	1.405(3)
C4	C5	1.458(4)
C5	C7	1.325(4)
C6	O1	1.455(3)

Bond		d (Å)
C6	C7	1.502(4)
C6	C19	1.525(4)
C6	C13	1.537(3)
C8	O1	1.372(3)
C8	C9	1.393(4)
C9	C10	1.375(4)
C9	C12	1.495(4)
C10	O2	1.383(3)
C13	C14	1.377(4)
C13	C18	1.378(4)
C9	C10	1.375(4)

Angle			ω (°)
N1	C1	O2	115.0(3)
N1	C1	C11	128.8(3)
O2	C1	C11	116.2(3)
C3	C2	C10	119.9(3)
C3	C2	N1	131.6(3)
C10	C2	N1	108.5(2)
C2	C3	C4	117.6(2)
C3	C4	C8	120.0(3)
C3	C4	C5	123.4(2)
C7	C5	C4	120.3(2)
O1	C6	C7	108.9(2)
O1	C6	C19	105.6(2)
C7	C6	C19	111.0(2)
O1	C6	C13	107.5(2)

Angle			ω (°)
C7	C6	C13	113.2(2)
C19	C6	C13	110.3(2)
C5	C7	C6	120.1(3)
O1	C8	C9	116.3(2)
O1	C8	C4	120.0(2)
C9	C8	C4	123.5(2)
C10	C9	C12	124.2(3)
C8	C9	C12	122.7(2)
C9	C10	C2	125.8(3)
C9	C10	O2	126.7(2)
C2	C10	O2	107.5(2)
C1	N1	C2	104.9(2)
C8	O1	C6	116.41(18)
C1	O2	C10	104.0(2)

7.2. NMR Spectra

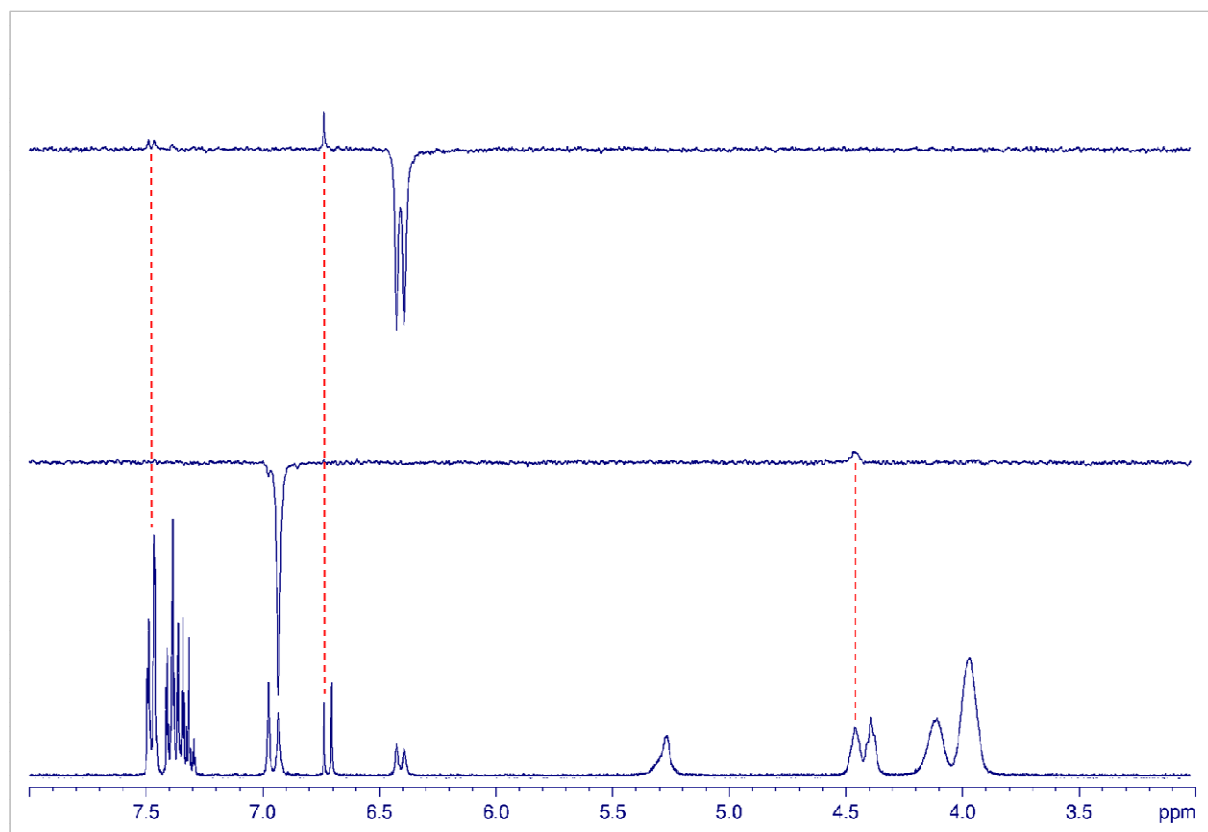


Figure 7.1. NOESY 1D NMR spectrum of a solution of **1a** in the presence of equimolar quantity of magnesium (II) cations (20°C). From top downward are shown spectra upon excitation of frequencies at δ 6.41 ppm, 6.92 ppm, and the ^1H NMR spectrum of the same solution.

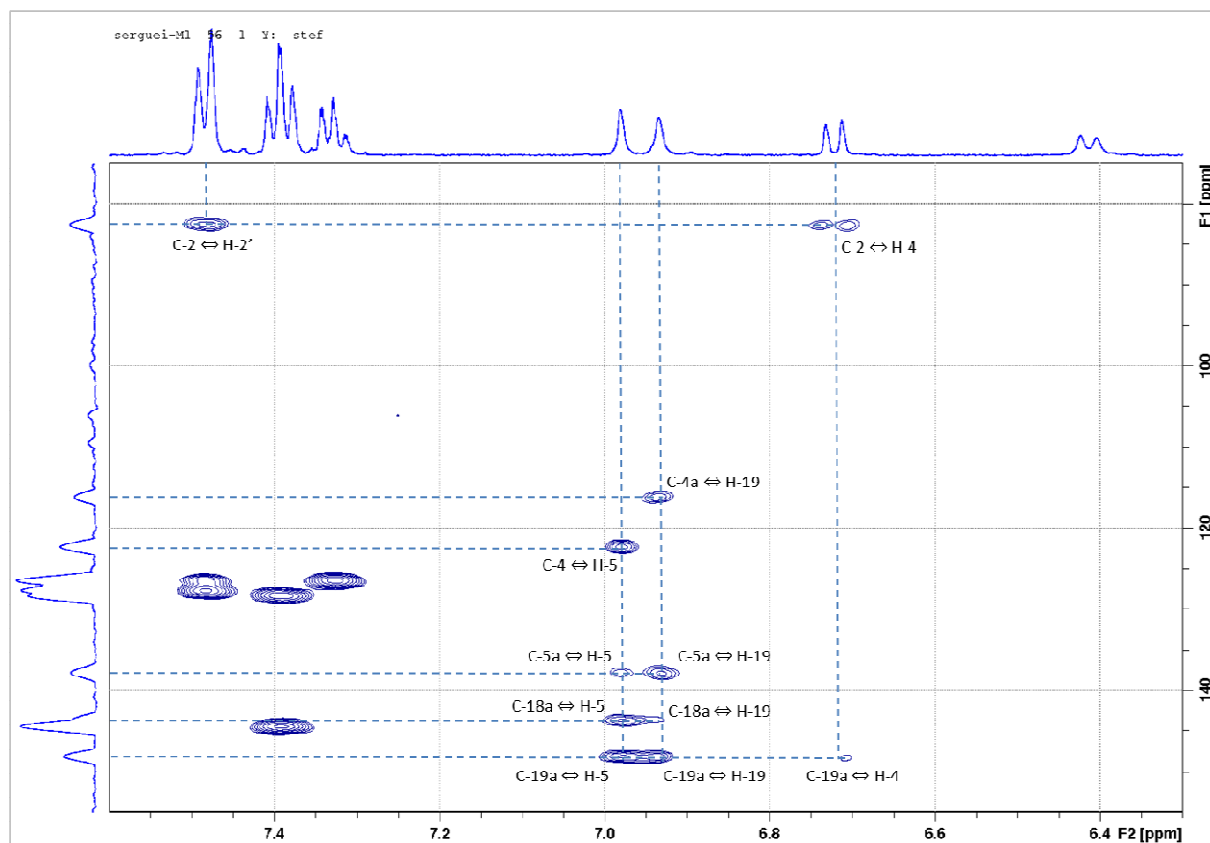


Figure 7.2. Low field part of HMBC spectrum of a solution of **1a** in CD_3CN in the presence of equimolar quantity of magnesium (II) cations (20°C). Some cross-peaks are marked.

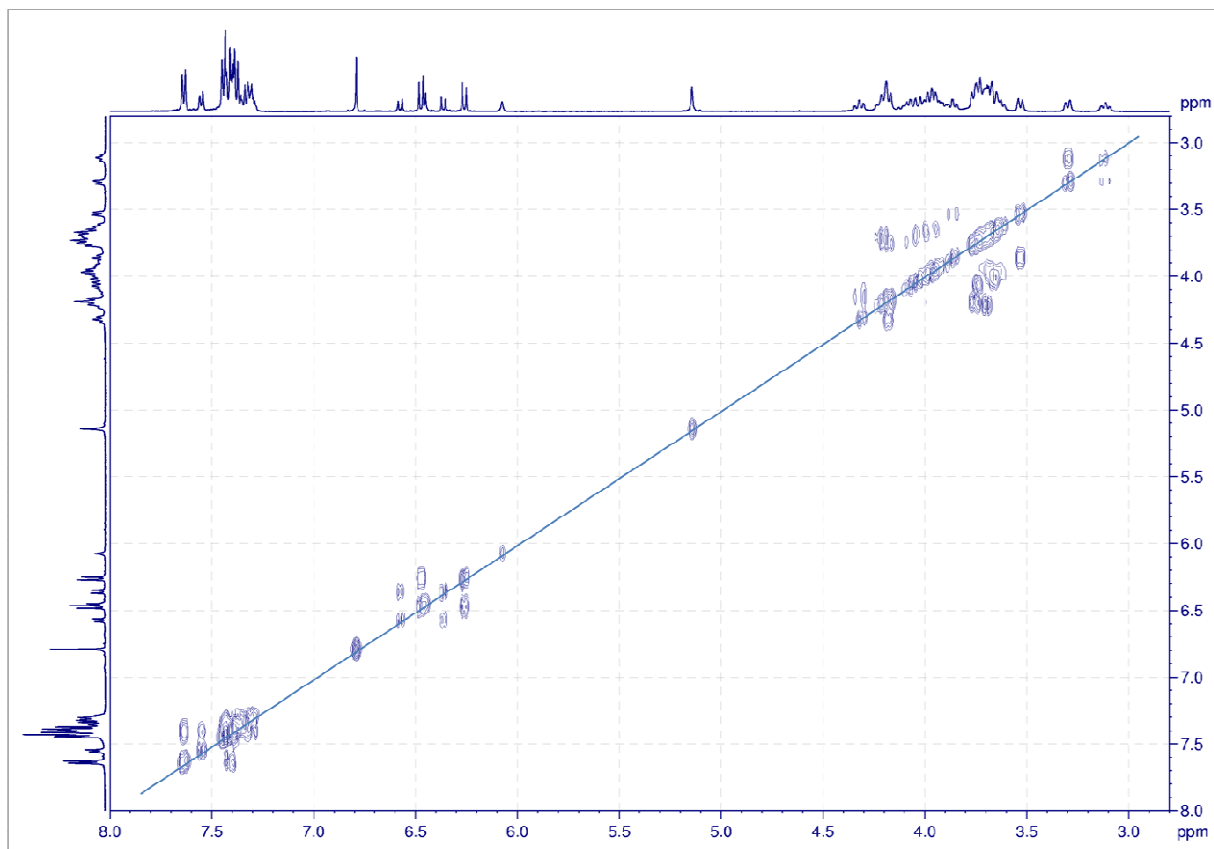


Figure 7.3. COSY spectrum of a solution of **1a** in CD_3CN in the presence of barium (II) cations ($C_M/C_{1a} = 0.5$) at -45°C .

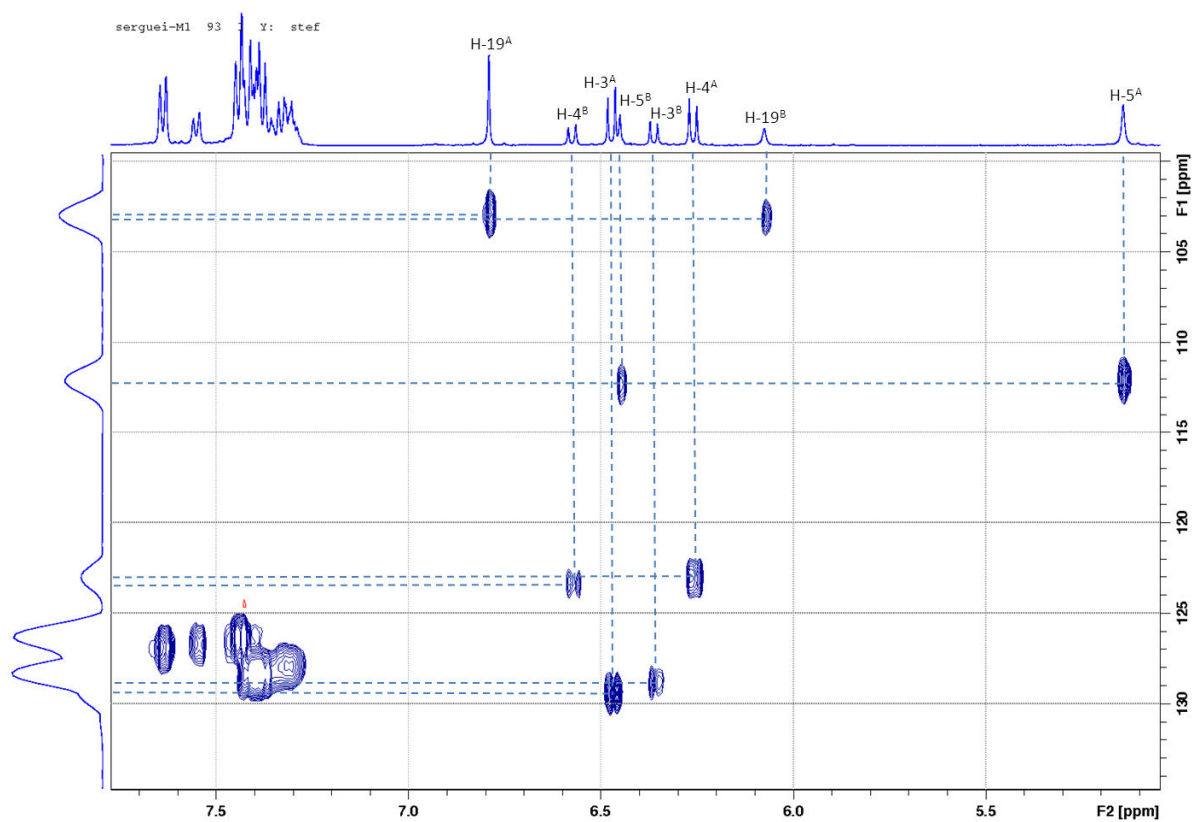


Figure 7.4. Low field part of HSQC spectrum of a solution of **1a** in CD_3CN in the presence of barium (II) cations ($C_M/C_{1a} = 0.5$) at -45°C . Some cross-peaks are marked.

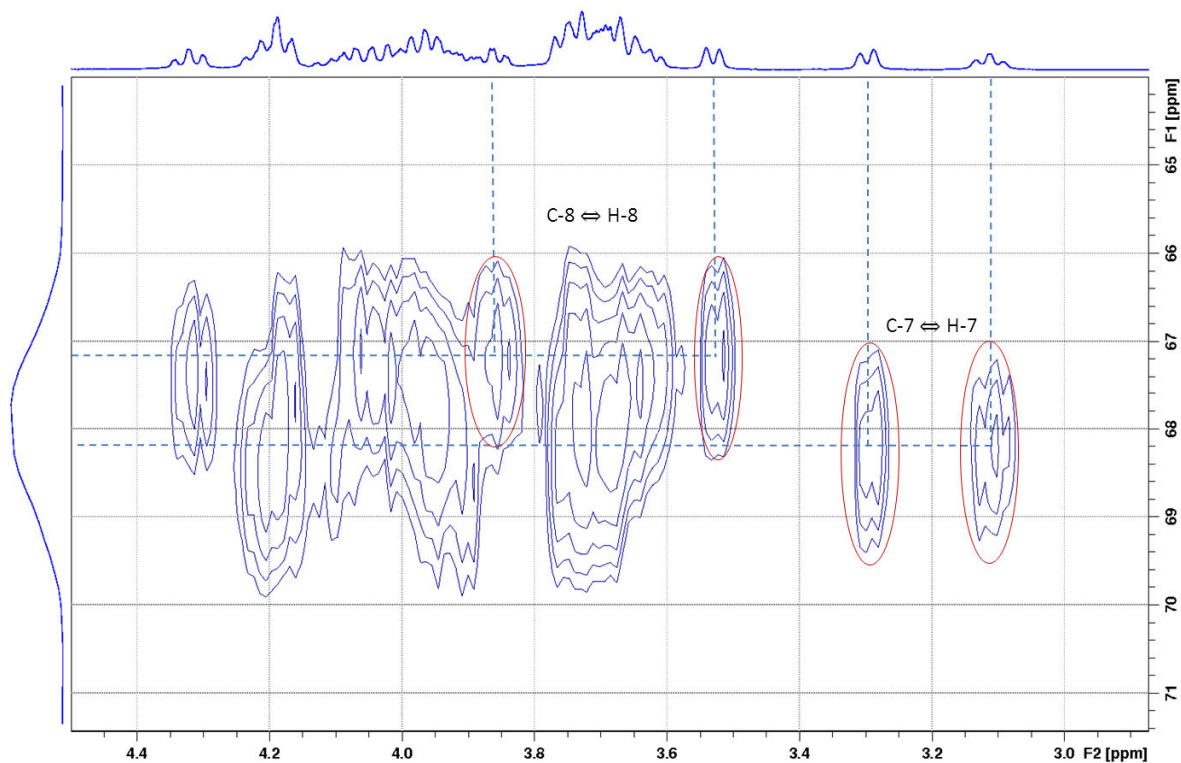


Figure 7.5. High field part of HSQC spectrum of a solution of **1a** in CD_3CN in the presence of barium (II) cations ($C_M/C_{1a} = 0.5$) at -45°C . Some cross-peaks are marked.

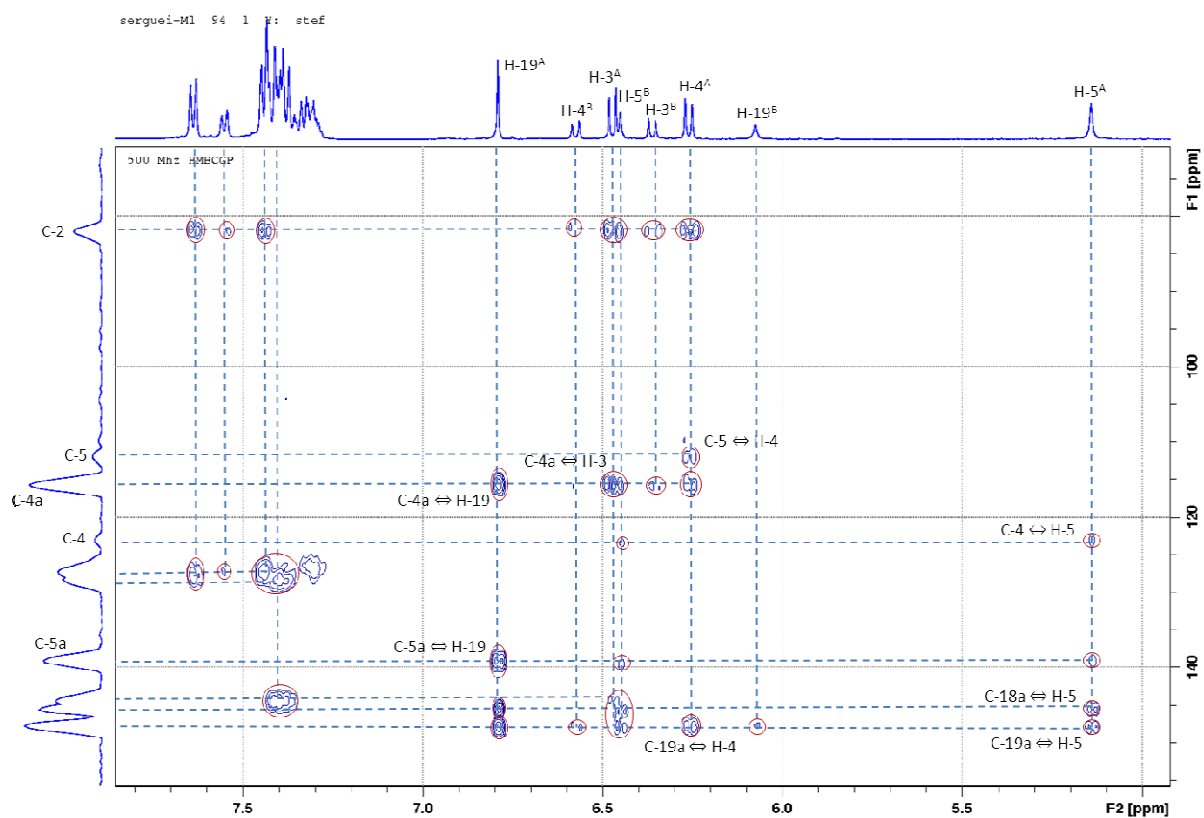


Figure 7.6. Low field part of HMBC spectrum of a solution of **1a** in CD_3CN in the presence of barium (II) cations ($C_M/C_{1a} = 0.5$) at -45°C . Some cross-peaks are marked.

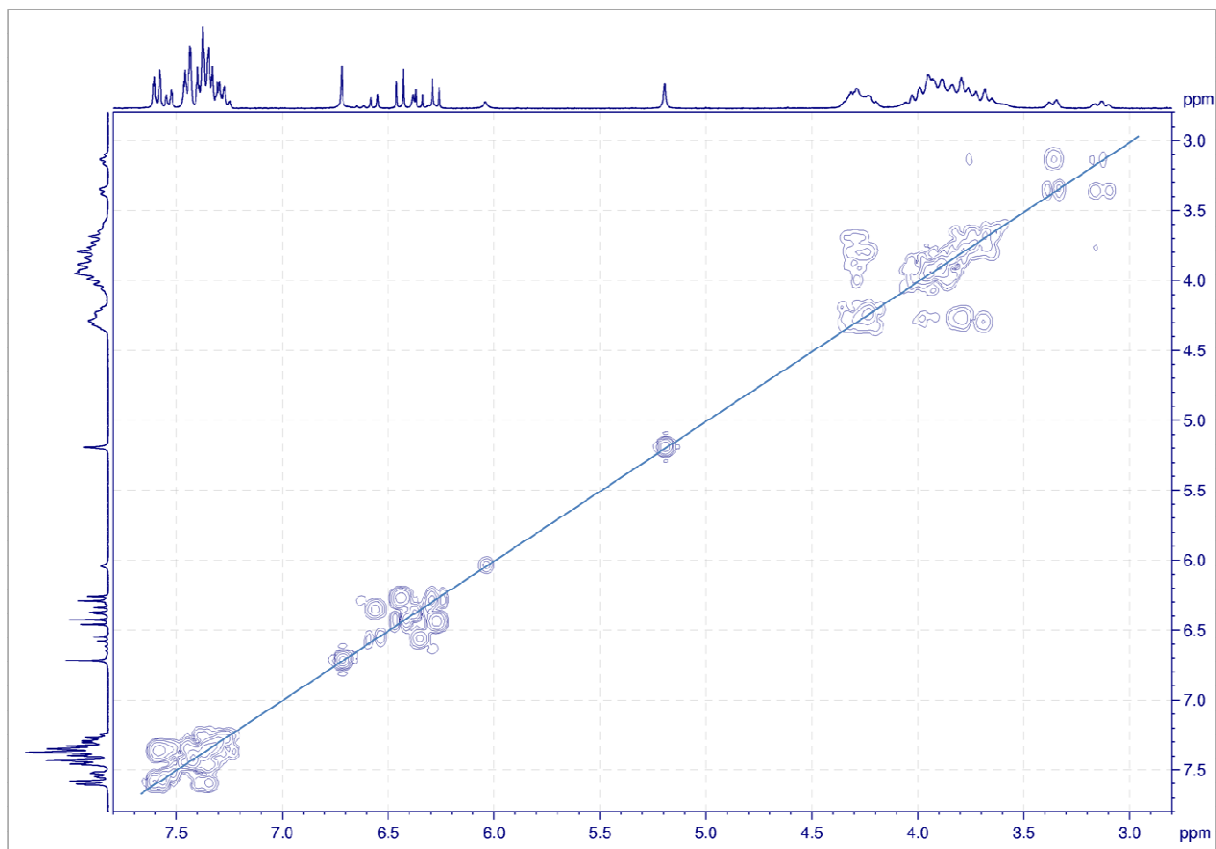


Figure 7.7. COSY spectrum of a solution of **1a** in CD_3CN in the presence of lead (II) cations ($C_M/C_{1a} = 0.5$) at -45°C .

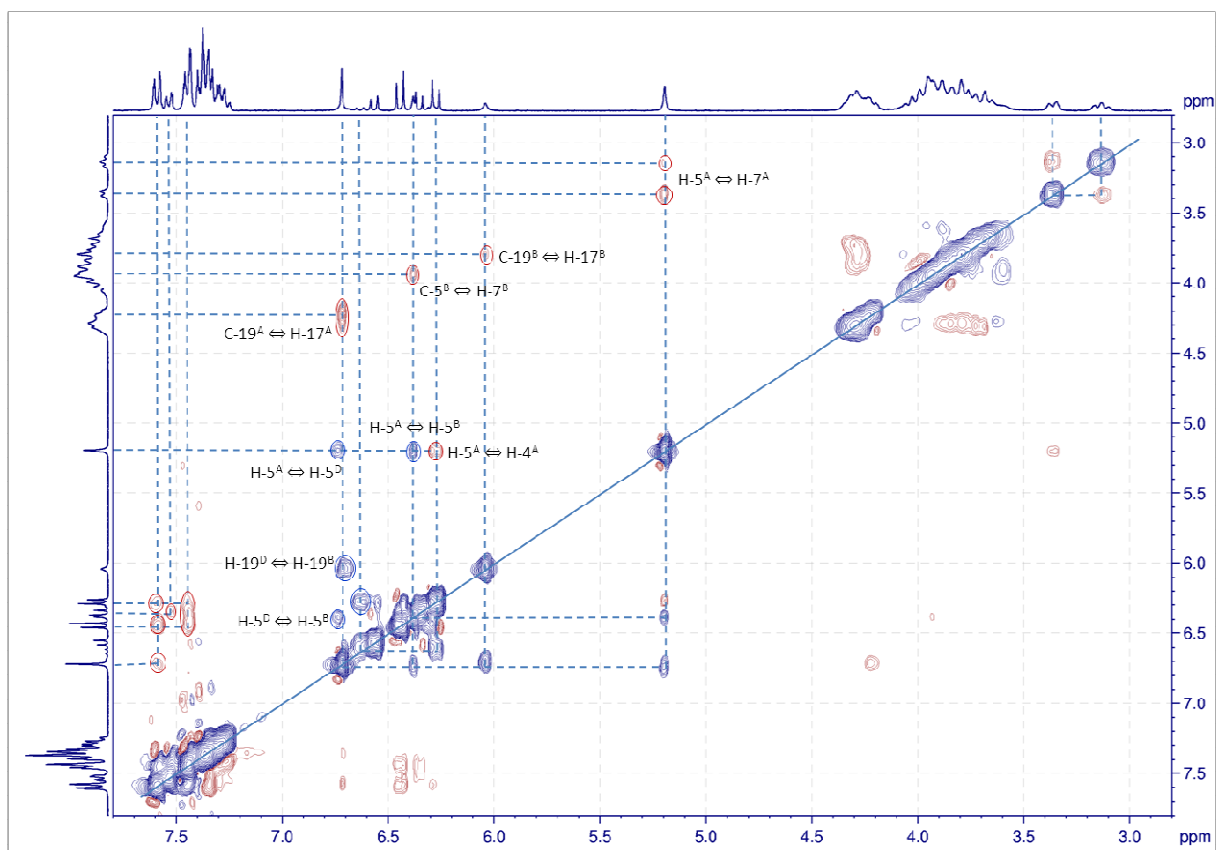


Figure 7.8. NOESY spectrum of a solution of **1a** in CD_3CN in the presence of lead (II) cations ($C_M/C_{1a} = 0.5$) at -45°C . Some cross-peaks are marked.

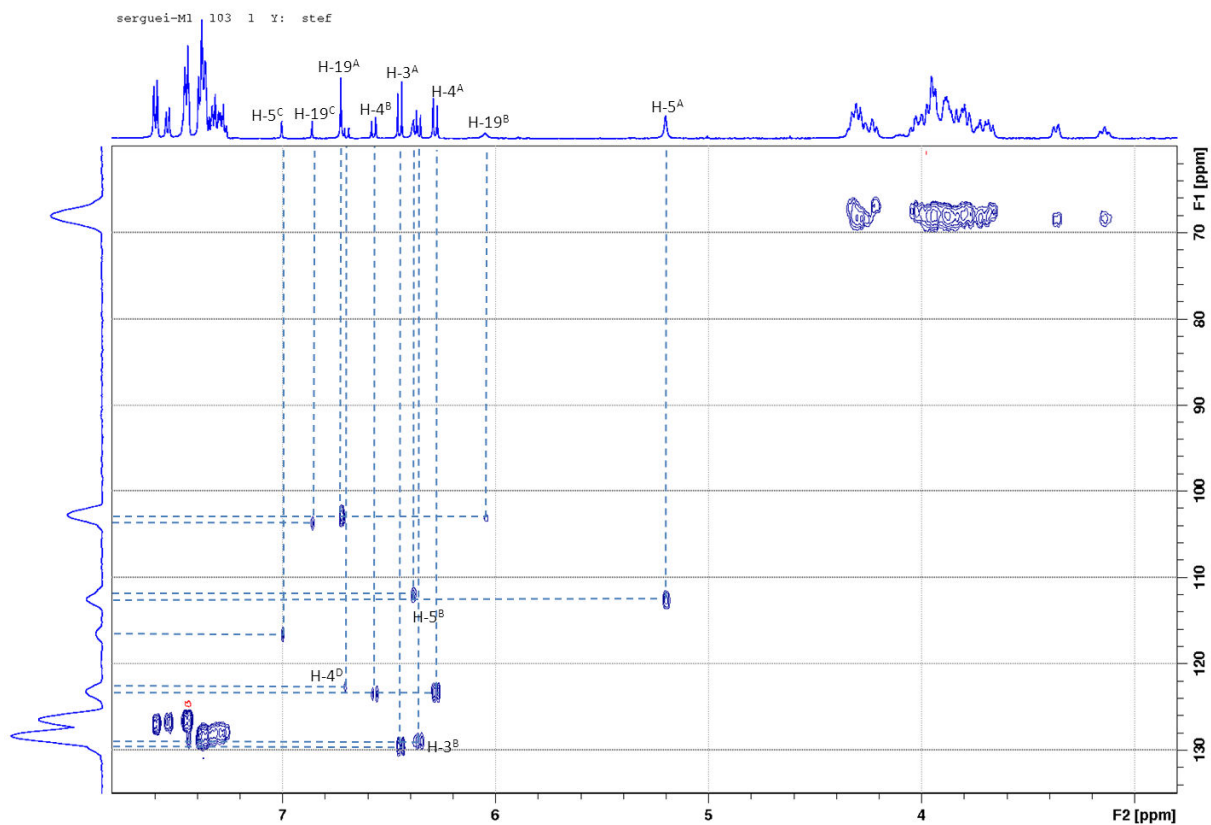


Figure 7.9. HSQC spectrum of a solution of **1a** in CD_3CN in the presence of lead (II) cations ($C_M/C_{1a} = 1$) at -45°C . Some cross-peaks are marked.

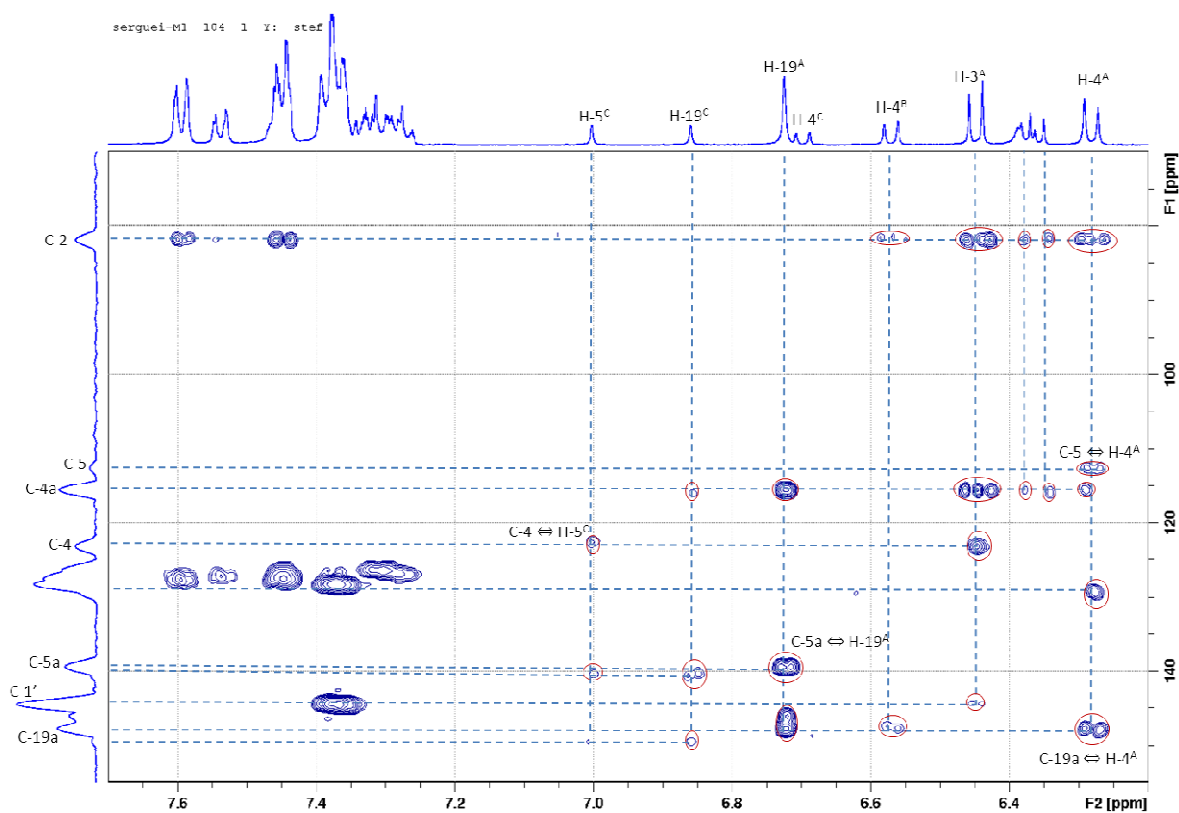


Figure 7.10. HMBC spectrum of a solution of **1a** in CD_3CN in the presence of barium (II) cations ($C_M/C_{1a} = 1$) at -45°C . Some cross-peaks are marked.

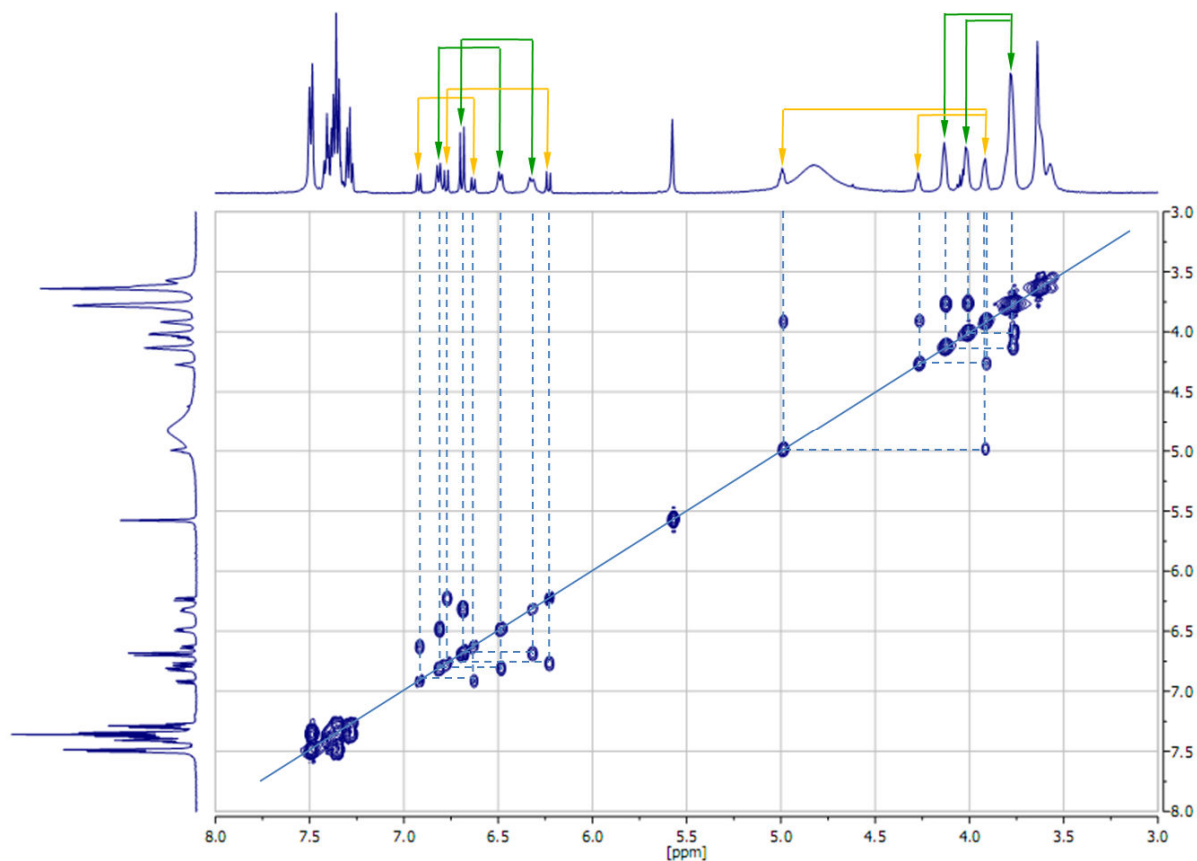


Figure 7.11. COSY spectrum of a solution of **3a** in CD_3CN in the presence of equimolar quantity of magnesium (II) cations at -45°C .

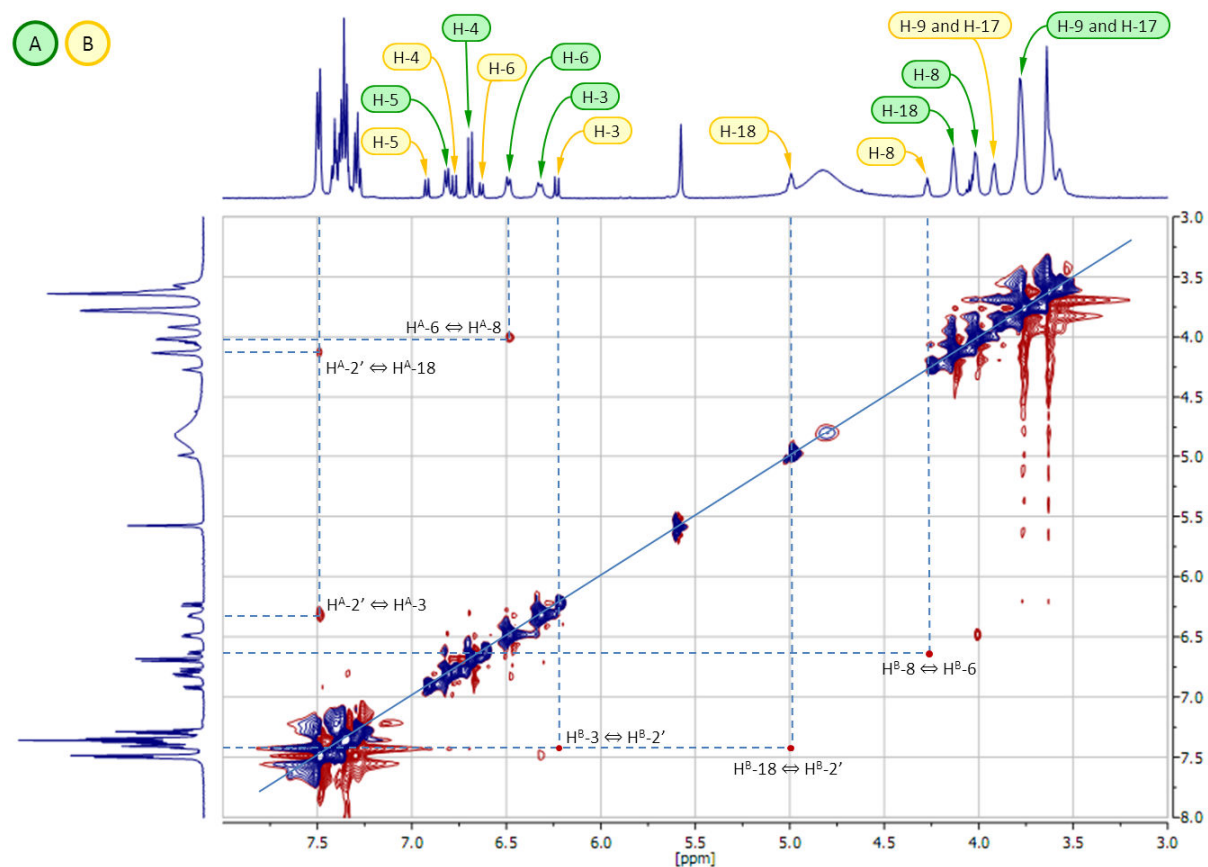


Figure 7.12. NOESY spectrum of a solution of **3a** in CD_3CN in the presence of equimolar quantity of magnesium (II) cations at -45°C .

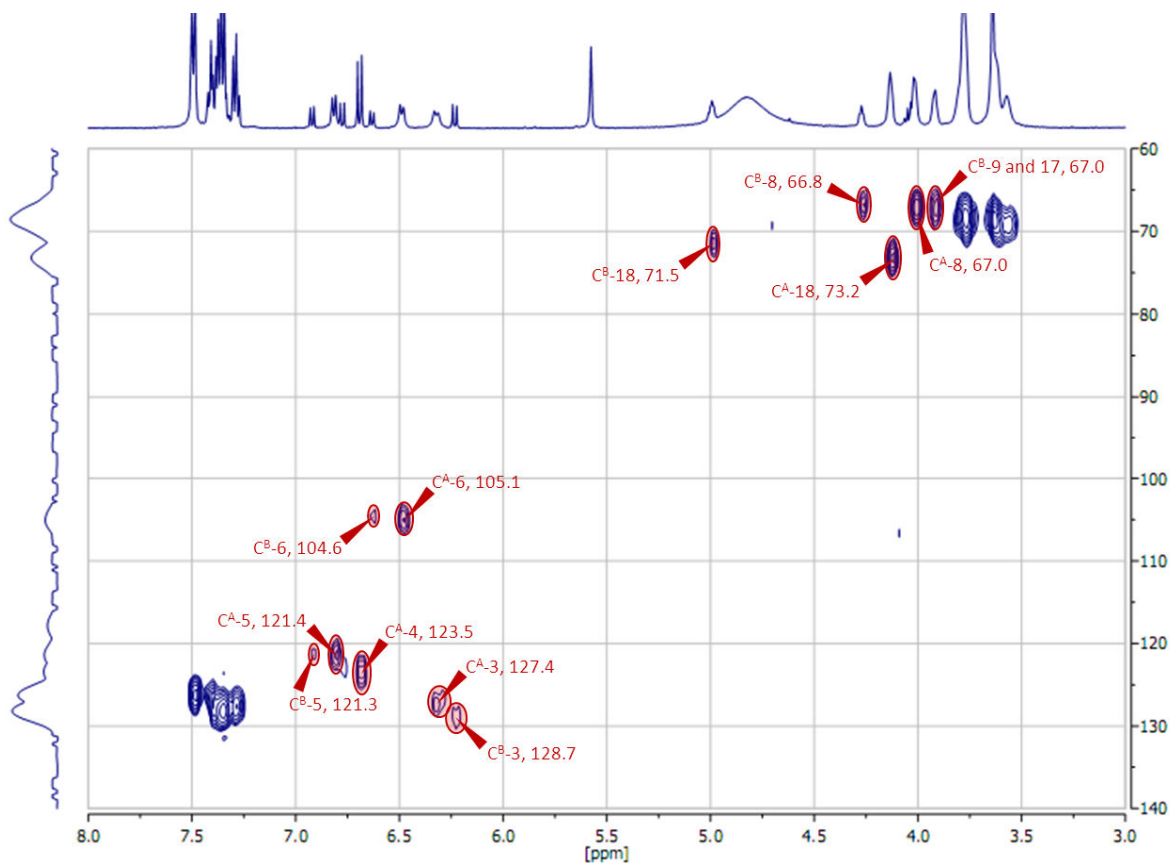


Figure 7.13. HSQC spectrum of a solution of **3a** in CD_3CN in the presence of equimolar quantity of magnesium (II) cations at $-45^\circ C$.

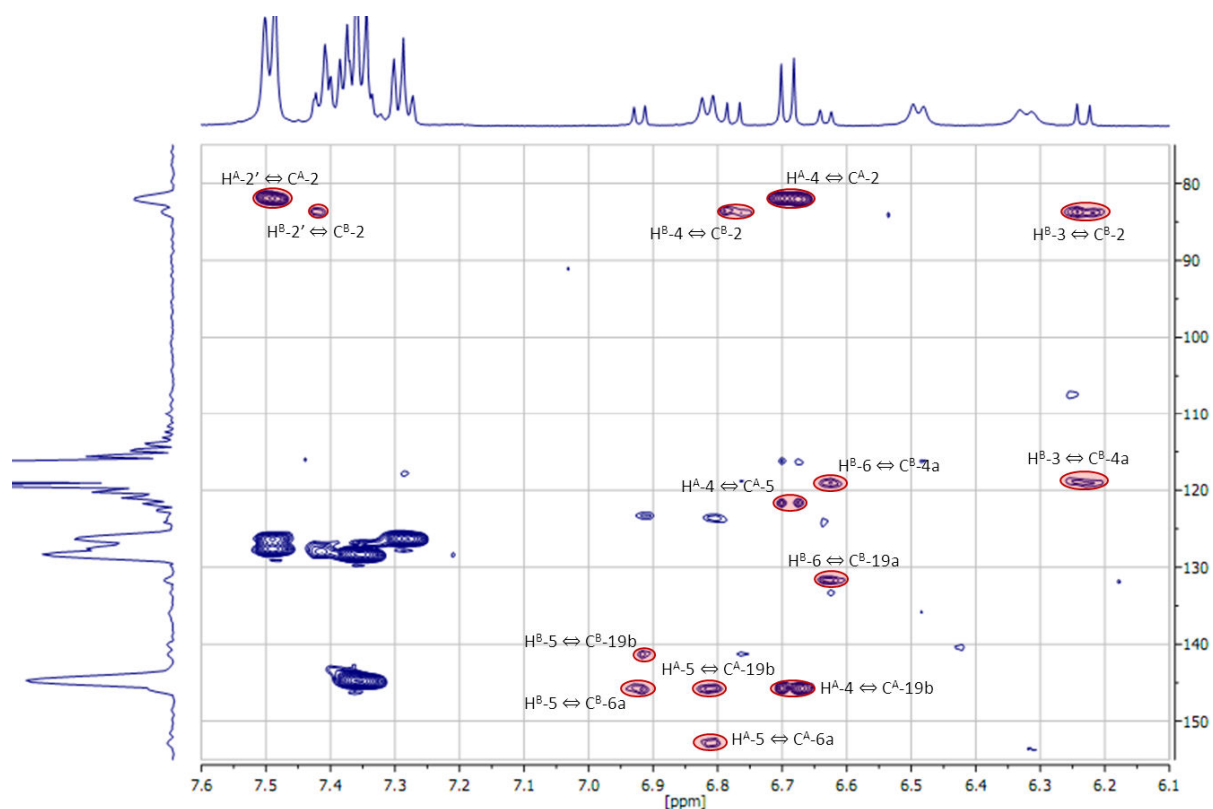


Figure 7.14. Low field part of HSQC spectrum of a solution of **3a** in CD_3CN in the presence of equimolar quantity of magnesium (II) cations at $-45^\circ C$.

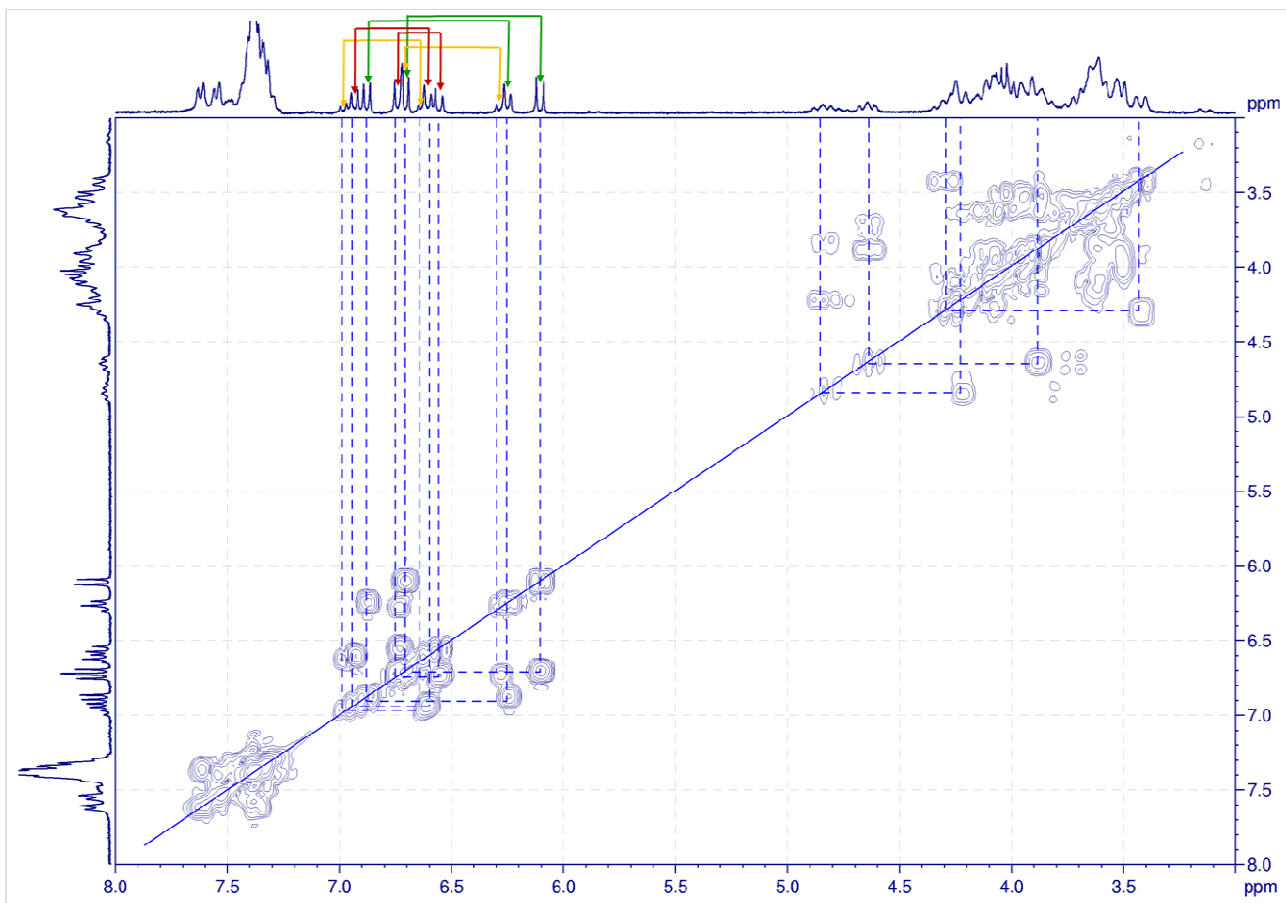


Figure 7.15. COSY spectrum of a solution of **3a** in CD_3CN in the presence of equimolar quantity of barium (II) cations at -45°C .

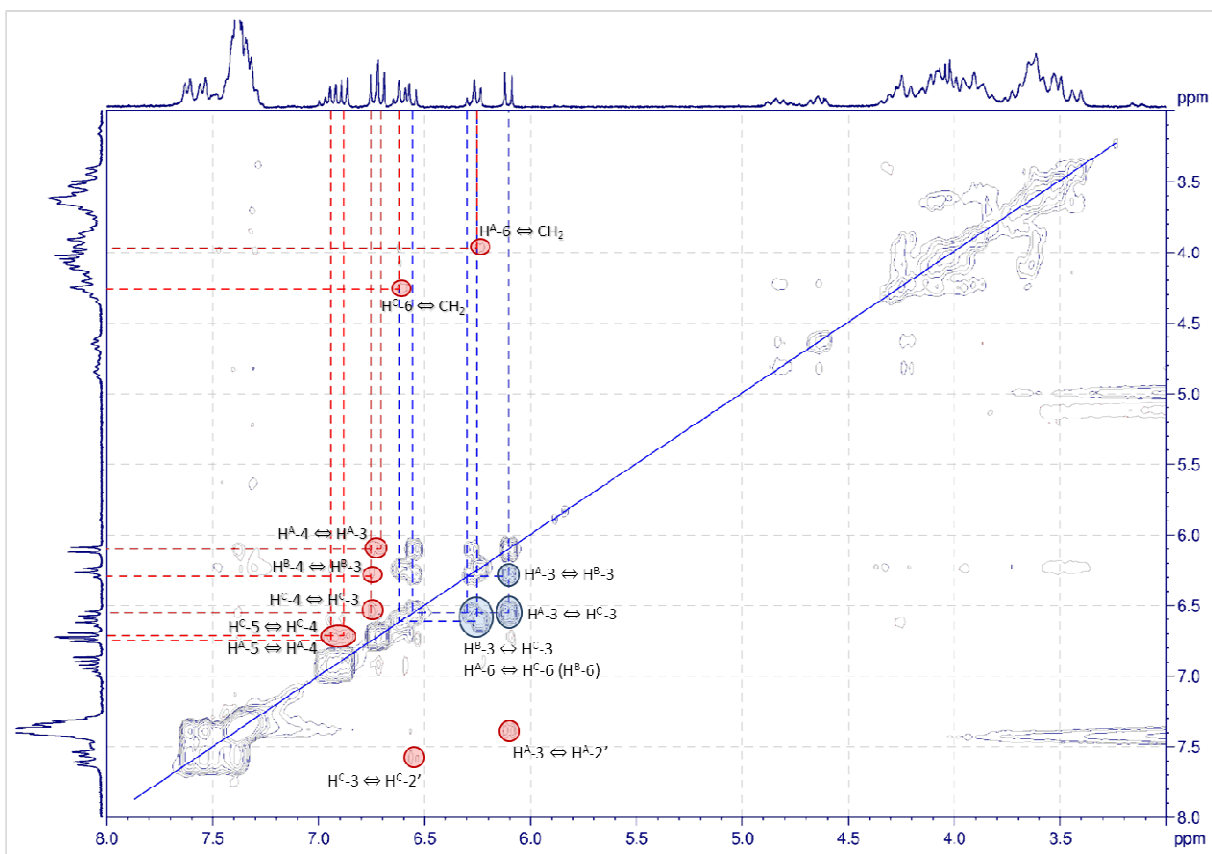


Figure 7.16. NOESY spectrum of a solution of **3a** in CD_3CN in the presence of equimolar quantity of barium (II) cations at -45°C .

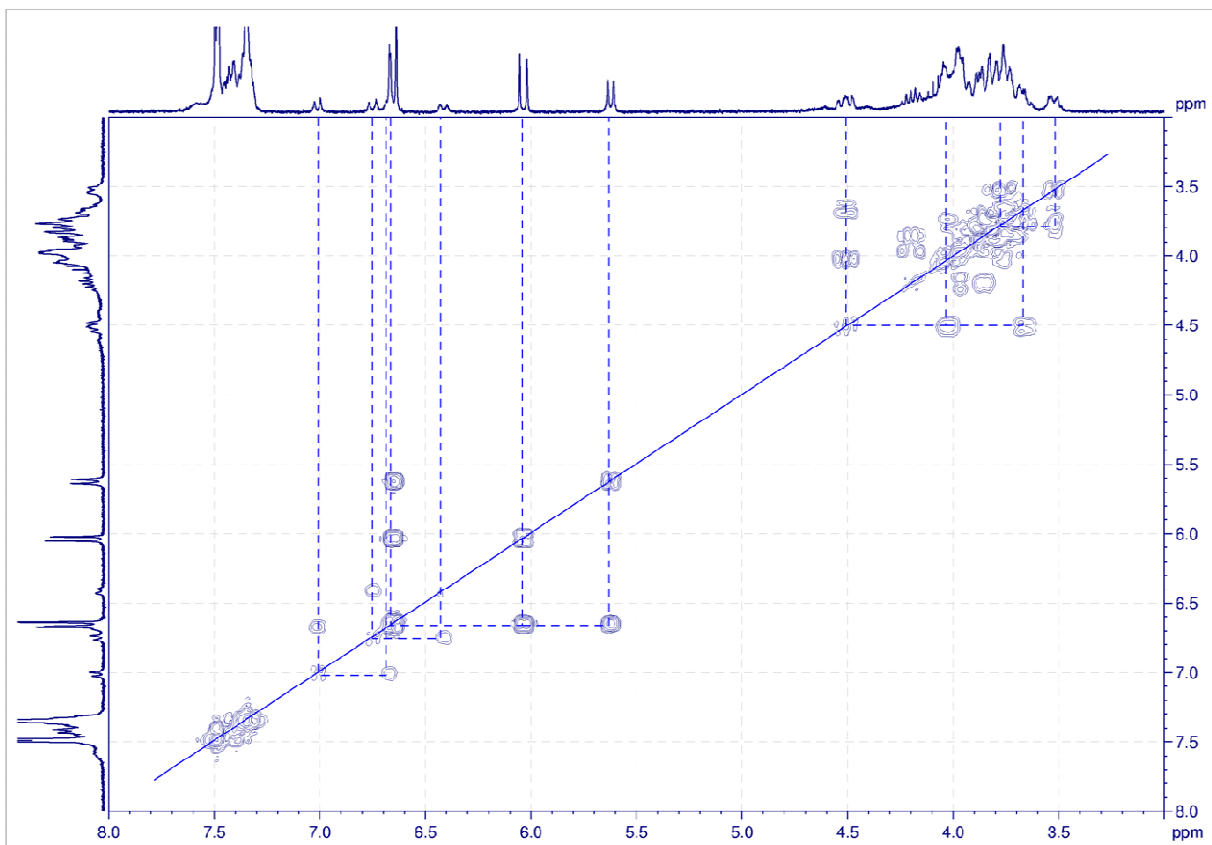


Figure 7.17. COSY spectrum of a solution of **3a** in CD_3CN in the presence of equimolar quantity of lead (II) cations at 20°C .

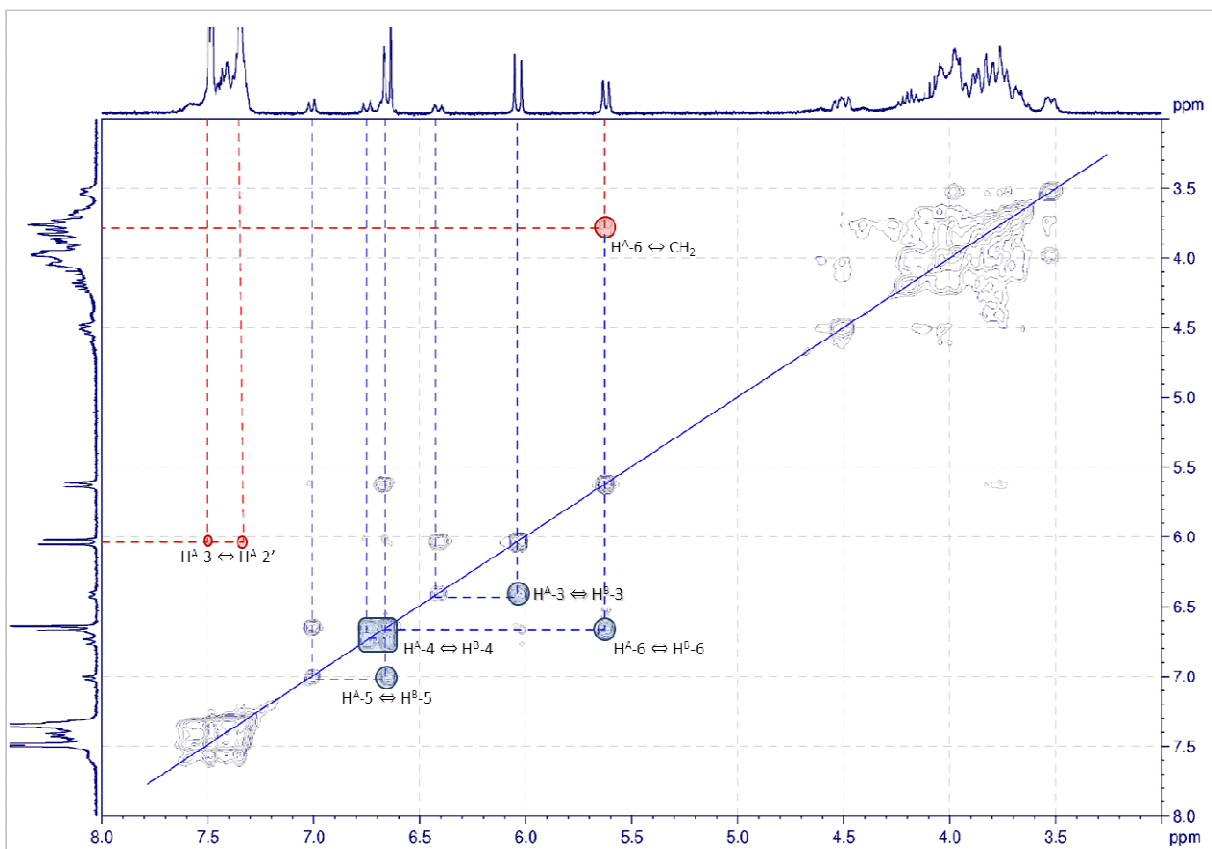


Figure 7.18. NOESY spectrum of a solution of **3a** in CD_3CN in the presence of equimolar quantity of lead (II) cations at 20°C .

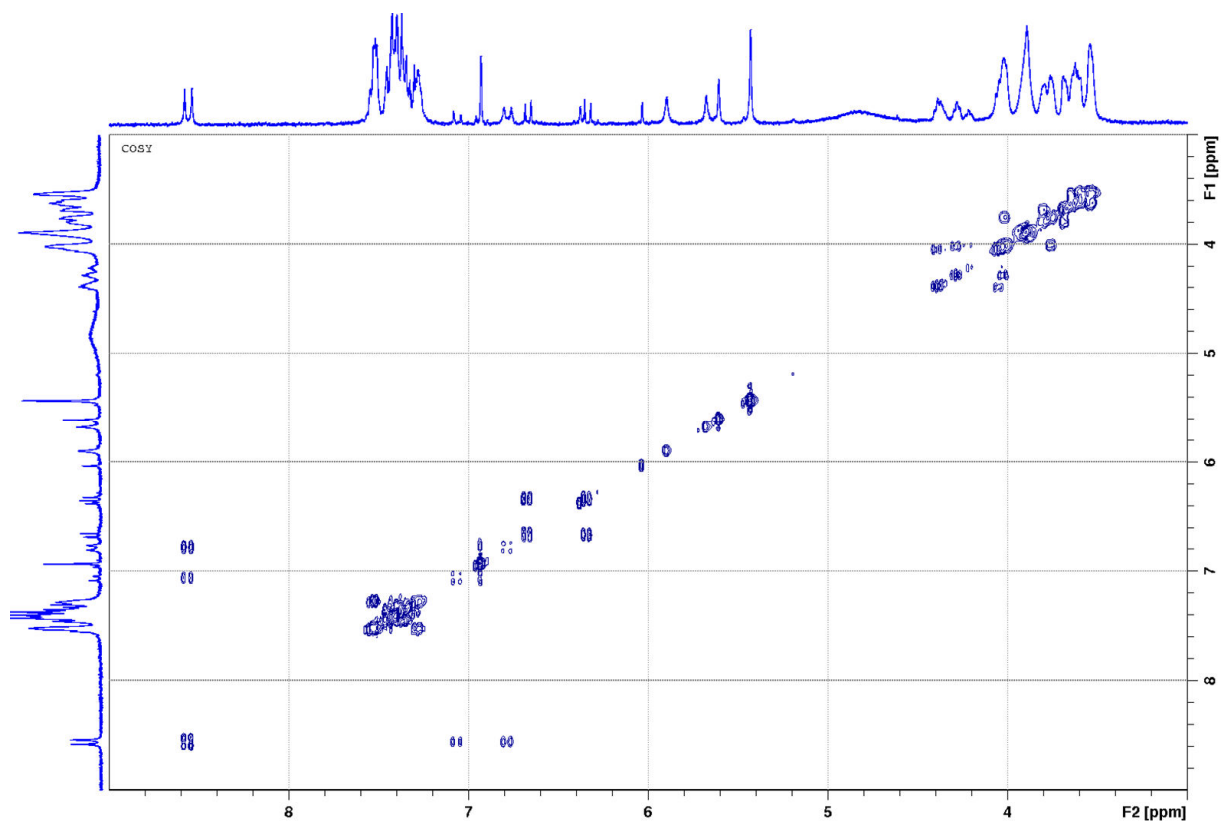


Figure 7.19. COSY spectrum of a solution of **1a** in CD_3CN in the presence of equimolar quantity of magnesium (II) cations at -45°C after 5 *min* of irradiation.

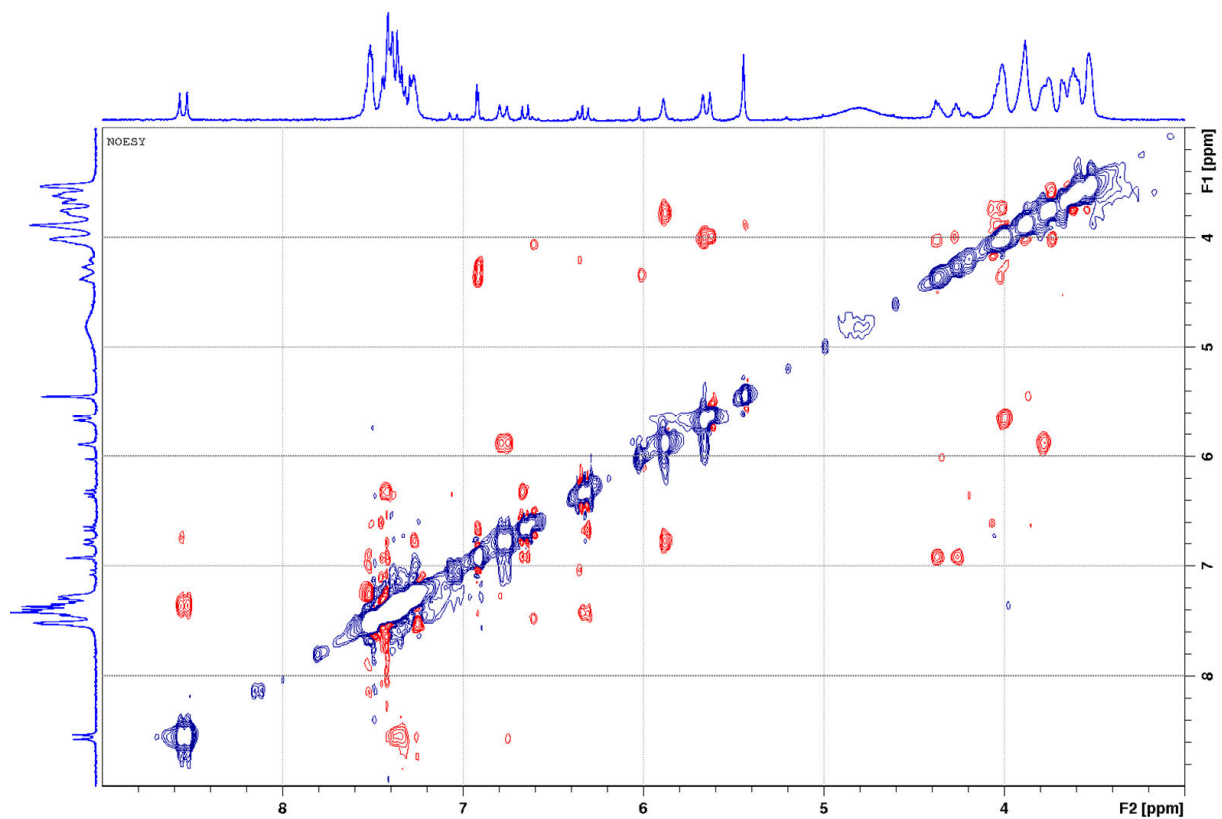


Figure 7.20. NOESY spectrum of a solution of **1a** in CD_3CN in the presence of equimolar quantity of magnesium (II) cations at -45°C after 5 *min* of irradiation.

7.3. List of Publications

Articles

1. Paramonov, S.V.; Fedorova, O.A.; Perevalov, V.P.; Lokshin, V.; Khodorkovsky, V. Synthesis of photochromic benzopyran annulated with 15(18)-crown-5(6) ether. *Russ. Chem. Bull.*, **2008**, *11*, pp. 2381-2384.
2. Glebov, E.M.; Smolentsev, A.B.; Korolev, V.V.; Plyusnin, V.F.; Chebunkova, A.V.; Paramonov, S.V.; Fedorova, O.A.; Lokshin, V.; Samat, A. Synthesis and photochromic properties of crown-containing styryl derivatives of naphthopyrans. *J. Phys. Org. Chem.*, **2009**, *22*, pp. 537–545.
3. Paramonov, S.; Delbaere, S.; Fedorova, O.; Fedorov, Yu.; Lokshin, V.; Samat, A.; Vermeersch, G. Structural and photochemical aspect of metal-ion-binding to a photochromic chromene annulated by crown-ether moiety. *J. Photoch. Photobio. A*, **2010**, *209*, pp. 111-120.
4. Aldoshin, S.M.; Sanina, N.A.; Morgunov, R.B.; Fedorova, O.A.; Paramonov, S.V.; Lokshin, V.; Mushenok, F.B.; Shilov, G.V.; Bozhenko, K.V.; Korchagin, D.V. Ferro-, para-, and thermoinduced magnetism of photomagnetic Cr^{III}/Mn^{II} and Cr^{III} oxalates with 7-methyl-3,3-diphenyl-3H-pyrano[3,2-f]quinolinium cation. *Izv. Akad. Nauk. Ser. Khim.*, **2010**, *59*, pp. 487-499. (*In Russian, to be translated and published in Russ. Chem. Bull.*)

Oral Presentations

1. Paramonov, S.V.; Fedorova, O.A.; Perevalov, V.P.; Lokshin, V.; Samat, A. Synthesis of crown-containing benzo- and naphthopyrans. *XIV International Conference of Students and Young Scientists – “Lomonosov”*, Moscow (Russia), **2007**. (*In Russian.*)
2. Paramonov, S.V. Development of synthetic approaches to benzo- and naphthopyrans annulated by crown ether moieties. *XLIII Russian Conference on Mathematics, Informatics, Physics, and Chemistry*, Moscow (Russia), **2007**. (*In Russian.*)
3. Paramonov, S.V. Synthesis and studies of photochromic chromenes annulated by crown ether fragments. *XV International Conference of Students and Young Scientists – “Lomonosov”*, Moscow (Russia), **2008**. (*In Russian.*)
4. Paramonov, S.V. Synthesis and photochromic properties of chromenes annulated by crown ether moieties. *XLIV Russian Conference on Mathematics, Informatics, Physics, and Chemistry*, Moscow (Russia), **2008**. (*In Russian.*)

5. Paramonov, S.; Delbaere, S.; Vermeersch, G.; Lokshin, V.; Samat, A.; Perevalov, V.; Fedorova, O. The design of photochemical sensor chromenes that reveal cation-dependent complex formation with different metal ions. *JSPS-CNRS "New Horizons of Photochromism – From Design of Molecules to Applications"*, Arras (France), **2008**.
6. Paramonov, S.V. Methods for preparation of chromenes annelated by crown ether fragments. *International Youth Scientific Forum "Lomonosov-2010"*, Moscow (Russia), **2010**. (In Russian.)
7. Paramonov, S.V. Development of methods for preparation of photochromic chromenes annelated by crown ether fragments. *XLV Russian Conference on Mathematics, Informatics, Physics, and Chemistry*, Moscow (Russia), **2010**. (In Russian.)

Posters

1. Paramonov, S.V.; Fedorova, O.A.; Perevalov, V.P.; Lokshin, V.; Samat, A. Synthesis of photochromic crown containing benzo- and naphthopyrans. *2nd International Symposium on Macrocyclic and Supramolecular Chemistry (ISMSC 2007)*, Pavia (Italy), **2007**.
2. Paramonov, S.V.; Fedorova, O.A.; Fedorov, Yu.V.; Strokach, Yu.P.; Valova, T.M.; Perevalov, V.P.; Lokshin, V.; Samat, A. Complex formation of benzopyran annelated by a crown ether fragment with different metal cations. *Joint XVI International Conference on Chemical Thermodynamics and X International Conference "Solvent and Complex Formation in Solutions"*, Suzdal (Russia), **2007**. (In Russian.)
3. Paramonov, S.V.; Fedorova, O.A.; Strokach, Yu.P.; Valova, T.M.; Perevalov, V.P.; Lokshin, V.; Samat, A. Spectral and photochromic properties of the benzopyran annelated with crown ether moiety. *International Conference on Photochemistry (ICP 2007)*, Köln (Germany), **2007**.
4. Paramonov, S.V.; Fedorova, O.A.; Strokach, Yu.P.; Valova, T.M.; Perevalov, V.P.; Lokshin, V.; Samat, A. Synthesis and photochromic properties of the benzopyran annelated with crown-ether moiety. *International Symposium on Photochromism (ISOP 07)*, Vancouver (Canada), **2007**.
5. Fedorova, O.A.; Perevalov, V.P.; Lokshin, V.; Samat, A.; Paramonov, S.V. Synthesis and photochromic properties of benzo- and naphthopyrans annelated with crown-ether moiety. *Russia-France Joint Seminar on Molecular Switching*, Saissac (France), **2007**.
6. Paramonov, S.; Delbaere, S.; Vermeersch, G.; Lokshin, V.; Samat, A.; Perevalov, V.; Fedorova, O. Cation-dependent photochromic supramolecular assemblies based on

- chromene derivatives. *XXIInd IUPAC Symposium on Photochemistry*, Gothenburg (Sweden), **2008**.
7. Paramonov, S.; Fedorova, O.; Perevalov, V. Studies of complex formation between chromenes annelated with crown ether moiety and metal cations. *IV International Summer School "Supramolecular Systems in Chemistry and Biology"*, Tuapse (Russia), **2008**.
 8. Paramonov, S.V.; Fedorova, O.A.; Fedorov, Yu.V.; Perevalov, V.P. Development of supramolecular complexes based on crown-containing chromenes. *XXIV International L.Chugaev Conference on Coordination Chemistry*, Saint-Petersburg (Russia), **2009**.
 9. Paramonov, S.; Fedorova, O.; Fedorov, Yu.; Lokshin, V.; Tulyakova, E.; Vermeersch, G.; Delbaered, S. Photoswitchable structures of the complexes of crown-annelated photochromic chromenes with amino acids. *The 6th International Symposium on Organic Photochromism (ISOP 2010)*, Yokohama (Japan), **2010**.
 10. Paramonov, S.V.; Fedorova, O.A.; Fedorov, Yu.V.; Lokshin, V.; Samat, A. Synthesis and photochromic properties of benzo- and naphthopyrans annelated by crown ether moiety. *The 6th International Symposium on Organic Photochromism (ISOP 2010)*, Yokohama (Japan), **2010**.

RESUME

Les chromènes photochromiques sont largement utilisés dans les technologies modernes en raison de leur capacité à changer les propriétés sous irradiation UV. Les chromènes présentés dans ce travail possèdent en outre des fragments pouvant participer à la coordination avec des cations métalliques, acides aminés, ou de l'ADN. Pour ce type de molécule, l'interdépendance éventuelle entre les propriétés photochromiques et complexantes permet d'envisager soit le photo-contrôle de la complexation, soit la modulation du photochromisme par le biais de coordination.

Ce travail est divisé en deux parties : la première est consacrée à la préparation des molécules cibles et la seconde à l'étude de la complexation. Les approches synthétiques élaborées ont permis d'obtenir une série de nouveaux chromènes annelés par des éthers couronnes de taille et de composition hétéroatomique différentes. Le processus de complexation de certains dérivés a été étudié en détail par spectroscopie RMN et absorption UV-Visible. Il a été établi que la nature des cations métalliques détermine la stœchiométrie du complexe formé ainsi que la structure spatiale. Pour tous les composés étudiés, la complexation affecte les paramètres photochromiques notamment la vitesse de décoloration. En ce qui concerne la complexation des chromènes synthétisés avec les acides aminés protonés, il a été établi qu'en fonction de la longueur de chaîne de ces acides, la formation de complexe mono- ou ditopique est favorisée.

De plus, l'interaction d'un nouveau chromène cationique avec l'ADN a été étudiée. Il a été constaté que contrairement à la forme initiale, la forme colorée de ce composé générée sous irradiation UV permet l'intercalation au sein de l'ADN.

MOTS CLES

Chromènes, photochromisme, éthers couronnes, complexation, acides aminés, cations métalliques.

SUMMARY

Photochromic chromenes are widely used in modern technologies due to their ability to change their properties upon UV irradiation. The chromenes presented in this work also possess fragments able to participate to the coordination with metal cations, amino acids, or DNA. These properties may sustain mutual influence on each other resulting in either photo-control of complexing ability or photochromism tunable by complex formation.

This work is divided in two parts, one devoted to the synthesis of the target compounds and the second to study on the complexing ability of the substances, respectively. Thus, the synthetic approaches to photochromic benzo- and naphthopyrans, annelated to the crown ether moieties of different size and heteroatomic composition, were developed. The complex formation of several chromenes with metal cations was investigated by means of UV-Vis absorption and NMR spectroscopies. The metal cation nature was found to determine the stoichiometry of the complexes as well as their spatial structure. The complex formation was found to affect the photochromic properties of the compounds, especially the bleaching rate. Investigation of complexation of the chromenes with protonated amino acids revealed that, depending on the length of the carbon chain of the acid used, mono- or ditopic complexes may be formed.

The interaction of the new chromene, possessing a positively charged group, with DNA was also studied. In contrast to the initial form, the photo-induced colored form was found to intercalate with DNA.

KEYWORDS

Chromenes, photochromism, crown ethers, complex formation, amino acids, metal cations.